

NASA TM X-73405

A THESIS

entitled

LIQUID JET IMPINGEMENT NORMAL TO

A DISK IN ZERO GRAVITY

(NASA-TM-X-73405) LIQUID JET IMPINGEMENT
NORMAL TO A DISK IN ZERO GRAVITY Ph.D.
Thesis - Toledo Univ. (NASA) 259 p HC 19.00
CSCI 201

876-22492

Unclas
26875

G3/34

by

Thomas L. Labus

as partial fulfillment of the requirements
of the Doctor of Philosophy Degree in
Engineering Science



Advisor

Dean of the Graduate School

The University of Toledo
July 1976

An Abstract of
LIQUID JET IMPINGEMENT NORMAL TO A
DISK IN ZERO GRAVITY

Thomas L. Labus

Submitted in partial fulfillment
of the requirements of the
Doctor of Philosophy in Engineering Science Degree

The University of Toledo
July 1976

An experimental and analytical investigation was conducted to determine the free surface shapes of circular liquid jets impinging normal to sharp-edged disks under both normal and zero gravity conditions. An order of magnitude analysis was conducted indicating regions where viscous forces were not significant when computing free surface shapes. The demarcation between the viscous and inviscid region was found to depend upon the flow Reynolds number and the ratio between the jet and disk radius.

Experiments conducted under zero gravity conditions yielded three distinct flow patterns. These flow patterns were defined as surface tension flow, transition flow, and inertia flow. The flow regions were classified in terms of the relative effects of surface tension and inertial forces. The transition between regions was correlated with the system Weber number and the ratio of the jet to the disk radius. The normal gravity plume shapes were observed to jump from one apparently stable flow pattern to another until steady-state was reached.

A zero gravity inviscid analysis was performed in which the governing equations and boundary conditions in the physical plane were transformed into an inverse plane. In the inverse plane, the stream function and velocity potential became the coordinates thus removing the prime difficulty in free surface problems, that of having to guess at the true position of the free surface. The governing equations were nonlinear in the inverse plane thus requiring a numerical solution in which sets of nonlinear algebraic equations were solved simultaneously. Comparisons between experiment and numerical computations were made for the infinite and finite plate cases with the result that good agreement for the free surface shapes were obtained.

ACKNOWLEDGMENTS

The author wishes to express his gratitude to the following people:

To Ken DeWitt, for his technical guidance and companionship.

To Frank Molls and Steve Sidik of Computer Services for supplying valuable subprograms and data analysis.

To Ray Sotos and the Support personnel at the 100-Foot Drop Tower and Zero Gravity Facility, for their assistance during the experimental tests.

To Bill Masica, Don Petrash, Tom Cochran, Gertrude Collins, and the NASA Lewis Training Branch, for supporting this research.

To Irene Snyder for being able to read my writing in order to type the rough draft of this thesis.

This thesis is dedicated to my wife, Janet, for her patience and understanding during the past ten years and to my parents, Janet and Ted, who provided the initial stimulation as well as continuing encouragement. It is in no small way dedicated to Frank, Jennifer, Eric,

TABLE OF CONTENTS

	Page
Abstract	ii
Acknowledgments	iii
Table of Contents	iv
List of Tables	vii
List of Figures	viii
Nomenclature	xi
I. INTRODUCTION	1
II. LITERATURE SURVEY	3
A. Experimental Studies	3
B. Analytical Studies	4
1. Steady two-dimensional potential flow	4
2. Steady axisymmetric viscous flow	6
C. Numerical Studies	6
1. Steady two-dimensional potential flow	6
2. Steady axisymmetric potential flow	7
3. Unsteady two-dimensional and axisymmetric potential flow	8
4. Steady potential flow including gravitational effects	8
5. Steady potential flow including surface tension	8
6. Steady three-dimensional potential flow	9
III. ORDER OF MAGNITUDE ANALYSIS	10
A. Formulation	10
B. Continuity Equation	17
C. Momentum Equations	17
D. Physics of z_0	18
E. Results	20
IV. ZERO GRAVITY EXPERIMENTATION	22
A. Apparatus and Procedure	22
1. Test facility	22
2. Experiment	22
3. Test liquids	24
4. Test procedure	24
B. Experimental Results	25
1. General considerations	25

2. Effect of nozzle height	27
3. Steady state flow patterns	27
4. Zero gravity results	29
V. POTENTIAL FORMULATION	30
A. Governing Equations and Boundary Conditions in Physical Plane Including Surface Tension	30
1. General formulation	30
2. Introduction of Stokes stream function	30
3. Derivation of boundary conditions in terms of ψ	34
4. Nondimensionalization of governing equations and boundary conditions in physical plane	35
5. Surface tension dominated model	36
B. Inverse Plane Formulations	38
1. Transformation formulas	38
2. Introduction of velocity potential	39
3. Relationships between ψ and ϕ	39
4. Inverse plane formulation	40
5. Governing equations for inverse functions	41
6. Infinite flat plate excluding surface tension	43
7. Derivation of boundary conditions in inverse plane for r formulation	44
8. Derivation of boundary conditions in inverse plane for z formulation	45
9. Finite plate excluding surface tension	46
10. Finite plate including surface tension	47
11. Surface tension dominated model-finite plate	48
VI. CENTRAL FINITE DIFFERENCE REPRESENTATION	50
A. Formulation	50
1. General considerations	50
2. Interior nodal points	51
B. Excluding Surface Tension	52
1. Infinite flat plate	52
2. Finite plate	53
C. Surface Tension	53
VII. DISCUSSION OF NUMERICAL TECHNIQUES	54
VIII. NUMERICAL RESULTS	56
A. Exclusion of Surface Tension	56
1. Infinite flat plate (Weber number = ∞)	56
2. Finite plate	57
B. Surface Tension Dominated Model	59
C. Discussion of Zero Gravity Results	63
IX. NORMAL GRAVITY EXPERIMENT SECTION	66
A. Apparatus and Procedure	66
1. Experiment	66
2. Test liquids	67
3. Test procedure	68

B. Results	68
1. Steady-state flow pattern	68
2. Unstable jumps	69
3. Experiment data	70
4. Data analysis	71
X. CONCLUSIONS	74
XI. APPENDIXES	77
XII. BIBLIOGRAPHY	198

LIST OF TABLES

Table		Page
1	Liquid Properties at 20° C	
2	Summary of Parameters - Zero Gravity	
3	Summary of Parameters - Normal Gravity	

LIST OF FIGURES

Figure	Page
1 Schematic of liquid jet impinging on a flat plate	
2 Flow pattern as a function of nozzle height	
3 Flow pattern as a function of jet radius	
4 Results of order of magnitude analysis	
5 Experiment package	
6 Flow system schematic	
7 (a) Top view of jet reservoir	
(b) Side view of jet reservoir	
8 Schematic diagram of sharp-edged disk	
9 Liquid jet impinging on flat solid plate	
10 Zero gravity experimental results	
11 Physical plane model of liquid jet impingement	
12 Dimensionless governing equation and boundary conditions in physical plane employing Stokes stream function	
13 Surface tension model in physical plane	
14 Dimensionless governing equations and boundary condi- tions	
15 (a) Inverse formulation excluding surface tension (r solution) for infinite plate	
(b) Inverse formulation excluding surface tension (z solution) for infinite plate	
16 (a) Inverse formulation excluding surface tension (r solution) for finite plate	
(b) Inverse formulation excluding surface tension (z solution) for finite plate	

17	Inverse formulation including surface tension (r solution) for finite plate
18	(a) Surface tension model - inverse formulation (r solution)
	(b) Surface tension model - inverse formulation (z solution)
19	Nodal point representation for rectangular mesh
20	(a) Finite difference representation for infinite plate (r solution)
	(b) Finite difference representation for infinite plate (z solution)
21	(a) Finite difference representation for finite plate (r solution)
	(b) Finite difference representation for finite plate (z solution)
22	(a) Finite difference representation for surface tension dominated model (r solution)
	(b) Finite difference representation for surface tension dominated model (z solution)
23	Numerical solution of liquid jet impinging on infinite flat plate (coarse mesh)
24	Print-plot of liquid jet impinging on infinite flat plate (fine mesh)
25	Numerical solution of liquid jet impinging on finite plate [(R_0/L) = 1/2]
26	Print-plot of numerical solution for impingement on a finite plate [(R_0/L) = 3/4]
27	Schematic diagram of velocity discontinuity occurring in surface tension model
28	Numerical solution of surface tension dominated model ($We = 4$, $R_0/L = 1/2$)
29	Comparison of numerical results for infinite plate with reference 39
30	Comparison of numerical results for finite plate - inertial flow with experiments ($R_0/L = 1/2$)

31	Comparison of numerical results for finite plate - inertial flow with experiments ($R_0/L = 3/4$)
32	(a) Experimental test rig - front view
	(b) Experimental test rig - side view
33	Cross-section of settling chamber
34	Photograph of sharp-edged disk
35	Schematic of steady state normal gravity impingement
36	Photographs indicating flow patterns before and after jump
37	Variation of plume width with Weber number

NOMENCLATURE

A	numerical constant
a	stream function increment
B	numerical constant
B_0	Bond number, $\rho g R_0^2 / \sigma$
b	numerical constant
C	numerical constant
C_0, C_1, C_2	numerical constants
c	numerical constant
D	$= 1/\alpha^2$
d	designated reference point
f_0	unknown scale factor, m
f, f_1, f_2	fictitious points
g	acceleration due to gravity, m/sec^2
g	gas
H	distance between plate and nozzle, m
i	any point on free surface
\hat{i}, \hat{j}	unit vectors
J	Jacobian
$K\phi$	numerical constant
L	disk radius, m
\hat{n}	unit normal on free surface
O	stagnation point
p	pressure, N/m^2

P_0	unknown scale factor, N/m^2
Q	$\frac{(r_1 - r_3)^2}{(r_f - r_4)^2} \cdot \frac{1}{\alpha^2}$
Q^*	$= \alpha^2 \frac{(f - z_4)^2}{(z_1 - z_3)^2}$
R^2	statistical variable
RD	$= L/R_0$
Re	Reynolds number, $\rho VR_0/\mu$
R_{max}	maximum radius for surface tension model, m
R_0	radius of nozzle, m
R_p	radius of plume, m
R_1, R_2	radii of curvature, m
r	radial coordinate, m
r_0	unknown scale factor, m
T^2	$= \alpha^2 r_0^2 \frac{(f - z_4)^2}{(z_1 - z_3)^2} + 1$
U_0	unknown scale factor, m/sec
u	radial velocity component, m/sec
v	jet velocity, m/sec
\vec{V}	vector velocity along free surface, m/sec
v	axial velocity component, m/sec
We	Weber number, $\rho V^2 R_0/\sigma$
y	dimensionless parameter
z	axial coordinate, m
z_1, z_2, z_3, z_4, z_5	dimensionless parameters

α	$\Delta\phi/\Delta\psi$
$\delta/\delta r$	finite difference analogy of $\partial/\partial r$
μ	liquid viscosity, $\text{g/m}^2\text{-sec}$
ρ	liquid density, kg/m^3
σ	liquid surface tension, N/m
ϕ	velocity potential, m^2/sec
x	$= r_f - r_4$, m
ψ	Stokes' stream function, m^3/sec

Superscripts and subscripts:

Cr	critical
'	differentiation with respect to r
*	denotes dimensionless quantities
1,2,3,4	nodal point locations
s	surface

I. INTRODUCTION

A knowledge of the dynamics of free liquid jets is required for the solution of a variety of problems associated with fluid flow within propellant tanks under low gravitational conditions. In particular, an understanding of the liquid jet - impact process, as occurs when liquid impinges upon baffles or tank walls during an inflow or reorientation maneuver, will be required in order to predict liquid-propellant location, heat transfer rates and pressure distributions. The area of liquid jet impingement also has direct applicability to the spacecraft fire safety problem, in which water jets are employed as extinguishant agents under low gravity conditions. In order to be able to predict required delivery flow rates, the accurate prediction of flow surface coverage as a function of jet momentum is needed.

There generally appears to be three chief obstacles which have in the past prohibited the attainment of solutions to steady-state liquid jet-solid interaction problems. The major obstacle is the presence of the free surface. In order to apply numerical techniques to the solution of free-jet problems it is necessary to define the area over which the computations are made by boundaries defined by the free liquid surface. Unfortunately, the location of the free-surface is one of the items sought from the solution so that various techniques must be devised to circumvent this situation. Furthermore, analytical techniques are restricted solely to two-dimensional problems, whether

a free surface exists or not. The second obstacle is gravity. Liquid jets in air (free jets), unlike liquid-into-liquid jets and gas-into-gas jets (submerged jets), are affected significantly by gravitational forces. The free-surface shape and velocity profiles are dependent on both the magnitude and the orientation of gravity. The addition of gravity necessarily complicates a model either through the governing equation or through the boundary conditions. Neglecting gravity in the model makes questionable the comparison of the theory with normal-gravity experimental data. The final obstacle is surface tension, an effect which has generally been neglected in almost all studies on free jets. The addition of surface tension into a model leads to non-linear free surface boundary conditions.

The purpose of this report is to present the results of an experimental and analytical study conducted at the NASA Lewis Research Center concerning zero gravity isothermal liquid jet impingement. An axisymmetric liquid jet was impinged normally onto a sharp-edged disk under conditions in which both inertial and surface tension forces are of importance. The experimental free surface shapes were correlated with known system parameters. An analytical model was formulated and the free surface shapes and streamlines were calculated for a number of discrete cases.

II. LITERATURE SURVEY

A. Experimental Studies

Very few experimental studies have been conducted to examine free jets impinging on solid surfaces. No work has been conducted where the major concern was either the shape of the free surface or the measurement of velocity profiles within the jet. Also, only one experiment has been conducted using a two-dimensional jet. A two-dimensional jet is one in which the flow emanates from a rectangular slot in which the width of the jet is very large relative to the thickness of the jet. Schach (38) measured the pressure distribution and analytically calculated the free surface shape and velocity distributions for jets impinging onto flat panels at various impingement inclinations relative to the direction of flow. The jet employed had dimensions of 21 by 115 mm. According to Schach, the jet diverged spatially after impinging upon the panel and thus it can only be considered as truly two-dimensional close to the centerline. An excellent account of an elaborate experimental apparatus for obtaining a quiescent circular water jet in normal gravity is given by Donnelly, et al. (11). Their major concern was jet stability under imposed audio frequency disturbances and, therefore, the impingement phenomenon was not directly observed. Rupe (37) and Stephens (41) experimentally measured the pressure distribution caused by circular jets striking solid surfaces in normal gravity. However, neither Rupe or Stephens meas-

ured the free-surface shape or discussed any instabilities which occurred.

In nearly all flows where a circular liquid jet strikes a large flat surface, typically what happens in normal gravity is that the liquid jet impinges on the surface and moves radially outward from the stagnation point until a certain radial distance is reached whereupon an instability known as a circular hydraulic jump occurs. The jump is characterized by an abrupt increase in the liquid depth and turbulent fluid motion. Koloseus, et al. (22) were concerned solely with predicting the behavior of the circular hydraulic jump. A water jet impinging on a flat plate of epoxy material was employed in these experiments. The circular hydraulic jump was the subject for a very complete study conducted by Nirapathdongporn (33), whose report contains an excellent description of various devices for measuring jet shapes and jet diameters.

All of the above mentioned studies deal with normal-gravity, liquid jet-solid impingement. There have been no experimental studies on the impingement of liquid jets under zero-gravity conditions.

B. Analytical Studies

1. Steady two-dimensional potential flow. - A number of papers and books have discussed steady-state two-dimensional free jets impinging on a variety of surfaces using analytical techniques. The majority of these studies were concerned with irrotational, incompressible, inviscid flow, in which the effects of gravity and surface tension were neglected. One of the major attractions of this type of problem is that it can be handled using complex potential theory and, therefore, can be treated analytically.

A two-dimensional jet striking an infinitely flat surface at various angles was examined by Batchelor (4), who solved for the limiting stream thickness as a function of flow impingement angle and jet diameter. However, no attempt was made to predict free-streamline shape. Schach (38) treated the impingement as a function of angle using Prandtl's hodograph method, and obtained the equations for the free surface shapes, flow distribution, and pressure distribution for the case of impingement on an infinitely wide plate. Kochin, et al. (21) also examined the impingement of a two-dimensional jet obliquely to an infinite flat plate, and discussed the case of impingement on a plate of finite length. The equation of the free-surface for the case of a two-dimensional jet striking a flat surface at right angles is presented by Milne-Thomson (30) who also solved for the velocity components within the jet. An excellent discussion of the techniques for handling two-dimensional free jet problems is presented by Gurevich (14). Some of the two-dimensional flows examined by Gurevich include flow around a finite wedge, perpendicular to a finite plate, obliquely to an infinite flat plate, and flows where a variety of solid objects are positioned adjacent to one wall or between two walls. Chang, et al. (9) analyzed the two-dimensional flow of a jet interacting with a number of flat segments at angles to one another. The results include flow turning angles but not free surface shapes or velocity profiles. The irrotational flow pattern of a free jet discharging from a slot and flowing past a wedge was analyzed by Arbhahirama (3). All of the above texts and articles were concerned with analytical techniques for obtaining solutions. The area of steady two-dimensional potential flow represents the most

complete area of research in the field of jet impingement.

2. Steady axisymmetric viscous flow. - Watson (43) has analytically investigated free jet-impingement for the case of large Reynolds numbers where the viscous forces are confined to a thin boundary layer adjacent to the plate. A similarity solution was obtained for both the two-dimensional and axisymmetric velocity profiles and free surface shapes for the case of normal impingement. As mentioned by Watson, the similarity solution can only be expected to be valid when the radial distance is sufficiently large for the incident jet to have lost its influence. The effects of gravity and surface tension were neglected in the analysis. Watson solved for the radial position of the circular hydraulic jump.

C. Numerical Studies

1. Steady two-dimensional potential flow. - When the shape of the solid upon which the jet impinges becomes complex, numerical techniques for the solution of free jet problems have to be applied. Jeppson (19) presents an excellent article in this regard. Jeppson employed the stream function and the velocity potential as the independent variables and the coordinates as the dependent variables. A similar inversion approach has been previously used to solve a variety of fluid dynamics problems as shown in references 5, 20, 31, 42, and 44 and is mainly attributable to Thom and Apelt (42). Using this technique, Jeppson was able to circumvent the problem of working in the physical plane and having to guess at the true position of the free surface. The latter iterative approach was used in references 1, 8, 13, 27, 32, 36, and 40 with limited success. Jeppson solved the problem of the two-dimensional flow over a wedge, and, as such, is

the only one to have attempted numerical solutions of this problem. Lastly, Chan (7) applied the finite element method to a number of free-surface flow problems, including the flow from a circular orifice.

2. Steady axisymmetric potential flow. - The solution of axisymmetric flow problems cannot utilize the powerful tool of complex analysis. For this reason, only numerical solutions can be attempted for problems of this nature.

LeClerc (25) studied the impingement of an axially symmetric liquid jet perpendicular to a flat surface. The shape of the free surface was found using an electrical analogy. This method thus fixed the position of the free surface and enabled the author to apply standard finite-differencing methods and employ Southwell's relaxation technique to solve Laplace's equation. Jeppson (19) applied his inversion technique to find the flow pattern and free-surface shape for the case of axisymmetric flow past a variety of bodies of revolution, including cones. Jeppson also applied his technique to the solution of a jet of inviscid, incompressible fluid issuing from a nozzle into the free atmosphere. He indicates how his method may be extended to a variety of other problems. Schach (39) used a semi-analytical technique based on Trefftz's approximate method to find the shape of an axisymmetric free jet impinging normally on a plate. Also presented in Schach's article was the pressure distribution on the plate which was calculated from the velocity distribution using Bernoulli's equation. Young, et al. (45) and Brunauer (6) determined the flow pattern past two disks immersed in axisymmetric flow. Both Young and Brunauer solved Laplace's equation in the physical plane.

No analyses have been conducted for the case in which an inviscid free jet impinges upon a plate of finite thickness.

The articles mentioned above encompass all the known solutions with regard to axisymmetric jet impingement. References 7, 8, 20, 27, and 40 deal specifically with numerical methods applied to free surface problems in which no impingement occurs. Jeppson (20) employed an inverse formulation while the others worked in the physical plane.

3. Unsteady two-dimensional and axisymmetric potential flow. - Huang (17, 18) has investigated unsteady flows and considered the impact phenomena for both two-dimensional and axisymmetric jets. The major interest in these articles was in obtaining the initial pressure distribution due to liquid impact.

4. Steady potential flow including gravitational effects. - The addition of gravity in analyses for potential flows causes no serious formulation problem for either the two-dimensional or axisymmetric case. The reason for this is because its effect enters only through the free-surface boundary conditions and not the governing equations. Jeppson (19) included gravity in his analysis of the impingement on a two-dimensional wedge. Moayeri, et al. (31) Southwell, et al. (40) and Chan (8), all considered the effect of gravity in dealing with steady, potential, free-surface problems in which no impingement occurs.

5. Steady potential flow including surface tension. - Zhukovskii (46) has indicated how to include the effects of surface tension. He examined a two-dimensional problem using complex analysis, but his method is not extendable to either axisymmetric or three-dimensional

flows.

6. Steady three-dimensional potential flow. - Until very recently, very little had been accomplished in the area of three-dimensional potential flow with a free surface, much less including impingement. Davis and Jeppson (10) developed a computer program to solve free-surface problems of this type using the inverse method. Michelson (28, 29) also examined jets under these conditions. He treated the case of an axisymmetric jet impinging obliquely on a flat surface, and analytically showed the occurrence of wedge-shaped dry zones when the impingement angle was less than a critical value. Free-surface shapes are not obtainable using Michelson's method.

III. ORDER OF MAGNITUDE ANALYSIS

A. Formulation

The problem under consideration is the viscous flow of a circular liquid jet as it impinges normally to an infinite flat plate, as shown in Figure 1. The objective is to determine the free surface shape of the impinging liquid and the velocity profiles within the jet. In general, flows of the type described will depend on viscous, surface tension, inertial and body forces. Physical intuition tells us that if the velocity is large and the diameter of the plate is sufficiently small, there will be regions wherein viscous forces are not of prime importance in determining the resulting flow behavior, particularly the free surface shape. The viscous forces, in this case, will be confined to a thin boundary layer on the plate which originates from the stagnation point. The location of the stagnation point is shown in Figure 1. The jet or nozzle radius is R_0 and the distance between the plate and nozzle is given as H . A cylindrical coordinate system (r, z) emanating from the stagnation point is chosen. An order of magnitude analysis will permit the governing equations to be simplified so that an analytical solution can be attempted. For axisymmetric, isothermal, incompressible steady flow under weightless conditions, the governing equations in cylindrical coordinates can be written:

Continuity:

$$\frac{1}{r} \frac{\partial}{\partial r} (ru) + \frac{\partial v}{\partial z} = 0 \quad (1)$$

Momentum:

r Component:

$$\rho \left(u \frac{\partial u}{\partial r} + v \frac{\partial u}{\partial z} \right) = - \frac{\partial P}{\partial r} + \mu \left\{ \frac{\partial}{\partial r} \left[\frac{1}{r} \frac{\partial}{\partial r} (ru) \right] + \frac{\partial^2 u}{\partial z^2} \right\} \quad (2)$$

z Component:

$$\rho \left(u \frac{\partial v}{\partial r} + v \frac{\partial v}{\partial z} \right) = - \frac{\partial P}{\partial z} + \mu \left[\frac{1}{r} \frac{\partial}{\partial r} \left(r \frac{\partial v}{\partial r} \right) + \frac{\partial^2 v}{\partial z^2} \right] \quad (3)$$

Boundary conditions are required on the flat plate, along the axis of symmetry, at the nozzle exit, on the free surface, and at $r = L$.

On plate

$$\begin{aligned} u &= 0 \\ v &= 0 \end{aligned} \quad \text{on } z = 0, \text{ all } r \quad (4)$$

Along axis of symmetry

$$\begin{aligned} u &= 0 \\ \frac{\partial v}{\partial r} &= 0 \end{aligned} \quad \text{on } r = 0, \text{ all } z \quad (5)$$

At the nozzle

$$\begin{aligned} v &= -V \\ u &= 0 \end{aligned} \quad \text{on } 0 \leq r \leq R_0, z = H \quad (6)$$

At $r = L$

$$\begin{aligned} u &= u(z) \\ v &= v(z) \end{aligned} \quad \text{on } r = L, 0 < z \leq f(L) \quad (7)$$

On the free surface, denoted by $z_s = f(r)$, two boundary conditions are required since the free surface position is an unknown to be determined as part of the solution. The details of the calculation

for the boundary conditions along the free surface can be found in Appendix A. (See eqs. (A.10) and (A.14).)

On the free surface

$$\frac{1}{2} (u^2 + v^2) - \frac{\sigma}{\rho r} \frac{d}{dr} \left[\frac{r \frac{df}{dr}}{\sqrt{1 + \left(\frac{df}{dr}\right)^2}} \right] = \frac{1}{2} v^2 - \frac{\sigma}{\rho R_0} \quad \text{on } z_s = f(r) \quad (8)$$

and

$$-u \frac{df}{dr} + v = 0 \quad \text{on } z_s = f(r) \quad (9)$$

In equation (4), the no-flow and no-slip boundary conditions are applied at the wall. Equation (5) is a statement involving the known geometrical symmetry of the problem, while equation (6) imposes an initially uniform velocity profile on the incoming jet. Equation (7) simply states the velocity distribution as the liquid leaves the control volume. Equation (8) is a statement of conservation of mechanical energy along a streamline, while equation (9) states that the normal velocity component on a streamline is zero. The second terms on the left and right sides of equation (8) are the contribution of surface tension to the mechanical energy balance.

The solution of the problem can be greatly facilitated by simplifying equations (1) to (8). Specifically, the method of obtaining the minimum parametric representation of a problem will be employed in order to simplify the governing equations. This method is described in detail by Krantz (23) and is the most systematic approach for scaling the governing equations. The initial step in the minimum parametric representation method is to form dimensionless variables by introducing characteristic scale factors for all dependent and independent

variables. The unknown scale factors are defined as $U_0, V_0, r_0, z_0,$
 $P_0,$ and $f_0.$

Dimensionless variables are now defined as:

$$u^* = \frac{u}{U_0}, \quad v^* = \frac{v}{V_0}, \quad r^* = \frac{r}{r_0}, \quad z^* = \frac{z}{z_0}, \quad p^* = \frac{P}{P_0}, \quad f^* = \frac{f}{f_0} \quad (10)$$

Introducing these dimensionless variables into the differential equations and boundary conditions, and arbitrarily making the coefficient of one term in each differential equation and boundary condition equal to unity, results in:

Continuity:

$$\frac{\partial v^*}{\partial z^*} + \frac{U_0 z_0}{V_0 r_0} \frac{1}{r^*} \frac{\partial}{\partial r^*} (r^* u^*) = 0 \quad (11)$$

Momentum:

r Component:

$$\begin{aligned} \frac{\rho U_0 z_0^2}{r_0 \mu} u^* \frac{\partial u^*}{\partial r^*} + \frac{\rho V_0 z_0}{\mu} v^* \frac{\partial u^*}{\partial z^*} = - \frac{P_0 z_0^2}{r_0 \mu U_0} \frac{\partial p^*}{\partial r^*} \\ + \frac{z_0^2}{r_0^2} \frac{\partial}{\partial r^*} \left[\frac{1}{r^*} \frac{\partial}{\partial r^*} (r^* u^*) \right] + \frac{\partial^2 v^*}{\partial z^{*2}} \end{aligned} \quad (12)$$

z Component:

$$\begin{aligned} \frac{U_0 z_0}{r_0 V_0} u^* \frac{\partial v^*}{\partial r^*} + v^* \frac{\partial v^*}{\partial z^*} = - \frac{P_0}{\rho V_0^2} \frac{\partial p^*}{\partial z^*} \\ + \frac{\mu z_0}{r_0^2 \rho V_0} \frac{1}{r^*} \frac{\partial}{\partial r^*} \left(r^* \frac{\partial v^*}{\partial r^*} \right) + \frac{\mu}{z_0 \rho V_0} \frac{\partial^2 v^*}{\partial z^{*2}} \end{aligned} \quad (13)$$

Boundary conditions:

On wall

$$\begin{aligned} u^* &= 0 \\ v^* &= 0 \end{aligned} \quad \text{on } z^* = 0, \text{ all } r^* \quad (14)$$

Along axis of symmetry

$$\begin{aligned} u^* &= 0 \\ \frac{\partial v^*}{\partial r^*} &= 0 \end{aligned} \quad \text{on } r^* = 0, \text{ all } z^* \quad (15)$$

At the nozzle

$$v^* = -\frac{V}{V_0} \quad 0 \leq r^* \leq \frac{R_0}{r_0} \quad (16)$$

$$u^* = 0 \quad z^* = \frac{H}{R_0}$$

At $r = L/R_0$

$$\begin{aligned} u^* &= u^*(z^*) \quad \text{on } r^* = \frac{L}{r_0} \\ v^* &= v^*(z) \end{aligned} \quad (17)$$

On the free surface

$$\begin{aligned} \frac{1}{2} \left(u^{*2} \frac{U_0^2}{V_0^2} + v^{*2} \right) - \frac{\sigma}{\rho r^* V_0^2} \frac{f_0}{r_0} \frac{d}{dr^*} \left[\frac{r^* \frac{df^*}{dr^*}}{\sqrt{1 + \frac{f_0^2}{r_0^2} \left(\frac{df^*}{dr^*} \right)^2}} \right] \\ = \frac{1}{2} \frac{V^2}{V_0^2} - \frac{\sigma}{\rho R_0 V_0^2} \quad \text{on } z_s^* = \frac{f^* f_0}{z_0} \end{aligned} \quad (18)$$

and

$$v^* - \frac{U_0 f_0}{V_0 r_0} u^* \frac{df^*}{dr^*} = 0 \quad \text{on } z_s^* = \frac{f^* f_0}{z_0} \quad (19)$$

The scale factors must now be determined. This is done by setting some of the resulting dimensionless groups in the equations and boundary conditions equal to zero or unity, the groups chosen depending upon the physical conditions for which the equations are being scaled (23). Characteristic lengths are usually determined from the dimensionless groups generated by the boundary conditions, while characteristic times, velocities, etc., are determined from dimensionless groups generated by the differential equations. The guidelines in determining the unknown scale factors are:

- (1) Do not introduce any mathematical contradictions
- (2) Do not violate physical intuition.

Boundary conditions. - Examining the boundary conditions, it is apparent that the following dimensionless groups are introduced:

$$\frac{v}{V_0}, \frac{R_0}{r_0}, \frac{H}{z_0}, \frac{L}{r_0}, \frac{f(L)}{z_0}, \frac{U_0^2}{V_0^2}, \frac{\sigma f_0}{\rho V_0^2 r_0^2}, \frac{f_0^2}{r_0^2}, \frac{\sigma}{\rho R_0 V_0^2}, \frac{f_0}{z_0}, \frac{U_0 f_0}{V_0 r_0}$$

It is known that v has the range 0 to $-V$, r has the range 0 to L , z has the range 0 to H and $f(r)$ also has the range 0 to H . Therefore, setting,

$$\frac{v}{V_0} = 1 \quad \text{and} \quad \frac{L}{r_0} = 1 \quad (20)$$

implies that

$$V_0 = V \quad \text{and} \quad r_0 = L \quad (21)$$

and yields two of the six unknown scale factors.

Some of the above remaining dimensionless groups cannot be set equal to one or zero without introducing contradictions. Setting $V_0 = V$ and $r_0 = L$ into the above ratios, and since it would be expected that

$$f_o = z_o \quad (22)$$

the following meaningful ratios remain:

$$\frac{H}{z_o}, \quad \frac{U_o^2}{V^2}, \quad \frac{\sigma z_o}{\rho V^2 L^2}, \quad \frac{z_o^2}{L^2}, \quad \frac{U_o z_o}{VL}$$

Setting the second or fourth ratio equal to one or zero would violate physical intuition. Therefore, the ratios to be considered are

$$\frac{H}{z_o}, \quad \frac{\sigma z_o}{\rho V^2 L^2}, \quad \frac{U_o z_o}{VL}$$

At this point an attempt was made to set $H/z_o = 1$ such that z_o would equal H . This seemed logical because 0 to H was the range of z . However, this leads to some confusing results in terms of the physics. For a given flow condition, it is argued that for a certain (minimum) value of H up to $H = \infty$, the flow pattern in the vicinity of the plate is not expected to change. This is shown schematically in Figure 2. This argument has been experimentally verified and will be discussed at some length in Section IV, Experimentation. The major point is that H cannot be a characteristic length in the problem either with reference to z_o or f_o . This leaves two remaining ratios from consideration of the boundary conditions.

$$\frac{\sigma z_o}{\rho V^2 L^2} \quad \text{and} \quad \frac{U_o z_o}{VL}$$

Accordingly, all possible information from the boundary conditions has been obtained. Two of the six scale factors and a relationship between two others has been determined. The governing equations must now be examined.

B. Continuity Equation

From the physics of the problem, it is known that mass must be conserved. Hence, the continuity equation must be valid in its dimensionless form (eq. (11)). If the dimensionless derivatives $\partial v^*/\partial z^*$ and $(1/r^*)(\partial/\partial r^*)(r^*u^*)$ are to be of the same order of magnitude, it is required that

$$\frac{U_o z_o}{V_o r_o} = 1 \quad (23)$$

With $V_o = V$ and $r_o = L$, it is found that

$$\frac{U_o z_o}{VL} = 1 \quad (24)$$

Solving for U_o ,

$$U_o = \frac{VL}{z_o} \quad (25)$$

This, of course, is an equation relating two unknowns, U_o and z_o . It is noted that the same information could have been obtained by setting the second of the two ratios remaining from the consideration of the boundary conditions equal to one.

C. Momentum Equations

It is the objective of this analysis to define that portion of the flow for which an inviscid solution is valid. For this case, the pressure forces are balanced by the inertia forces. This fact allows us to determine the scale factor for the pressure, P_o . If the dimensionless pressure gradient in equation (13) is to be the same order of magnitude as the dimensionless inertia term,

$$\frac{P_o}{\rho V_o^2} = 1 \quad (26)$$

This implies that

$$P_o = \rho V_o^2 = \rho V^2 \quad (27)$$

thus, the characteristic pressure is the stagnation value.

D. Physics of z_o

The remaining unknown to be determined is z_o . At this point some physical arguments are necessary. Recall that it has been shown that H cannot be considered as a characteristic scale factor for the problem at hand for reasonably large values of H . However, the free surface shape is expected to change as R_o varies (see Fig. 3). Therefore, from physical considerations this suggests that characteristic values of z_o vary as R_o . Defining

$$z_o = R_o \quad (28)$$

then U_o can be found from equation (25).

$$U_o = \frac{VL}{R_o} \quad (29)$$

Summarizing, the following has been determined

$$V_o = V$$

$$r_o = L$$

$$z_o = R_o$$

$$f_o = R_o$$

$$U_o = \frac{VL}{R_o}$$

$$P_o = \rho V^2$$

These scale factors can now be substituted into the governing equations to obtain the minimum parametric representation of the problem. The results are as follows:

$$\begin{aligned} \text{Re } u^* \frac{\partial u^*}{\partial r^*} + \text{Re } v^* \frac{\partial u^*}{\partial z^*} = -\text{Re} \left(\frac{R_0}{L} \right)^2 \frac{\partial p^*}{\partial r^*} \\ + \left(\frac{R_0}{L} \right)^2 \frac{\partial}{\partial r^*} \left[\frac{1}{r^*} \frac{\partial}{\partial r^*} (r^* u^*) \right] + \frac{\partial^2 v^*}{\partial z^{*2}} \end{aligned} \quad (30)$$

$$\begin{aligned} \text{Re } u^* \frac{\partial v^*}{\partial r^*} + \text{Re } v^* \frac{\partial v^*}{\partial z^*} = -\text{Re} \frac{\partial p^*}{\partial z^*} \\ + \left(\frac{R_0}{L} \right)^2 \frac{1}{r^*} \frac{\partial}{\partial r^*} \left(r^* \frac{\partial v^*}{\partial r^*} \right) + \frac{\partial^2 v^*}{\partial z^{*2}} \end{aligned} \quad (31)$$

where Re is the Reynolds number defined as

$$\text{Re} = \frac{\rho V R_0}{\mu} \quad (32)$$

The equations are now in the form in which it can be determined what the conditions must be such that viscous forces are not significant. The major parameters in this problem are (R_0/L) and Re . Since all the starred or dimensionless terms in equations (30) and (31) are of unit order, only the coefficients of the individual terms need be considered in order to make statements regarding simplifications. Considering equation (30), it can be seen that since $(R_0/L)^2 \ll 1$, both the inertia and pressure forces will be an order of magnitude greater than the viscous forces provided that,

$$\text{Re} \gg 1$$

$$\text{Re} \left(\frac{R_0}{L} \right)^2 \gg 1 \quad (33)$$

From equation (31), since $(R_0/L)^2 \ll 1$, no new information is obtained. The governing equations will be reduced to a simplified form of Euler's equations of motion.

$$u^* \frac{\partial u^*}{\partial r^*} + v^* \frac{\partial u^*}{\partial z^*} = - \left(\frac{R_o}{L} \right)^2 \frac{\partial p^*}{\partial r^*} \quad (34)$$

$$u^* \frac{\partial v^*}{\partial r^*} + v^* \frac{\partial v^*}{\partial z^*} = - \frac{\partial p^*}{\partial z^*} \quad (35)$$

E. Results

Restricting the viscous forces to be at least two orders of magnitude smaller than the inertial or pressure forces, there results

$$Re \geq 100$$

$$Re \left(\frac{R_o}{L} \right)^2 \geq 100 \quad (36)$$

Since (R_o/L) is less than one by definition, the coefficient to consider is the second one in equation (36), since this will be the limiting one. Under the following restrictions,

$$(1) \quad Re \geq 100$$

$$(2) \quad \frac{R_o}{L} < 1 \quad (37)$$

the Euler's equation of motion are obtained. The equation $Re(R_o/L)^2 = 100$ is shown graphically in Figure 4. The line shown in Figure 4 separates the inviscid from the viscous region. A physical understanding of the problem is made clearer by reference to this plot. The higher the incoming jet Reynolds number becomes, the thinner will be the boundary layer at some fixed radial position from the stagnation point. As seen from Figure 4, at lower values of the ratio R_o/L (perhaps obtained by increasing the disk radius L), higher Reynolds numbers are required in order to avoid viscous influence. Finally, within the viscous region, the boundary layer will

grow until a radial length is reached where it becomes equal to the free surface height. The effective design of an experiment is now possible so that the flow can be considered essentially inviscid.

IV. ZERO GRAVITY EXPERIMENTATION

A. Apparatus and Procedure

1. Test facility. - The experimental investigation was conducted in the 2.2-second drop tower. The exact specifications of the facility, the mode of operation, and release and recovery systems are described in detail in Appendix B. The drop tower provides us with a 2.2 second weightless environment in which to conduct the tests.

2. Experiment. - The experiment package used to obtain the data for this study is shown in Figure 5. It consists of an aluminum frame in which were mounted the jet reservoir, disk, a 16 millimeter high speed motion picture camera, supply tank, backlighting scheme, and batteries. The major functions were controlled by on-board sequence timers.

A diagram indicating the manner in which the flow system operates is shown in Figure 6. This is a pressure controlled system in which the flow was initiated by opening the solenoid valve. Prior to the drop, liquid was contained in the line between the liquid supply tank and the jet reservoir. In addition, the jet reservoir was completely filled with the test liquid.

Initially, the object was to employ two-dimensional jets during the experiments. Schach (38), was the only author who investigated two-dimensional jets, although it is impossible to determine how rectangular his jets really were. Several attempts were made to fabricate a two-dimensional nozzle (slot) for use in the zero gravity studies.

Initially, the slots built were quite crude; a rectangular hole cut in a section of plexiglass; a balsa wood jet sealed with epoxy cement. Later, slots were accurately designed in order to achieve the desired flow. The slot length was arbitrarily chosen as 5 centimeters and its width as 0.25 centimeters. Approximately 45° tapers were made to the opening along both the wide and narrow sides. The results of the zero gravity testing were as follows: The jet contracted in the long direction (5 cm) and expanded in the narrow direction (0.25 cm). A tendency to become cylindrical probably due to the effects of surface tension, was observed. A redesigned version of the slot was tested, which employed absolutely no taper in the narrow direction. This also failed to yield a rectangular jet. When these approximate slot jets impinged on various flat plates, the jet diverged radially. In other words, it was impossible to prevent spreading in the lateral direction for an unconstrained surface. Various methods were tried to eliminate this lateral spreading and to force the impingement flow to be completely two-dimensional. The flow was impinged on rectangular plates having the same width as that of the slot, 5 centimeters. The result of these tests was that the liquid simply fell off or went around the plate. A large rectangular plate was used and the region greater in width than 5 centimeters was sprayed with fluorocarbon since distilled water does not wet a fluorocarbon surface. This also failed. All attempts at using a two-dimensional slot jet were subsequently abandoned and axisymmetric jets were pursued.

A schematic drawing of the jet reservoir, which was fabricated out of acrylic plastic, is shown in Figures 7(a) and (b). The critical feature of the jet reservoir is the 45° taper to a circular hole of

diameter D . The range of diameters studied was from 0.5 to 1.5 centimeters. In addition, the transition between the circular hole and conical taper was rounded smooth. The taper prohibits boundary layer buildup and allows the liquid jet to exit from the reservoir with a nearly uniform velocity profile. Based on the experimental results of reference 24, a total angle of 90° is more than sufficient to insure a uniform exiting velocity profile over the range of Reynolds numbers studied.

Sharp-edge disks, also fabricated from acrylic plastic, were mounted above the jet reservoir by means of a threaded rod such that the flat surface of the disk was at right angles to the impinging liquid jet. Sharp-edged disks were employed in the study rather than finite thickness disks in order to develop an analytical model for the flow. As was learned later, the thickness of the disk edge is only of importance for those flows dominated by the effects of surface tension. The diameters, $2L$, of the disks were 2.0 and 3.0 centimeters. A schematic drawing of the disks is shown in Figure 8.

3. Test liquids. - Two test liquids were employed, anhydrous ethanol and trichlorotrifluoroethane. Their properties at 20°C are listed in Table 1. No attempt was made to correct the fluid properties for temperature changes. It is noted that both of these test fluids possess a nearly 0° contact angle on an acrylic plastic surface. However, this was not the reason why they were chosen as test fluids. They were chosen because of their relatively low viscosity and availability.

4. Test procedure. - Prior to a test run, the jet reservoir, disk and supply tanks were cleaned ultrasonically with a mild detergent.

After these parts were rinsed with methanol, they were dried in a warm air dryer. The supply tank was subsequently filled with the test liquid and the jet reservoir was filled by pressurizing the supply tank. This procedure eliminated air bubbles from the lines ensuring accurate flow rates. After the jet reservoir was completely full, the supply tank was sealed and two accumulator bottles (not shown in Fig. 5) were pressurized with gaseous nitrogen to a predetermined value. The accumulator bottles were designed to be of such a volume that no appreciable pressure drop occurred during the drop.

Electrical timers on the experiment package were set to control the initiation and duration of all functions programmed during the drop. The experiment package was then balanced and positioned within the prebalanced drag shield. The wire support was attached to the experiment package through an access hole in the shield (see Fig. B3(a) in Appendix B). Properly sized spikes tips were installed on the drag shield. Then the drag shield, with the experiment package inside, was hoisted to the predrop position at the top of the facility (Fig. B1) and connected to an external electrical power source. The wire support was attached to the release system, and the entire assembly was suspended from the wire. After final electrical checks were made and the experiment package was switched to internal power, the system was released. After completion of the test, the experiment package and drag shield were returned to the preparation area.

B. Experimental Results

1. General considerations. - In addition to the measurement and observation of steady state liquid flow patterns, two separate phenomena were observed. First, no circular hydraulic jump occurred during any

of the tests even though they are a common occurrence under normal gravity conditions. Secondly, the initial impact of the jet upon the solid surface provided another unusual phenomena, that of the rebounding liquid droplet. At high flow rates, the jet broke up prior to impinging upon the disk. The first droplet tended to impinge upon and stick to the disk, spreading as it did. However, the second droplet impinged and rebounded off this wetted surface sometimes into the incoming liquid jet. This provided no serious problem with the attainment of a steady state flow pattern since this all occurred during the transient phase.

The jet generally appeared to go through three phases during the impingement process. The initial phase, including the droplet pinch-off and subsequent impingement, was termed the transient phase. After a certain period of time, a steady state flow pattern was achieved from which the free surface shapes were measured and observations were made. A third phase was reached shortly after the jet had reached its equilibrium configuration. The flow pattern developed an instability. Initially, the instability started from the jet which began to oscillate, and then spread to the plume. Since the time over which the jet and flow pattern appeared stable and smooth was finite, steady state data could be obtained. It was observed that the time before breakdown was inversely proportional to the back pressure during the flow. At 1 psia, for example, the jet remained stable for 1.5 seconds while at 10 psi, it was stable for approximately 0.4 seconds. An attempt was made to lengthen the time over which stability occurred by packing the nozzle chamber with steel wool. This appeared to be effective in improving the overall stability but had the negative

effect of introducing a low level perturbation throughout the test and, thus, was not employed during any of the experiments.

2. Effect of nozzle height. - Several tests were conducted initially to determine the effect of H , the distance between the nozzle and the disk, on the experimental flow pattern. It was determined that there is no effect on the liquid flow provided that the ratio of the nozzle height H to the jet diameter is greater than 3. As a result, all zero gravity experiments were conducted in order to eliminate this effect. This fact, which was determined experimentally, supports the argument made in Section III, Order of Magnitude Analysis, concerning the assertion that H could not be a scale factor for the axial coordinate.

3. Steady state flow patterns. - The approximate steady state flows for three different jet velocities are shown photographically in Figure 9. The direction of flow of the liquid jet is vertically upwards. The threaded rod and bolt observed in the film clips is the disk holder which connects the sharp-edged disk assembly to the rig frame. The jet velocity increases from left to right in the figure. Three distinct classifications of flow patterns were observed to occur and are shown labeled in Figure 9 as surface tension flow, transition flow, and inertia flow. Surface tension flow (Fig. 9(a)) is defined as that flow in which the liquid flows completely around the disk with no separation occurring from the disk edge. In transition flow (Fig. 9(b)), surface tension and inertia forces are both important. Transition flow is defined as flow in which separation occurs from the disk and the resulting liquid sheet either collects upon itself forming an envelope or has the tendency to do so. Inertia flow (Fig. 9(c))

is defined as that flow in which the liquid separates from the disk with no liquid turning towards the jet centerline attempting to form an envelope. The flow pattern shown for transition flow is not really the steady state flow pattern one would expect if steady state conditions could have been reached. The reason for this is as follows: Some liquid is always traveling toward the disk from the point at which the envelope meets. This liquid flow strikes the back of the baffle and subsequently disrupts the initially formed envelope. The recirculation flow then is a strong function of the geometry of the disk holder, an uncontrollable parameter. This important distinction means that an analysis for free surface shapes would have to account for the geometry of the disk holder in the transition region. The surface tension flow is generally slow and, as a result, does not quite reach a steady state configuration on the back side of the disk. The inertia flow tests (represented by Fig. 9(c)) always reached steady state.

The experimental tests were conducted in the inviscid region of Figure 4. Depending on the particular ratio of (R_0/L) , there exists a minimum Reynolds number below which the runs can no longer be considered as viscous-free. The experimental results are listed in tabular form in Table 2 in which all the important parameters as well as the flow classifications are contained. One additional parameter, the Weber number, is listed in Table 1. As will be shown in the next section, when the Reynolds number is no longer a parameter to consider for flow classifications, the Weber number and ratio (R_0/L) remain. The Weber number $\rho V^2 R_0 / \sigma$, is basically the ratio of inertia to surface tension forces. In the flow category column, S indicates

surface tension flow, T indicates transition flow, and I is inertia flow. Finally, it is noted that the designated flow classification for some cases, particularly those bordering transition or inertia flow, could easily fit into either category.

4. Zero gravity results. - The data contained in Table 2 is shown graphically in Figure 10. The lines indicated in the figure were faired in by hand and separate the various flow classifications. It is observed that at any particular value of the ratio (R_o/L), the flow classification is dependent only on the system Weber number. Two critical Weber numbers occur at a constant value of (R_o/L). The lowest critical Weber number separates the surface tension flow from the transition flow while the higher critical Weber number separates the transition flow from the inertia flow. In addition, the critical Weber number between regimes was found to decrease as (R_o/L) was increased.

V. POTENTIAL FORMULATION

A. Governing Equations and Boundary Conditions in Physical Plane Including Surface Tension

In Section III, Order of Magnitude Analysis, it was shown that at any particular value of R_0/L if $Re > Re_{cr}$ the flow in the region of the disk can be considered as viscous free. It is further assumed that the jet will continue to remain viscous free after leaving the disk. There will be no shear stress between the exiting radial jet and the ambient air surrounding it.

1. General formulation. - Consider the flow of a circular liquid jet impinging normally on a circular disk as shown in Figure 11. R_0 is the jet radius, L is the disk radius, and H is the distance between the jet reservoir and the disk. The incoming jet velocity is given as V and the initial velocity profile is assumed to be uniform. There will be two free surfaces involved. The upper free surface is defined as $z_s = f_1(r)$ and the lower surface as $z_s = f_2(r)$. In addition, a third surface is required for the complete formulation of the boundary value problem. Initially, this surface was chosen as the straight line FE shown in Figure 11. However, this proved to be inconvenient since FE is arbitrary and, thus, has no known boundary condition. It was found convenient to instead choose the surface $z = f_3(r)$ to be a surface along which the velocity potential is constant. Various points in the physical plane have been designated with letters ranging from A to G for convenience. In cylindrical coordinates, the governing

equations and boundary conditions in terms of primary variables (u,v)

are given as follows:

Continuity:

$$\frac{1}{r} \frac{\partial}{\partial r} (ru) + \frac{\partial v}{\partial z} = 0 \quad (38)$$

Momentum:

r Component:

$$\rho \left(u \frac{\partial u}{\partial r} + v \frac{\partial u}{\partial z} \right) = - \frac{\partial p}{\partial r} \quad (39)$$

z Component:

$$\rho \left(u \frac{\partial v}{\partial r} + v \frac{\partial v}{\partial z} \right) = - \frac{\partial p}{\partial z} \quad (40)$$

The following boundary conditions are applied,

On DC

$$v = 0 \quad \text{on } z = 0, 0 \leq r \leq L \quad (41)$$

On AB

$$u = 0 \quad 0 \leq r \leq R_0, z = H \quad (42)$$

On BC

$$\frac{\partial v}{\partial r} = 0 \quad r = 0, 0 < z \leq H \quad (43)$$

On AG

$$\frac{1}{2} (u^2 + v^2) - \frac{\sigma}{\rho r} \frac{d}{dr} \left(\frac{rf_1'}{\sqrt{1+f_1'^2}} \right) = \frac{1}{2} v^2 - \frac{\sigma}{\rho R_0} \quad \text{on } z_s = f_1(r) \quad (44)$$

And

$$-uf_1' + v = 0 \quad \text{on } z_s = f_1(r) \quad (45)$$

On DE

$$\frac{1}{2} (u^2 + v^2) - \frac{\sigma}{\rho r} \frac{d}{dr} \left(\frac{rf_2'}{\sqrt{1+f_2'^2}} \right) = \frac{1}{2} v^2 - \frac{\sigma}{\rho R_0} \quad \text{on } z_s = f_2(r) \quad (46)$$

And

$$-uf_2' + v = 0 \quad \text{on } z_g = f_2(r) \quad (47)$$

On GE

$$u + vf_3'(r) = 0 \quad \text{on } z = f_3(r) \quad (48)$$

The derivation for the boundary condition along GE is as follows. Along GE, the velocity potential ϕ is constant. By definition, the velocity vector \vec{V} is normal to an equipotential surface.

This means that

$$\vec{V} \times \hat{n} = 0 \quad \text{on } z = f_3(r) \quad (49)$$

The unit normal to $f_3(r)$ is

$$\hat{n} = \frac{-f_3' \hat{i} + \hat{j}}{\sqrt{f_3'^2 + 1}} \quad (50)$$

where \hat{i} is the unit vector in the radial direction and \hat{j} is the unit vector in the axial direction, and

$$\vec{V} = u\hat{i} + v\hat{j} \quad (51)$$

Application of equation (49) results in

$$\frac{u + vf_3'(r)}{\sqrt{f_3'^2 + 1}} = 0 \quad (52)$$

From which equation (48) follows.

2. Introduction of Stokes Stream Function. - The primary variables contained in the governing equations are the scalar velocity components u and v . The fact that two functions are required to describe one vector field is cumbersome. As shown in the theory of hydrodynamics, the number of functions can be reduced for several important cases, one of these being axisymmetric flow. A function ψ , defined as Stokes stream function, can be introduced which automatically satisfies

the continuity equation. With the additional requirement of irrotationality, the governing equation in terms of Stokes stream function will result. According to Chan (7), Stokes stream function is a mathematical device used to describe the flow and has the following properties. First, when the stream function is set equal to a constant, it results in different annular stream surfaces in axisymmetric flow. Secondly, when it is differentiated properly, it yields the velocity components. Thirdly, taking the difference between the values at two adjacent stream surfaces yields the flow rate.

Starting with equation (38), the continuity equation for axisymmetric flow, a guess is made at what u and v are in order to satisfy continuity identically. Assume

$$u = -\frac{1}{r} \frac{\partial \psi}{\partial z} \quad (53)$$

And

$$v = \frac{1}{r} \frac{\partial \psi}{\partial r} \quad (54)$$

Substitution of equations (53) and (54) into equation (38) shows that continuity is identically satisfied by these two guesses. In addition, the assumption is made that the flow is also irrotational. As a result

$$\text{Curl } \vec{V} = 0 \quad (55)$$

For axisymmetric flow, this can be written,

$$\frac{\partial u}{\partial z} - \frac{\partial v}{\partial r} = 0 \quad (56)$$

Replacing u and v in the above by their relationships to ψ results in the governing equation for axisymmetric flow in terms of Stokes stream function

$$\frac{\partial^2 \psi}{\partial z^2} - \frac{1}{r} \frac{\partial \psi}{\partial r} + \frac{\partial^2 \psi}{\partial r^2} = 0 \quad (57)$$

3. Derivation of boundary conditions in terms of ψ . - Since BC, CD, and DE are all a part of the same streamline, they must all have the same value for Stokes stream function. Let us arbitrarily set that value equal to zero. The value of ψ along AB and AG can be calculated from equation (54).

On AB

$$-v = \frac{1}{r} \frac{\partial \psi}{\partial r} \quad (58)$$

Integrating this yields

$$\psi = -\frac{Vr^2}{2} \quad (59)$$

On AG since AG is a line of constant ψ ,

$$\psi = -\frac{VR_o^2}{2} \quad (60)$$

In addition, equation (44) applies. Substitution of equation (53) and (54) into (44) yields

$$\frac{1}{2r^2} \left[\left(\frac{\partial \psi}{\partial z} \right)^2 + \left(\frac{\partial \psi}{\partial r} \right)^2 \right] - \frac{\sigma}{\rho r} \frac{d}{dr} \left(\frac{rf_1'}{\sqrt{1+f_1'^2}} \right) = \frac{1}{2} v^2 - \frac{\sigma}{\rho R_o} \quad \text{on } z_s = f_1(r) \quad (61)$$

On DE

$$\frac{1}{2r^2} \left[\left(\frac{\partial \psi}{\partial z} \right)^2 + \left(\frac{\partial \psi}{\partial r} \right)^2 \right] - \frac{\sigma}{\rho r} \frac{d}{dr} \left(\frac{rf_2'}{\sqrt{1+f_2'^2}} \right) = \frac{1}{2} v^2 - \frac{\sigma}{\rho R_o} \quad \text{on } z_s = f_2(r) \quad (62)$$

It is noted that the second boundary conditions on the free surfaces, namely $-uf_1' + v = 0$ and $-uf_2' + v = 0$, are fully equivalent to the specification of the value of Stokes stream function along that

surface. Since $\psi = \psi(r, z)$, it can be expanded and $d\psi$ set equal to zero along AG and ED.

On GE, equation (48) becomes

$$-\frac{\partial\psi}{\partial z} + \frac{\partial\psi}{\partial r} f_3'(r) = 0 \quad \text{on } z = f_3(r) \quad (63)$$

4. Nondimensionalization of governing equations and boundary conditions in physical plane. - The governing equation in terms of Stokes stream function (eq. (57)) and the boundary conditions (eqs. (58) to (63)) are now put into dimensionless form by introducing arbitrary scale factors. Let the scale factor for the stream function be $-VR_0^2$. Let dimensionless quantities be represented by stars, i.e., ψ^* is dimensionless. The results of this manipulation are shown in Figure 12. Three parameters appear in the specification of boundary conditions. They include the Weber number, We , and the dimensionless length ratios L/R_0 and H/R_0 . Recalling the arguments in the Order of Magnitude Analysis section, H/R_0 is not really a parameter provided it is larger than some minimum value. The dimensionless velocity components can be calculated from the following expressions

$$\frac{u}{V} = \frac{1}{r^*} \frac{\partial\psi^*}{\partial z^*} \quad (64)$$

$$\frac{v}{V} = -\frac{1}{r^*} \frac{\partial\psi^*}{\partial r^*} \quad (65)$$

The procedure for solution of the boundary value problem as set up in dimensionless form in the physical plane (Fig. 12) would be as follows: Initially, realistic variations for $f_1^*(r)$, $f_2^*(r)$, and $f_3^*(r)$ are assumed. Using only one of the two given boundary conditions on AG and GE (i.e., $\psi^* = 1/2$ and $\psi^* = 0$) solve for ψ^* using finite difference methods. With the initial solution for ψ^* check the va-

lidity of the second of the two boundary conditions on AG and GE. If the boundary conditions are not satisfied, new variations in f_1^* , f_2^* , and f_3^* must be assumed. A second iteration to ψ^* must be obtained and so on. One of the serious drawbacks of this outlined iteration scheme is the lack of knowledge concerning how to update assumed values of f_1^* , f_2^* , and f_3^* based on previous solutions. In other words, there is no logical way in which to make changes to the shape of the initially assumed control volume.

5. Surface tension dominated model. - For Weber numbers between 5 and 30 (depending on the ratio R_0/L), experimental data shows that the resulting steady-state flow pattern is surface tension dominated (see Fig. 9(a)). By previous definition, surface tension flow is defined as that flow in which the liquid flows completely around the disk with no separation from the edge. It is the intent to model this flow in order to solve for the theoretical free surface shapes and velocity profiles. Assuming axisymmetry, the physical plane model is shown in Figure 13. In the model, at some cross-section far downstream, the flow is assumed to approach the initially uniform flow it possessed at AB. The exiting plane is denoted by GE in the model. C and C' are both located at $r = 0$, $z = 0$. C is located on top of the plate while C' is on the bottom. The free surface $f_1(r)$, is not assumed to possess mirror symmetry about the $z = 0$ position. In cylindrical coordinates, the governing equations and boundary conditions in terms of the primary variables (u,v) are given as follows:
Continuity:

$$\frac{1}{r} \frac{\partial}{\partial r} (ru) + \frac{\partial v}{\partial z} = 0 \quad (66)$$

Momentum:

r Component

$$\rho \left(u \frac{\partial u}{\partial r} + v \frac{\partial u}{\partial z} \right) = - \frac{\partial p}{\partial r} \quad (67)$$

z Component

$$\rho \left(u \frac{\partial v}{\partial r} + v \frac{\partial v}{\partial z} \right) = - \frac{\partial p}{\partial z} \quad (68)$$

The following boundary conditions are applied

On DC

$$v = 0 \quad \text{on } z = 0, 0 \leq r \leq L \quad (69)$$

On DC'

$$v = 0 \quad \text{on } z = 0, 0 \leq r \leq L \quad (70)$$

On AB

$$u = 0 \quad 0 \leq r \leq R_0, z = H \quad (71)$$

On BC

$$\frac{\partial v}{\partial r} = 0 \quad \text{on } r = 0, 0 < z \leq H \quad (72)$$

On C'E

$$\frac{\partial v}{\partial r} = 0 \quad \text{on } r = 0, -H \leq z < 0 \quad (73)$$

On GE

$$u = 0 \quad 0 \leq r \leq R_0, z = -H \quad (74)$$

On AG

$$\frac{1}{2} (u^2 + v^2) - \frac{\sigma}{\rho r} \frac{d}{dr} \left(\frac{r f_1'}{\sqrt{1 + f_1'^2}} \right) = \frac{1}{2} v^2 - \frac{\sigma}{\rho R_0} \quad \text{on } z_s = f_1(r) \quad (75)$$

and

$$-u f_1' + v = 0 \quad \text{on } z_s = f_1(r) \quad (76)$$

Equations (75) and (76) represent two distinct pieces of information concerning $z_s = f_1(r)$. It is noted that f_1' can be eliminated from

the set of equations by means of simple substitution. This fact will have implications later in the development leading to a major simplification. The following expression would result,

$$\frac{1}{2} (u^2 + v^2) - \frac{\sigma}{\rho r} \frac{d}{dr} \left(\frac{r}{\sqrt{\frac{u^2}{v^2} + 1}} \right) = \frac{1}{2} v^2 - \frac{\sigma}{\rho R_0} \quad \text{on } z_s = f_1(r) \quad (77)$$

Direct substitution of equations (53) and (54), the relations between the velocity components and Stokes stream function, into the governing equation and boundary conditions for the surface tension model results in the formulation shown in Figure 14 after nondimensionalization.

Similar to the general formulation in the last section, the various lengths in the problem are scaled with respect to R_0 and the scale factor for Stokes stream function is $-VR_0^2$.

B. Inverse Plane Formulations

The procedure for solving for the free surface shapes in the physical plane has been outlined previously. The difficulties encountered when making adjustments to the free surfaces between iterations and the lack of a logical manner in which to make the adjustments have been cited. This would be a time consuming task even in the absence of surface tension. A computerized scheme is sought which offers the possibility of achieving the free-surface results with a minimum of computer iteration time and user interaction.

1. Transformation formulas. - An alternate approach to the physical plane solution is discussed in detail by Jeppson (19). In his article, Jeppson discusses a transformation technique into what is defined as the inverse plane. The coordinate axes in the inverse plane are the velocity potential ϕ and Stokes stream function ψ . The ad-

vantage to using the $\phi\psi$ space, or inverse plane, is that the free surface lies along a line of constant ψ and is, therefore, at a known position. Of course, one must pay the price for knowing the position of the free surface. As will be shown shortly, the governing equation is no longer linear as it was in the physical plane.

2. Introduction of velocity potential. - The use of a scalar function defined as the velocity potential has been used previously in the specification of the boundary GE (the exiting plane). The continuity equation for steady incompressible axisymmetric flow is given by equation (38). The flow is also assumed to be irrotational such that the condition given by equation (56) is also valid. Equation (56) implies that there exists a scalar potential function ϕ such that

$$\vec{V} = \text{grad } \phi \quad (78)$$

from which it follows

$$u = \frac{\partial \phi}{\partial r} \quad (79)$$

and

$$v = \frac{\partial \phi}{\partial z} \quad (80)$$

Substitution of equations (79) and (80) yields the governing equation for steady axisymmetric flow in terms of the velocity potential

$$\frac{\partial^2 \phi}{\partial z^2} + \frac{1}{r} \frac{\partial \phi}{\partial r} + \frac{\partial^2 \phi}{\partial r^2} = 0 \quad (81)$$

3. Relationship between ψ and ϕ . - It can now be stated that the relationships between the velocity potential and Stokes's stream function are given as:

$$u = \frac{\partial \phi}{\partial r} = -\frac{1}{r} \frac{\partial \psi}{\partial z} \quad (82)$$

and

$$v = \frac{\partial \phi}{\partial z} = \frac{1}{r} \frac{\partial \psi}{\partial r} \quad (83)$$

4. Inverse plane formulation. - In order to formulate the problem in the physical plane, r and z must be known as functions of ψ and ϕ . In other words, we are attempting to reverse the roles of the dependent and independent variables in the inverse plane. The required relationships are obtained noting that if $\psi = \psi(r, z)$ and $\phi = \phi(r, z)$, then there exist inverse functions $r = r(\phi, \psi)$ and $z = z(\phi, \psi)$ as shown in reference 13 such that

$$\frac{\partial r}{\partial \phi} = - \frac{1}{J} \frac{\partial \psi}{\partial z} \quad (84)$$

$$\frac{\partial z}{\partial \psi} = - \frac{1}{J} \frac{\partial \phi}{\partial r} \quad (85)$$

$$\frac{\partial z}{\partial \phi} = \frac{1}{J} \frac{\partial \psi}{\partial r} \quad (86)$$

$$\frac{\partial r}{\partial \psi} = \frac{1}{J} \frac{\partial \phi}{\partial z} \quad (87)$$

and where the Jacobian J is defined as

$$J = \begin{vmatrix} \frac{\partial \phi}{\partial r} & \frac{\partial \phi}{\partial z} \\ \frac{\partial \psi}{\partial r} & \frac{\partial \psi}{\partial z} \end{vmatrix} = \left(\frac{\partial \phi}{\partial r} \right) \left(\frac{\partial \psi}{\partial z} \right) - \left(\frac{\partial \phi}{\partial z} \right) \left(\frac{\partial \psi}{\partial r} \right) \quad (88)$$

From the above set of equations follow two important relations. Substituting into equation (82) the values of $\partial \phi / \partial r$ and $\partial \psi / \partial z$ obtained from equations (84) and (85) yields

$$\frac{\partial z}{\partial \psi} = - \frac{1}{r} \frac{\partial r}{\partial \phi} \quad (89)$$

Similarly, substitution of the values of $\partial \phi / \partial z$ and $\partial \psi / \partial r$ from equations (86) and (87) into equation (83) yields

$$\frac{\partial r}{\partial \psi} = \frac{1}{r} \frac{\partial z}{\partial \phi} \quad (90)$$

For subsequent relations, it is necessary to express the Jacobian in terms of the inverse function $r(\psi, \phi)$ and $z(\psi, \phi)$. Substituting equations (84) to (87) into equation (88) results in

$$J = J^2 \left[\left(\frac{\partial z}{\partial \psi} \right) \left(\frac{\partial r}{\partial \phi} \right) - \left(\frac{\partial r}{\partial \psi} \right) \left(\frac{\partial z}{\partial \phi} \right) \right] \quad (91)$$

Now, using equations (89) and (90) in the above yields,

$$J = - \frac{1}{r \left[\left(\frac{\partial z}{\partial \psi} \right)^2 + \left(\frac{\partial r}{\partial \psi} \right)^2 \right]} = - \frac{r}{\left(\frac{\partial r}{\partial \phi} \right)^2 + \left(\frac{\partial z}{\partial \phi} \right)^2} \quad (92)$$

5. Governing equations for inverse functions. - Differentiating equation (89) with respect to ψ yields

$$\frac{\partial^2 z}{\partial \psi^2} = - \frac{1}{r} \frac{\partial^2 r}{\partial \psi \partial \phi} + \frac{1}{r^2} \frac{\partial r}{\partial \psi} \frac{\partial r}{\partial \phi} \quad (93)$$

and combining this with the derivatives of equation (90) with respect to ϕ , which is

$$\frac{\partial^2 r}{\partial \phi \partial \psi} = - \frac{1}{r^2} \left(\frac{\partial r}{\partial \phi} \right) \left(\frac{\partial z}{\partial \phi} \right) + \frac{1}{r} \frac{\partial^2 z}{\partial \phi^2} \quad (94)$$

it is found that

$$\frac{\partial^2 z}{\partial \psi^2} = \frac{1}{r^3} \frac{\partial r}{\partial \phi} \frac{\partial z}{\partial \phi} - \frac{1}{r^2} \frac{\partial^2 z}{\partial \phi^2} + \frac{1}{r^2} \frac{\partial r}{\partial \phi} \frac{\partial r}{\partial \psi} \quad (95)$$

By using equations (89) and (90), the terms involving derivatives in equation (95) can be expressed entirely in terms of z , giving the important equation,

$$r^2 \frac{\partial^2 z}{\partial \psi^2} + \frac{\partial^2 z}{\partial \phi^2} = -2 \frac{\partial z}{\partial \psi} \frac{\partial z}{\partial \phi} \quad (96)$$

On the other hand, differentiating equation (89) with respect to ϕ and equation (90) with respect to ψ and combining the result leads to the equation

$$\frac{\partial^2 r}{\partial \psi^2} = -\frac{1}{r^2} \frac{\partial^2 r}{\partial \phi^2} + \frac{1}{r^3} \left(\frac{\partial r}{\partial \phi} \right)^2 - \frac{1}{r^2} \frac{\partial r}{\partial \psi} \frac{\partial z}{\partial \phi} \quad (97)$$

By substitution for $\partial z / \partial \phi$ from equation (90), the following equation for $r(\phi, \psi)$ is obtained:

$$\frac{\partial^2 r}{\partial \psi^2} + \frac{1}{r^2} \frac{\partial^2 r}{\partial \phi^2} - \frac{1}{r^3} \left(\frac{\partial r}{\partial \phi} \right)^2 + \frac{1}{r} \left(\frac{\partial r}{\partial \psi} \right)^2 = 0 \quad (98)$$

For further discussion, equation (96) will be referred to as the z equation while equation (98) will be called the r equation. Both of these equations are nonlinear with the nonlinearity in the z equation also involving r . It is further noted that both of these equations are of the elliptic type, as shown in reference 19. This means that boundary conditions are required for all boundaries in the flow region. Since the r equation (eq. (98)) only involves that variable, a solution to the problem begins with its solution.

One final point involves the fact that the variables discussed in the above inverse transformations are all dimensional. It is noted that nondimensionalization of the above equations similar to the nondimensionalization done in the physical plane allows us to recover the same equation.

Let

$$\left. \begin{aligned} z^* &= \frac{z}{z_0} & \text{where } z_0 &= R_0 \\ r^* &= \frac{r}{r_0} & \text{where } r_0 &= R_0 \\ \psi^* &= \frac{\psi}{\psi_0} & \text{where } \psi_0 &= -VR_0^2 \\ \phi^* &= \frac{\phi}{\phi_0} & \text{where } \phi_0 &= -VR_0 \end{aligned} \right\} \quad (99)$$

The results of this substitution yields exactly the same governing equations and transformation formulas in starred notation. In other words,

$$r^{*2} \frac{\partial^2 z^*}{\partial \psi^{*2}} + \frac{\partial^2 z^*}{\partial \phi^{*2}} = -2 \frac{\partial z^*}{\partial \psi^*} \frac{\partial z^*}{\partial \phi^*} \quad (100a)$$

and

$$\frac{\partial^2 r^*}{\partial \psi^{*2}} + \frac{1}{r^{*2}} \frac{\partial^2 r^*}{\partial \phi^{*2}} - \frac{1}{r^{*3}} \left(\frac{\partial r^*}{\partial \phi^*} \right)^2 + \frac{1}{r^*} \left(\frac{\partial r^*}{\partial \psi^*} \right)^2 = 0 \quad (100b)$$

6. Infinite flat plate excluding surface tension. - The first problem to be examined in which we employ the inverse transformation is the flow of a circular liquid jet normal to a flat plate. At this point, we drop the starred notation to designate dimensionless quantities. It is assumed that all quantities appearing henceforth are dimensionless unless otherwise stated (i.e., r , z , ψ , ϕ , are now dimensionless). For the case in which surface tension is excluded, the physical plane model depicted in Figure 12 must necessarily change. The model in Figure 12 is for the general case of a finite disk in which surface tension effects are important. For the case of an infinite flat plate, since the free surface ED no longer exists, the designation D does not appear in the model. Furthermore, for the case in which surface tension forces are unimportant, the boundary condition along the upper surface (referring to Fig. 12) can be written as follows:

On AG

$$\frac{1}{r^2} \left[\left(\frac{\partial \psi}{\partial z} \right)^2 + \left(\frac{\partial \psi}{\partial r} \right)^2 \right] = 1 \quad (101)$$

This expression is obtained by allowing the Weber number to approach

infinity. The reasoning for letting the Weber number become large is because it is the ratio of inertial to surface tension forces. The case we are examining is one in which the surface tension forces become vanishingly small or the inertial forces becoming large. Finally, the boundary GE will be nearly vertical implying that the velocity there is purely radial.

7. Derivation of boundary conditions in inverse plane for r
formulation. -

On AB

$$\left. \begin{array}{l} \text{In the physical plane, } \psi = \frac{1}{2} r^2 \\ \text{In the inverse plane, } r = \sqrt{2\psi} \end{array} \right\} \quad (102)$$

On BC

$$\left. \begin{array}{l} \text{In the physical plane, } \psi = 0 \\ \text{In the inverse plane, } r = 0 \end{array} \right\} \quad (103)$$

On EC

$$\left. \begin{array}{l} \text{In the physical plane, } \psi = 0 \\ \text{Also } v = 0, \text{ by equation (83) this implies that } \frac{\partial \phi}{\partial z} \text{ and } \\ \frac{\partial \psi}{\partial r} = 0. \\ \text{In the inverse plane (via eq. (87)), } \frac{\partial r}{\partial \psi} = 0 \end{array} \right\} \quad (104)$$

On GE

$$\left. \begin{array}{l} \text{In the physical plane, } \frac{\partial \psi}{\partial r} = 0 \\ \text{In the inverse plane, } \frac{\partial r}{\partial \psi} = 0 \end{array} \right\} \quad (105)$$

On AG

$$\text{In the physical plane, } \frac{1}{r^2} \left[\left(\frac{\partial \psi}{\partial z} \right)^2 + \left(\frac{\partial \psi}{\partial r} \right)^2 \right] = 1$$

In the inverse plane, using equations (82) and (83), this becomes

$$\left(\frac{\partial \phi}{\partial r}\right)^2 + \left(\frac{\partial \phi}{\partial z}\right)^2 = 1$$

and upon using relations (85) and (87)

$$J^2 \left[\left(\frac{\partial z}{\partial \psi}\right)^2 + \left(\frac{\partial r}{\partial \psi}\right)^2 \right] = 1$$

Substituting in for J^2 from equation (92) and then using (89) and (90) yields the final form

$$\left(\frac{\partial r}{\partial \phi}\right)^2 + r^2 \left(\frac{\partial r}{\partial \psi}\right)^2 = 1 \quad (106)$$

The results of the above calculations are shown in Figure 15(a) in the inverse plane. For the case of flow normal to an infinite flat plate, the r values can now be completely found once we solve the nonlinear governing equation. The variable z does not appear anywhere in the formulation. In addition, the boundary conditions for the z formulation were also derived and are indicated in Figure 15(b). It follows that the z solution cannot be obtained until after r values are known since the r values are required on the free surface boundary and within the interior flow. The boundary conditions for the z formulation were derived as follows:

8. Derivation of boundary conditions in inverse plane for z formulation. -

On AB

In the physical plane, $u = 0$ which implies $\frac{\partial \phi}{\partial r} = 0$

From equation (85), $\frac{\partial z}{\partial \psi} = 0$

This implies that $z = z(\phi)$ alone and since

AB is a line of constant ϕ ,
in the inverse plane $z = \text{constant}$

(107)

On BC

$$\left. \begin{array}{l} \text{In physical plane, } u = 0 \\ \text{From which it follows, in the inverse plane } \frac{\partial z}{\partial \psi} = 0 \end{array} \right\} \quad (108)$$

On EC

$$\left. \begin{array}{l} \text{In physical plane } \psi = 0 \\ \text{In inverse plane } z = 0 \end{array} \right\} \quad (109)$$

On GE

$$\left. \begin{array}{l} \text{In physical plane, } v = 0 \\ \text{From equation (83), it follows that } \frac{\partial \psi}{\partial r} = 0 \\ \text{and from equation (86), we have in the inverse plane } \frac{\partial z}{\partial \phi} = 0 \end{array} \right\} \quad (110)$$

On AG

$$\left. \begin{array}{l} \text{In the physical plane } \frac{1}{r^2} \left[\left(\frac{\partial \psi}{\partial z} \right)^2 + \left(\frac{\partial \psi}{\partial r} \right)^2 \right] = 1 \\ \text{In the inverse plane we can take over the equivalent ex-} \\ \text{pression given by equation (106) } \left(\frac{\partial r}{\partial \phi} \right)^2 + r^2 \left(\frac{\partial r}{\partial \psi} \right)^2 = 1 \\ \text{Using equations (89) and (90) to eliminate the derivative} \\ \text{involving } r \text{ results in } r^2 \left(\frac{\partial z}{\partial \psi} \right)^2 + \left(\frac{\partial z}{\partial \phi} \right)^2 = 1 \end{array} \right\} \quad (111)$$

9. Finite plate excluding surface tension. - A second problem to be formulated is concerned with the impingement of a circular liquid jet normal to a disk of finite width. For the case in which surface tension effects are neglected, the model depicted in Figure 12 will vary only slightly. The only difference being that the boundary conditions along the top and bottom free surfaces are now expressed as

$$\frac{1}{r^2} \left[\left(\frac{\partial \psi}{\partial z} \right)^2 + \left(\frac{\partial \psi}{\partial r} \right)^2 \right] = 1$$

The r formulation in the inverse plane is shown in Figure 16(a). The only boundary condition that bears some explanation is that along GE, the exiting plane in the physical plane, from Figure 12,

$$\frac{\partial \psi}{\partial z} - \frac{\partial \psi}{\partial r} f_3' = 0 \quad (112)$$

Using equations (84) and (86) this can be written

$$\frac{\partial r}{\partial \phi} + \frac{\partial z}{\partial \phi} f_3' = 0 \quad (113)$$

Finally, using equation (90) to eliminate $\partial z / \partial \phi$,

$$\frac{\partial r}{\partial \phi} + r \frac{\partial r}{\partial \psi} f_3' = 0 \quad (114)$$

or

$$\frac{\partial r}{\partial \phi} + r \left(\frac{\partial r}{\partial \psi} \right) \left(\frac{dz}{dr} \right) = 0 \quad (115)$$

The z formulation in the inverse plane is shown in Figure 16(b). Here again, only the boundary condition along GE bears some explanation. Continuing with equation (115) and using equations (89) and (90) we obtain

$$r \left(\frac{\partial z}{\partial \psi} \right) - \left(\frac{\partial z}{\partial \phi} \right) \left(\frac{dz}{dr} \right) = 0 \quad (116)$$

The formulation of the problem of flow of a circular liquid jet normal to a finite disk in the inverse plane is now complete. The r solution (Fig. 16(a)) can no longer be obtained independent of the z solution due to the exiting jet boundary condition. Thus, the problem will necessitate a simultaneous solution of two partial differential equations of the nonlinear elliptic type.

10. Finite plate including surface tension. - A third problem that is formulated but not solved due to the complexity of applying it to a

real system involves the normal impingement to a finite disk in which both surface tension and inertial forces are important. These would include all the flows experimentally labeled as transition flows. This represents a complete inverse formulation for the exact physical model represented in Figure 12. The results of the inverse formulation for the r solution are shown in Figure 17. The way in which the inverse boundary conditions along the free surface were derived will be made more clear in the next section.

11. Surface tension dominated model - finite plate. - The final problem to be examined involves the surface tension dominated flow, described in Figure 14. The inverse plane formulation for the r solution is indicated in Figure 18(a). The boundary conditions are the same as derived previously with the exception of the free surface boundary. Along AG in the physical plane,

$$\frac{1}{2r^2} \left[\left(\frac{\partial \psi}{\partial z} \right)^2 + \left(\frac{\partial \psi}{\partial r} \right)^2 \right] - \frac{1}{We} \frac{1}{r} \frac{d}{dr} \left[\frac{r}{\sqrt{\left(\frac{\partial \psi}{\partial z} \right)^2 + 1}} \right] = \frac{1}{2} - \frac{1}{We} \quad (117)$$

In the derivation of equation (106), it was shown that

$$\frac{1}{r^2} \left[\left(\frac{\partial \psi}{\partial z} \right)^2 + \left(\frac{\partial \psi}{\partial r} \right)^2 \right] = \frac{1}{\left(\frac{\partial r}{\partial \phi} \right)^2 + r^2 \left(\frac{\partial r}{\partial \psi} \right)^2} \quad (118)$$

In addition, using equations (84) and (86),

$$\left(\frac{\frac{\partial \psi}{\partial z}}{\frac{\partial \psi}{\partial r}} \right)^2 = \frac{1}{r^2} \left(\frac{\frac{\partial r}{\partial \phi}}{\frac{\partial r}{\partial \psi}} \right)^2 \quad (119)$$

Therefore, the inverse boundary condition along AG becomes

$$\frac{1}{2} \frac{1}{\left(\frac{\partial r}{\partial \phi}\right)^2 + r^2 \left(\frac{\partial r}{\partial \psi}\right)^2} - \frac{1}{We} \frac{1}{r} \frac{d}{dr} \left[\frac{r}{\sqrt{\frac{1}{r^2} \left(\frac{\partial r}{\partial \phi}\right)^2 + 1}} \right] = \frac{1}{2} - \frac{1}{We} \quad (120)$$

which can be written

$$\frac{1}{2} \frac{1}{\left(\frac{\partial r}{\partial \phi}\right)^2 + r^2 \left(\frac{\partial r}{\partial \psi}\right)^2} - \frac{1}{We} \frac{1}{r} \frac{d}{dr} \left[\frac{r^2}{\sqrt{\left(\frac{\partial r}{\partial \phi}\right)^2 + r^2}} \right] = \frac{1}{2} - \frac{1}{We} \quad (121)$$

Multiplying through by 2, and rearranging yields,

$$\left(\frac{\partial r}{\partial \phi}\right)^2 + r^2 \left(\frac{\partial r}{\partial \psi}\right)^2 = \frac{1}{\left\{ 1 - \frac{2}{We} + \frac{2}{We} \frac{1}{r} \frac{d}{dr} \left[\frac{r^2}{\sqrt{\left(\frac{\partial r}{\partial \phi}\right)^2 + r^2}} \right] \right\}} \quad (122)$$

There has been no symmetry assumed for the r formulation, only axisymmetry. It is noted that the r formulation does not involve the variable z . This means that the r and z solutions can be obtained independently. The z formulation is indicated in Figure 18(b).

VI. CENTRAL FINITE DIFFERENCE REPRESENTATION

The finite difference operators for the nonlinear r and z elliptic partial differential equations resulting from the inversion were put into difference form. It was found from experience that considerable flexibility resulted if the difference equations were derived employing rectangular mesh. The reason for this becomes clearer as we progress into the numerical solution. Suffice to say that this allowed us to control the size of the flow region. Square meshes were originally attempted, but only led to solutions in the cases where the mesh sizes became vanishingly small.

A. Formulation

1. General considerations. - The partial derivatives appearing in the r and z governing equations are replaced by algebraic central finite difference operators. A complete derivation of the various operators is contained in reference 35. The notation used in this report is that shown in Figure 19. If the finite difference analogy of $\partial/\partial r$ is $\delta/\delta r$, the r derivatives can be written at point 0 as follows,

$$\frac{\delta r}{\delta \phi} = \frac{r_1 - r_3}{2 \Delta \phi} \quad (123)$$

$$\frac{\delta r}{\delta \psi} = \frac{r_2 - r_4}{2 \Delta \psi} \quad (124)$$

$$\frac{\delta^2 r}{\delta \phi^2} = \frac{r_1 + r_3 - 2r_0}{\Delta \phi^2} \quad (125)$$

$$\frac{\delta^2 r}{\delta \psi^2} = \frac{r_2 + r_4 - 2r_0}{\Delta \psi^2} \quad (126)$$

Similarly, the central finite difference representations for the z derivatives are,

$$\frac{\delta z}{\delta \phi} = \frac{z_1 - z_3}{2 \Delta \phi} \quad (127)$$

$$\frac{\delta z}{\delta \psi} = \frac{z_2 - z_4}{2 \Delta \psi} \quad (128)$$

$$\frac{\delta^2 z}{\delta \phi^2} = \frac{z_1 + z_3 - 2z_0}{\Delta \phi^2} \quad (129)$$

$$\frac{\delta^2 z}{\delta \psi^2} = \frac{z_2 + z_4 - 2z_0}{\Delta \psi^2} \quad (130)$$

2. Interior nodal points. - If equations (123) to (126) are substituted into the r governing equation (eq. (98)) with $\alpha = \Delta \phi / \Delta \psi$, the finite difference expression for all interior nodal points is obtained,

$$r_0^4 - \frac{r_0^3}{2} (r_2 + r_4) + r_0^2 \left[\frac{1}{\alpha^2} - \frac{1}{8} (r_2 - r_4)^2 \right] - \frac{r_0}{2\alpha^2} (r_1 + r_3) + \frac{1}{8\alpha^2} (r_1 - r_3)^2 = 0 \quad (131)$$

In addition, if equations (127) to (130) are substituted into the z governing equation (eq. (96)), the finite difference expression for all interior nodal points is obtained

$$z_0 = \frac{r_0^2}{2 \left(r_0^2 + \frac{1}{\alpha^2} \right)} (z_2 + z_4) + \frac{1}{2 \left(r_0^2 \alpha^2 + 1 \right)} (z_1 + z_3) + \frac{1}{4 \left(r_0^2 \alpha^2 + \frac{1}{\alpha} \right)} (z_2 - z_4)(z_1 - z_3) \quad (132)$$

where, as in the derivation of equation (131),

$$\alpha = \frac{\Delta\phi}{\Delta\psi} \quad (133)$$

B. Excluding Surface Tension

1. Infinite flat plate. - The finite difference representation for the infinite flat plate is shown in Figures 20(a) and (b). The algebraic expressions for the boundaries is derived by simultaneous application of the governing equation and boundary conditions at a fixed point. This application involves a fictitious point, *f*, outside the boundary which is subsequently eliminated. Point *G* represents a special point in the finite difference representation for the *z* solution since it is a part of two separate boundaries. The governing *z* equation (eq. (132)) was applied at point *G* which resulted in two fictitious points. Then the boundary conditions along both *AG* and *GE* were applied at point *G*. This allowed the elimination of the two fictitious points from the resulting finite difference expression. Detailed calculations for the boundaries are contained in Appendix C.

2. Finite plate. - The inverse formulation for the finite plate problem (Fig. 16), is shown in difference form in Figure 21. For this case, the difference operator along *GE* is more complicated than in the infinite plate case. In fact, both *G* and *E* represent special points in the formulation. However, one of these, point *E*, is specified as a known position (*r* = constant). At point *G* the equation to be satisfied in the *r* formulation is shown at the top of Figure 21(a). In the formulation (Fig. 21(b)), both points *G* and *E* are special points. The following equations hold there.

At point G

$$z_0 = \frac{r_0}{\left(r_0^2 + \frac{1}{\alpha^2}\right)} \left\{ \frac{1}{r_0} \sqrt{\left[a^2 - r_0^2(r_0 - r_4)^2\right]} + z_4 \right\} + \frac{z_1 - r_0 \alpha (r_0 - r_4)}{r_0^2 \alpha^2 + 1} + \frac{r_0 - r_4}{r_0^2 + \frac{1}{\alpha^2}} \sqrt{\left[a^2 - r_0^2(r_0 - r_4)^2\right]} \quad (134)$$

At point E

$$z_0 = \frac{r_0^2}{r_0^2 + \frac{1}{\alpha^2}} \left\{ z_2 - \frac{1}{r_0} \sqrt{\left[a^2 - r_0^2(r_2 - r_0)^2\right]} \right\} + \frac{z_1 - r_0 \alpha (r_2 - r_0)}{r_0^2 \alpha^2 + 1} + \frac{r_2 - r_0}{r_0^2 + \frac{1}{\alpha^2}} \sqrt{\left[a^2 - r_0^2(r_2 - r_0)^2\right]} \quad (135)$$

Detailed calculations for all the additional boundaries encountered for the finite plate case are contained in Appendix C.

C. Surface Tension

The difference formulation corresponding to the Surface Tension model (shown in Fig. 18) is indicated in Figure 22(a) and (b). The only boundary condition that must be explained is the one along the free surface AG. Details of this calculation are contained in Appendix C. It is noted that (see Fig. 22(a)) the r solution can be obtained independent of the z solution.

VII. DISCUSSION OF NUMERICAL TECHNIQUES

Since the governing equations for the r and z formulations are nonlinear in the inverse plane, in general, the finite difference operations at the interior and boundary points will be nonlinear (see eqs. (131) and (132)). For the infinite flat plate case, as described in Figure 20, the solution begins with $r = r(\psi, \phi)$ from Figure 20(a). Secondly, with a knowledge of the r solution, the z formulation, shown in Figure 20(b), is solved for $z(\psi, \phi)$. However, in the case where the plate is finite, the r formulation also contains z along the exiting plane GE (see Fig. 21(a)). As a result, the r and z formulations must be solved simultaneously. The surface tension model, described in Figure 22, also allows the solution of the r equation independent of the z equations since z appears nowhere in the formulation.

In any case, when solving the r equation, the finite difference representation of the problem results in N nonlinear algebraic equations in N unknowns. A variety of methods were applied in order to obtain a solution to the simultaneous nonlinear equations. These included Lieberstein's extension of Youngs' work on over-relaxation to nonlinear elliptic partial differential equations (26), and the familiar Newton-Raphson method. None of the above methods were successful in obtaining a convergent solution. The technique suggested by Powell (34) resulted in the method used in this paper to obtain solutions. Basically, Powell developed a subroutine which was essentially

a "compromise between the Newton-Raphson algorithm and the methods of steepest descents." In his paper, a Fortran subroutine is described for solving the nonlinear set of equations,

$$f_K(x_1, x_2, \dots, x_N) = 0 \quad K = 1, 2, \dots, N \quad (138)$$

The objective is to minimize the function

$$F(x_1, x_2, \dots, x_N) = \sum_{K=1}^N [f_K(x_1, x_2, \dots, x_N)]^2 \quad (139)$$

As with many iteration schemes, initial guesses are required for X_i . This particular algorithm has an advantage in that the initial guessed values do not have to be that close to the exact solution. The computer program for the r solution contains the main program and three subroutines. The subroutine EQNS is the one supplied by Powell. The user supplies the subroutine MATINV which inverts the matrices and the subroutine CALFUN which contains the nonlinear functions $F(X_i)$. A knowledge of the r solution makes the z formulation explicit in the unknown z_0 at each nodal point. As a result, a Gauss-Siedel linear iteration scheme was employed to obtain the solution.

For details of the subroutines, the reader is referred to reference 34. As we get into the computer results in the next section, a complete printout of the subroutine will be presented.

VIII. NUMERICAL RESULTS

A. Exclusion of Surface Tension

1. Infinite flat plate (Weber number = ∞). - Initially, the finite flat plate problem was numerically solved employing a very coarse mesh. Referring to Figure 20(a), the total stream function was divided into five equal parts. Recall that $\psi_G = 1/2$ and $\psi_B = 0$ which meant that the parameter $a = \Delta\psi$ was set equal to 0.1. In addition, the ϕ axis was divided up into eight equal parts. This division was purely arbitrary. One consideration was that there would be at least two vertical lines of constant ϕ between points C and B. This resulted in a total of 39 unknown nodal points for the r formulation indicated in Figure 20(a), and 41 unknown nodal points for the z formulation shown in Figure 20(b). The value of $D = \alpha^2$ where $\alpha = \Delta\phi/\Delta\psi$, was set equal to 0.0204. In Figure 20(a), the value of C along GE was arbitrarily chosen as 4.0 while the value of C for z along AB was chosen as 3.315. The major reason for the assignment of these two values for r and z was to be able to compare our numerical solution with the semi-analytical results for the infinite flat plate case with Schach (39). Actually, the major variable choice in the entire program is $D = 1/\alpha^2$. Basically, D is a measure of how large the flow system is since rectangular mesh is being used, i.e., a measure of $\Delta\phi$ and ψ total. The only concern is that $\Delta\phi$ is not chosen too small. In that event, ψ total would be too small to satisfy the incoming and exiting flow boundary conditions.

$\Delta\phi$ is chosen too large, i.e., α chosen too large or D chosen too small, all that is lost is accuracy due to larger mesh spacings. For the coarse mesh infinite flat plate problem, the results of the numerical solution as well as the computer listing and final output can be found in Appendix D - "Computer Solutions/Listings." The solution to the r formulation (Fig. 20(a)) required 1098 calls of the subroutine used to solve the simultaneous nonlinear equation. The sum of the squares of the error to the exact solution was reduced to 0.00357 at the last iteration.

The final values for the coarse mesh solution (r, z) were used to make initial guesses for the values for the fine mesh solution. The r solution required the simultaneous solution of 159 nonlinear algebraic equations. The z equation, again being explicit in z_0 , resulted in 164 unknown values of z_0 . The plot of the results from the computer program (details shown in Appendix D) are presented in Figure 24 in a print plot. The computer connected the nodal points with straight line segments. In general, there is very little difference between the fine mesh and coarse mesh solution. The fine mesh solution required the extended storage space option on the 1106 machine. The sum of the squares for the final r solution was reduced to 0.024 after approximately 1000 calls of the subroutine CALFUN used to solve the simultaneous nonlinear equations. For this case 1000 iterations were required to obtain a satisfactory z solution.

2. Finite plate. - As mentioned in Section VII, Discussions of Numerical Techniques, the finite plate formulation also contains z on the exiting jet surface (see Fig. 21(a)). As a result, the method of solution consisted of the following steps:

Initially, assumed values of z along GE were chosen. These values were used to compute an r solution. The computed r solution used 161 calls of the subroutine CALFUN to reduce the sum of the squares of the residuals at the nodal points to 0.00066. With this r solution, the linear iteration technique was used to calculate the complete z solution. Since the computed z solution resulted in refined approximations to the values of z along GE, changes could then be reflected in a new r computation.

For the finite disk case in which the ratio of the radius of the liquid jet to the radius of the disk was one-half, a second r calculation did not change when the z values were updated. A curve was faired through the calculated nodal points and is shown in Figure 25. Only two of the four available streamlines are shown in the figure. No attempt was made to refine the solution by completely doubling the number of vertical and horizontal grid lines. For this particular case, since no comparison with any existing analytical techniques existed, a more convenient value of 3.3 was chosen for $K\phi$. The value of D employed in the solution was 0.0138. The only specification along GE was that Z was set equal to 0.25. The computer listing as well as the calculated r and z values at each nodal point can be found in Appendix D.

The same method was used to numerically compute the finite plate case in which the ratio of the jet diameter to the disk diameter was three-fourths. There were 38 nodal points required for the r solution and 45 for the z solution. A complete print-plot of the results is shown in Figure 26. Two iterations were required for the z solution as well as for the r solution. The sum of the squares for the

r solution at the final iteration was 0.001. The computer listing and printout can be found in Appendix D. Again, the value of $K\phi$ was arbitrarily chosen as 3.3.

The z solution corresponding to the r solution was obtained and is also presented in Appendix D along with its complete computer listing. The method applied to obtain the solution was a simple linear iteration technique since equations explicit in Z_0 can be derived both in the interior and along the boundary points. There were 249 iterations required for the Z solution. Changes between the 248th and 249th iteration occurred in the fifth decimal point.

A physical plane description of the infinite flat plate solution is presented in Figure 23. Only two of the four internal streamlines are shown in the figure. Curves were faired through the available calculated nodal points (r,z) by a best fit process. There appeared, at the onset, the question of whether or not the coarse mesh employed could sufficiently describe the flow. When applying boundary conditions at the free surface, a larger number of nodal points are desirable. As a result, the existing mesh was doubled. The total ψ was divided up into ten equal parts such that $a = \Delta\psi = 0.05$, and the total ϕ was divided up into 16 equal parts.

B. Surface Tension Dominated Model

As previously mentioned, the r formulation for the surface tension dominated flow can be solved independent of the z formulation (refer to Figs. 22(a) and (b)). The initial case examined had a Weber number of 4 and the ratio of the radius of the jet to the radius of the disk was one-half. Also, the first solution to this problem as-

sumed only axisymmetry. The results of the numerical solution, employing a coarse mesh, resulted in a symmetrical r solution; symmetrical about the equipotential line emanating from point D. This allowed us to make a simplification to the problem in that not only could axisymmetry be assumed, but also mirror image symmetry (i.e., symmetry about the $z = 0$ plane). This is significant for problems in which the surface tension effects are to be taken into account since the surface tension forces are highly dependent on the curvature of the free surface. By taking advantage of the symmetry involved, additional nodal points can be placed on the free surface without using extended computer storage.

Referring now to Figure 22(a), a vertical line was drawn (equipotential line) emanating from point D, where $r = RD$. RD is the dimensionless disk radius. The intersection of this equipotential line with the free surface AG was defined as point M. Along DM, it is known that $z = 0$. In addition, the variation of r with ψ can be computed. Let us now refer to Figure 27 in which the equipotential line DM is depicted. Since DM is an equipotential line, the velocity along this line must be equal to V , the incoming jet velocity with the exception of the point $r = L$ in the physical plane. At point D, a velocity discontinuity will exist. However, we can specify how r varies with ψ along this line as follows:

In the physical plane,

On DM

$$u = 0 \quad \text{on } z = 0, L \leq r \leq R_{\max} \quad (140)$$

$$v = -V$$

where R_{\max} is the maximum radius of the liquid flow pattern.

An expression for the stream function along DM can now be derived since the radial velocity component along DM is 0, we have

$$0 = -\frac{1}{r} \frac{\partial \psi}{\partial z} \quad (141)$$

This implies that $\psi = \psi(r)$ alone. In order to find what the function is, the definition of the axial velocity is employed, namely,

$v = (1/r)(\partial\psi/\partial r)$, on DM

$$-v = \frac{1}{r} \frac{\partial \psi}{\partial r} \quad (142)$$

Integrating this

$$\psi = -\frac{vr^2}{2} + \text{Constant} \quad (143)$$

Applying the boundary condition that $\psi = 0$ at $r = L$, the constant in (143) can be calculated. The following expression results,

$$\psi = -\frac{vr^2}{2} + \frac{vL^2}{2} \quad (144)$$

If this equation is nondimensionalized,

$$\psi^* = \frac{r^{*2}}{2} - \frac{1}{2} \left(\frac{L}{R_0} \right)^2 \quad (145)$$

As we have done in the past derivations, the starred notation is dropped.

$$\psi = \frac{r^2}{2} - \frac{1}{2} \left(\frac{L}{R_0} \right)^2 \quad (146)$$

Solving for r ,

$$r = +\sqrt{2\psi + (RD)^2} \quad (147)$$

where

$$\frac{L}{R_0} = RD \quad (148)$$

Equation (147) represents the boundary condition employed along DM in the inverse plane for the r formulation. The condition $z = 0$ was used for the z formulation.

In the course of finding the solution to the z formulation, depicted in Figure 22(b), it was necessary to solve a cubic equation for the parameter T along the free surface. Physical as well as mathematical interpretation was required when choosing the proper root of the cubic since a possibility of three real roots existed. Referring to equation (C-78) in Appendix C, the only mathematically meaningful roots are those in which the absolute value of the parameter T was greater than or equal to one. However, the possibility still existed that all three roots would be real and in addition satisfy the requirement that their absolute values were greater than one. As a result, some physical insight was required when deciding upon which roots to employ in the equation relating T to the fictitious point f , (eq. (C-84)). For example, it is known that as the nozzle exit is approached along the free surface, $z = f(r)$ becomes steeper (i.e., $f'(r)$ approaches infinity). This would coincide with the curvature terms dropping out of the boundary condition in the physical plane formulation. An alternate approach to viewing this is that the fictitious point f approaches the image point z_4 . As a result, the value of the parameter T approaches unity. The algorithm selected for choosing the proper root of the cubic was to select the value of T closest to unity but ensuring that its absolute value was greater than or equal to one. During the course of finding the solution, problems in implementing this algorithm occurred, particularly when close to the nozzle, since the T values closest to one were slightly less than

one and were automatically discarded by the algorithm. The resulting potential lines and streamlines appeared inaccurate when plotted up. The only way found to circumvent this problem was to set up an additional algorithm which set T identically equal to one for several free surface nodal points in the vicinity of the nozzle (i.e., those nodal points in which the computed r value was $\leq 1.00 N$). Physically, this reasoning is justified since it is known that $f'(r)$ must approach infinity there.

The results of the numerical solution are indicated in Figure 28. The Weber number for this solution was 4 and the ratio of the radius of the liquid jet to the radius of the disk was $1/2$. A value of 3.5 was chosen for $K\phi$, and D was set equal to 0.0204. The computer listing can be found in Appendix D along with the computed r and z values for the nodal points. The sum of the squares for the r solution was 0.77×10^{-6} and since the r solution was independent of the z solution, a second iteration was unnecessary.

C. Discussion of Zero Gravity Results

The numerical solutions were compared with the available semi-analytical results of Schach (39) for the case of the infinite flat plate. The method employed by Schach is attributed to Trefftz. The method used by Schach did not appear readily extendable to more complicated geometrical flows and could not be employed to account for the effects of surface tension. In making the comparison between reference 39 and the numerical results, the fine mesh solution presented in Figure 24 was used. The results of the comparison for the infinite flat plate are shown in Figure 29. The symbols indicated in the figure were obtained from Figure 11 of Schach's paper by using an expandable

scale. As a result there is some unknown error associated with the process of taking the results from the reference. In any case, the agreement looks particularly well with the sole exception of the first r coordinate greater than unity. One final point with respect to the infinite flat plate solution concerns the extreme left coordinate in Figure 29, namely, $r = 4$, $z = 0.125$. These two values are fixed by continuity, both in our numerical program and in the semi-analytical results of Schach. This result was obtained as follows; assuming constant density, the volumetric flow rate into the control volume at AB must balance the flow out of the control volume at GE. In physical coordinates, the flow is given as $\pi R_o^2 V$ and the flow out by $2\pi R_{jet} Z_G V$. Equating these and cancelling leads to the fact that Z_G must equal $R_o^2 / (2R_{jet})$. Nondimensionalizing with respect to R_o yields

$$z_G^* = \frac{1}{2R_{jet}^*} \quad (149)$$

Dropping the starred notation and observing that $R_{jet} = 4$ at the left boundary of the control volume shows that Z_o must equal $1/8$.

As far as the finite plate is concerned, there was no available comparisons with past experimental or analytical work. As a result, comparisons were made with respect to our own zero gravity experimental data. The results are shown in dimensionless coordinates in Figures 30 and 31. Figure 30 is for the case where the ratio of the jet radius to the disk radius is one-half and Figure 31 indicates the comparison when the ratio of the jet radius to the disk radius is three-fourths. The comparisons were made with respect to the outer or top free surface since it was impossible to view the lower free surface

because of the way in which the flow occurred. The results were generally good for both ratios compared. Experimental data points were obtained from both sides of the axisymmetric sheet as it flowed around the disk. An averaging procedure was subsequently used to plot the continuous lines indicated in Figures 30 and 31. The analysis corroborated the experiments in the sense that as the ratio (R_0/L) becomes smaller, the jet appears to leave the disk more tangentially.

IX. NORMAL GRAVITY EXPERIMENT SECTION

A. Apparatus and Procedure

1. Experiment. - The experimental test rig used to obtain the normal gravity data is shown in Figures 32(a) and (b). The rig consisted of an angle-iron frame in which was mounted a 10 gallon supply tank, a settling chamber, a 56 gallon catch basin, a return pump, a control box, a clock, sequence timers, a regulator, and a supply tank. The major functions were controlled through the control box. A high-speed Mitchell Monitor motion picture camera (nominal speed 400 frames/sec) was located directly in front of the experimental test rig. The camera was mounted on a Wollensak camera stand which was fastened to a concrete floor by means of conduit clamps.

The experiment could be conducted in either a pressurized or non-pressurized mode (gravity-feed). To operate in the pressurized mode, two vent valves located above the supply tank were closed and the system was pressurized through the regulator. The pressure level was recorded on the gage located immediately to the right of the regulator as shown in Figure 32(a). For both modes, the return pump was used to resupply liquid to the supply tank in order to maintain a nearly constant level of liquid. Since the supply tank was fabricated from stainless steel and provided no visible means for monitoring liquid level, attempts were made to connect a plastic hose between the needle valve located just upstream of the solenoid valve and the side of the supply tank. This system was generally inaccurate and as a rule the

return pump was normally activated after completing two or three test runs.

In order to maintain a circular liquid jet having an initially uniform velocity profile, a settling chamber was designed to quiet the incoming flow. A similar technique was employed by Donnelly et al. (11) in their study of liquid jet stability. The settling chamber, Fig. 33, was fabricated from stainless-steel and had a 30° tapered approach to a circular hole in order to prevent boundary layer buildup. A total angle of 60° was employed in order to ensure a nearly uniform velocity profile at the exit to the settling chamber. Three settling chambers were employed having outlet diameters of 0.25, 0.50, and 1.0 centimeters. Problems developed when using an un baffled settling chamber in that the entire flow developed a swirling action between 2 and 10 seconds after flow was initiated. In order to circumvent the swirling problem, the cylindrical section of the settling chamber was fitted with a $1\frac{3}{4}$ inch honeycomb spacer. A sixteen mesh stainless steel screen was mounted below the first screen and both screens were butted up against the bottom of the spacer. This technique seemed to eliminate any noticeable swirl in the flow.

Sharp-edged disks, fabricated from stainless steel, were mounted below the settling chamber and positioned at right angles to the impinging liquid jet. A photograph of the disks employed in the study is shown in Figure 34. Their diameters ranged from 1 to 4 centimeters. The disks were mounted onto a stainless steel device capable of being adjusted at any angle to the incoming flow. However, in this study the impingement was restricted to 90°.

2. Test liquids. - Two test liquids were employed, anhydrous

ethanol and distilled water. Their properties at 20° C are listed in Table 1. No attempt was made to correct these fluid properties for temperature changes.

3. Test procedure. - Prior to a test run the settling chamber was filled with the test liquid by opening the solenoid valve while holding the bottom of the settling chamber closed. The liquid completely filled the settling chamber until it flowed out of the relief screw. At that point, the relief screw was closed and the outlet could be opened without loss of liquid from the settling chamber since it was a stable pressure supported system. This method worked when using distilled water for all the nozzle openings. It did not work for anhydrous ethanol in conjunction with the largest or 1 centimeter diameter opening. As a result, for those tests, the nozzle opening was kept sealed until the solenoid was opened at the start of each test.

Calibration tests were made prior to every series of test runs. Electrical sequence times in the control box were used along with graduated cylinders to determine the volumetric flow rate. At least three calibration tests were made before each series of runs, and an average value for the flow rate was thus determined. The impingement velocity (velocity at the disk) was calculated by correcting for the effect of gravitational forces.

B. Results

1. Steady-state flow patterns. - Basically, two types of flow patterns were observed in the course of normal gravity liquid jet impingement. The first type occurred when a very high speed jet impinged upon a solid surface and spread out radially as a thin sheet. The sheet became thinner until it became unstable and broke up into

small liquid droplets. A second pattern is shown schematically in Figure 35. No breakup was observed in this pattern; the jet curved upon itself to form a surface of revolution or plume. The incoming jet velocity is V and the radius of the circular liquid jet is R_0 . The disk radius is denoted as L while H is the distance between the nozzle and the disk. The maximum radius that the plume possessed is denoted as R_p . The maximum plume radius was the primary experimental variable for the normal gravity study since it was easily measurable and characteristic of the entire flow pattern. For the case when the plume was not visibly disturbed, the plume would slowly move to a final R_p , with visible surface ripples.

2. Unstable jumps. - In attempting to obtain steady-state impingement profiles, an unusual phenomenon was discovered. Instead of a single steady-state flow pattern, a number of unstable flow patterns were observed prior to the attaining of a stable steady state. Typically, the jet impinged upon the solid and formed a plume of some given radius with surface ripples present. If disturbed, either upstream or downstream of the plume, the jet would jump to another apparently stable configuration of larger plume radius. Normally, only one jump would occur in a single test run, but occasionally two jumps or three apparently stable configurations were observed. A series of tests indicating the flow patterns before and after a jump are shown in Figure 36. Figures 36(a), (c), and (e) illustrate the behavior before the respective jumps, while Figures 36(b), (d), and (f) occur after the jumps. The plume size for the final configurations appear to be nearly double what they were initially. However, there does not appear to be any correlation between initial and final size. The jumps

are natural in occurrence, such as when a small liquid droplet rebounds off the disk holder and impinges upon this film, but can be initiated by a disturbance, such as a pencil penetrating the flow. The final steady-state configuration is stable to any additional disturbances, i.e., it remains at some fixed plume shape. Under no circumstances was the plume observed to jump to a smaller plume configuration; all jumps were to larger plume sizes.

The actual cause of these jumps remains unanswered at this writing. Some possible causes have been eliminated, such as swirling flow. If the flow were swirling, the steady-state flow patterns would be significantly affected if half the flow over the disk was obstructed. However, the pattern was not affected at all when this was done. It is tentatively concluded that the jumps are natural in occurrence. The initial states and all transition states are unstable to small disturbances. For the purpose of the experimental investigation, then, the steady-state was chosen as the state in which further disturbances caused no change in the liquid flow pattern.

3. Experimental data. - The experimental runs were conducted such that the viscous dependence would be small. As shown in section III, depending upon the ratio (R_0/L), there exists a critical Reynolds number above which the flow can be considered as essentially inviscid. The Reynolds number was calculated at the point of impingement on the disk (i.e., the approach velocity to the disk was corrected for gravitational effects). From analytical considerations, numerous dimensionless parameters arise and thus form the basis for correlating the primary variable, the plume size. These parameters include the Weber number, which is the ratio of inertial to surface tension forces, and

the Bond number, which is the ratio between gravitational and surface tension forces. In addition, several geometrical ratios appear, such as R_o/L , the ratio of jet to the disk radius, and H/R_o , the ratio of the nozzle height to the jet radius. The experimental results are listed in tabular form in Table 3. The last column contains the plume radius, nondimensionalized with respect to the jet radius. In examining the difference between zero and normal gravity liquid jet impingement, it can be seen that two additional parameters are required in order to completely define this phenomena in normal gravity. They are the Bond number, Bo , and the dimensionless nozzle height, H/R_o . The Bond number relates the relative contribution of gravitational forces, while H/R_o has an effect in that jets flowing downward under the effect of gravity accelerate and thus shrink in size, thereby having an effect on the resulting flow.

4. Data analysis. - A linear regression analysis was employed in order to correlate the independent variable, R_p/R_o , with the remaining system parameters. Let us define the following variables,

$$Y = \frac{R_p}{R_o} \quad (150)$$

$$Z_1 = \frac{R_o}{L} \quad (151)$$

$$Z_2 = \frac{H}{R_o} \quad (152)$$

$$Z_3 = We \quad (153)$$

$$Z_4 = Re \quad (154)$$

$$Z_5 = Bo \quad (155)$$

The parameter Z_4 , the Reynolds number, was included to see what

the viscous influence was. The experimental data was fitted to the following complex model

$$\begin{aligned} \frac{R_p}{R_o} = & 22.8241 + 7.67129 X_1 - 41.2001 X_1^2 + 42.9330 X_1^3 + 1.91085 X_2 \\ & + 8.90368 X_3 + 1.46319 X_4 - 2.07823 X_5 + 0.0696939 X_2 X_5 \end{aligned} \quad (156)$$

where

$$X_1 = \frac{\frac{R_o}{L} - 0.371839}{0.154239} \quad (157)$$

$$X_2 = \frac{\frac{H}{R_o} - 9.22727}{7.19571} \quad (158)$$

$$X_3 = \frac{We - 129.227}{75.7108} \quad (159)$$

$$X_4 = \frac{Re - 4663.89}{1897.57} \quad (160)$$

$$X_5 = \frac{Bo - 2.15602}{1.12058} \quad (161)$$

The value of R^2 for the above statistical model was 0.981. This means that 98.1 percent of the total variance in R_p/R_o is accounted for by the model. An examination of the signs in the equation for the complex model tells us how R_p/R_o varies with each of the parameters; R_p/R_o increases slightly as H/R_o and Re are increased, and increases significantly with X_3 , the Weber number. Since X_5 is involved in two terms in the correlation, its variation depends on the strongest term (i.e., the one with the largest coefficient). As a result, R_p/R_o decreases with increasing Bo . The variation with X_1 is more confusing since it is involved in three terms. The actual data

bears this out, R_p/R_o sometimes increasing, or sometimes decreasing. The coefficient for X_3 is essentially the largest of all (X_3 is related to We). As a result, a simpler model was pursued using only We as the independent variable. The following equation resulted;

$$\frac{R_p}{R_o} = 21.7059 + 10.1410 \frac{We - 129.227}{75.7108} \quad (162)$$

For this simple model $R^2 = 0.916$, which means that the correlation accounts for 91.6 percent of the variance in the data. A plot of the data is displayed in Figure 37.

The Weber number turns out to be the most statistically significant variable. This is not to say that the other variables are not significant, but that the Weber number is the most dominant variable in determining R_p/R_o .

X. CONCLUSIONS

Zero gravity. - An experimental and analytical investigation was conducted to determine the free surface shape of circular liquid jets impinging normal to sharp-edged disks in zero gravity. The test liquids employed were anhydrous ethanol and trichlorotrifluoroethane. Jet radii were varied from 0.25 to 0.75 centimeter and disk radii of 1.0 and 1.5 centimeters were employed. The jet velocity was varied between 12 and 365 centimeters per second. Under the stipulation that the nozzle was located at least 5 centimeters from the disk, the investigation yielded the following results:

1. It was analytically determined that there exist flow regions where viscous forces are not significant when computing free surface shapes. It was shown that the Reynolds number $\rho VR_0/\mu$ and the ratio of jet to disk radius R_0/L uniquely define the flow regions. It was further shown that the Reynolds number specifying the transition between viscous and nonviscous flow decreased with increasing jet to disk radius ratio.
2. Within the inviscid region, three distinct flow regimes were experimentally found which depend uniquely on the Weber number $\rho V^2 R_0/\sigma$ and the ratio of the jet to disk radius R_0/L . These flows were defined as Surface Tension Flow, Transition Flow, and Inertia Flow. The critical Weber number between regimes was found to decrease with increasing jet to disk radius ratio.
3. A numerical solution yielding free surface shapes and stream-

lines was obtained for the case of impingement normal to an infinite flat plate and compared favorably with semi-analytical techniques in the literature.

4. A numerical solution yielding free surface shapes and streamlines was obtained for inertially dominated flows at ratios of jet to disk radius of one-half and three-fourths. The comparison with experiments showed good agreement for the upper free surface.

5. A surface tension dominated flow was formulated and solved numerically. The system Weber number was 4.0 and the ratio of the jet to the disk radius was one-half.

Normal gravity. - An experimental investigation was conducted to determine the characteristics of circular liquid jets impinging normal to a sharp-edged disk in normal gravity. The test liquids employed were distilled water and anhydrous ethanol. Jet radii between 0.125 and 0.50 centimeter were employed and the disk radii were varied between 0.5 and 2.0 centimeters. The jet velocity had the range of 75.5 to 484 centimeters per second. The distance between the nozzle and disk was varied between 0.25 and 5.0 centimeters. Under the stipulation that the Reynolds numbers were such that they exceeded the minimum value required to avoid viscous influence, the investigation yielded the following results:

1. The liquid flow pattern was observed to jump from one apparently stable flow pattern to another until a completely stable configuration was reached. The jumps were triggered by disturbances both upstream and downstream of the disk and were apparently natural in occurrence.

2. The dimensionless plume radius R_p/R_0 was correlated by means

of a linear regression analysis. A simple model, employing only the Weber number, accounted for nearly 92 percent of the experimental data.

The following empirical formula resulted

$$\frac{R_p}{R_o} = 21.7059 + 10.140 \frac{We - 129.227}{75.7108}$$

where R_p is the plume radius, R_o the nozzle radius, and We the system Weber number.

XI, APPENDIXES

Appendix A - Detailed Calculations of Free Surface Boundary Conditions

There are two boundary conditions required for the case of a free surface in a fluid dynamics problem. This is in comparison to known boundaries in which only one boundary condition is required. The two conditions to be satisfied are:

- (1) Conservation of energy along a streamline
- (2) The velocity normal to the streamline is zero.

Consider the following geometry:

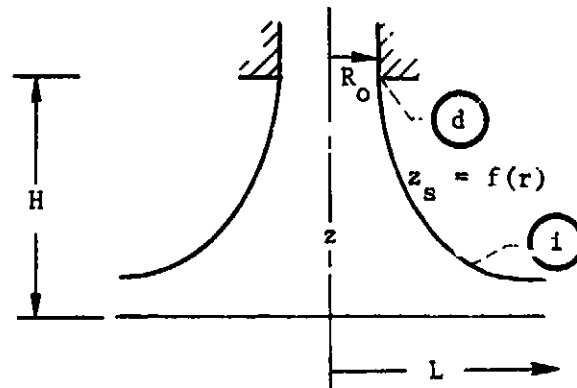


Figure A.1. - Schematic of Liquid Jet Impingement

where "i" represents any point on the free surface $z_s = f(r)$ and "d" designates the reference point which is chosen as the point where the liquid jet exits from the nozzle.

- (1) Conservation of energy along a streamline

Bernoulli's equation written between points "i" and "d" becomes

$$\frac{1}{2} (u^2 + v^2) + \frac{P_i}{\rho} = \frac{1}{2} V^2 + \frac{P_d}{\rho} \quad \text{on } z_s = f(r) \quad (\text{A } 1)$$

The pressure at point 1, p_1 , is not the same as it is at point d, P_d , due to the effects of surface tension. In general,

$$P_g - P = \sigma J \quad (A-2)$$

where P_g = known gas pressure, and

$$J = \frac{1}{R_1} + \frac{1}{R_2} \quad (A-3)$$

where R_1, R_2 are radii of curvature where

$$\frac{1}{R_1} = \frac{f''}{(1 + f'^2)^{3/2}} \quad (A-4)$$

and

$$\frac{1}{R_2} = \frac{f'}{r(1 + f'^2)^{1/2}} \quad (A-5)$$

Combining (A-4) and (A-5) with (A-2) we find

$$P_g - P = \sigma \left[\frac{f''}{(1 + f'^2)^{3/2}} + \frac{f'}{r(1 + f'^2)^{1/2}} \right] \quad (A-6)$$

which can be combined to yield,

$$P_g - P = \frac{\sigma}{r} \frac{d}{dx} \left(\frac{rf'}{\sqrt{1 + f'^2}} \right) \quad (A-7)$$

Applying at point "d"

$$z = H, \quad r = R_o, \quad \text{and} \quad \frac{df}{dr} = f' = \infty$$

For large f' ,

$$\sqrt{1 + f'^2} \doteq \sqrt{f'^2} = f'$$

Therefore, substitution into (A-7) yields

$$P_g - P_d = \frac{\sigma}{R_o} \quad (A-8)$$

Applying at point "i"

$$P_g - P_i = \frac{\sigma}{r} \frac{d}{dr} \left(\frac{rf'}{\sqrt{1+f'^2}} \right) \quad (\text{A-9})$$

Now (A-8) and (A-9) can be substituted into (A-1) to obtain

$$\frac{1}{2} (u^2 + v^2) - \frac{\sigma}{\rho r} \frac{d}{dr} \left(\frac{rf'}{\sqrt{1+f'^2}} \right) = \frac{1}{2} v^2 - \frac{\sigma}{\rho R_o} \quad \text{on } z_s = f(r) \quad (\text{A-10})$$

(2) The velocity normal to the free surface is zero

A portion of the free surface $z_s = f(r)$ is shown in Figure A.2

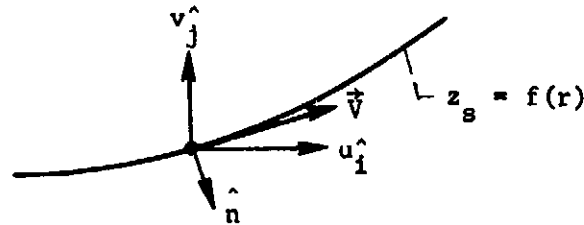


Figure A.2. - Velocity Vector at Free Surface

\hat{n} is the unit outward normal to the surface at some point and u and v are the velocity components such that $\vec{V} = u\hat{i} + v\hat{j}$. Since the velocity normal to the surface is zero

$$\vec{V} \cdot \hat{n} = 0 \quad (\text{A-11})$$

With the surface given by $z_s = f(r)$, the unit normal is given as

$$\hat{n} = \frac{-f'\hat{i} + \hat{j}}{\sqrt{1+f'^2}} \quad (\text{A-12})$$

Hence

$$\vec{V} \cdot \hat{n} = -\frac{uf'}{\sqrt{1+f'^2}} + \frac{v}{\sqrt{1+f'^2}} = 0 \quad (\text{A-13})$$

which simplifies to

$$-uf' + v = 0 \quad \text{on } z_s = f(r) \quad (\text{A-14})$$

Appendix B - Zero Gravity Drop Tower Test Facility

The experimental data for this study were obtained in the Lewis Research Center's 2.2-Second Zero Gravity Facility. A schematic diagram of this facility is shown in Figure B.1. The facility consists of a building 6.4 meters square by 30.5 meters tall. Contained within the building is a drop area 27 meters long with a cross section 1.5 by 2.75 meters.

The service building has a shop and service area, a calibration room, and a controlled environment room. Those components of the experiment that required special handling were prepared in the controlled environment room of the facility. This air-conditioned and filtered room (shown in Fig. B.2) contains an ultrasonic cleaning system and the laboratory equipment necessary for handling test liquids.

Mode of operation - A 2.2-second period of weightlessness is obtained by allowing the experiment package to free fall from the top of the drop area. In order to minimize drag on the experiment package, it is enclosed in a drag shield designed with a high ratio of weight to frontal area and a low drag coefficient. The relative motion of the experiment package with respect to the drag shield during a test is shown in Figure B.3. Throughout the test, the experiment package and drag shield fall freely and independently of each other; that is, no guide wires, electrical lines, etc., are connected to either. Therefore, the only force acting on the freely falling experiment package

is the air drag associated with the relative motion of the package within the enclosure of the drag shield. This air drag results in an equivalent gravitational acceleration acting on the experiment, which is estimated to be below 10^{-5} g's.

Release system. - The experiment package, installed within the drag shield, is suspended at the top of the drop area by means of a highly stressed music wire attached to the release system. This release system consists of a double-acting air cylinder with a hard-steel knife edge attached to the piston. Pressurization of the air cylinder drives the knife edge against the wire, which is backed by an anvil. The resulting notch causes the wire to fail, smoothly releasing the experiment. No measurable disturbances are imparted to the package by this release procedure.

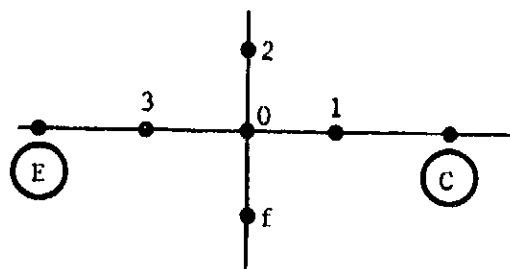
Recovery system. - After the experiment package and drag shield have traversed the total length of the drop area, they are recovered by deceleration in a 2.2-meter-deep container filled with sand. The deceleration rate (averaging 15 g's) is controlled by selectively varying the tips of the deceleration spikes mounted on the bottom of the drag shield (Fig. B.1). At the time of impact of the drag shield in the decelerator container, the experiment package has traversed the vertical distance within the drag shield (compare Figs. B3(a) and (c)).

Appendix C - Detailed Derivations of Finite Difference
Operators Along Boundaries

A. Infinite Flat Plate

The finite difference representations for the derivatives are those shown in the text (eqs. (123) to (130)). Refer to Figures 15(a) and (b).

$$\underline{\frac{\partial r}{\partial \psi} = 0 \text{ on EC}}$$



Applying the r difference equation (eq. (131)) at point 0, where f is a fictitious point outside boundary

$$r_0^4 - \frac{r_0^3}{2} (r_2 + r_f) + r_0^2 \left[\frac{1}{\alpha^2} - \frac{1}{8} (r_2 - r_f)^2 \right] - \frac{r_0}{2\alpha^2} (r_1 + r_3) + \frac{1}{8\alpha^2} (r_1 - r_3)^2 = 0 \quad (C-1)$$

Along EC, $\frac{\partial r}{\partial \psi} = 0$. This implies

$$\frac{r_2 - r_f}{2 \Delta \psi} = 0 \quad (C-2)$$

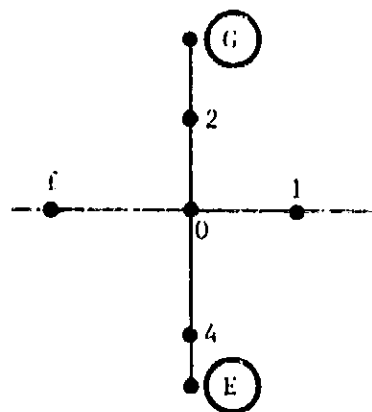
Therefore,

$$r_2 = r_f \quad (C-3)$$

Equation (C-1) becomes

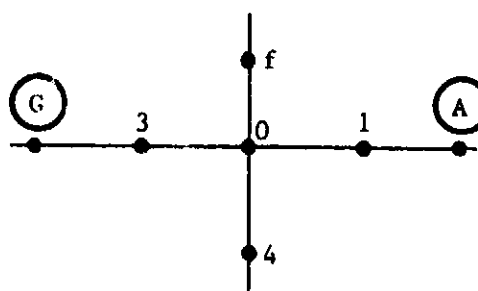
$$r_0^4 - r_0^3 r_2 + r_0^2 \frac{1}{\alpha^2} - \frac{r_0}{2\alpha^2} (r_1 + r_3) + \frac{1}{8\alpha^2} (r_1 - r_3)^2 = 0 \quad (C-4)$$

$$\frac{\partial r}{\partial \psi} = 0 \quad \text{on GE}$$



Application of $\partial r / \partial \psi$ on GE yields the fact that $r_2 = r_4$ and does not involve the unknown fictitious point f. However, $\partial r / \partial \psi = 0$ implies $r \neq r(\psi)$. Therefore, r must only be a function of ϕ , $r = r(\phi)$. But, along GE, $\phi = \text{constant}$, ($\phi = 0$). Hence, $r = \text{constant}$ along GE.

$$\left(\frac{\partial r}{\partial \phi}\right)^2 + r^2 \left(\frac{\partial r}{\partial \psi}\right)^2 = 1 \quad \text{on AG}$$



The r difference equation can be written

$$r_o^4 - \frac{r_o^3}{2} (r_f + r_4) + r_o^2 \left[\frac{1}{\alpha^2} - \frac{1}{8} (r_f - r_4)^2 \right] - \frac{r_o}{2\alpha^2} (r_1 + r_3) + \frac{1}{8\alpha^2} (r_1 - r_3)^2 = 0 \quad (C-5)$$

Along AC

$$\left(\frac{\partial r}{\partial \phi} \right)^2 + r^2 \left(\frac{\partial r}{\partial \psi} \right)^2 = 1$$

This implies

$$\left(\frac{r_1 - r_3}{2 \Delta \phi} \right)^2 + r_o^2 \left(\frac{r_f - r_4}{2 \Delta \psi} \right)^2 = 1 \quad (C-6)$$

Rearranging and letting $\Delta \psi = a$ (recalling $a = b_4 / \Delta \psi$)

$$(r_f - r_4)^2 = \frac{1}{r_o^2} \left[4a^2 - \frac{1}{\alpha^2} (r_1 - r_3)^2 \right] \quad (C-7)$$

Whereupon we can calculate the two expressions

$$r_f - r_4 = \frac{1}{r_o} \sqrt{\left[4a^2 - \frac{1}{\alpha^2} (r_1 - r_3)^2 \right]} \quad (C-8)$$

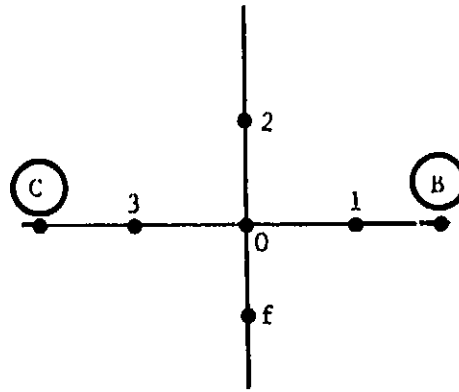
$$r_f + r_4 = \frac{1}{r_o} \sqrt{\left[4a^2 - \frac{1}{\alpha^2} (r_1 - r_3)^2 \right]} + 2r_4 \quad (C-9)$$

Inserting (C-8) and (C-9) into (C-5) yields the desired relation

$$r_o^4 - r_o^3 r_4 + r_o^2 \left\{ \frac{1}{\alpha^2} - \frac{1}{2} \sqrt{\left[4a^2 - \frac{1}{\alpha^2} (r_1 - r_3)^2 \right]} \right\} - \frac{r_o}{2\alpha^2} (r_1 + r_3) + \frac{1}{8} \left[\frac{2}{\alpha^2} (r_1 - r_3)^2 - 4a^2 \right] = 0 \quad (C-10)$$

$z = \text{Constant}$ on AB, let $z = R_0$.

$$\underline{\frac{\partial z}{\partial \phi} = 0 \text{ on BC}}$$



Applying the z difference equation (eq. (132)) at point 0, where f is a fictitious point outside of boundary

$$z_0 = \frac{r_0^2}{2\left(r_0^2 + \frac{1}{\alpha^2}\right)} (z_2 + z_f) + \frac{1}{2\left(r_0^2 \alpha^2 + 1\right)} (z_1 + z_3) + \frac{1}{4\left(r_0^2 \alpha^2 + \frac{1}{\alpha}\right)} (z_2 - z_f)(z_1 - z_3) \quad (\text{C-11})$$

Along BC, $\frac{\partial z}{\partial \psi} = 0$. This implies

$$z_2 - z_f = 0$$

or

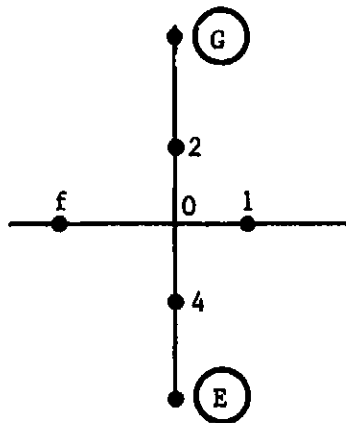
$$z_f = z_2 \quad (\text{C-12})$$

Therefore, equation (C-11) becomes

$$z_0 = \frac{r_0^2 z_2}{r_0^2 + \frac{1}{\alpha^2}} + \frac{1}{2\left(r_0^2 \alpha^2 + 1\right)} (z_1 + z_3) \quad (\text{C-13})$$

(C-13)

$$\frac{\partial z}{\partial \phi} = 0 \text{ on GE}$$



The z difference equation can be written

$$z_0 = \frac{r_0^2}{2\left(r_0^2 + \frac{1}{\alpha^2}\right)} (z_2 + z_4) + \frac{1}{2\left(r_0^2 \alpha^2 + 1\right)} (z_1 + z_f) + \frac{1}{4\left(r_0^2 \alpha + \frac{1}{\alpha}\right)} (z_2 - z_4)(z_1 - z_f) \quad (\text{C-14})$$

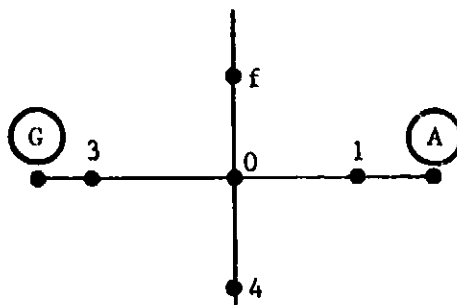
Along GE, $\frac{\partial z}{\partial \phi} = 0$ this implies $z_1 - z_f = 0$ or

$$z_f \equiv z_1 \quad (\text{C-15})$$

Therefore, equation (C-14) becomes

$$z_0 = \frac{r_0^2}{2\left(r_0^2 + \frac{1}{\alpha^2}\right)} (z_2 + z_4) + \frac{z_1}{r_0^2 \alpha^2 + 1} \quad (\text{C-16})$$

$$r^2 \left(\frac{\partial z}{\partial \psi}\right)^2 + \left(\frac{\partial z}{\partial \phi}\right)^2 = 1 \text{ on GA}$$



The z difference equation can be written

$$z_o = \frac{r_o^2}{2\left(r_o^2 + \frac{1}{\alpha^2}\right)} (z_f - z_4) + \frac{1}{2\left(r_o^2 \alpha^2 + 1\right)} (z_1 + z_3) + \frac{1}{4\left(r_o^2 \alpha + \frac{1}{\alpha}\right)} (z_f - z_4)(z_1 - z_3) \quad (\text{C-17})$$

Along AG, $r^2 \left(\frac{\partial z}{\partial \psi}\right)^2 + \left(\frac{\partial z}{\partial \phi}\right)^2 = 1$. Hence,

$$r_o^2 \left(\frac{z_f - z_4}{2 \Delta \psi}\right)^2 + \left(\frac{z_1 - z_3}{2 \Delta \phi}\right)^2 = 1 \quad (\text{C-18})$$

which can be expressed as

$$(z_f - z_4)^2 = \frac{1}{r_o^2} \left[4a^2 - \frac{1}{\alpha^2} (z_1 - z_3)^2 \right] \quad (\text{C-19})$$

This yields the two relations,

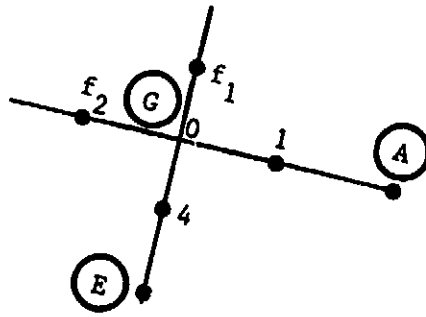
$$z_f - z_4 = \frac{1}{r_o} \sqrt{\left[4a^2 - \frac{1}{\alpha^2} (z_1 - z_3)^2 \right]} \quad (\text{C-20})$$

$$z_f + z_4 = \frac{1}{r_o} \sqrt{\left[4a^2 - \frac{1}{\alpha^2} (z_1 - z_3)^2 \right]} + 2z_4 \quad (\text{C-21})$$

Inserting these last two equations in (C-17) eliminates the fictitious point z_f , yielding

$$z_0 = \frac{r_0^2}{2\left(r_0^2 + \frac{1}{\alpha^2}\right)} \left\{ \frac{1}{r_0} \sqrt{\left[4a^2 - \frac{1}{\alpha^2}(z_1 - z_3)^2\right] + 2z_4} \right. \\ \left. + \frac{1}{2\left(r_0^2\alpha^2 + 1\right)} (z_1 + z_3) \right. \\ \left. + \frac{z_1 - z_3}{4r_0\left(r_0^2\alpha + \frac{1}{\alpha}\right)} \sqrt{\left[4a^2 - \frac{1}{\alpha^2}(z_1 - z_3)^2\right]} \right\} \quad (C-22)$$

A special boundary condition is required for point G since it is a part of two separate boundaries



Applying the z difference equation,

$$z_0 = \frac{r_0^2}{2\left(r_0^2 + \frac{1}{\alpha^2}\right)} (f_1 + z_4) + \frac{1}{2\left(r_0^2\alpha^2 + 1\right)} (z_1 + f_2)$$

$$+ \frac{1}{4\left(r_0^2\alpha + \frac{1}{\alpha}\right)} (f_1 - z_4)(z_1 - f_2)$$

Applying the boundary condition along GE, namely $\frac{\partial z}{\partial \phi} = 0$, it is found that $f_2 = z_1$. Therefore, we write

(C-23)

$$z_o = \frac{r_o^2}{2\left(r_o^2 + \frac{1}{\alpha^2}\right)} (f_1 + z_4) + \frac{z_1}{r_o^2 \alpha^2 + 1} \quad (C-24)$$

Applying the boundary condition along AG (see eq. (C-20))

$$f_1 = z_4 + \frac{1}{r_o} \sqrt{\left[4a^2 - \frac{1}{\alpha^2} (z_1 - f_2)^2\right]} \quad (C-25)$$

but $f_2 = z_1$, hence we write

$$f_1 = z_4 + \frac{2a}{r_o} \quad (C-26)$$

Equation (C-23) becomes

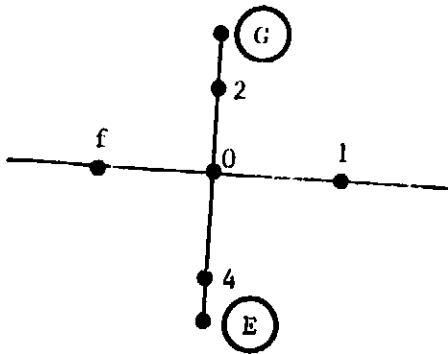
$$z_o = \frac{r_o \left(z_4 + \frac{a}{r_o}\right)}{r_o^2 + \frac{1}{\alpha^2}} + \frac{z_1}{r_o^2 \alpha^2 + 1} \quad (C-27)$$

such that $z_o = z_o(z_1, z_4)$ at point G.

B. Finite Plate

Referring to Figures 16(a) and (b), the changes in the boundary conditions between the infinite and finite plate occur on GE and the addition of the free surface ED. In addition, G becomes a special point in the r formulation while both G and E become special points in the z formulation.

$$\underline{\left(\frac{\partial r}{\partial \phi}\right) + r \left(\frac{\partial r}{\partial \psi}\right) \left(\frac{dz}{dr}\right) = 0 \text{ on GE}}$$



Along GE, the r difference equation is

$$r_o^4 - \frac{r_o^3}{2} (r_2 + r_4) + r_o^2 \left[\frac{1}{\alpha^2} - \frac{1}{8} (r_2 - r_4)^2 \right] - \frac{r_o}{2\alpha^2} (r_1 + f) + \frac{1}{8\alpha^2} (r_1 - f)^2 = 0 \quad (C-28)$$

in finite difference form, the boundary condition is,

$$\frac{r_1 - f}{\Delta\phi} + \frac{r_o}{\Delta\psi} (z_2 - z_4) = 0 \quad (C-29)$$

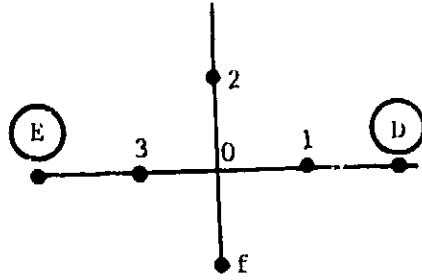
solving for f ,

$$f = r_1 + \alpha r_o (z_2 - z_4) \quad (C-30)$$

and, inserting this into the r difference equation yields the desired result.

$$r_o^4 - \frac{r_o^3}{2} (r_2 + r_4) + r_o^2 \left[\frac{1}{\alpha^2} - \frac{1}{8} (r_2 - r_4)^2 \right] - \frac{r_o}{2\alpha^2} [2r_1 + \alpha r_o (z_2 - z_4)] + \frac{r_o^2}{8} (z_2 - z_4)^2 = 0 \quad (C-31)$$

$$\left(\frac{\partial r}{\partial \phi} \right)^2 + r^2 \left(\frac{\partial r}{\partial \psi} \right)^2 = 1 \quad \text{on ED}$$



The r difference equation can be written

$$r_o^4 - \frac{r_o^3}{2} (r_2 + r_f) + r_o^2 \left[\frac{1}{\alpha^2} - \frac{1}{8} (r_2 - r_f)^2 \right] - \frac{r_o}{2\alpha^2} (r_1 + r_3) + \frac{1}{8\alpha^2} (r_1 - r_3)^2 = 0 \quad (C-32)$$

Using $\left(\frac{\partial r}{\partial \phi}\right)^2 + r^2 \left(\frac{\partial r}{\partial \psi}\right)^2 = 1$ on ED,

$$\left(\frac{r_1 - r_3}{2 \Delta \phi}\right)^2 + r_o^2 \left(\frac{r_2 - r_f}{2 \Delta \psi}\right)^2 = 1 \quad (C-33)$$

Yields

$$(r_2 - r_f)^2 = \frac{1}{r_o^2} \left[4a^2 - \frac{1}{\alpha^2} (r_1 - r_3)^2 \right] \quad (C-34)$$

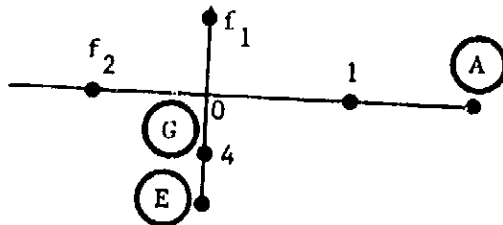
and

$$r_2 + r_f = 2r_2 - \frac{1}{r_o} \sqrt{\left[4a^2 - \frac{1}{\alpha^2} (r_1 - r_3)^2 \right]} \quad (C-35)$$

Substituting (C-34) and (C-35) into (C-32) we obtain

$$r_o^4 - r_o^3 r_2 + r_o^2 \left\{ \frac{1}{\alpha^2} + \frac{1}{2} \sqrt{\left[4a^2 - \frac{1}{\alpha^2} (r_1 - r_3)^2 \right]} \right\} - \frac{r_o}{2\alpha^2} (r_1 + r_3) + \frac{1}{8} \left[-4a^2 + \frac{2}{\alpha^2} (r_1 - r_3)^2 \right] = 0 \quad (C-36)$$

Now, points E and G will be special points since equation (C-31) cannot be directly applied there. One of these positions can be specified as known, $r_E = \text{constant}$. Let us examine special point G



Applying equation (C-10) at point G,

$$r_o^4 - r_o^3 r_4 + r_o^2 \left\{ \frac{1}{\alpha^2} - \frac{1}{2} \sqrt{4a^2 - \frac{1}{\alpha^2} (r_1 - f_2)^2} \right\} - \frac{r_o}{2\alpha^2} (r_1 + f_2) + \frac{1}{8} \left[\frac{2}{\alpha^2} (r_1 - f_2)^2 - 4a^2 \right] = 0 \quad (C-37)$$

Now, applying $\left(\frac{\partial r}{\partial \phi}\right) + r \left(\frac{\partial r}{\partial \psi}\right) \left(\frac{dz}{dr}\right) = 0$ along GE without involving f_1 ,

$$\left(\frac{r_1 - f_2}{2 \Delta \phi}\right) + r_o \left(\frac{r_o - r_4}{\Delta \psi}\right) \left(\frac{z_o - z_4}{r_o - r_4}\right) = 0 \quad (C-38)$$

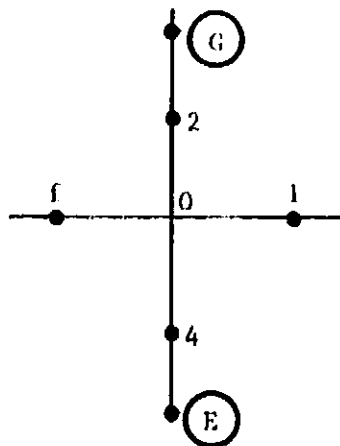
Solving for f_2 ,

$$f_2 = r_1 + 2\alpha r_o (z_o - z_4) \quad (C-39)$$

Therefore, equation (C-37) becomes

$$r_o^4 - r_o^3 r_4 + r_o^2 \left\{ \frac{1}{\alpha^2} - \sqrt{a^2 - r_o^2 (z_o - z_4)^2} \right\} - \frac{r_o}{\alpha^2} \left[r_1 + \alpha r_o (z_o - z_4) \right] + \left[r_o^2 (z_o - z_4)^2 - \frac{a^2}{2} \right] = 0 \quad (C-40)$$

$$\underline{r \left(\frac{\partial z}{\partial \psi}\right) - \left(\frac{\partial z}{\partial \phi}\right) \left(\frac{dz}{dr}\right) = 0 \text{ on GE}}$$



Application of z difference equation yields,

$$z_o = \frac{r_o^2}{2\left(r_o^2 + \frac{1}{\alpha^2}\right)} (z_2 + z_4) + \frac{z_1 + f}{2\left(r_o^2 \alpha^2 + 1\right)} + \frac{(z_2 - z_4)(z_1 - f)}{4\left(r_o^2 \alpha + \frac{1}{\alpha}\right)} \quad (C-41)$$

Now, along GE, $r\left(\frac{\partial z}{\partial \psi}\right) - \left(\frac{\partial z}{\partial \phi}\right)\left(\frac{dz}{dr}\right) = 0$, which in difference form can be written,

$$r_o \left(\frac{z_2 - z_4}{2 \Delta \psi} \right) - \left(\frac{z_1 - f}{2 \Delta \phi} \right) \left(\frac{z_2 - z_4}{r_2 - r_4} \right) = 0 \quad (C-42)$$

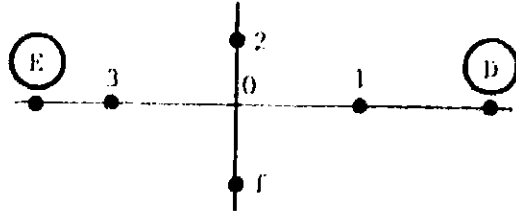
Solving for f ,

$$f = z_1 - r_o \alpha (r_2 - r_4) \quad (C-43)$$

Hence, equation (C-41) becomes

$$z_o = \frac{r_o^2}{2\left(r_o^2 + \frac{1}{\alpha^2}\right)} (z_2 + z_4) + \frac{2z_1 - r_o \alpha (r_2 - r_4)}{2\left(r_o^2 \alpha^2 + 1\right)} + \frac{(z_2 - z_4)[r_o \alpha (r_2 - r_4)]}{4\left(r_o^2 \alpha + \frac{1}{\alpha}\right)} \quad (C-44)$$

$$\underline{r^2 \left(\frac{\partial z}{\partial \psi} \right)^2 + \left(\frac{\partial z}{\partial \phi} \right)^2 = 1 \text{ on ED}}$$



The z difference equation can be written,

$$z_o = \frac{r_o^2}{2\left(r_o^2 + \frac{1}{\alpha^2}\right)} (z_2 + z_f) + \frac{1}{2\left(r_o^2 \alpha^2 + 1\right)} (z_1 + z_3) + \frac{1}{4\left(r_o^2 \alpha + \frac{1}{\alpha}\right)} (z_2 - z_f)(z_1 - z_3) \quad (C-45)$$

Applying $r^2 \left(\frac{\partial z}{\partial \psi}\right)^2 + \left(\frac{\partial z}{\partial \phi}\right)^2 = 1$ on ED,

$$r_o^2 \left(\frac{z_2 - z_f}{2 \Delta \psi}\right)^2 + \left(\frac{z_1 - z_3}{2 \Delta \phi}\right)^2 = 1 \quad (C-46)$$

Solving for $(z_2 - z_f)$.

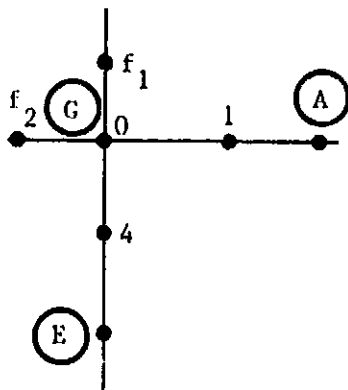
$$z_2 - z_f = \frac{1}{r_o} \sqrt{\left[4a^2 - \frac{1}{\alpha^2} (z_1 - z_3)^2\right]} \quad (C-47)$$

Also,

$$z_f + z_2 = 2z_2 - \frac{1}{r_o} \sqrt{\left[4a^2 - \frac{1}{\alpha^2} (z_1 - z_3)^2\right]} \quad (C-48)$$

Substitution of these last two equations into equation (C-43) yields the desired expression

$$z_0 = \frac{r_0^2}{2\left(r_0^2 + \frac{1}{\alpha^2}\right)} \left\{ 2z_2 - \frac{1}{r_0} \sqrt{\left[4a^2 - \frac{1}{\alpha^2} (z_1 - z_3)^2\right]} \right\} + \frac{z_1 + z_3}{2\left(r_0^2 \alpha^2 + 1\right)} \\ + \frac{z_1 - z_3}{4\left(r_0^2 \alpha + \frac{1}{\alpha}\right)} \frac{1}{r_0} \sqrt{\left[4a^2 - \frac{1}{\alpha^2} (z_1 - z_3)^2\right]} \quad (C-49)$$



Applying equation (C-22) at point G yields,

$$z_0 = \frac{r_0^2}{2\left(r_0^2 + \frac{1}{\alpha^2}\right)} \left\{ \frac{1}{r_0} \sqrt{\left[4a^2 - \frac{1}{\alpha^2} (z_1 - f_2)^2\right]} + 2z_4 \right\} + \frac{z_1 + f_2}{2\left(r_0^2 \alpha^2 + 1\right)} \\ + \frac{z_1 - f_2}{4r_0\left(r_0^2 \alpha + \frac{1}{\alpha}\right)} \sqrt{\left[4a^2 - \frac{1}{\alpha^2} (z_1 - f_2)^2\right]} \quad (C-50)$$

To find f_2 , we apply $r\left(\frac{\partial z}{\partial \psi}\right) - \left(\frac{\partial z}{\partial \phi}\right)\left(\frac{dz}{dr}\right) = 0$ without involving f_1 ,

$$r_0 \left(\frac{z_0 - z_4}{\Delta \psi} \right) - \left(\frac{z_1 - f_2}{2 \Delta \phi} \right) \left(\frac{z_0 - z_4}{r_0 - r_4} \right) = 0 \quad (C-51)$$

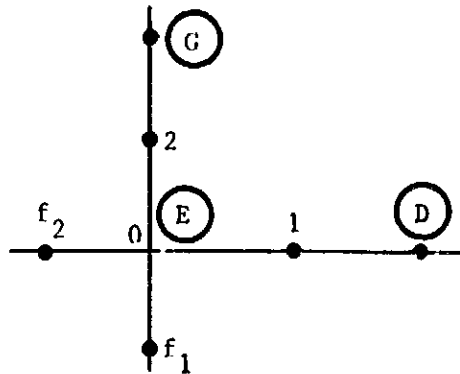
Solving for f_2 ,

$$f_2 = z_1 - 2r_0 \alpha (r_0 - r_4) \quad (C-52)$$

Substitution into (C-50) yields

$$z_0 = \frac{r_0}{r_0^2 + \frac{1}{\alpha^2}} \left\{ \frac{1}{r_0} \sqrt{[a^2 - r_0^2(r_0 - r_h)^2]} + z_h \right\} + \frac{z_1 - r_0 \alpha (r_0 - r_h)}{r_0^2 \alpha^2 + 1} + \frac{r_0 - r_h}{r_0^2 + \frac{1}{\alpha^2}} \sqrt{[a^2 - r_0^2(r_0 - r_h)^2]} \quad (C-53)$$

Let us examine the special point at E



Application of equation (C-49) at point E results in,

$$z_0 = \frac{r_0^2}{2\left(r_0^2 + \frac{1}{\alpha^2}\right)} \left\{ 2z_2 - \frac{1}{r_0} \sqrt{\left[4a^2 - \frac{1}{\alpha^2} (z_1 - f_2)^2\right]} \right\} + \frac{1}{2\left(r_0^2 \alpha^2 + 1\right)} (z_1 + f_2) + \frac{z_1 - f_2}{4r_0\left(r_0^2 + \frac{1}{\alpha}\right)} \sqrt{\left[4a^2 - \frac{1}{\alpha^2} (z_1 - f_2)^2\right]} \quad (C-54)$$

In order to find the fictitious point, f_2 , we apply

$$r \left(\frac{\partial z}{\partial \psi} \right) - \left(\frac{\partial z}{\partial \phi} \right) \left(\frac{dz}{d\tau} \right) = 0 \quad \text{on GE, without involving } f_1$$

$$\frac{r_0(z_2 - z_0)}{\Delta\psi} - \frac{z_1 - f_2}{2\Delta\psi} \frac{z_2 - z_0}{r_2 - r_0} = 0 \quad (C-55)$$

Solving for f_2 ,

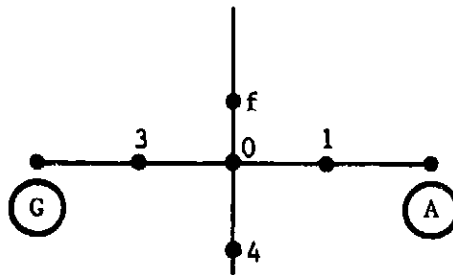
$$f_2 = z_1 - 2r_0\alpha(r_2 - r_0) \quad (C-56)$$

Finally, obtaining from equation (C-54),

$$z_0 = \frac{r_0^2}{r_0^2 + \frac{1}{\alpha^2}} \left\{ z_2 - \frac{1}{r_0} \sqrt{\left[a^2 - r_0^2(r_2 - r_0)^2 \right]} \right\} + \frac{z_1 - r_0\alpha(r_2 - r_0)}{r_0^2\alpha^2 + 1} + \frac{r_2 - r_0}{r_0^2 + \frac{1}{\alpha^2}} \sqrt{\left[a^2 - r_0^2(r_2 - r_0)^2 \right]} \quad (C-57)$$

C. Surface Tension

$$\left(\frac{\partial r}{\partial \phi} \right)^2 + r^2 \left(\frac{\partial r}{\partial \psi} \right)^2 = \frac{1}{\left\{ 1 - \frac{2}{We} + \frac{2}{We} \frac{1}{r} \frac{d}{dr} \left[\frac{r^2}{\sqrt{\left(\frac{\partial r}{\partial \phi} \right)^2 + r^2}} \right]} \right\}} \quad \text{on } \Delta G$$



Applying r difference equation (eq. (131)) at point 0 where f is a fictitious point outside the boundary

$$r_o^4 - \frac{r_o^3}{2} (r_f + r_4) + r_o^2 \left[\frac{1}{\alpha^2} - \frac{1}{8} (r_f - r_4)^2 \right] - \frac{r_o}{2\alpha^2} (r_1 + r_3) + \frac{1}{8\alpha^2} (r_1 - r_3)^2 = 0 \quad (C-58)$$

in difference form, the free surface boundary condition becomes

$$\left(\frac{r_1 - r_3}{2 \Delta\phi} \right)^2 + r_o^2 \left(\frac{r_f - r_4}{2 \Delta\psi} \right)^2 = \frac{1}{1 - \frac{2}{We} + \frac{2}{We} \frac{1}{r_o} \frac{d}{dr_o} \left\{ \frac{r_o^2}{\sqrt{\left[\frac{(r_1 - r_3)/2 \Delta\phi}{(r_f - r_4)/2 \Delta\psi} \right]^2 + r_o^2}} \right\}} \quad (C-59)$$

Simplifying by using $\alpha = \Delta\phi/\Delta\psi$ and defining $Q = \Delta\psi$ yields,

$$\frac{1}{\alpha^2} (r_1 - r_3)^2 + r_o^2 (r_f - r_4)^2 = \frac{4\alpha^2}{1 - \frac{2}{We} + \frac{2}{We} \frac{1}{r_o} \frac{d}{dr_o} \left(\frac{r_o^2}{\sqrt{Q + r_o^2}} \right)} \quad (C-60)$$

Now, examine

$$\frac{1}{r_o} \frac{d}{dr_o} \left(\frac{r_o^2}{\sqrt{Q + r_o^2}} \right)$$

As an approximation to this derivative Q is assumed as a constant.

In actuality, $Q = f(r_f)$ and $r_f = f(r_o)$. Expanding

$$\frac{1}{r_o} \frac{d}{dr_o} \left(\frac{r_o^2}{\sqrt{Q + r_o^2}} \right)$$

yields

$$\frac{1}{r_c} \frac{d}{dr_o} \left(\frac{r_o^2}{\sqrt{Q + r_o^2}} \right) = \left[\frac{2Q + r_o^2}{\sqrt{(Q + r_o^2)}(Q + r_o^2)} \right] \quad (C-61)$$

Therefore, the finite difference representation for the free surface becomes

$$\frac{1}{\alpha^2} (r_1 - r_3)^2 + r_o^2 (r_f - r_4)^2 = \frac{4a^2}{1 - \frac{2}{We} + \frac{2}{We} \left[\frac{2Q + r_o^2}{\sqrt{Q + r_o^2}(Q + r_o^2)} \right]} \quad (C-62)$$

r_f must be eliminated between equations (C-58) and (C-62). Let us define

$$x = r_f - r_4 \quad (C-63)$$

Equation (C-62) can be written

$$\frac{1}{\alpha^2} (r_1 - r_3)^2 + r_o^2 x^2 = \frac{4a^2}{1 - \frac{2}{We} + \frac{2}{We} \left[\frac{2Q + r_o^2}{\sqrt{Q + r_o^2}(Q + r_o^2)} \right]} \quad (C-64)$$

Where

$$Q = \frac{(r_1 - r_3)^2}{x^2} \cdot \frac{1}{\alpha^2} \quad (C-65)$$

Inserting (C-63) into (C-58) yields

$$\frac{r_o^2 x^2}{8} + \frac{r_o^3}{2} x - r_o^4 + r_o^3 r_4 - \frac{r_o^2}{\alpha^2} + \frac{r_o}{2\alpha^2} (r_1 + r_3) - \frac{1}{8\alpha^2} (r_1 - r_3)^2 = 0 \quad (C-66)$$

This is of the form

$$A'x^2 + B'x + C' = 0$$

Hence

$$\chi = \frac{-B' + \sqrt{B'^2 - 4A'C'}}{2A'} \quad (C-67)$$

where

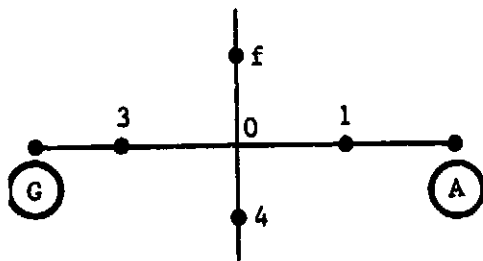
$$A' = \frac{r_0^2}{8} \quad (C-68)$$

$$B' = \frac{r_0^3}{2} \quad (C-69)$$

$$C' = -r_0^4 + r_0^3 r_4 - \frac{r_0^2}{\alpha^2} + \frac{r_0}{2\alpha^2} (r_1 + r_3) - \frac{1}{8\alpha^2} (r_1 - r_3)^2 \quad (C-70)$$

The sign in front of the square root in equation (C-67) was chosen as positive since χ must be greater than or equal to zero. In addition,

$$r^2 \left(\frac{\partial z}{\partial \psi} \right)^2 + \left(\frac{\partial z}{\partial \phi} \right)^2 = \frac{1}{1 - \frac{2}{We} + \frac{2}{We} \frac{1}{r} \frac{d}{dr} \left[\frac{r}{\sqrt{r^2 \left(\frac{\partial z}{\partial \psi} \right)^2 + 1}} \right]} \quad \text{on AG}$$



Applying z difference equation (132) at point 0 where f is a fictitious point outside the boundary

$$z_0 = \frac{r_0^2}{2 \left(r_0^2 + \frac{1}{\alpha^2} \right)} (f + z_4) + \frac{1}{2 \left(r_0^2 \alpha^2 + 1 \right)} (z_1 + z_3) + \frac{(f - z_4)(z_1 - z_3)}{4 \left(r_0^2 \alpha + \frac{1}{\alpha} \right)} \quad (C-71)$$

In finite difference form, the free surface boundary condition can be written,

$$r_o^2 (f - z_4)^2 + \frac{1}{\alpha^2} (z_1 - z_3)^2 = \frac{4a^2}{1 - \frac{2}{We} + \frac{2}{We} \frac{1}{r_o} \frac{d}{dr_o} \left(\frac{r_o}{\sqrt{r_o^2 Q^* + 1}} \right)} \quad (C-72)$$

where,

$$Q^* = \alpha^2 \frac{(f - z_4)^2}{(z_1 - z_3)^2} \quad (C-73)$$

As an approximation, Q^* is assumed to be a constant. Expanding

$$\frac{1}{r_o} \frac{d}{dr_o} \left(\frac{r_o}{\sqrt{r_o^2 Q^* + 1}} \right)$$

obtaining

$$\frac{1}{r_o} \frac{d}{dr_o} \left(\frac{r_o}{\sqrt{r_o^2 Q^* + 1}} \right) = \frac{1}{r_o (r_o^2 Q^* + 1) \sqrt{r_o^2 Q^* + 1}} \quad (C-74)$$

Therefore, the finite difference representation along the free surface becomes

$$r_o^2 (f - z_4)^2 + \frac{1}{\alpha^2} (z_1 - z_3)^2 = \frac{4a^2}{\left[1 - \frac{2}{We} + \frac{2}{We} \frac{1}{r_o} \frac{1}{(r_o^2 Q^* + 1) \sqrt{r_o^2 Q^* + 1}} \right]} \quad (C-75)$$

f must now be eliminated between equation (C-71) and (C-75). The manner in which this is done is as follows: Equation (C-75) is solved for $f = F_{ct}(z_1, z_3, z_4)$. The results are then inserted into equation (C-71). In this way, equation (C-71) remains explicit in z_o . Actually, it will be more convenient to solve for the variable $(f - z_4)$ instead of

f since equation (C-71) can be expressed as,

$$z_0 = \frac{r_0^2 z_4}{r_0^2 + \frac{1}{\alpha^2}} + \frac{z_1 + z_3}{2(r_0^2 \alpha^2 + 1)} + (f - z_4) \left[\frac{2\alpha r_0^2 + (z_1 - z_3)}{4\alpha \left(r_0^2 + \frac{1}{\alpha^2} \right)} \right] \quad (C-76)$$

Turning our attention to equation (C-74), it is solved for $(f - z_4)$

$$\frac{\alpha^2 r_0^2 (f - z_4)^2}{(z_1 - z_3)^2} + 1 =$$

$$\frac{4a^2 \alpha^2}{(z_1 - z_3)^2} \left\{ 1 - \frac{2}{We} + \frac{2}{We} \frac{1}{r_0} \left[\frac{r_0^2 \alpha^2 (f - z_4)^2}{(z_1 - z_3)^2} + 1 \right] \sqrt{\frac{r_0^2 \alpha^2 (f - z_4)^2}{(z_1 - z_3)^2} + 1} \right\} \quad (C-77)$$

A new variable T^2 is introduced

$$T^2 = \frac{\alpha^2 r_0^2 (f - z_4)^2}{(z_1 - z_3)^2} + 1 \quad (C-78)$$

Also, let

$$C_0 = \frac{4a^2 \alpha^2}{(z_1 - z_3)^2} \quad (C-79)$$

$$C_1 = 1 - \frac{2}{We} \quad (C-80)$$

$$C_2 = \frac{2}{We} \cdot \frac{1}{r_0} \quad (C-81)$$

Making these substitutions into equation (C-77) results in a cubic equation for T

$$T^3 - \frac{c_0}{c_1} T + \frac{c_2}{c_1} = 0 \quad (\text{C-82})$$

Rewriting this as follows:

$$T^3 + aT + b = 0 \quad (\text{C-83})$$

Once T is found from (C-83), $(f - z_4)$ is calculated from equation (C-78) as follows:

$$f - z_4 = \pm \frac{z_1 - z_3}{\alpha r_0} \sqrt{T^2 - 1} \quad (\text{C-84})$$

Appendix D - "Computer Solutions/Listings"

A. Infinite Flat Plate

- I. Computer Listing
- II. Coarse Mesh Solution for r and z
- III. Computer Listing
- IV. Fine Mesh Solution for r and z

B. Finite Plate

- V. Computer Listing ($R_o/L = 1/2$)
- VI. Coarse Mesh Solution
- VII. Computer Listing ($R_o/L = 3/4$)
- VIII. Coarse Mesh Solution

C. Surface Tension Model

- IX. Computer Listing
- X. r Solution
- XI. z Solution

I. F AND Z COMPUTER PROGRAM/INFINITE PLATE/COARSE SOLUTION

DATE 070274 PAGE 1

INFINITE FLAT PLATE

FOR=IS MAIN
FOR 011A-070274-15 79 09 (,0)

MAIN PROGRAM

STORAGE USED CODE(1) 000050; DATA(0) 017271; BLANK COMMON(2) 000000

EXTERNAL REFERENCES (BLOCK, NAME)

CODE FCMS
0006 NINTRS
0005 MPDUS
0004 MIOIS
0007 MIOCS
0010 MSTOP5

STORAGE ASSIGNMENT (BLOCK, TYPE, RELATIVE LOCATION, NAME)

0000 017261 100F 0001 000014 1076 0000 R 017256 ACC 0000 R 000188 AJIMV 0000 F 017260 DMAX
0000 R 030062 F 0000 I 017254 IPRINT 0000 I 017253 J 0000 I 017257 MAXFUN 0000 I 017252 M
0000 R 017245 STEP 0000 R 005050 M 0000 R 000000 X

00101 10 DIMENSION X(50),F(50),AJIMV(50),MIS(250)
00102 20 100 FORMAT (R1F10.23)
00103 30 N=50
00104 40 READ(5,100)X(I),J=1,M
00105 50 IPRINT=1
00106 60 STEP=0001
00107 70 ACC=000001
00108 80 MAXFUN=190
00109 90 DMAX=1.0
00110 100 CALL FOWSIN,X,F,AJIMV,STEP,DMAX,ACC,MAXFUN,IPRINT,M
00111 110 END

END OF COMPILATION NO DIAGNOSTICS.

COPYRIGHT PAGE IS
OF POOR QUALITY

DATE 070274 PAGE 3

INFINITE FLAT PLATE

```

00103 DIMENSION X(1),F(1),AJINVM(N),M(1)
00104 DIMENSION BJIN(50,50)
00105 C
00106 C
00107 C
00108 C
00109 C
00110 C
00111 C
00112 C
00113 C
00114 C
00115 C
00116 C
00117 C
00118 C
00119 C
00120 C
00121 C
00122 C
00123 C
00124 C
00125 C
00126 C
00127 C
00128 C
00129 C
00130 C
00131 C
00132 C
00133 C
00134 C
00135 C
00136 C
00137 C
00138 C
00139 C
00140 C
00141 C
00142 C
00143 C
00145 C
00146 C
00147 C
00148 C
00149 C
00150 C
00151 C
00152 C
00153 C
00154 C
00155 C
00156 C
00157 C
00158 C
00159 C
00160 C
00161 C
00162 C
00163 C
00164 C
00165 C
00166 C
00167 C
00168 C
00169 C
00170 C
00171 C
00172 C
00173 C
00174 C
00175 C
00176 C
00177 C
00178 C
00179 C
00180 C
00181 C
00182 C
00183 C
00184 C
00185 C
00186 C
00187 C
00188 C
00189 C
00190 C
00191 C
00192 C
00193 C
00194 C
00195 C
00196 C
00197 C
00198 C
00199 C
00200 C
00201 C
00202 C
00203 C
00204 C
00205 C
00206 C
00207 C
00208 C
00209 C
00210 C
00211 C
00212 C
00213 C
00214 C
00215 C
00216 C
00217 C
00218 C
00219 C
00220 C
00221 C
00222 C
00223 C
00224 C
00225 C
00226 C
00227 C
00228 C
00229 C
00230 C
00231 C
00232 C
00233 C
00234 C
00235 C
00236 C
00237 C
00238 C
00239 C
00240 C
00241 C
00242 C
00243 C
00244 C
00245 C
00246 C
00247 C
00248 C
00249 C
00250 C
00251 C
00252 C
00253 C
00254 C
00255 C
00256 C
00257 C
00258 C
00259 C
00260 C
00261 C
00262 C
00263 C
00264 C
00265 C
00266 C
00267 C
00268 C
00269 C
00270 C
00271 C
00272 C
00273 C
00274 C
00275 C
00276 C
00277 C
00278 C
00279 C
00280 C
00281 C
00282 C
00283 C
00284 C
00285 C
00286 C
00287 C
00288 C
00289 C
00290 C
00291 C
00292 C
00293 C
00294 C
00295 C
00296 C
00297 C
00298 C
00299 C
00300 C
00301 C
00302 C
00303 C
00304 C
00305 C
00306 C
00307 C
00308 C
00309 C
00310 C
00311 C
00312 C
00313 C
00314 C
00315 C
00316 C
00317 C
00318 C
00319 C
00320 C
00321 C
00322 C
00323 C
00324 C
00325 C
00326 C
00327 C
00328 C
00329 C
00330 C
00331 C
00332 C
00333 C
00334 C
00335 C
00336 C
00337 C
00338 C
00339 C
00340 C
00341 C
00342 C
00343 C
00344 C
00345 C
00346 C
00347 C
00348 C
00349 C
00350 C
00351 C
00352 C
00353 C
00354 C
00355 C
00356 C
00357 C
00358 C
00359 C
00360 C
00361 C
00362 C
00363 C
00364 C
00365 C
00366 C
00367 C
00368 C
00369 C
00370 C
00371 C
00372 C
00373 C
00374 C
00375 C
00376 C
00377 C
00378 C
00379 C
00380 C
00381 C
00382 C
00383 C
00384 C
00385 C
00386 C
00387 C
00388 C
00389 C
00390 C
00391 C
00392 C
00393 C
00394 C
00395 C
00396 C
00397 C
00398 C
00399 C
00400 C
00401 C
00402 C
00403 C
00404 C
00405 C
00406 C
00407 C
00408 C
00409 C
00410 C
00411 C
00412 C
00413 C
00414 C
00415 C
00416 C
00417 C
00418 C
00419 C
00420 C
00421 C
00422 C
00423 C
00424 C
00425 C
00426 C
00427 C
00428 C
00429 C
00430 C
00431 C
00432 C
00433 C
00434 C
00435 C
00436 C
00437 C
00438 C
00439 C
00440 C
00441 C
00442 C
00443 C
00444 C
00445 C
00446 C
00447 C
00448 C
00449 C
00450 C
00451 C
00452 C
00453 C
00454 C
00455 C
00456 C
00457 C
00458 C
00459 C
00460 C
00461 C
00462 C
00463 C
00464 C
00465 C
00466 C
00467 C
00468 C
00469 C
00470 C
00471 C
00472 C
00473 C
00474 C
00475 C
00476 C
00477 C
00478 C
00479 C
00480 C
00481 C
00482 C
00483 C
00484 C
00485 C
00486 C
00487 C
00488 C
00489 C
00490 C
00491 C
00492 C
00493 C
00494 C
00495 C
00496 C
00497 C
00498 C
00499 C
00500 C
00501 C
00502 C
00503 C
00504 C
00505 C
00506 C
00507 C
00508 C
00509 C
00510 C
00511 C
00512 C
00513 C
00514 C
00515 C
00516 C
00517 C
00518 C
00519 C
00520 C
00521 C
00522 C
00523 C
00524 C
00525 C
00526 C
00527 C
00528 C
00529 C
00530 C
00531 C
00532 C
00533 C
00534 C
00535 C
00536 C
00537 C
00538 C
00539 C
00540 C
00541 C
00542 C
00543 C
00544 C
00545 C
00546 C
00547 C
00548 C
00549 C
00550 C
00551 C
00552 C
00553 C
00554 C
00555 C
00556 C
00557 C
00558 C
00559 C
00560 C
00561 C
00562 C
00563 C
00564 C
00565 C
00566 C
00567 C
00568 C
00569 C
00570 C
00571 C
00572 C
00573 C
00574 C
00575 C
00576 C
00577 C
00578 C
00579 C
00580 C
00581 C
00582 C
00583 C
00584 C
00585 C
00586 C
00587 C
00588 C
00589 C
00590 C
00591 C
00592 C
00593 C
00594 C
00595 C
00596 C
00597 C
00598 C
00599 C
00600 C
00601 C
00602 C
00603 C
00604 C
00605 C
00606 C
00607 C
00608 C
00609 C
00610 C
00611 C
00612 C
00613 C
00614 C
00615 C
00616 C
00617 C
00618 C
00619 C
00620 C
00621 C
00622 C
00623 C
00624 C
00625 C
00626 C
00627 C
00628 C
00629 C
00630 C
00631 C
00632 C
00633 C
00634 C
00635 C
00636 C
00637 C
00638 C
00639 C
00640 C
00641 C
00642 C
00643 C
00644 C
00645 C
00646 C
00647 C
00648 C
00649 C
00650 C
00651 C
00652 C
00653 C
00654 C
00655 C
00656 C
00657 C
00658 C
00659 C
00660 C
00661 C
00662 C
00663 C
00664 C
00665 C
00666 C
00667 C
00668 C
00669 C
00670 C
00671 C
00672 C
00673 C
00674 C
00675 C
00676 C
00677 C
00678 C
00679 C
00680 C
00681 C
00682 C
00683 C
00684 C
00685 C
00686 C
00687 C
00688 C
00689 C
00690 C
00691 C
00692 C
00693 C
00694 C
00695 C
00696 C
00697 C
00698 C
00699 C
00700 C
00701 C
00702 C
00703 C
00704 C
00705 C
00706 C
00707 C
00708 C
00709 C
00710 C
00711 C
00712 C
00713 C
00714 C
00715 C
00716 C
00717 C
00718 C
00719 C
00720 C
00721 C
00722 C
00723 C
00724 C
00725 C
00726 C
00727 C
00728 C
00729 C
00730 C
00731 C
00732 C
00733 C
00734 C
00735 C
00736 C
00737 C
00738 C
00739 C
00740 C
00741 C
00742 C
00743 C
00744 C
00745 C
00746 C
00747 C
00748 C
00749 C
00750 C
00751 C
00752 C
00753 C
00754 C
00755 C
00756 C
00757 C
00758 C
00759 C
00760 C
00761 C
00762 C
00763 C
00764 C
00765 C
00766 C
00767 C
00768 C
00769 C
00770 C
00771 C
00772 C
00773 C
00774 C
00775 C
00776 C
00777 C
00778 C
00779 C
00780 C
00781 C
00782 C
00783 C
00784 C
00785 C
00786 C
00787 C
00788 C
00789 C
00790 C
00791 C
00792 C
00793 C
00794 C
00795 C
00796 C
00797 C
00798 C
00799 C
00800 C
00801 C
00802 C
00803 C
00804 C
00805 C
00806 C
00807 C
00808 C
00809 C
00810 C
00811 C
00812 C
00813 C
00814 C
00815 C
00816 C
00817 C
00818 C
00819 C
00820 C
00821 C
00822 C
00823 C
00824 C
00825 C
00826 C
00827 C
00828 C
00829 C
00830 C
00831 C
00832 C
00833 C
00834 C
00835 C
00836 C
00837 C
00838 C
00839 C
00840 C
00841 C
00842 C
00843 C
00844 C
00845 C
00846 C
00847 C
00848 C
00849 C
00850 C
00851 C
00852 C
00853 C
00854 C
00855 C
00856 C
00857 C
00858 C
00859 C
00860 C
00861 C
00862 C
00863 C
00864 C
00865 C
00866 C
00867 C
00868 C
00869 C
00870 C
00871 C
00872 C
00873 C
00874 C
00875 C
00876 C
00877 C
00878 C
00879 C
00880 C
00881 C
00882 C
00883 C
00884 C
00885 C
00886 C
00887 C
00888 C
00889 C
00890 C
00891 C
00892 C
00893 C
00894 C
00895 C
00896 C
00897 C
00898 C
00899 C
00900 C
00901 C
00902 C
00903 C
00904 C
00905 C
00906 C
00907 C
00908 C
00909 C
00910 C
00911 C
00912 C
00913 C
00914 C
00915 C
00916 C
00917 C
00918 C
00919 C
00920 C
00921 C
00922 C
00923 C
00924 C
00925 C
00926 C
00927 C
00928 C
00929 C
00930 C
00931 C
00932 C
00933 C
00934 C
00935 C
00936 C
00937 C
00938 C
00939 C
00940 C
00941 C
00942 C
00943 C
00944 C
00945 C
00946 C
00947 C
00948 C
00949 C
00950 C
00951 C
00952 C
00953 C
00954 C
00955 C
00956 C
00957 C
00958 C
00959 C
00960 C
00961 C
00962 C
00963 C
00964 C
00965 C
00966 C
00967 C
00968 C
00969 C
00970 C
00971 C
00972 C
00973 C
00974 C
00975 C
00976 C
00977 C
00978 C
00979 C
00980 C
00981 C
00982 C
00983 C
00984 C
00985 C
00986 C
00987 C
00988 C
00989 C
00990 C
00991 C
00992 C
00993 C
00994 C
00995 C
00996 C
00997 C
00998 C
00999 C

```

INFINITE FLAT PLATE

DIMENSION X(1),F(1),AJINVM(N),M(1)
DIMENSION BJIN(50,50)

SET VARIOUS PARAMETERS

MAXC = 0
MAXC COUNTS THE NUMBER OF CALLS OF CALFUM

MF = N+4
MTEST = MY

MY AND MTEST CAUSE AN ERROR RETURN IF FIXJ DOES NOT DECREASE

DTEST = FLOAT(N) -0.5
DTEST IS USED TO MAINTAIN LINEAR INDEPENDENCE

MX = N+1
MY = N+2
MZ = N+3
ND = NDC+N

THESE PARAMETERS SEPARATE THE WORKING SPACE ARRAY M

FMIN = 0.0

USUALLY FMIN IS THE LEAST CALCULATED VALUE OF F(X)
AND THE BEST X IS 'N'*(MFX+1) TO MINX+M)

DD = 0.0
DSS = DSTEP*DSTEP
DM = DMAX*DMAX
DMM = D*DD*DM
IS = 5

IS CONTROLS A GO TO STATEMENT FOLLOWING A CALL OF CALFUM

TINC = 1.0

TINC IS USED IN THE CRITERION TO INCREASE THE STEP LENGTH
START A NEW PAGE FOR PRINTING

IS IPRINT) 1,1,85
B5 WRITE(6,*5)
B6 FORMAT(11M)

CALL SUBROUTINE CALFUM

MAXC = MAXC+1
CALL CALFUM(X,F)

BEST FOR CONVERGENCE

F50 = 0.0
DO 7 F=1,M
F50 = F50 + F(1)*F(1)
2 CONTINUE
IF(F50-ACC) 3,3,4

DATE 070274 PAGE

INFINITE FLAT PLATE

```

00195
00196
00197
00198
00199
00200
00201
00202
00203
00204
00205
00206
00207
00208
00209
00210
00211
00212
00213
00214
00215
00216
00217
00218
00219
00220
00221
00222
00223
00224
00225
00226
00227
00228
00229
00230
00231
00232
00233
00234
00235
00236
00237
00238
00239
00240
00241
00242
00243
00244
00245
00246
00247
00248
00249
00250
00251
00252
00253
00254
00255
00256
00257
00258
00259
00260
00261
00262
00263
00264
00265
00266
00267
00268
00269
00270
00271
00272
00273
00274
00275
00276
00277
00278
00279
00280
00281
00282
00283
00284
00285
00286
00287
00288
00289
00290
00291
00292
00293
00294
00295
00296
00297
00298
00299
00300
00301
00302
00303
00304
00305
00306
00307
00308
00309
00310
00311
00312
00313
00314
00315
00316
00317
00318
00319
00320
00321
00322
00323
00324
00325
00326
00327
00328
00329
00330
00331
00332
00333
00334
00335
00336
00337
00338
00339
00340
00341
00342
00343
00344
00345
00346
00347
00348
00349
00350
00351
00352
00353
00354
00355
00356
00357
00358
00359
00360
00361
00362
00363
00364
00365
00366
00367
00368
00369
00370
00371
00372
00373
00374
00375
00376
00377
00378
00379
00380
00381
00382
00383
00384
00385
00386
00387
00388
00389
00390
00391
00392
00393
00394
00395
00396
00397
00398
00399
00400
00401
00402
00403
00404
00405
00406
00407
00408
00409
00410
00411
00412
00413
00414
00415
00416
00417
00418
00419
00420
00421
00422
00423
00424
00425
00426
00427
00428
00429
00430
00431
00432
00433
00434
00435
00436
00437
00438
00439
00440
00441
00442
00443
00444
00445
00446
00447
00448
00449
00450
00451
00452
00453
00454
00455
00456
00457
00458
00459
00460
00461
00462
00463
00464
00465
00466
00467
00468
00469
00470
00471
00472
00473
00474
00475
00476
00477
00478
00479
00480
00481
00482
00483
00484
00485
00486
00487
00488
00489
00490
00491
00492
00493
00494
00495
00496
00497
00498
00499
00500

```

C PROVIDE PRINTING OF FINAL SOLUTION IF REQUESTED
3 IF (IPRINT) 5,5,6
6 WRITE(6,7) MAXC
7 FORMAT (1MK,5X 20THE FINAL SOLUTION REQUIRED IS,2X2ZHCALLS OF C
1ALFUM AND IS)
WRITE (6,8) (I,X(I),F(1),I=1,N)
8 FORMAT(1MK,4XIMI,2XIMH(I),1X4MFI(I))//((15,2E17.8))
WRITE (6,9) FSO
9 FORMAT (1MK,6X22THE SUM OF SQUARES IS E17.8)
5 RETURN
C
C TEST FOR ERROR RETURN BECAUSE FIXI DOES NOT DECREASE
C
* GO TO 110,11,11,10,11,15
10 IF (FSO - FMIN) 15,20,20
20 IF (DD - DSS) 12,12,11
12 NTEST = NTEST - 1
IF (NTEST) 13,14,11
14 WRITE (6,16) NI
16 FORMAT (1MK,6X23ERROR RETURN BECAUSE IS,2X6HCALLS OF CALFUM FAIL
IED TO IMPROVE THE RESIDUALS)
17 DO 18 1,1+N
NFI = NI + 1
MFI = NI + 1
X(1) = MIN(X(1),
F(1) = MIN(F(1),
FSO = FMIN
GO TO 3
C
C ERROR RETURN BECAUSE A NEW JACOBIAN IS UNSUCCESSFUL
C
13 WRITE(6,19)
19 FORMAT(1MK,6X20ERROR RETURN BECAUSE FIXI FAILED TO DECREASE USING
1A NEW JACOBIAN)
GO TO 17
15 NTEST = NI
C
C TEST WHETHER THERE HAVE BEEN MAXFUN CALLS OF CALFUM
C
11 IF (MAXFUN - MAXC) 21,21,27
21 WRITE(6,27) MAXC
22 FORMAT(1MK,6X27ERROR RETURN BECAUSE THERE HAVE BEEN IS,2X 15HCAL
LS OF CALFUM)
IF (FSO - FMIN) 3,17,17
C
C PROVIDE PRINTING IF REQUESTED
C
27 IF (IPRINT) 28,28,25
25 WRITE(6,28) MAXC
26 FORMAT(1MK,6X28THE TIME IS,1X25THE CALL OF CALFUM AT MAXET
WRITE(6,29) (I,X(I),F(1),I=1,N)
WRITE(6,9) FSO
28 GO TO 17,28,29,27,30,15
C
C STOPS THE RESULT OF THE INITIAL CALL OF CALFUM
C

INFINITE FLAT PLATE

```

0000* 1750
00005 1760
0001P 1750
00011 1760
00012 1770
00013 1780
00014 1790
00016 1800
00017 1810
00020 1820
00021 1830
00021 1840
00021 1850
00021 1860
00021 1870
00023 1880
00023 1890
00023 1900
00023 1910
00026 1910
00026 1920
00026 1930
00031 1940
00031 1950
00032 1960
00033 1970
00037 1980
00037 1990
00040 2000
00041 2010
00043 2020
00043 2030
00043 2040
00043 2050
00045 2060
00045 2070
00050 2080
00051 2090
00052 2100
00053 2110
00056 2120
00057 2130
00057 2140
00057 2150
00057 2160
00061 2170
00062 2180
00065 2190
00066 2200
00071 2210
00072 2220
00073 2230
00075 2240
00076 2250
00080 2260
00081 2270
00081 2280
00501 2290

```

```

00 90 J=1,N
MPPJ = MF + J
X(I) = X(I) - W(I)*M(FPJ)
F(I) = F(I) - R(I)*W(I),J=MIN(FPJ)
M = M*W
*0 CONTINUE
DS = DS + X(I)*X(I)
DME DM+FAID*F(I)
SP = SP+X(I)*F(I)
*9 CONTINUE
C TEST WHETHER A NEARBY STATIONARY POINT IS PREDICTED
C
C IF FMIN*FMIN-DM*DS) N1,N1,*2
C
C IF SO THEN RETURN OR REVISE JACOBIAN
C
*2 GO TO (N3,N3,N3),IS
*4 WRITE (6,N5)
*5 FORMAT (1H,*, BIGGEROR RETURN BECAUSE A NEARBY STATIONARY POINT
10F FIX) IS PREDICTED)
GO TO 17
*3 WTEST = 0
DO *6 I=1,M
NXP1 = NX + I
X(I) = W(XP1)
*6 CONTINUE
*6 GO TO 32
C TEST WHETHER TO APPLY THE FULL NEWTON CORRECTION
C
C N1 IS = 2
IF (DM-DM) N7,N7,*8
*7 DD = AMAX1(DM,DS)
DS = -25*DM
TIME = 1.0
IF (DM-DS) N9,58,58
*9 IS = *4
GO TO 90
C CALCULATE THE LENGTH OF THE STEEPEST DESCENT STEP
C
*8 M=0
DMULT = 0.0
DO 51 I=1,M
DM = 0.0
DO 52 J=1,N
M = M+1
DM = DM + W(I)*X(I)
*52 CONTINUE
DMULT = DMULT+DM*DM
*51 CONTINUE
DMULT = DS/DMULT
DS = DS* DMULT*DMULT
C TEST WHETHER TO USE THE STEEPEST DESCENT DIRECTION
C

```

ORIGINAL PAGE IS
OF POOR QUALITY

DATE 07027M PAGE 7

```

INFINITE FLAT PLATE
C 2300 IF (DS-DD) 53,54,56
C 2310 TEST WHETHER INITIAL VALUE OF DD HAS BEEN SET
C 2320
C 2330
C 2340
C 2350
C 2360
C 2370
C 2380
C 2390
C 2400
C 2410
C 2420
C 2430
C 2440
C 2450
C 2460
C 2470
C 2480
C 2490
C 2500
C 2510
C 2520
C 2530
C 2540
C 2550
C 2560
C 2570
C 2580
C 2590
C 2600
C 2610
C 2620
C 2630
C 2640
C 2650
C 2660
C 2670
C 2680
C 2690
C 2700
C 2710
C 2720
C 2730
C 2740
C 2750
C 2760
C 2770
C 2780
C 2790
C 2800
C 2810
C 2820
C 2830
C 2840
C 2850
C 2860
C 2870
C 2880
C 2890
C 2900
C 2910
C 2920
C 2930
C 2940
C 2950
C 2960
C 2970
C 2980
C 2990
C 3000
C 3010
C 3020
C 3030
C 3040
C 3050
C 3060
C 3070
C 3080
C 3090
C 3100
C 3110
C 3120
C 3130
C 3140
C 3150
C 3160
C 3170
C 3180
C 3190
C 3200
C 3210
C 3220
C 3230
C 3240
C 3250
C 3260
C 3270
C 3280
C 3290
C 3300
C 3310
C 3320
C 3330
C 3340
C 3350
C 3360
C 3370
C 3380
C 3390
C 3400
C 3410
C 3420
C 3430
C 3440
C 3450
C 3460
C 3470
C 3480
C 3490
C 3500
C 3510
C 3520
C 3530
C 3540
C 3550
C 3560
C 3570
C 3580
C 3590
C 3600
C 3610
C 3620
C 3630
C 3640
C 3650
C 3660
C 3670
C 3680
C 3690
C 3700
C 3710
C 3720
C 3730
C 3740
C 3750
C 3760
C 3770
C 3780
C 3790
C 3800
C 3810
C 3820
C 3830
C 3840
C 3850
C 3860
C 3870
C 3880
C 3890
C 3900
C 3910
C 3920
C 3930
C 3940
C 3950
C 3960
C 3970
C 3980
C 3990
C 4000
C 4010
C 4020
C 4030
C 4040
C 4050
C 4060
C 4070
C 4080
C 4090
C 4100
C 4110
C 4120
C 4130
C 4140
C 4150
C 4160
C 4170
C 4180
C 4190
C 4200
C 4210
C 4220
C 4230
C 4240
C 4250
C 4260
C 4270
C 4280
C 4290
C 4300
C 4310
C 4320
C 4330
C 4340
C 4350
C 4360
C 4370
C 4380
C 4390
C 4400
C 4410
C 4420
C 4430
C 4440
C 4450
C 4460
C 4470
C 4480
C 4490
C 4500
C 4510
C 4520
C 4530
C 4540
C 4550
C 4560
C 4570
C 4580
C 4590
C 4600
C 4610
C 4620
C 4630
C 4640
C 4650
C 4660
C 4670
C 4680
C 4690
C 4700
C 4710
C 4720
C 4730
C 4740
C 4750
C 4760
C 4770
C 4780
C 4790
C 4800
C 4810
C 4820
C 4830
C 4840
C 4850
C 4860
C 4870
C 4880
C 4890
C 4900
C 4910
C 4920
C 4930
C 4940
C 4950
C 4960
C 4970
C 4980
C 4990
C 5000
C 5010
C 5020
C 5030
C 5040
C 5050
C 5060
C 5070
C 5080
C 5090
C 5100
C 5110
C 5120
C 5130
C 5140
C 5150
C 5160
C 5170
C 5180
C 5190
C 5200
C 5210
C 5220
C 5230
C 5240
C 5250
C 5260
C 5270
C 5280
C 5290
C 5300
C 5310
C 5320
C 5330
C 5340
C 5350
C 5360
C 5370
C 5380
C 5390
C 5400
C 5410
C 5420
C 5430
C 5440
C 5450
C 5460
C 5470
C 5480
C 5490
C 5500
C 5510
C 5520
C 5530
C 5540
C 5550
C 5560
C 5570
C 5580
C 5590
C 5600
C 5610
C 5620
C 5630
C 5640
C 5650
C 5660
C 5670
C 5680
C 5690
C 5700
C 5710
C 5720
C 5730
C 5740
C 5750
C 5760
C 5770
C 5780
C 5790
C 5800
C 5810
C 5820
C 5830
C 5840
C 5850
C 5860
C 5870
C 5880
C 5890
C 5900
C 5910
C 5920
C 5930
C 5940
C 5950
C 5960
C 5970
C 5980
C 5990
C 6000
C 6010
C 6020
C 6030
C 6040
C 6050
C 6060
C 6070
C 6080
C 6090
C 6100
C 6110
C 6120
C 6130
C 6140
C 6150
C 6160
C 6170
C 6180
C 6190
C 6200
C 6210
C 6220
C 6230
C 6240
C 6250
C 6260
C 6270
C 6280
C 6290
C 6300
C 6310
C 6320
C 6330
C 6340
C 6350
C 6360
C 6370
C 6380
C 6390
C 6400
C 6410
C 6420
C 6430
C 6440
C 6450
C 6460
C 6470
C 6480
C 6490
C 6500
C 6510
C 6520
C 6530
C 6540
C 6550
C 6560
C 6570
C 6580
C 6590
C 6600
C 6610
C 6620
C 6630
C 6640
C 6650
C 6660
C 6670
C 6680
C 6690
C 6700
C 6710
C 6720
C 6730
C 6740
C 6750
C 6760
C 6770
C 6780
C 6790
C 6800
C 6810
C 6820
C 6830
C 6840
C 6850
C 6860
C 6870
C 6880
C 6890
C 6900
C 6910
C 6920
C 6930
C 6940
C 6950
C 6960
C 6970
C 6980
C 6990
C 7000
C 7010
C 7020
C 7030
C 7040
C 7050
C 7060
C 7070
C 7080
C 7090
C 7100
C 7110
C 7120
C 7130
C 7140
C 7150
C 7160
C 7170
C 7180
C 7190
C 7200
C 7210
C 7220
C 7230
C 7240
C 7250
C 7260
C 7270
C 7280
C 7290
C 7300
C 7310
C 7320
C 7330
C 7340
C 7350
C 7360
C 7370
C 7380
C 7390
C 7400
C 7410
C 7420
C 7430
C 7440
C 7450
C 7460
C 7470
C 7480
C 7490
C 7500
C 7510
C 7520
C 7530
C 7540
C 7550
C 7560
C 7570
C 7580
C 7590
C 7600
C 7610
C 7620
C 7630
C 7640
C 7650
C 7660
C 7670
C 7680
C 7690
C 7700
C 7710
C 7720
C 7730
C 7740
C 7750
C 7760
C 7770
C 7780
C 7790
C 7800
C 7810
C 7820
C 7830
C 7840
C 7850
C 7860
C 7870
C 7880
C 7890
C 7900
C 7910
C 7920
C 7930
C 7940
C 7950
C 7960
C 7970
C 7980
C 7990
C 8000
C 8010
C 8020
C 8030
C 8040
C 8050
C 8060
C 8070
C 8080
C 8090
C 8100
C 8110
C 8120
C 8130
C 8140
C 8150
C 8160
C 8170
C 8180
C 8190
C 8200
C 8210
C 8220
C 8230
C 8240
C 8250
C 8260
C 8270
C 8280
C 8290
C 8300
C 8310
C 8320
C 8330
C 8340
C 8350
C 8360
C 8370
C 8380
C 8390
C 8400
C 8410
C 8420
C 8430
C 8440
C 8450
C 8460
C 8470
C 8480
C 8490
C 8500
C 8510
C 8520
C 8530
C 8540
C 8550
C 8560
C 8570
C 8580
C 8590
C 8600
C 8610
C 8620
C 8630
C 8640
C 8650
C 8660
C 8670
C 8680
C 8690
C 8700
C 8710
C 8720
C 8730
C 8740
C 8750
C 8760
C 8770
C 8780
C 8790
C 8800
C 8810
C 8820
C 8830
C 8840
C 8850
C 8860
C 8870
C 8880
C 8890
C 8900
C 8910
C 8920
C 8930
C 8940
C 8950
C 8960
C 8970
C 8980
C 8990
C 9000
C 9010
C 9020
C 9030
C 9040
C 9050
C 9060
C 9070
C 9080
C 9090
C 9100
C 9110
C 9120
C 9130
C 9140
C 9150
C 9160
C 9170
C 9180
C 9190
C 9200
C 9210
C 9220
C 9230
C 9240
C 9250
C 9260
C 9270
C 9280
C 9290
C 9300
C 9310
C 9320
C 9330
C 9340
C 9350
C 9360
C 9370
C 9380
C 9390
C 9400
C 9410
C 9420
C 9430
C 9440
C 9450
C 9460
C 9470
C 9480
C 9490
C 9500
C 9510
C 9520
C 9530
C 9540
C 9550
C 9560
C 9570
C 9580
C 9590
C 9600
C 9610
C 9620
C 9630
C 9640
C 9650
C 9660
C 9670
C 9680
C 9690
C 9700
C 9710
C 9720
C 9730
C 9740
C 9750
C 9760
C 9770
C 9780
C 9790
C 9800
C 9810
C 9820
C 9830
C 9840
C 9850
C 9860
C 9870
C 9880
C 9890
C 9900
C 9910
C 9920
C 9930
C 9940
C 9950
C 9960
C 9970
C 9980
C 9990
C 10000

```

ORIGINAL PAGE IS
OF POOR QUALITY

INFINITE FLAY PLATE

00572 2870
00574 2880
00575 2890
00577 2900
00577 2910
00577 2920
00577 2930
00577 2940
00600 2950
00601 2960
00602 2970
00605 2980
00606 2990
00607 3000
00610 3010
00613 3020
00614 3030
00615 3040
00617 3050
00620 3060
00621 3070
00622 3080
00625 3090
00626 3100
00627 3110
00630 3120
00631 3130
00632 3140
00633 3150
00634 3160
00636 3170
00636 3180
00636 3190
00636 3200
00637 3210
00642 3220
00643 3230
00646 3240
00647 3250
00650 3260
00653 3270
00654 3280
00655 3290
00656 3300
00650 3310
00661 3320
00661 3330
00661 3340
00661 3350
00663 3360
00666 3370
00667 3380
00670 3390
00672 3400
00673 3410
00674 3420
00677 3430

63 CONTINUE
M(K) = SP
62 CONTINUE
60 TO I
C
C EXPRESS THE NEW DIRECTION IN TERMS OF THOSE OF THE DIRECTION
C MATRIX, AND UPDATE THE COUNTS IN WINDC(I) ETC.
C
50 SP = 0.
K = ND
DO 64 I=1,M
WDCPI = NDC * I
X(I) = 0W
DW = 0.
DO 65 J=1,M
K = K+I
DW = DW+(J)*W(K)
65 CONTINUE
60 TO 168,66)) IS
66 WINDC(I) = WINDCPI+1.0
SP = SP+DW*DW
IF (SP-DS) 64,66,.67
67 IS=1
KK = I
X(I) = DW
60 TO 69
68 X(I) = DW
WDCPI = NDC * I
69 WINDC(I) = WINDCPI+1.0
64 CONTINUE
WIND) = 1.0
C
C REORDER THE DIRECTIONS SO THAT KK IS FIRST
C
IF(KK-1) 70,70,71
71 K5 = WDC*W(K)
DO 72 I=1,M
K = K5+I
SP = W(K)
DO 73 J=2,M
W(K) = W - W
W(K) = W(K)
K = K-N
73 CONTINUE
W(K) = SP
72 CONTINUE
C
C GENERATE THE NEW ORTHOGONAL DIRECTION MATRIX
C
70 DO 74 I=1,M
W(K) = W * I
WINDC(I) = 0.0
74 CONTINUE
SP = X(I)*X(I)
K = ND
DO 75 I=2,M
DS = SORT(SP*(SP+X(I))*X(I)))

DATE 070274 PAGE 9

DATE 070274 PAGE 9

INFINITE FLAT PLATE

```

00700 3880  DB = SP/DS
00701 3450  DS = X(1)/DS
00702 3460  SP = SP*X(1)*X(1)
00703 3470  DO 76 J=1,N
00704 3480  K= K+1
00705 3490  MNPJ = NU + J
00706 3500  NPN = N + N
00707 3510  W(NPJJ)=W(NPJJ)+X(1)*X(1)
00708 3520  W(K) = DMW(NPN)-DS*(MNPJ)
00709 3530  76 CONTINUE
00710 3540  78 CONTINUE
00711 3550  SP= 1.0/SORT(DM)
00712 3560  DO 77 I=1,N
00713 3570  K= K+1
00714 3580  W(K) = SP*(F(I)
00715 3590  77 CONTINUE
00716 3600  C
00717 3610  C
00718 3620  C
00719 3630  80 FMP= 0.0
00720 3640  K=0
00721 3650  DO 78 I=1,N
00722 3660  MXPJ = MX + I
00723 3670  MNPJ = NU + I
00724 3680  MFPJ = MF + I
00725 3690  X(I) = MXPJ*(F(I)
00726 3700  W(MNPJ) = W(MFPJ)
00727 3710  DO 79 J=1,N
00728 3720  K= K+1
00729 3730  W(MNPJ) = W(MNPJ)+W(MFPJ)
00730 3740  79 CONTINUE
00731 3750  FMP= FMP+W(MNPJ)**2
00732 3760  78 CONTINUE
00733 3770  C
00734 3780  C
00735 3790  C
00736 3800  60 TO 1
00737 3810  C
00738 3820  C
00739 3830  C
00740 3840  27 DMULT = .9*(FMIN+.1)*FMP-FSQ
00741 3850  IF (DMULT) 82,81,81
00742 3860  82 DD = AMAX1(DSS,0.25*DD)
00743 3870  TINC = 1.0
00744 3880  IF(FSQ-FMIN) 83,28,28
00745 3890  C
00746 3900  C
00747 3910  C
00748 3920  C
00749 3930  81 SP= D+C
00750 3940  SS = 0.0
00751 3950  DO 84 I=1,N
00752 3960  MNPJ = NU + I
00753 3970  SS = SP*(ABS(F(I)*F(I)-W(MNPJ)))
00754 3980  84 CONTINUE
00755 3990  PJ = 1.0*(DMULT/SP+SORT(SS)*SP+DMULT*SS)
00756 4000  SP= AMIN1(N,0,TINC,PJ)
01000

```

INFINITE FLAT PLATE

```

401* 01001
402* 01002
403* 01003
404* 01003
405* 01003
406* 01003
407* 01004
408* 01007
409* 01010
410* 01013
411* 01014
412* 01015
413* 01016
414* 01017
415* 01020
416* 01021
417* 01022
418* 01023
419* 01024
420* 01025
421* 01027
422* 01027
423* 01027
424* 01027
425* 01032
426* 01035
427* 01036
428* 01037
429* 01040
430* 01041
431* 01041
432* 01041
433* 01041
434* 01043
435* 01044
436* 01047
437* 01050
438* 01051
439* 01052
440* 01053
441* 01056
442* 01057
443* 01060
444* 01061
445* 01063
446* 01065
447* 01066
448* 01067
449* 01072
450* 01073
451* 01076
452* 01077
453* 01101
454* 01102
455* 01103
456* 01104
457* 01104

TIME = PJ/SP
DO = AMINI(DM,SP*DD)
GO TO 83
C IF F(X) IMPROVES STORE THE NEW VALUE OF X
C
87 IF (F50 - FMIN) 03,50,50
88 FMIN = F50
89 DO 88 I=1,M
SP = X(I)
MXP1 = MX + I
MFP1 = MF + I
X(I) = MINXP1
MINMPI = SP
SP = F(I)
F(I) = MINFPI
MINMPI = SP
MINMPI = -MINMPI
88 CONTINUE
IF (I5 - I) 28,28,50
C CALCULATE THE CHANGES IN F AND X
C
28 DO 89 I=1,M
MXP1 = MX + I
MFP1 = MF + I
X(I) = X(I) - MINMPI
F(I) = F(I) - MINMPI
89 CONTINUE
C UPDATE THE APPROXIMATIONS TO J AND AJINW
C
N = 0
DO 90 I=1,M
MUP1 = MU + I
MUP1 = MU + I
MINMPI = X(I)
MINMPI = F(I)
DO 91 J=1,M
MINMPI = MINMPI - AJINW(I,J)*F(J)
K=K+1
MINMPI = MINMPI - MINMPI*X(I)
91 CONTINUE
90 CONTINUE
SP = D.O
SS = 0.O
DO 92 I=1,M
DS = 0.O
DO 93 J=1,M
DS = DS + AJINW(I,J)*X(I)
93 CONTINUE
SP = SP + DS*F(I)
SS = SS + X(I)*X(I)
F(I) = DS
92 CONTINUE
DMULT = 1.O

```

INFINITE FLAT PLATE

```

01107 *58*
01112 *59*
01113 *60*
01114 *61*
01115 *62*
01116 *63*
01121 *64*
01122 *65*
01123 *66*
01124 *67*
01125 *68*
01130 *69*
01131 *70*
01132 *71*
01133 *72*
01135 *73*
01137 *74*
01140 *75*

IF (ABS(SP)-.1)SS) 94,95,95
94 DMULT = 0.8
95 PJ = DMULT/SS
PA = DMULT/DMULT*SP*(1.0-DMULT)*SS)
K = 0
DO 96 I=1,N
  MPI = MU * I
  MPPI = MU * I
  SP = PJO(MMPI)
  SS = PA(MMPI)
  DO 97 J=1,N
    K = K+1
  MINJ = MINJ*SP*(I,J)
  AJINVI+J) = AJINVI+J)*SS*(I,J)
97 CONTINUE
96 CONTINUE
GO TO 38
END

```

END OF COMPILATION NO DIAGNOSTICS.

DATE 070274 PAGE 11

INFINITE FLAT PLATE

FOR 15 MATIN
FOR 011A-07/0279-15 29 31 (,0)

SUBROUTINE MATIMV ENTRY POINT 000655

STORAGE USED CODE(1) 000715: DATA(0) 012003: BLANK COMMON(2) 000000

EXTERNAL REFERENCES (BLOCK, NAME)

0003 WEP235

STORAGE ASSIGNMENT

ADDRESS	TYPE	RELATIVE LOCATION, NAME
0001	00007 1L	0001 000327 11L
0001	00023 15L	0001 000174 1556
0001	000250 2056	0001 000562 21L
0001	000352 2356	0001 000284 2136
0001	000444 2726	0001 000412 2516
0001	000525 3206	0001 000085 3L
0001	000206 7L	0001 000602 3406
0001	000077 1	0000 R 000072 DELT
0000 I 000074 L00P5		0000 R 000104 DELT
0000 I 000102 M		0000 I 000000 K
0000 D 000105 Z1		0000 I 000076 MM
		0000 D 000105 T
		0001 000127 1376
		0001 000231 1736
		0001 000302 2216
		0001 000427 2636
		0001 000520 3116
		0001 000053 4L
		0000 R 000073 EPS
		0000 I 000101 L
		0000 I 000071 MMAX
		0000 R 000103 TEST
		0001 000133 1436
		0001 000040 2L
		0001 000614 23L
		0001 000435 2676
		0001 000522 3146
		0001 000060 5L

EXTERNAL REFERENCES (BLOCK, NAME)

ADDRESS	TYPE	RELATIVE LOCATION, NAME
00101	MINV	2
00101	MINV	5
00103	MINV	8
00109	MINV	9
00105	MINV	13
00106	MINV	14
00107	MINV	15
00114	MINV	16
00115	MINV	17
00116	MINV	18
00117	MINV	20
00121	MINV	21
00123	MINV	24
00124	MINV	25
00125	MINV	26
00126	MINV	27
00130	MINV	28
00131	MINV	29
00132	MINV	30
00133	MINV	31
00134	MINV	32
00135	MINV	33
00136	MINV	34

```

SUBROUTINE MATIMV(S,MY,KSI6)
MATRIX INVERSION BY GAUSS-JORDAN ELIMINATION
DIMENSION S(50,50),T(50,50),Z(150,50),Z2(150,50),K(150)
DOUBLE PRECISION A,R,PROD,T,Z1,Z2
EQUVALENCE T,Z1,Z2)
LOGICAL MATIN
DATA MMAX, DELT, EPS, L00P5/ 5.0,0001,1.0E-8,1/
MATIN=.TRUE.
GO TO 1
C.....INITIALIZE ROUTINE AND TEST MX (=ORDER OF MATRIX)
1 NCM
IF(M-ST.1-AND-M.LE.MMAX) GO TO 5
IF(M.EQ.1) GO TO 2
MSIG=MSIG+1
RETURN
2 PROD=S(1,1)
THE TEST FOR EQUALITY BETWEEN NON-INTEGERS MAY NOT BE MEANINGFUL.
IF(PROD-NE.0.0) GO TO 4
3 MSIG=MSIG+2
4 RETURN
5 GO TO 23
6 PROD=1.0
MM=N-1
DO 6 I=1,M

```

ORIGINAL PAGE IS
OF POOR QUALITY

```

00191 INFINITE FLAT PLATE
00192
00193
00194
00195
00196
00197
00198
00199
00200
00201
00202
00203
00204
00205
00206
00207
00208
00209
00210
00211
00212
00213
00214
00215
00216
00217
00218
00219
00220
00221
00222
00223
00224
00225
00226
00227
00228
00229
00230
00231
00232
00233
00234
00235
00236
00237
00238
00239
00240
00241
00242
00243
00244
00245
00246
00247
00248
00249
00250
00251
00252
00253
00254
00255
00256
00257
00258
00259
00260
00261
00262
00263
00264
00265
00266
00267
00268
00269
00270
00271
00272
00273
00274
00275
00276
00277
00278
00279
00280
00281
00282
00283
00284
00285
00286
00287
00288
00289
00290
00291
00292
00293
00294
00295
00296
00297
00298
00299
00300
00301
00302
00303
00304
00305
00306
00307
00308
00309
00310
00311
00312
00313
00314
00315
00316
00317
00318
00319
00320
00321
00322
00323
00324
00325
00326
00327
00328
00329
00330
00331
00332
00333
00334
00335
00336
00337
00338
00339
00340
00341
00342
00343
00344
00345
00346
00347
00348
00349
00350
00351
00352
00353
00354
00355
00356
00357
00358
00359
00360
00361
00362
00363
00364
00365
00366
00367
00368
00369
00370
00371
00372
00373
00374
00375
00376
00377
00378
00379
00380
00381
00382
00383
00384
00385
00386
00387
00388
00389
00390
00391
00392
00393
00394
00395
00396
00397
00398
00399
00400
00401
00402
00403
00404
00405
00406
00407
00408
00409
00410
00411
00412
00413
00414
00415
00416
00417
00418
00419
00420
00421
00422
00423
00424
00425
00426
00427
00428
00429
00430
00431
00432
00433
00434
00435
00436
00437
00438
00439
00440
00441
00442
00443
00444
00445
00446
00447
00448
00449
00450
00451
00452
00453
00454
00455
00456
00457
00458
00459
00460
00461
00462
00463
00464
00465
00466
00467
00468
00469
00470
00471
00472
00473
00474
00475
00476
00477
00478
00479
00480
00481
00482
00483
00484
00485
00486
00487
00488
00489
00490
00491
00492
00493
00494
00495
00496
00497
00498
00499
00500
00501
00502
00503
00504
00505
00506
00507
00508
00509
00510
00511
00512
00513
00514
00515
00516
00517
00518
00519
00520
00521
00522
00523
00524
00525
00526
00527
00528
00529
00530
00531
00532
00533
00534
00535
00536
00537
00538
00539
00540
00541
00542
00543
00544
00545
00546
00547
00548
00549
00550
00551
00552
00553
00554
00555
00556
00557
00558
00559
00560
00561
00562
00563
00564
00565
00566
00567
00568
00569
00570
00571
00572
00573
00574
00575
00576
00577
00578
00579
00580
00581
00582
00583
00584
00585
00586
00587
00588
00589
00590
00591
00592
00593
00594
00595
00596
00597
00598
00599
00600
00601
00602
00603
00604
00605
00606
00607
00608
00609
00610
00611
00612
00613
00614
00615
00616
00617
00618
00619
00620
00621
00622
00623
00624
00625
00626
00627
00628
00629
00630
00631
00632
00633
00634
00635
00636
00637
00638
00639
00640
00641
00642
00643
00644
00645
00646
00647
00648
00649
00650
00651
00652
00653
00654
00655
00656
00657
00658
00659
00660
00661
00662
00663
00664
00665
00666
00667
00668
00669
00670
00671
00672
00673
00674
00675
00676
00677
00678
00679
00680
00681
00682
00683
00684
00685
00686
00687
00688
00689
00690
00691
00692
00693
00694
00695
00696
00697
00698
00699
00700
00701
00702
00703
00704
00705
00706
00707
00708
00709
00710
00711
00712
00713
00714
00715
00716
00717
00718
00719
00720
00721
00722
00723
00724
00725
00726
00727
00728
00729
00730
00731
00732
00733
00734
00735
00736
00737
00738
00739
00740
00741
00742
00743
00744
00745
00746
00747
00748
00749
00750
00751
00752
00753
00754
00755
00756
00757
00758
00759
00760
00761
00762
00763
00764
00765
00766
00767
00768
00769
00770
00771
00772
00773
00774
00775
00776
00777
00778
00779
00780
00781
00782
00783
00784
00785
00786
00787
00788
00789
00790
00791
00792
00793
00794
00795
00796
00797
00798
00799
00800
00801
00802
00803
00804
00805
00806
00807
00808
00809
00810
00811
00812
00813
00814
00815
00816
00817
00818
00819
00820
00821
00822
00823
00824
00825
00826
00827
00828
00829
00830
00831
00832
00833
00834
00835
00836
00837
00838
00839
00840
00841
00842
00843
00844
00845
00846
00847
00848
00849
00850
00851
00852
00853
00854
00855
00856
00857
00858
00859
00860
00861
00862
00863
00864
00865
00866
00867
00868
00869
00870
00871
00872
00873
00874
00875
00876
00877
00878
00879
00880
00881
00882
00883
00884
00885
00886
00887
00888
00889
00890
00891
00892
00893
00894
00895
00896
00897
00898
00899
00900
00901
00902
00903
00904
00905
00906
00907
00908
00909
00910
00911
00912
00913
00914
00915
00916
00917
00918
00919
00920
00921
00922
00923
00924
00925
00926
00927
00928
00929
00930
00931
00932
00933
00934
00935
00936
00937
00938
00939
00940
00941
00942
00943
00944
00945
00946
00947
00948
00949
00950
00951
00952
00953
00954
00955
00956
00957
00958
00959
00960
00961
00962
00963
00964
00965
00966
00967
00968
00969
00970
00971
00972
00973
00974
00975
00976
00977
00978
00979
00980
00981
00982
00983
00984
00985
00986
00987
00988
00989
00990
00991
00992
00993
00994
00995
00996
00997
00998
00999
01000

```

DATE 070274 PAGE 19

```

MINV 28
MINV 29
MINV 31
MINV 32
MINV 33
MINV 34
MINV 37
MINV 38
MINV 39
MINV 40
MINV 41
MINV 42
MINV 43
MINV 44
MINV 48
MINV 50
MINV 51
MINV 54
MINV 55
MINV 56
MINV 58
MINV 62
MINV 63
MINV 64
MINV 65
MINV 66
MINV 67
MINV 68
MINV 69
MINV 70
MINV 74
MINV 75
MINV 76
MINV 77
MINV 78
MINV 79
MINV 80
MINV 81
MINV 82

```

DIAGNOSTIC THE TEST FOR EQUALITY BETWEEN NON-INTEGERS MAY NOT BE MEANINGFUL.

OF A HIGH QUALITY

```

00302 IF(LE(J) R=0)
00303 TEST=ABS(1/TEST,ABSARD)
00304 17 Z211,L1-R
00305 00 19 I=1,M
00306 00 19 J=1,M
00307 A=0.0
00308 00 18 L=1,M
00309 18 A=A+Z111,L3+Z211,J)
00310 19 Z111,J=Z111,J)+A
00311 IF(1/TEST-LE(DEL)) GO TO 21
00312 20 CONTINUE
00313 1516=K516+J
00314 C.....TRANSFER FINAL INVERSE
00315 21 DO 22 I=1,M
00316 -2 511,J=Z111,J)
00317 .3 IF(1/TEST) RETURN
00318 DET=PROD
00319 RETURN
00320 END
00321
00322
00323
00324
00325
00326
00327
00328
00329
00330
00331
00332
00333
00334
00335
00336
00337
00338
00339
00340
00341
00342
00343
00344
00345
00346
00347
00348
00349
00350
00351

```

DATE 070274 PAGE 14

MINV 84
MINV 85
MINV 87
MINV 88
MINV 89
MINV 90
MINV 93
MINV 94
MINV 95
MINV 96
MINV 97
MINV 98
MINV 100
MINV 101
MINV 102
MINV 103

END OF COMPILATION 2 DIAGNOSTICS.

DATE 070274 PAGE 15

INFINITE FLAT PLATE

8P00.15 CAL
FOR 011A-07/02/74-15 29 39 1,01

SUBROUTINE CALFUN ENTRY POINT 001224

STORAGE USED CODE(1) 0012*7; DATA(0) 000203; BLANK COMMON(2) 000000

EXTERNAL REFERENCES (BLOCK, NAME)

0003 SORT
0004 WERR35

STORAGE ASSIGNMENT (BLOCK, TYPE, RELATIVE LOCATION, NAME)

0001	0002*6	I216	0001	000*14	I366	0001	000517	I466	0001	000600	I616	0001	000666	I706	
0001	000736	I766	0001	001001	I20*6	0001	001050	I2126	0001	001112	I2206	0001	001151	I2266	
0001	000*57	I62L	0000	R	000066	AL	0000	R	000064	D	0000	I	000070	IS	
0000	I	000071	I7	0000	I	000067	K	0000	R	000072	MR	0000	R	000065	PS16
0000	W	000000	U	0000	R	000063	US	0000	R	000062	MS	0000	R	000065	PS16

00101	14	SUBROUTINE CALFUN(N,Y,F)
00103	24	DIMENSION UFSOJ
00104	34	DIMENSION YFSOJ
00105	44	DIMENSION FFSOJ
00106	54	REAL MS
00107	64	MS=1.
00110	74	US=MS*2
00111	84	D=-0204
00112	94	AL=PS16*5.
00113	104	AL=PS16*5.
00114	114	C ALL STATEMENT NUMBERS LOCAL TO CAL
00115	124	C DEFINE F(I) IN TERMS OF Y(I)
00116	134	SD U(I)=4.*AL*2/US-DefY(I)-4.*J*2
00117	144	IF(U(I)-LE.O-0)U(I)=0.D
00118	154	F(I)=Y(I)*2*MS-Y(I)*Y(I)*2*MS
00119	164	Y(I)=2*MS*U(I)-5*SORT(U(I))-Y(I)*2*MS
00120	174	Z(I)=DefY(I)-4.*J*2-4.*AL*2/US*J*2.
00121	184	DO 60 N=2,6
00122	194	U(N)=4.*AL*2/US-DefY(N)-Y(N)-J*2
00123	204	Y(N)=LE.O-0)U(N)=0.D
00124	214	F(N)=Y(N)*2*MS-Y(N)*Y(N)*2*MS
00125	224	Y(N)=2*MS*U(N)-5*SORT(U(N))-Y(N)*2*MS
00126	234	Z(N)=DefY(N)-4.*J*2-4.*AL*2/US*J*2.
00127	244	60 CONTINUE
00131	254	U(7)=4.*AL*2/US-11.-Y(6)*2*MS
00132	264	Y(7)=LE.O-0)U(7)=0.D
00133	274	F(7)=Y(7)*2*MS-Y(7)*Y(7)*2*MS
00134	284	Y(7)=2*MS*U(7)-5*SORT(U(7))-Y(7)*2*MS
00135	294	Z(7)=DefY(7)-4.*J*2-4.*AL*2/US*J*2.
00136	304	DO 61 N=8,29,7

INFINITE FLAT PLATE

```

00140 F(1)=Y(1)000-Y(1)003*(Y(1)-7)*Y(1)+7)/2.0
00140 Y(1)002*(10-.125*(Y(1)-7)*Y(1)+7)/2.0
00141 Z(Y(1))=D*(Y(1)+1)*.9)/2.-D*(Y(1)+1)*.9)/2.0
00143 61 CONTINUE
00144 IS=9
00145 62 IT=IS+8
00150 DO 63 N=IS,JI
00150 F(K)=Y(K)000-Y(K)003*(Y(K)-7)*Y(K)+7)/2.0
00150 Y(K)002*(10-.125*(Y(K)-7)*Y(K)+7)/2.0
00151 Z*(D*(Y(K)+1)-Y(K)-1)/2.0
00153 63 CONTINUE
00154 IS=IS+7
00156 IF (IS-LE-23)60 TO 62
00157 REAL MR
00160 MR=1.
00163 DO 64 N=18,28,7
00163 F(K)=Y(K)000-Y(K)003*(Y(K)-7)*Y(K)+7)/2.0
00163 Y(K)002*(10-.125*(Y(K)-7)*Y(K)+7)/2.0
00164 Z*(D*(Y(K)+1)-Y(K)-1)/2.0
00165 MR=MR+1.
00167 64 CONTINUE
00172 DO 65 N=30,32
00172 F(K)=Y(K)000-Y(K)003*(Y(K)-7)*Y(K)+7)/2.0
00172 Y(K)002*(10-.125*(Y(K)-7)*Y(K)+7)/2.0
00173 Z*(D*(Y(K)+1)-Y(K)-1)/2.0
00175 65 CONTINUE
00200 DO 67 N=33,34
00200 F(K)=Y(K)000-Y(K)003*(Y(K)-7)*Y(K)+7)/2.0
00200 Y(K)002*(10-.125*(Y(K)-7)*Y(K)+7)/2.0
00201 Z*(D*(Y(K)+1)-Y(K)-1)/2.0
00203 67 CONTINUE
00206 DO 68 N=35,35
00206 F(K)=Y(K)000-Y(K)003*(Y(K)-7)*Y(K)+7)/2.0
00206 Y(K)002*(10-.125*(Y(K)-7)*Y(K)+7)/2.0
00207 Z*(D*(Y(K)+1)-Y(K)-1)/2.0
00211 68 CONTINUE
00214 DO 21 N=36,36
00214 F(K)=Y(K)000-Y(K)003*(Y(K)-7)*Y(K)+7)/2.0
00214 Y(K)002*(10-.125*(Y(K)-7)*Y(K)+7)/2.0
00215 Z*(D*(Y(K)+1)-Y(K)-1)/2.0
00217 21 CONTINUE
00222 DO 22 N=37,38
00222 F(K)=Y(K)000-Y(K)-7)*Y(K)003*(D*(Y(K)002
00222 1-D*(Y(K)002*(Y(K)+1)*Y(K)-1)/2.0
00223 1-D*(Y(K)+1)*Y(K)-1)/2.0
00225 22 CONTINUE
00230 DO 130 N=39,39
00230 F(K)=Y(K)000-Y(K)003*(Y(K)-7)*Y(K)+7)/2.0
00231 1-D*(Y(K)002*(Y(K)+1)*Y(K)-1)/2.0
00233 130 CONTINUE
00234 RETURN
00234 END

```

END OF COMPILATION NO DIAGNOSTICS.

INFINITE FLAT PLATE

AT THE 310 TH CALL OF CALFUM WE HAVE

F11

1	-26591012+01	-56294629-02
2	-26165588+01	-63966683-02
3	-22680399+01	-10192208-01
4	-15253005+01	-19077991-02
5	-10540853+01	-77230529-02
6	-10291688+01	-36837752-02
7	-19074260+01	-32102639-02
8	-16554089+01	-10294695-01
9	-26161788+01	-14457418-01
10	-22327907+01	-21219265-01
11	-19919475+01	-35230514-02
12	-96886716+00	-59360909-02
13	-91838167+00	-92781783-03
14	-90938066+00	-50812014-03
15	-36525446+01	-10723169-01
16	-26160266+01	-13809766-01
17	-22123906+01	-20670719-01
18	-14605228+01	-57012009-02
19	-89933027+00	-10842451-02
20	-80062543+00	-13186946-02
21	-78436679+00	-86075103-03
22	-36509966+01	-11411039-01
23	-26161283+01	-12569365-01
24	-21977497+01	-20706584-01
25	-14338906+01	-38107553-02
26	-70283066+00	-91968715-04
27	-65509960+00	-88849347-03
28	-64302110+00	-99666334-03
29	-36492280+01	-11610316-01
30	-26163998+01	-11036446-01
31	-21800788+01	-22334901-01
32	-14129902+01	-74147554-02
33	-49379254+00	-10728177-04
34	-45625703+00	-93313694-03
35	-44746430+00	-89681619-03
36	-36487271+01	-58850507-02
37	-26164698+01	-51837265-02
38	-21868144+01	-11770664-01
39	-14038445+01	-42180993-02

THE SUM OF SQUARES IS -35713191-02
ERROR RETURN BECAUSE FIX FAILED TO DECREASE USINGA NEW JACOBEAN

ORIGINAL PAGE IS
OF POOR QUALITY

DATE 091770 PAGE 1

SPOR.75-MAIN
FOR 011A-09/17/74-10 26 18 6.01

MAIN PROGRAM

STORAGE USED CODE(1) 000752; DATA(1) 000315; BLANK COMMON(2) 000000

EXTERNAL REFERENCES (BLOCK, NAME)

0003 MINTPS
0004 MRCUS
0005 MIOIS
0006 MIOZS
0007 MWDUS
0010 SORS
0011 MSTOP

STORAGE ASSIGNMENT (BLOCK, TYPE, RELATIVE LOCATION, NAME)

0000	000284	100F	0001	000032	1206	0001	000044	1266			
0001	000372	2005	0001	000450	2106	0001	000517	2216			
0001	000415	3L	0001	000553	50L	0000	000257	8F			
0000	1	000237	COUNT	0000	R	000232	0	0000	I	000240	I
0000	1	000234	J	0000	I	000241	K	0000	R	000227	K0
0000	R	000226	MS	0000	R	000233	PS16	0000	R	000000	U
0000	R	000144	Z								

0001	000125	1506	0001	000211	1676		
0001	000575	2306	0000	000246	247		
0001	000750	99L	0000	R	000234	AL	
0000	1	000242	IS	0000	I	000243	IT
0000	I	000230	MM	0000	I	000235	M
0000	R	000231	US	0000	R	000062	V

00101	14	DIMENSION	U450J
00103	24	DIMENSION	Y450J
00104	34	DIMENSION	Z450J
00105	44	REAL	NS
00106	54	REAL	K0
00107	64	MM	=250
00110	74	MS	=1
00111	84	US	=MS**2
00112	94	D	=-0204
00113	104	PSIG	=MS/2
00114	114	AL	=PS16/5
00115	124	M	=N1
00116	134	READ(5,100)	(Y(I),J=1,M)
00124	144	READ(5,100)	(Z(I),J=1,M)
00133	164	100	FORMAT(16,F10.2)
00134	174	NO	=3.315
00135	184	INTEGER	COUNT
00136	194	COUNT	=D
00137	204	90	COUNT=COUNT+1
00141	214	IF	COUNT=CE-MMI 60 TO 99
00142	224	THIS	STATEMENT HAS TOO MANY LEFT PARENTHESES.
00143	234	24	FORMAT(16H,6X)M4I THE 15,1425MIN ITERATION WE HAVE!
00144	244	WRITE	(16,26) COUNT
00145	254	9	FORMAT(16H,4X)M1,9X4N2(I1)/415,(E17.8))
00146	264	WRITE	(16,8) (1,Z(I),I=1,M)

INFINITE PLATE 2 SOLUTION

```

00155 250 U115= N*AL**2/US-D*(Z12)-.125**2
00156 260 IF(U11)LE-0.0) U115= 0.0
00160 270 Z11)=Y11**2+(SORT(U11))/Y11**2-.2*(Y11)/12.*(Y11**2+D)**-
00160 280 1/2*(2)*.125/12.*(Y11**2/D+1.1)**
00160 290 Z12(2)=.125*(SORT(U11))/14.*(Y11**2/SORT(D)+SORT(D))
00161 300 DO 7 K=2,6
00164 310 UTK)= N*AL**2/US-D*(Z1K-1)-Z1K-1)****2
00165 320 IF(U1K)LE-0.0) U1K)=0.0
00167 330 Z1K)=Y1K**2+(SORT(U1K))/Y1K**2-.2*(Y1K)/12.*(Y1K**2+D)**-
00167 340 1/2*(2)*.125/12.*(Y1K**2/D+1.1)**
00167 350 Z12(K+1)-Z1K-1) /12.*(Y1K**2/D+1.1)**
00170 360 7 CONTINUE
00172 370 U17)= N*AL**2/US-D*(K0-Z16)**2
00175 380 IF(U17)LE-0.0) U17)=0.0
00175 390 Z17)=Y17**2+(SORT(U17))/Y17**2-.2*(Y17)/12.*(Y17**2+D)**-
00175 400 1/2*(2)*.125/12.*(Y17**2/D+1.1)**
00175 410 Z1K0-Z16)**2/SORT(U17))/14.*(Y17**2/SORT(D)+SORT(D))
00176 420 Z18)=Y18**2+.125*(Z16)/12.*(Y18**2+D)**-
00176 430 1/2*(1) /18)**2/D+1.1)**
00177 440 DO 2 K=16,24,8
00202 450 Z1K)= Y1K**2+(Z1K-8)**2*(Y1K)/12.*(Y1K**2+D)**-
00202 460 1/2*(1) /Y1K)**2/D+1.1)**
00203 470 2 CONTINUE
00205 480 3 IS= 5
00206 490 DO 4 K=35,47
00207 500 Z1K)=Y1K**2+(Z1K-8)**2*(Y1K)/12.*(Y1K**2+D)**-
00212 510 1/2*(1) /Y1K)**2/D+1.1)**
00212 520 Z12(K-8)-Z1K-1) /12.*(Y1K**2/D+1.1)**
00212 530 Z12(K-8)-Z1K-1) /14.*(Y1K)**2/SORT(D)+SORT(D))
00215 540 4 CONTINUE
00215 550 5 IS= 8
00216 560 IF 15,LE.,25)60 TO 3
00220 570 DO 5 K=15,31,8
00223 580 Z1K)=Y1K**2+(Z1K-8)**2*(Y1K)/12.*(Y1K**2+D)**-
00223 590 1/2*(1) /Y1K)**2/D+1.1)**
00223 600 Z12(K-8)-Z1K-1) /14.*(Y1K)**2/SORT(D)+SORT(D))
00224 610 5 CONTINUE
00226 620 Z132)=Y132**2+(Z12)**2*(Y132)/12.*(Y132**2+D)**-
00227 630 DO 6 K=35,37
00232 640 Z1K)=Y1K**2+(Z1K-8)**2*(Y1K)/12.*(Y1K**2+D)**-
00232 650 1/2*(1) /Y1K)**2/D+1.1)**
00232 660 Z12(K-8)-Z1K-1) /14.*(Y1K)**2/SORT(D)+SORT(D))
00233 670 6 CONTINUE
00235 680 Z138)=Y138**2+(Z130)**2*(Y138)/12.*(Y138**2+D)**-
00235 690 1/2*(1) /Y138)**2/D+1.1)**
00235 700 Z12(30)-Z140) /14.*(Y138)**2/SORT(D)+SORT(D))
00236 710 Z139)=Y139**2+(Z131)**2*(Y139)/12.*(Y139**2+D)**-
00236 720 1/2*(1) /Y139)**2/D+1.1)**
00236 730 Z12(31)-Z140) /14.*(Y139)**2/SORT(D)+SORT(D))
00237 740 Z140)=Y140**2+(Z136)**2*(Y140)**2+D)**-
00237 750 1/2*(1) /Y140)**2/D+1.1)**
00240 760 Z141)=Y141**2+(Z139)**2*(Y141)**2+D)**-
00241 770 1/2*(1) /Y141)**2/D+1.1)**
00241 780 DO 10 50
00242 790 99 END

```


AT THE 249 TH ITERATION WE HAVE

Iteration	Value
1	.13719856+CC
2	.19091899+00
3	.22606329+00
4	.36715700+00
5	.87868027+00
6	.19526295+01
7	.23448205+01
8	.10003767+00
9	.10985776+00
10	.15276201+00
11	.18180807+00
12	.30835310+00
13	.81400262+00
14	.14495683+01
15	.23491339+01
16	.75050307+01
17	.82451005+01
18	.11458908+00
19	.13698362+00
20	.23995656+00
21	.73781828+00
22	.14382671+01
23	.23461986+01
24	.50044250+01
25	.54999402+01
26	.78401815+01
27	.91624808+01
28	.16600324+02
29	.62519258+02
30	.14139405+01
31	.23390695+01

DATE 001778 PAGE 196

ORIGINAL PAGE IS
OF POOR QUALITY

INFINITE PLATE 2 SOLUTION

32	..25025193-01
33	..27505639-01
34	..38203740-01
35	..45913611-01
36	..65872217-01
37	..45195695-00
38	..13611927-01
39	..23212266-01
40	..11050000-01
41	..22100000-01

OFIN

VI. INFINITE FLAT PLATE/COARSE MESH

$\psi = \frac{1}{2}$	G								A
4	3.659	2.616	2.258	1.525	1.054	1.024	1.007	$K\phi = 3.315$	
.125	.137	.191	.226	.367	.878	1.45	2.35	1.0	
	z_1	z_2	z_3	z_4	z_5	z_6	z_7		
4	3.655	2.616	2.232	1.492	.965	.918	.904	$K\phi = 3.315$	
.100	.109	.152	.181	.306	.814	1.44	2.35	.895	
z_8	z_9	z_{10}	z_{11}	z_{12}	z_{13}	z_{14}	z_{15}		
4	3.652	2.616	2.212	1.460	.848	.8006	.986	$K\phi = 3.315$	
.075	.082	.114	.136	.239	.733	1.43	2.34	.775	
z_{16}	z_{17}	z_{18}	z_{19}	z_{20}	z_{21}	z_{22}	z_{23}		
4	3.650	2.616	2.198	1.433	.702	.655	.643	$K\phi = 3.315$	
.05	.055	.076	.091	.166	.625	1.41	2.34	.632	
z_{24}	z_{25}	z_{26}	z_{27}	z_{28}	z_{29}	z_{30}	z_{31}		
4	3.649	2.616	2.189	1.412	.494	.456	.4474	$K\phi = 5.315$	
.025	.027	.038	.045	.085	.45	1.36	2.32	.447	
z_{32}	z_{33}	z_{34}	z_{35}	z_{36}	z_{37}	z_{38}	z_{39}		
4	3.648	2.616	2.187	1.404	0	0	0	$K\phi = 3.315$	
0	0	0	0	0	0	1.10	2.21	.447	
					z_{40}	z_{41}			

$\psi=0$

E

C

B

ϕ

CONFIDENTIAL
 SECURITY INFORMATION

III. Y AND Z COMPUTER PROGRAM/INFINITE PLATE/FINE SOLUTION

DATE 082779 PAGE 3

INFINITE FLAT PLATE

3FCR.15 MAYN
FCP 0118-06/2779-17 12 12 (1.0)

MAIN PROGRAM
STORAGE USED CODE(1) 00051; DATA(1) 000516; BLANK COMMON(2) 000000

COMMON BLOCKS

0003 A 061301
0004 B 061301
0005 C 165140
0006 D 061301

EXTERNAL REFERENCES (BLOCK, NAME)

0007 EQNS
0010 NINTRA
0011 MROUS
0012 NI018
0013 NI028
0014 NSTOPS

STORAGE ASSIGNMENT (BLOCK, TYPE, RELATIVE LOCATION, NAME)

0000 000505 LOGF 0001 00017 1156 0000 R 000502 ACC 0004 000000 AJ1AV 0006 000000 BJ1AV
0000 R 000504 DMAX 0000 R 000237 F 0000 I 200500 IPRINT 0000 I 000477 J 0000 I 000503 MAXFUN
0000 I 000476 N 0000 R 000501 STEP 0003 000000 T 0005 000000 W 0000 R 000000 X

00101 1* COMPILER(XM=1)
00102 2* DIMENSION X(159),F(159)
00103 3* COMMON/A/1(159,159)
00104 4* COMMON/B/AJ1AV(159,159)
00105 5* COMMON/C/A(60000)
00106 6* COMMON/D/BJ1AV(159,159)
00107 7* 100 FORMAT (81F10.2)
00108 8* N=159
00109 9* READ(5,100)X,Y,Z,I,M
00110 10* IPRINT=1
00111 11* STEP=0001
00112 12* ACC=00000
00113 13* MAXFUN=700
00114 14* DMAX=1.0
00115 15* CALL EQRSTWT,F,STEP,DMAX,TCC,MAXFUN,IPRINT
00116 16* END

END OF COMPILATION NO DIAGNOSTICS.

ORIGINAL PAGE IS
OF POOR QUALITY

INFINITE FLAT PLATE

FOR IS EC
FOR 011A-08/2774-17 12 21 6.01

SUBROUTINE EOMS ENTRY POINT 002525

STORAGE USED CODE(1) 002652; DATA(0) 000276; BLANK COMMON(2) 000000

COMMON BLOCKS

0003 A 061301
0004 B 061301
0005 C 165190
0006 D 061301

EXTERNAL REFERENCES (BLOCK, NAME)

0007 CALFUM
0010 MATINY
0011 MUDUS
0012 MIOZS
0013 MIDIS
0014 NERZS
0015 SORT
0016 NERFIS

STORAGE ASSIGNMENT (BLOCK, TYPE, RELATIVE LOCATION, NAME)

0001	000110	IL	0001	000216	JOL	0001	002137	10266	0001	002221	10406	0001	002253	10526
0001	002277	10616	0001	000335	10750	0001	000306	111	0001	002341	11016	0001	002424	11246
0001	002452	11316	0001	000276	13L	0001	000126	1450	0001	000304	15L	0000	000114	16F
0001	000163	1666	0001	000242	17L	0000	000133	19F	0001	000325	22L	0001	000252	2226
0000	000150	23F	0001	000370	28L	0000	000164	26F	0001	000352	264E	0001	001777	27L
0001	002201	28L	0001	000451	29L	0001	000136	3L	0001	000402	30L	0001	000414	30C6
0001	000463	3176	0001	000435	32L	0001	000440	33L	0001	000533	3356	0001	000535	34C6
0001	002465	3576	0001	000606	3626	0001	000641	3716	0001	000642	3746	0001	000654	38L
0001	000204	4L	0001	000700	4056	0001	001025	41L	0001	000707	4136	0001	001003	43L
0001	000775	44L	0001	001012	442C	0000	000175	45F	0001	001063	4706	0001	001067	4746
0001	001055	49L	0001	000201	5L	0001	001262	50L	0001	001153	53L	0001	001221	5316
0001	001300	5526	0001	001141	56L	0001	001337	5656	0001	001350	5726	0001	001374	58L
0001	001264	60L	0001	001467	6106	0001	001421	6166	0001	001501	64L	0001	001523	6516
0001	001534	656C	0001	001442	66L	0001	001567	6716	0001	001465	68L	0001	001472	69L
0000	000061	7F	0001	001557	70L	0001	001610	7026	0001	001635	7116	0001	001703	7266
0001	001725	7376	0001	001755	7476	0001	002036	7756	0000	000075	8F	0001	001714	80L
0001	002026	81L	0001	001725	83L	0000	000060	86F	0001	002121	87L	0000	000105	9F
0001	002474	95L	0001	001204	98L	0004	000000	AJ1W	0000	000083	ANMULY	0006	000000	8J1W
0000	000013	0D	0000	000015	0M	0000	000016	0M	0000	000041	0MULY	0000	000000	0M
0000	000035	0S	0000	000014	0SS	0000	000003	0TEST	0000	000042	0M	0000	000000	0M
0001	000051	FMP	0000	000021	F50	0000	000022	I	0000	000025	IC	0000	000025	INJPS
0001	000017	I	0000	000030	J	0000	000026	K	0000	000046	KK	0000	000050	MMN
0001	000095	KPN	0000	000047	MS	0000	000034	MS16	0000	000000	MAXC	0000	000007	MM
0001	000056	MJPI	0000	000011	ND	0000	000010	NDC	0000	000032	NDCPI	0000	000033	NDCPIP
0001	000044	N0PT	0000	000031	N0PM	0000	000005	MF	0000	000023	NFPJ	0000	000040	NFPJ
0000	000001	NY	0000	000002	NTEST	0000	000006	NU	0000	000051	NVPI	0000	000052	NVJ

ORIGINAL PAGE IS
OF POOR QUALITY

INFINITE FLAT PLATE
 0000 I 000004 M 0000 I 000024 MXPIC 0000 R 000055 PJ 0000 R 000055 PJ
 0000 P 000037 SP 0000 P 000054 SS 0003 000000 T 0000 R 000020 TINC 0000 R 000000 M

```

00101 10 COMPILER=11
00102 20 SUBROUTINE EGASIN,X,F,DSILP,DMAX,ACC,MAXFUN,IPRINT)
00103 30 DIMENSION X(11),F(11)
00104 40 COMMON/A/T(159,159)
00105 50 COMMON/B/AUTNM(159,159)
00106 60 COMMON/C/N(6,000)
00107 70 COMMON/D/BUTNM(159,159)
00108 80
00109 90 SET VARIOUS PARAMETERS
00110 100 MAXC = 0
00111 110
00112 120 MAXC COUNTS THE NUMBER OF CALLS OF CALFUN
00113 130
00114 140 NT = N+4
00115 150 NTES = N1
00116 160
00117 170 NT AND NTEST CAUSE AN ERROR RETURN IF F(X) DOES NOT DECREASE
00118 180
00119 190 DTEST = FLOAT(N) * 0.5
00120 200
00121 210 DTEST IS USED TO MAINTAIN LINEAR INDEPENDENCE
00122 220
00123 230 NX = N*N
00124 240 NY = N*N*N
00125 250
00126 260 NM = N*N*N
00127 270 NN = N*N*N
00128 280 NDC = N*N*N
00129 290 ND = NDC*N
00130 300
00131 310 THESE PARAMETERS SEPARATE THE WORKING SPACE ARRAY M
00132 320
00133 330 FMIN = 0.0
00134 340
00135 350 USUALLY FMIN IS THE LEAST CALCULATED VALUE OF F(X)
00136 360 AND THE BEST X IS IN MIN(1) TO MIN(N)
00137 370
00138 380 DD = 0.0
00139 390 DSS = DSTEP*DSTEP
00140 400 DM = DMAX*DMAX
00141 410 DMN = 4.0*DM
00142 420 IS = 5
00143 430
00144 440 IS CONTROLS A GO TO STATEMENT FOLLOWING A CALL OF CALFUN
00145 450 TINC = 1.0
00146 460
00147 470 TINC IS USED IN THE CRITERION TO INCREASE THE STEP LENGTH
00148 480 START A NEW PAGE FOR PRINTING
00149 490 IF IPRINT) 1,1785
00150 500
00151 510
00152 520
00153 530
00154 540
00155 550
00156 560
00157 570
00158 580
00159 590
00160 600
00161 610
00162 620
00163 630
00164 640
00165 650
00166 660
00167 670
00168 680
00169 690
00170 700
00171 710
00172 720
00173 730
00174 740
00175 750
00176 760
00177 770
00178 780
00179 790
00180 800
00181 810
00182 820
00183 830
00184 840
00185 850
00186 860
00187 870
00188 880
00189 890
00190 900
00191 910
00192 920
00193 930
00194 940
00195 950
00196 960
00197 970
00198 980
00199 990
00200 1000
  
```

INFINITE FLAT PLATE

```

52* 00140 C CALL SUBROUTINE CALFUN
53* 00141 C 1 MAXC = MAXC*1
54* 00142 C CALL CALFUN(X,F)
55* 00143 C
56* 00144 C TEST FOR CONVERGENCE
57* 00145 C FSO = D.O
58* 00146 C DO 2 I=1,N
59* 00147 C FSO = FSO + F(I)*F(I)
60* 00148 C 2 CONTINUE
61* 00149 C IF(FSO-ACC) 3,3,N
62* 00150 C
63* 00151 C PROVIDE PRINTING OF FINAL SOLUTION IF REQUESTED
64* 00152 C
65* 00153 C 3 IF(IPRINT) 5,5,6
66* 00154 C 5 WRITE(6,7) MAXC
67* 00155 C 7 FORMAT (1HM,5X 28M THE FINAL SOLUTION REQUIRED 15,2X22M CALLS OF C
68* 00156 C 8 WRITE(6,8) 11,X11,F11,11,ND
69* 00157 C 8 FORMAT(1HM,4X1M,9X4M11),11X11F11//15,2E17,8)
70* 00158 C 9 WRITE(6,9) FSO
71* 00159 C 9 FORMAT (1HM,6X22M THE SUM OF SQUARES IS E17,8)
72* 00160 C
73* 00161 C 5 RETURN
74* 00162 C
75* 00163 C TEST FOR ERROR RETURN BECAUSE FIXI DOES NOT DECREASE
76* 00164 C
77* 00165 C 9 GO TO (10,11,11,10,11),15
78* 00166 C 10 IF (FSO - FMIN) 15,20,20
79* 00167 C 20 IF (100 - OSS) 12,12,11
80* 00168 C 12 NTEST = NTEST - 1
81* 00169 C IF NTEST = 13,19,11
82* 00170 C 14 WRITE (6,16) NT
83* 00171 C 16 FORMAT(1HM,6X21M ERROR RETURN BECAUSE 15,2X26M CALLS OF CALFUN FAIL
84* 00172 C 17 DO 18 I=1,N
85* 00173 C 18 NPFI = NF + I
86* 00174 C 18 NPFI = NA + I
87* 00175 C X11 = X(NXP1)
88* 00176 C F11 = F(NFP1)
89* 00177 C 18 CONTINUE
90* 00178 C FSO = FMIN
91* 00179 C 60 TO 3
92* 00180 C
93* 00181 C ERROR RETURN BECAUSE A NEW JACOBIAN IS UNSUCCESSFUL
94* 00182 C
95* 00183 C 13 WRITE(6,19)
96* 00184 C 19 FORMAT(1HM,6X5M ERROR RETURN BECAUSE F(X) FAILED TO DECREASE USING
97* 00185 C 1A NEW JACOBIAN)
98* 00186 C GO TO 17
99* 00187 C 15 NTEST = NT
100* 00188 C
101* 00189 C TEST WHETHER THERE HAVE BEEN YARFUNG CALLS OF CALFUN
102* 00190 C
103* 00191 C 11 IF (MFXUN - MAXC) 21,21,22
104* 00192 C 21 WRITE(6,23) MAXC
105* 00193 C 23 FORMAT (1HM,6X37M ERROR RETURN BECAUSE THERE HAVE BEEN 15,2X 15M CAL
106* 00194 C 1LS OF CALFUN)
107* 00195 C IF (FSG - FMIN) 3,17,17
108* 00196 C

```

INFINITE FLAT PLATE

DATE 082774 PAGE 5

```

00250 1099 C
00250 1100 C
00250 1110 C
00253 1120 C
00256 1130 C
00261 1140 C
00262 1150 C
00272 1160 C
00275 1170 C
00275 1180 C
00275 1190 C
00275 1200 C
00275 1210 C
00277 1220 C
00302 1230 C
00303 1240 C
00304 1250 C
00305 1260 C
00308 1270 C
00308 1280 C
00306 1290 C
00306 1300 C
00310 1310 C
00311 1320 C
00312 1330 C
00313 1340 C
00314 1350 C
00315 1360 C
00316 1370 C
00321 1380 C
00322 1390 C
00323 1400 C
00324 1410 C
00326 1420 C
00327 1430 C
00330 1440 C
00330 1450 C
00330 1460 C
00330 1470 C
00333 1480 C
00334 1490 C
00337 1500 C
00342 1510 C
00343 1520 C
00344 1530 C
00345 1540 C
00346 1550 C
00350 1560 C
00351 1570 C
00352 1580 C
00353 1590 C
00354 1600 C
00354 1610 C
00361 1620 C
00364 1630 C
00367 1640 C
00370 1650 C

```

C PROVIDE PRINTING IF REQUESTED
 22 IF (IPRINT) 20,20,25
 25 WRITE(6,26) MAXC
 26 FORMAT(1X,4X,7H) THE IS,1X,25NH CALL OF CALFUM WE HAVE)
 WRITE(6,87) (I,X(I),F(11),F(11),F(11))
 24 GO TO 127,28,20,87,30,1,15
 C STORE THE RESULT OF THE INITIAL CALL OF CALFUM
 30 TRIN = FSO
 DO 31 I=1,N
 MXPI = MX + I
 MFPI = MF + I
 MINMPI = XII
 MINMPI = FII
 31 CONTINUE
 C CALCULATE A NEW JACOBIAN APPROXIMATION
 32 IC = 0
 33 IC = IC + 1
 34 CONTINUE
 29 K = IC
 DO 34 I=1,N
 MFPI = MF + I
 WPK = (F(I)-MINMPI)/DSTEP
 W = M * N
 34 CONTINUE
 C CALCULATE THE INVERSE OF THE JACOBIAN AND SET THE DIRECTION MATRIX
 35 R=0
 DO 36 I=1,N
 DO 37 J=1,N
 W = R + J
 AJINVI(J)=W
 NDKR = ND + W
 WINDPKI = 1.-D/FLOAT(N-I)
 37 CONTINUE
 NDCPI = NDC + I
 NDCPI = NDCPI + W
 WINDCPI = 1.-D
 WINDCPI = 1.-D/FLOAT(N-I)
 36 CONTINUE
 DO 1000 I = 1,N
 DO 1000 J = 1,N
 CALL PJINVI(J) = AJINVI(J)
 CALL MATINV(J) = WINDCPI
 DO 1001 I = 1,N

INFINITE FLAT PLATE DATE 082774 PAGE 6

```

1668 00173 DD 1001 J = 1,N
1678 00174 1001 AJINVI,J) = RJINVI,J)
1688 00175 C
1698 00176 C START ITERATION BY PREDICTING THE DESCENT AND NEWTON MINIMA
1708 00177 C
1718 00178 10 DS = 0.0
1728 00179 10 GM = 0.0
1738 00180 10 SP = 0.5
1748 00181 DO 30 I=1,N
1758 00182 X(I) = 0.0
1768 00183 F(I) = 0.0
1778 00184 M = 1
1788 00185 DO 40 J=1,N
1798 00186 MFPJ = NF + J
1808 00187 X(I) = X(I) - W(J)*MFPJ
1818 00188 F(I) = F(I) - AJINVI,J)*MFPJ
1828 00189 M = M*N
1838 00190 40 CONTINUE
1848 00191 DS = DS + X(I)*X(I)
1858 00192 DN = DN + F(I)*F(I)
1868 00193 SP = SP + X(I)*F(I)
1878 00194 30 CONTINUE
1888 00195 C
1898 00196 C TEST WHETHER A NEARBY STATIONARY POINT IS PREDICTED
1908 00197 C
1918 00198 IF (FMIN - DM*DS) < 1.0E-4
1928 00199 42 GO TO 193
1938 00200 42 WRITE (6,*) IS
1948 00201 42 FORMAT (1H, 6X) ERROR RETURN BECAUSE A NEARBY STATIONARY POINT
1958 00202 10F FIX IS PREDICTED
1968 00203 43 NEXT = 0
1978 00204 DO 60 I=1,N
1988 00205 XPI = X(I)
1998 00206 XII = X(I)*PI
2008 00207 46 CONTINUE
2018 00208 60 TO 52
2028 00209 C
2038 00210 C TEST WHETHER TO APPLY THE FULL NEWTON CORRECTION
2048 00211 C
2058 00212 41 IS = 2
2068 00213 IF (DN - 0.1) < 1.0E-6
2078 00214 47 DO AMAXIUM, DSS)
2088 00215 DS = .25*DN
2098 00216 TIME = 1.0
2108 00217 IF (DN - DSS) < 1.0E-6
2118 00218 49 IS = 4
2128 00219 60 TO 80
2138 00220 C
2148 00221 C CALCULATE THE LENGTH OF THE STEEPEST DESCENT STEP
2158 00222 C
2168 00223 48 M=0
2178 00224 D=0
2188 00225 DO 51 I=1,N
2198 00226 2248
    
```

ORIGINAL PAGE IS
OF POOR QUALITY

INFINITE FLAT PLATE DATE 002774 PAGE 7

00472	2230	00 E 0.0
00473	2240	00 S2 0.1,N
00476	2250	M = M+1
00477	2260	00 = 00 + MIN(X,FJ)
00500	2270	S2 CONTINUE
00502	2280	00MULT = 00MULT+00
00503	2290	S1 CONTINUE
00505	2300	00MULT = DS/00MULT
00506	2310	DS = DS+ 00MULT*00MULT
00506	2320	C
00506	2330	C
00506	2340	C
00507	2350	IF 00S=0001 53,54,55
00507	2360	C
00507	2370	C
00507	2380	C
00512	2390	54 IF 00S 55,55,56
00515	2400	55 00 = AMAX(00S,AMIN(00,DS))
00516	2410	DS = DS/00MULT*00MULT
00517	2420	60 Y0 41
00517	2430	C
00517	2440	C
00517	2450	C
00520	2460	56 00MULT = 0.0
00521	2470	00MULT = 00MULT*00/00S
00522	2480	60 TO 98
00522	2490	C
00522	2500	C
00522	2510	C
00523	2520	53 SP = SP*00MULT
00524	2530	00MULT = 00S/(1+SP-00S)+SORT(1+SP-00S)*00MULT*(00-00S)
00525	2540	00MULT = 00MULT*00-00MULT
00525	2550	C
00525	2560	C
00525	2570	C
00526	2580	08 00 = 0.0
00527	2590	SP = 0.0
00530	2600	00 57 I=1,N
00533	2610	F(I) = 00MULT*(X(I)+00MULT*(F(I))
00534	2620	00E 00MULT*(F(I))
00535	2630	00PI = 00 + I
00536	2640	SP = SP*(F(I)+00MULT*PI)
00537	2650	S7 CONTINUE
00541	2660	05 = +25* 00
00541	2670	C
00541	2680	C
00541	2690	C
00542	2700	IF 00MULT<10-00MULT 58,58,59
00545	2710	58 IF (SP+SP-DS) 60,58,58
00545	2720	C
00545	2730	C
00545	2740	C
00545	2750	C
00545	2760	C
00545	2770	C
00545	2780	C
00545	2790	C
00545	2800	C
00545	2810	C
00545	2820	C
00545	2830	C
00545	2840	C
00545	2850	C
00545	2860	C
00545	2870	C
00545	2880	C
00545	2890	C
00545	2900	C
00545	2910	C
00545	2920	C
00545	2930	C
00545	2940	C
00545	2950	C
00545	2960	C
00545	2970	C
00545	2980	C
00545	2990	C
00545	3000	C

ORIGINAL PAGE IS
OF POOR QUALITY

DATE 0827N PAGE 8

INFINITE FLAT PLATE

```

00557 2834      (I1) = WINDPI3 + DSTIP*WINDPI1
00558 2835      WINDCPI3 = WINDCPI1 + 1.0
00559 2836      61 CONTINUE
00560 2837      WIND3 = I1*G
00561 2838      GO 52 I=1,N
00562 2839      W = ND*1
00563 2840      SP = W*1
00564 2841      DO 63 J=1,M
00565 2842      KPN = K + N
00566 2843      WIK = WIKPN
00567 2844      W = K*N
00568 2845      63 CONTINUE
00569 2846      WIK1 = SP
00570 2847      62 CONTINUE
00571 2848      GO TO 1
00572 2849
00573 2850      C      EXPRESS THE NEW DIRECTION IN TERMS OF THOSE OF THE DIRECTION
00574 2851      C      MATRIX, AND UPDATE THE COUNTS IN WINDCPI3 ETC.
00575 2852
00576 2853      58 SP = J*
00577 2854      W = ND
00578 2855      DO 64 I=1,N
00579 2856      WDCPI = WDC + I
00580 2857      X(I) = DM
00581 2858      DW = O*
00582 2859      DO 65 J=1,M
00583 2860      W = K*1
00584 2861      CW = DW*FIJ*WIK(I)
00585 2862      65 CONTINUE
00586 2863      GO TO (64,66),I5
00587 2864      66 WINDCPI3 = WINDCPI3 + 1.0
00588 2865      SP = SP + DW*DM
00589 2866      IF (SP-DS) 64,64,67
00590 2867      67 IS=1
00591 2868      KK = I
00592 2869      X(I) = DM
00593 2870      GO TO 69
00594 2871      68 X(I) = DM
00595 2872      WDCPI = WDC + 1
00596 2873      69 WINDCPI3 = WINDCPI3 + 1.0
00597 2874      64 CONTINUE
00598 2875      WIND3 = 1.0
00599 2876
00600 2877      C      REORDER THE DIRECTIONS SO THAT KK IS FIRST
00601 2878      C
00602 2879      IF (KK-1) 70,70,71
00603 2880      71 NS = WDC*WIK*W
00604 2881      DO 72 I=1,M
00605 2882      W = NS*1
00606 2883      SP = W*1
00607 2884      DO 73 J=1,N
00608 2885      WKN = K + N
00609 2886      WIKW = WIK*WKN
00610 2887      W = K*N
00611 2888      73 CONTINUE
00612 2889      WIK1 = SP
00613 2890      72 CONTINUE
00614 2891
00615 2892
00616 2893
00617 2894
00618 2895
00619 2896
00620 2897
00621 2898
00622 2899
00623 2900
00624 2901
00625 2902
00626 2903
00627 2904
00628 2905
00629 2906
00630 2907
00631 2908
00632 2909
00633 2910
00634 2911
00635 2912
00636 2913
00637 2914
00638 2915
00639 2916
00640 2917
00641 2918
00642 2919
00643 2920
00644 2921
00645 2922
00646 2923
00647 2924
00648 2925
00649 2926
00650 2927
00651 2928
00652 2929
00653 2930
00654 2931
00655 2932
00656 2933
00657 2934
00658 2935
00659 2936
00660 2937
00661 2938
00662 2939
00663 2940
00664 2941
00665 2942
00666 2943
    
```


INFINITE FLAT PLATE

```

01072 4514 03 CONTINUE
01073 4520 DO 92 J=1,N
01074 4524 DS = D*J
01077 4528 DO 93 J=1,N
01100 4534 DS = DS + AJINVIJ,IBOR(J)
01132 4538 03 CONTINUE
01134 4540 SP = SP + DS*F(I)
01136 4544 SS = SS + X(I)*F(I)
01137 4548 F(I) = G5
01138 4552 02 CONTINUE
01141 4600 CMULT = 1-C
01142 4610 IF (ABS(SS)-.1)SS) 94,95,95
01144 4620 94 CMULT = 7.8
01147 4630 95 FJ = CMULT/SS
01150 4640 PA = CMULT/CMULT*SP+.11-D*CMULT*SS)
01151 4650 KE C
01152 4660 DO 96 I=1,N
01153 4670 WPI = W + I
01154 4680 PPI = P + I
01157 4684 SP = PPI*WPI
01158 4700 SS = PPI*WPI
01161 4710 DO 97 J=1,N
01162 4720 WJ = W + J
01163 4730 WJ = WJ*SP*F(I)
01164 4740 WJ = WJ*SP*F(I)
01167 4750 07 CONTINUE
01168 4760 06 CONTINUE
01169 4770 DO 10 JR
01170 4780 ENO

```

END OF COMPILATION NO DIAGNOSTICS.

OF FOUR QUALITY

DATE 082774 PAGE 12

INFINITE FLAT PLATE

FOR ILLI MATIN
FOR J11A-082777-17 12 AS 1.00

SUBROUTINE MATIN ENTRY POINT 000741

STORAGE USED CODE(1) CODE(1) DATA(3) 000760: BLANK COMMON(2) 000000

COMMON BLOCKS

0001 A JN2002
0008 B 061301
0009 C 165140
0006 D 061301

EXTERNAL REFERENCES (BLOCK, NAME)

0007 NEAR33

STORAGE ASSIGNMENT (BLOCK, TYPE, RELATIVE LOCATION, NAME)

0001	000386 IL	0001	000373 11L	0001	000451 13L	0001	000500 15L	0001	000161 153E
0001	000395 155G	0001	001114 167G	0001	000236 167G	0001	000667 2L	0001	000275 205E
0001	000445 21L	0001	003112 217C	0001	000327 225E	0001	000700 23L	0001	000346 233E
0001	000470 240C	0001	001440 254G	0001	000470 263G	0001	000505 275G	0001	000074 3L
0001	000512 201G	0001	000525 314G	0001	000527 310C	0001	000602 323E	0001	000605 324E
0001	000519 137G	0001	000565 147G	0001	000666 352G	0001	000102 3L	0001	000107 5L
0001	000551 7L	0000	000237 A	0004	000000 AJINV	0006	000003 8JINV	0000	000287 DELT
0000	000000 M	0000	000254 L	0000	000254 I	0000	000271 INJPS	0000	000255 J
0000	000000 W	0000	000254 M	0000	000251 LOOPS	0000	000252 M	0000	000245 MATIN
0001	000001 Y	0000	000265 125I	0005	000000 W	0000	000243 PROD	0000	000241 R
0001	000001 Z	0000	000265 125I	0005	000000 W	0003	000000 21	0003	000000 22

0001E	10	COMPLETE(1), (000200M)	MINV	2
0001F	20	SUBROUTINE MATIN(S,PARANSIS)		
0001G	30	DIMENSION 5(159,159)		
0001H	40	C-----WATER INVERSION BY GAUSS-JORDAN ELIMINATION	MINV	2
0001I	50	DIMENSION 4(159)		
0001J	60	DIMENSION 2(159,159)		
0001K	70	DIMENSION 2(159,159)		
0001L	80	COMMON/AT(159,159)		
0001M	90	COMMON/R/AG(159,159)		
0001N	100	COMMON/W/ABCDEF		
0001O	110	COMMON/C/2(159,159)		
0001P	120	COMMON/PRECISION A,B,FC(0),21,422		
0001Q	130	COMMON/SCALE(1,1)		
0001R	140	COMMON/SCALE(2,1)		
0001S	150	COMMON/MATIN		
0001T	160	DATA W(4), DELT, SP, LOOPS/ N,C,DCCL(1),CF-R,17	MINV	5
0001U	170	MATIN, ITRDCL	MINV	8
0001V	180	DC CL, I	MINV	9

COPIES MADE
DATE 082774

INFINITE FLAY PLATE

LINE	CODE	TEXT	MINV
00127	198	C.....INITIALIZE ROUTINE AND TEST MAX L(ORDER OF MATRIX)	MINV 13
00130	206	1 MEM	MINV 14
00131	218	IF M.GT.1 AND M.LE.M*MAXI GO TO 5	MINV 15
00132	220	IF M.GT.1 GO TO 2	MINV 16
00133	230	MSEMSIG=1	MINV 17
00136	240	RETURN	MINV 18
00137	258	Z PRODSIG=1	
00140	*DIAGNOSTIC*	THE TEST FOR EQUALITY BETWEEN NON-INTEGERS MAY NOT BE MEANINGFUL.	MINV 20
00141	264	IF IPROD.NE.C.D) GO TO 4	MINV 21
00142	274	3 MISEKSI=2	MINV 22
00143	280	RETURN	
00144	290	4 SEI=1;1-0/PROD	
00145	300	GO TO 73	MINV 24
00146	310	5 PRODEL=0	MINV 25
00147	320	M=1	MINV 26
00150	330	GO 5 I=1,M	MINV 27
00153	340	M=1;1	MINV 28
00154	350	DO 6 J=1,M	MINV 29
00157	360	7 TEST=TEST+J	
00157	370	C.....BEGIN BY FINDING LARGEST PIVOTAL ELEMENT	MINV 31
00162	380	DO 11 I=1,M	MINV 32
00165	390	ATC=0	MINV 33
00166	400	DO 7 J=1,M	MINV 34
00171	410	IF ABS(ABS(I)-J) LE AT GO TO 7	
00173	420	A=ABS(I)-J	
00174	430	LEJ	MINV 37
00175	440	7 CONTINUE	MINV 38
00177	*DIAGNOSTIC*	THE TEST FOR EQUALITY BETWEEN NON-INTEGERS MAY NOT BE MEANINGFUL.	MINV 39
00177	450	IF I.E.O.D) GO TO 3	MINV 40
00177	460	C.....REARRANGE ROWS AND ORDER ARRAY	MINV 41
00201	470	M=1;1	MINV 42
00202	480	M=1;1;1	MINV 43
00207	490	M=1;1;1	MINV 44
00207	500	DO 3 J=1,M	
00207	510	AT(I)=J	MINV 45
00207	520	IF ABS(ABS(I)-J) LE AT	MINV 50
00207	530	AT(I)=J	MINV 51
00211	540	C.....REDUCE PIVOTAL POW	
00211	550	AT(I)=1	MINV 54
00214	560	IF ABS(ABS(I)-J) LE AT	MINV 55
00214	570	GO 9 J=1,M	MINV 56
00214	580	9 TEST=TEST+J+1/J	MINV 58
00217	590	10 TEST=TEST+J	MINV 59
00217	600	C.....REDUCE REMAINING ROWS	
00217	610	DO 11 I=1,M	
00217	620	IF I.E.O.D) GO TO 11	
00217	630	A=I;1;1	
00217	640	DO 12 J=1,M	
00217	650	IF ABS(ABS(I)-J) LE AT	
00217	660	AT(I)=J	
00217	670	IF ABS(ABS(I)-J) LE AT	
00217	680	AT(I)=J	
00217	690	11 CONTINUE	
00217	700	C.....INTEGRAL INVERTED MATRIX	
00217	710	DO 13 I=1,M	
00217	720	IF I.E.O.D) GO TO 13	
00217	730	AT(I)=1	
00217	740	DO 14 J=1,M	
00217	750	IF ABS(ABS(I)-J) LE AT	
00217	760	AT(I)=J	
00217	770	13 CONTINUE	
00217	780	14 CONTINUE	

ORIGINAL SOURCE
OF INFORMATION

INFINITE FLAT PLATE DATE 082774 PAGE 15

FOR IS CAL
FOR C11A-08/2774-17 12 56 (40)

SUBROUTINE CALCON ENTRY POINT 001236

STORAGE USED CODE(1) 001262; DATA(0) 000361; BLANK COMMON(2) 000000

COMMON BLOCKS

0003 A 061301
0004 B 061301
0005 C 165140
0006 D 061301

EXTERNAL REFERENCES (BLOCK, NAME)

0007 SORT
0010 MERR3S

STORAGE ASSIGNMENT (BLOCK, TYPE, RELATIVE LOCATION, NAME)

0001 000255 127G 0001 000425 1446 0001 000530 154G 0001 000677 1766
0001 000747 204G 0001 001012 212G 0001 001061 220G 0001 001162 234G
0001 000470 62L 0004 000000 AJ1M 0000 R 030243 AL 0000 P 000243 D
0000 003262 INJPS 0003 I 030245 IS 0030 Y 000246 IT 0000 I 000244 M 0000 R 000247 MR
0000 R 000237 NS 0000 W 000242 PS1G 0005 000000 Y 0000 R 000240 US
0005 000000 V

00101 COMPILER(XM=1)

00103 SUBROUTINE CALFORIN(Y,F)
00104 DIMENSION U(159)
00106 DIMENSION Y(159)
00107 5* DIMENSION F(159)
00110 7* COMMON/A/T(159,159)
00111 7* COMMON/B/AJ1M(159,159)
00112 COMMON/C/W(6000)
00113 9* COMMON/D/BJ1M(159,159)
00114 10* REAL NS
00115 11* MS=1
00116 12* US=NS+2
00117 13* D=-0082
00120 PSIG=MS/2.

00121 15* AL=PSIG/10.
00121 16* C ALL STATEMENT NUMBERS LOCAL TO CAL
00121 17* C DEFINE F(1) IN TERMS OF Y(I)
00122 18* 50 U(1)=A*AL+2/US-D*Y(2)-4.1+2
00123 19* IF(U(1)-LE-D*U(1))=D-0
00123 20* F(1)=Y(1)+6-Y(15)*Y(1)+3*
00125 21* F(1)+2*10-5*SORT(U(1))-Y(1)+D*Y(2)+4.1/2*
00125 22* ZTZ=0*(Y(2)-3.1+2-8*AL+2/US)/8.

INFINITE FLAT PLATE

```

00126 230
00131 240 DO 60 M=2,10
00132 250 URM=9.0AL002/US-DR(Y(K+1)-Y(K-1))/B.
00134 260 IF(UIM).LE.0.0UTRIS=0.0
00139 270 F(K)=Y(K)*9-Y(K+15)*2
00139 280 Y(K)=2*Y(K)-5*SORT(UIS))
00139 290 DO CONTINUE
00140 300 UUIS=9.0AL002/US-11.-(Y(1))/2.0
00142 310 IF(UUIS).LE.0.0Y(UIS)=0.0
00142 320 F(15)=Y(15)*9-Y(10)/2.0
00142 330 Y(15)=2*Y(10)-5*SORT(UUIS))
00143 340 DO 61 K=10,136,15
00146 350 F(K)=Y(K)*9-Y(K+15)*2
00146 370 Y(K)=2*Y(K)-5*SORT(UUIS))
00147 380 Y(K)=2*Y(K)-125*(Y(K-15)-Y(K+15))/2.0
00151 390 61 CONTINUE
00152 400 IS=15
00152 410 IF(UIS).LE.122)GO TO 62
00153 420 62 IT=IS+12
00156 430 DO 53 M=15,17
00156 440 F(M)=Y(M)*9-Y(M+15)*2
00156 450 Y(M)=2*Y(M)-125*(Y(M-15)-Y(M+15))/2.0
00157 460 2*Y(M)=Y(M+15)-Y(M-15)*2
00161 470 63 CONTINUE
00162 480 IS=IS+15
00164 490 IF(UIS).LE.122)GO TO 62
00165 500 REAL MR
00166 510 MR=1.
00171 520 DO 64 M=30,135,15
00171 530 F(M)=Y(M)*9-Y(M+15)*2
00171 540 Y(M)=2*Y(M)-125*(Y(M-15)-Y(M+15))/2.0
00172 550 2*Y(M)=Y(M+15)-Y(M-15)*2
00173 560 ZD=ISORT(2.0*Y(M)-Y(M+15)-Y(M-15))/2.0
00175 570 MR=MR*1.
00200 590 DO 55 K=17,144
00200 600 F(K)=Y(K)*9-Y(K+15)*2
00200 610 Y(K)=2*Y(K)-125*(Y(K-15)-Y(K+15))/2.0
00203 620 2*Y(K)=Y(K+15)-Y(K-15)*2
00206 630 65 CONTINUE
00206 640 DO 67 M=15,149
00206 650 F(M)=Y(M)*9-Y(M+15)*2
00207 660 Y(M)=2*Y(M)-125*(Y(M-15)-Y(M+15))/2.0
00211 670 2*Y(M)=Y(M+15)-Y(M-15)*2
00214 690 67 CONTINUE
00214 700 DO 68 M=150,150
00214 710 F(M)=Y(M)*9-Y(M+15)*2
00215 720 2*Y(M)=Y(M+15)-Y(M-15)*2
00217 730 68 CONTINUE
00222 740 DO 21 K=151,151
00222 750 F(K)=Y(K)*9-Y(K+15)*2
00223 760 Y(K)=2*Y(K)-125*(Y(K-15)-Y(K+15))/2.0
00224 770 2*Y(K)=Y(K+15)-Y(K-15)*2
00224 780 69 CONTINUE
00224 790 F(M)=Y(M)*9-Y(M+15)*2
00224 800 Y(M)=2*Y(M)-125*(Y(M-15)-Y(M+15))/2.0

```

DATE 002770 PAGE 16

INFINITE FLAT PLATE

DATE 092774

PAGE 17

```
00251 80* .....22 CONTINUE
00252 81* DO 130 M=159,159
00253 82* FEN=YENK1000-P1K100030Y10-JS1-D0Y1K1002
00254 83* I-D0Y1N01Y1N-1111/2..0+Y1K-11002/9.
00255 84* 130 CONTINUE
00256 85* RETURN
00257 86* END
```

END OF COMPILATION NO DIAGNOSTICS.

ORIGINAL PAGE IS OF POOR QUALITY

INFINITE FLAT PLATE

THE SUM OF SQUARES IS .28419073-01
 AT THE 247 TH CALL OF CALCULATION WE HAVE
 I XII

1	.35782708+01	-.25943897-01
2	.3693767+01	-.11803987-01
3	.3135326+01	-.22705568-02
4	.26529124+01	-.12444856-01
5	.24702245+01	-.13217318-01
6	.22716574+01	-.53595324-72
7	.1892873+01	-.47812623-02
8	.15520390+01	-.55619132-02
9	.13039200+01	.26925764-02
10	.10592116+01	.32742186-03
11	.13403279+01	-.50723355-03
12	.1212715+01	-.40999346-03
13	.10153921+01	.14006924-02
14	.10081590+01	.16916617-02
15	.10039740+01	.76044100-03
16	.16583476+01	-.43987804-01
17	.26901187+01	-.22641685-01
18	.4126145+01	-.11711255-01
19	.24374201+01	.23134743-01
20	.24518697+01	-.19077322-01
21	.22534223+01	-.10415060-01
22	.14799610+01	-.76425035-02
23	.12260547+01	-.51631511-02
24	.12680419+01	.12622547-02
25	.12113753+01	-.94445866-03
26	.02144919+00	.52441813-03
27	.07144856+00	.55613314-03
28	.06761350+00	-.73801924-03
29	.05789875+00	-.11324055-02
30	.05165323+00	-.49602234-03
31	.03479794+01	-.40374468-01
32	.03415440+01	-.20637518-01
33	.01219312+01	.61907623-02
34	.26253943+01	-.22058824-01
35	.04350747+01	-.15187123-01
36	.22372173+01	-.70203774-02
37	.18228279+01	-.56927804-02
38	.15224855+01	-.24964497-02
39	.12295474+01	.22543803-02
40	.06115463+00	.42153371-03
41	.03016921+00	.40507743-03
42	.01761503+00	.27313177-04
43	.01057323+00	.51264487-03
44	.00310314+00	.05634428-03
45	.49825249+00	-.30165501-03

DATE 082778 PAGE 998

INFINITE FLAT PLATE

46	.38389188*01	-.38706297-01
47	.36780452*01	-.28197899-01
48	.31201432*01	-.89057230-02
49	.26184805*01	-.16703597-01
50	.24221447*01	-.13802154-01
51	.22229895*01	-.8779057-02
52	.18975638*01	-.45987181-02
53	.14799534*01	-.46388752-02
54	.11874722*01	-.38466383-02
55	.90510487*00	-.56823805-03
56	.86231392*00	-.38250503-03
57	.86017171*00	-.20055662-03
58	.85280239*00	-.44289521-04
59	.84510340*00	-.10085039-03
60	.84014207*00	-.57532954-04
61	.8310136*01	-.26344608-01
62	.81676018*01	-.20513883-01
63	.81169724*01	-.61903790-02
64	.26057286*01	-.15248948-01
65	.24101623*01	-.12482065-01
66	.22105391*01	-.77308029-02
67	.18336841*01	-.81287756-02
68	.14949760*01	-.38940654-02
69	.11394441*01	-.24453780-02
70	.84445985*00	-.19575331-03
71	.82034443*00	-.56284290-03
72	.79777423*00	-.35806775-03
73	.79068265*00	-.39781119-03
74	.78315047*00	-.27732580-03
75	.77812924*00	-.21727524-03
76	.78244888*01	-.55651930-01
77	.76627369*01	-.14936449-01
78	.75142508*01	-.61575244-02
79	.25980272*01	-.15174482-01
80	.2399427*01	-.11578275-01
81	.21998200*01	-.76504316-02
82	.18212493*01	-.55705432-02
83	.14423754*01	-.25729887-02
84	.10862246*01	-.32284358-02
85	.77541749*00	-.25583759-01
86	.75107636*00	-.24652378-03
87	.72831528*00	-.13081171-03
88	.72350990*00	-.95537917-04
89	.71457072*00	-.59446581-04
90	.70702825*00	-.96217276-05
91	.68192244*01	-.35742138-01
92	.65577310*01	-.20363044-01
93	.63119849*01	-.75230513-02
94	.60913869*01	-.14478319-01
95	.59198612*01	-.17716955-01
96	.11310741*01	-.80629537-02
97	.14265759*01	-.73292132-02
98	.10253264*01	-.34431104-02
99	.6876470*00	-.23450435-02
100	.6732323*00	-.12705961-03
101	.65040725*00	-.47315728-03
102	.65040725*00	-.274966434-03

INFINITE FLAT PLATE

107	.67441901*00	.27023094*03
108	.63629708*00	.25988274*03
109	.61766577*00	.15301702*03
106	.38152350*01	-.31873726*01
107	.36543093*01	-.20015015*01
108	.31102727*01	-.62071178*02
109	.25867629*01	-.15118289*01
110	.21846911*01	-.12317716*01
111	.2137790*01	-.84554083*02
112	.18028888*01	-.61725091*02
113	.14139583*01	-.35246652*02
114	.95452069*00	-.87481745*03
115	.60458644*00	-.87672418*03
116	.58187800*00	-.26508491*03
117	.55968283*00	-.34865030*03
118	.54030135*00	-.31286708*03
119	.54621821*00	-.30996475*03
120	.36123794*01	-.30219482*03
121	.36519618*01	-.30452651*01
122	.31090327*01	-.67789138*02
123	.25832305*01	-.1583001*01
124	.23798207*01	-.13538847*01
125	.21786797*01	-.89943574*02
126	.17973544*01	-.58854267*02
127	.14043501*01	-.23707625*02
128	.87640801*00	-.21482436*02
129	.49678179*00	-.58371871*03
130	.47661173*00	-.49337271*04
131	.45596735*00	-.14605851*03
132	.65172288*00	-.86756361*04
133	.44739817*00	-.44401183*04
134	.44599661*00	.30522881*04
135	.38107846*01	-.37951367*01
136	.36505533*01	-.19526803*01
137	.11083069*01	-.84611035*02
138	.75817189*01	-.16796501*01
139	.23769787*01	-.14634226*01
140	.21756909*01	-.9673702*02
141	.17939216*01	-.65851919*02
142	.13076636*01	-.42003277*02
143	.79864386*00	-.26023505*02
144	.35883618*00	-.77200018*03
145	.34214295*00	.83770480*03
146	.32432985*00	.53506468*03
147	.32055851*00	.49948927*03
148	.31593683*00	.40651101*03
149	.31502096*00	.40653087*03
150	.318105192*01	-.14179888*01
151	.36502033*01	-.10307302*01
152	.31087098*01	-.19307238*02
153	.25807864*01	-.09584091*02
154	.23763276*01	-.87446792*02
155	.21749593*01	-.55673543*02
156	.17930288*01	-.44125743*02
157	.15956358*01	-.27900659*02
158	.72634997*00	-.25339310*01

ORIGINAL PAGE IS
OF POOR QUALITY

FOR IS MAIN
FOR 311A-11704/74-15 07 30 (L0)

MAIN PROGRAM

STORAGE USED CODE(1) 001001 DATA(0) 001044 SLAN* COMMON(2) 000000

EXTERNAL REFERENCES (BLOCK NAME)

0003 NINTPS
0004 NPDUS
0005 NIOIS
0006 NIOZS
0007 SORT
0010 NACUS
0011 NSTOP8

STORAGE ASSIGNMENT (BLOCK, TYPE, RELATIVE LOCATION, NAME)

0000	000772	I00F	0001	000032	I206	0001	000044	I266	0001	000162	I166	0001	000345	I166					
0001	000423	I74C	0001	000467	Z056	0001	000545	Z146	0001	000602	Z226	0001	000712	Z326					
0001	000770	Z51C	0001	000774	Z6F	0001	000370	ZL	0001	000053	S0L	0000	001005	8F					
0001	000782	Y9L	0000	000782	AL	0000	I	000785	COUNT	0000	P	000780	D	0000	I	000771	I		
0000	I	000787	IS	0000	I	000770	IT	0000	I	000784	J	0000	I	000786	K	0000	R	000755	K0
0000	I	000756	M4	0000	I	000763	N	0000	R	000754	NS	0000	R	000761	PSIG	0000	R	000000	U
0000	E	000767	US	0000	P	000244	Y	0000	P	000510	Z								

0101	10	DIMENSION Y(164)
0102	20	DIMENSION X(164)
0103	30	DIMENSION Z(164)
0104	40	REAL NS
0105	50	REAL MO
0106	60	MM*ICCO
0107	70	NS21
0108	80	USE NS**2
0109	90	CR*CC2
0110	100	PSIGR5/2
0111	110	ALP*SIG*IC
0112	120	NS184
0113	130	SELECTED(Y(I),J,ELN)
0114	140	SELECTED(X(I),J,ELN)
0115	150	SELECTED(Z(I),J,ELN)
0116	160	FORMATT(10,2)
0117	170	FORMATT(10,2)
0118	180	FORMATT(10,2)
0119	190	FORMATT(10,2)
0120	200	FORMATT(10,2)
0121	210	FORMATT(10,2)
0122	220	FORMATT(10,2)
0123	230	FORMATT(10,2)
0124	240	FORMATT(10,2)
0125	250	FORMATT(10,2)
0126	260	FORMATT(10,2)
0127	270	FORMATT(10,2)
0128	280	FORMATT(10,2)
0129	290	FORMATT(10,2)
0130	300	FORMATT(10,2)
0131	310	FORMATT(10,2)
0132	320	FORMATT(10,2)
0133	330	FORMATT(10,2)
0134	340	FORMATT(10,2)
0135	350	FORMATT(10,2)
0136	360	FORMATT(10,2)
0137	370	FORMATT(10,2)
0138	380	FORMATT(10,2)
0139	390	FORMATT(10,2)
0140	400	FORMATT(10,2)
0141	410	FORMATT(10,2)
0142	420	FORMATT(10,2)
0143	430	FORMATT(10,2)
0144	440	FORMATT(10,2)
0145	450	FORMATT(10,2)
0146	460	FORMATT(10,2)
0147	470	FORMATT(10,2)
0148	480	FORMATT(10,2)
0149	490	FORMATT(10,2)
0150	500	FORMATT(10,2)

A STUDY
OF POOR QUALITY

```

2145 260 DO 1 M=2,14
2146 270 URM=4.*AL**2/US-D*(Z(K+1)-Z(K-1))**2
2147 280 IF(UH*ALE.D.O) UH=Z(0)
2148 290 Z(K)=Y(K)**2+SQRT(UH**2+Y(K)**2)/(Z(K+16)))/(Z*(Y(K)**2+D))
2149 300 1*(Z(K+1)-Z(K-1))**2/(Z*(Y(K)**2+D)+1)**2
2150 310 Z(K)=Z(K-1)+SQRT(UH**2+Y(K)**2)/(Z*(Y(K)**2+D))
2151 320 1 CONTINUE
2152 330 U(15)=4.*AL**2/US-D*(NO-Z(14))**2
2153 340 IF(U(15).LE.D.O) U(15)=C.O
2154 350 C(15)=Y(15)**2+SQRT(U(15)**2+Y(15)**2)/(Z*(Y(15)**2+D))
2155 360 1*(C(15)-Z(14))**2/(Z*(Y(15)**2+D)+1)**2
2156 370 Z(K)=Z(K-1)+SQRT(U(15)**2+Y(15)**2)/(Z*(Y(15)**2+D))
2157 380 1*(16)**2/(Z*(Y(16)**2+D)+1)**2
2158 390 C(2)=32.*128.*16
2159 400 DO 2 M=32,128,16
2160 410 Z(M)=Y(M)**2+SQRT(U(16))**2/(Z*(Y(M)**2+D))
2161 420 1*(Z(M)-Z(M-1))**2/(Z*(Y(M)**2+D)+1)**2
2162 430 2 CONTINUE
2163 440 IS=17
2164 450 IF(15.*13
2165 460 DO 4 M=15,13
2166 470 Z(M)=Y(M)**2+SQRT(U(15))**2/(Z*(Y(M)**2+D))
2167 480 1*(Z(M)-Z(M-1))**2/(Z*(Y(M)**2+D)+1)**2
2168 490 Z(K)=Z(K-1)+SQRT(U(15))**2/(Z*(Y(K)**2+D))
2169 500 4 CONTINUE
2170 510 IS=15+16
2171 520 IF(15.*129)GO TO 3
2172 530 DO 5 M=1,16,16
2173 540 Z(M)=Y(M)**2+SQRT(U(16))**2/(Z*(Y(M)**2+D))
2174 550 1*(Z(M)-Z(M-1))**2/(Z*(Y(M)**2+D)+1)**2
2175 560 Z(K)=Z(K-1)+SQRT(U(16))**2/(Z*(Y(K)**2+D))
2176 570 5 CONTINUE
2177 580 DO 6 M=145,156
2178 590 Z(M)=Y(M)**2+SQRT(U(16))**2/(Z*(Y(M)**2+D))
2179 600 1*(Z(M)-Z(M-1))**2/(Z*(Y(M)**2+D)+1)**2
2180 610 Z(K)=Z(K-1)+SQRT(U(16))**2/(Z*(Y(K)**2+D))
2181 620 6 CONTINUE
2182 630 DO 7 M=155,156
2183 640 Z(M)=Y(M)**2+SQRT(U(16))**2/(Z*(Y(M)**2+D))
2184 650 1*(Z(M)-Z(M-1))**2/(Z*(Y(M)**2+D)+1)**2
2185 660 Z(K)=Z(K-1)+SQRT(U(16))**2/(Z*(Y(K)**2+D))
2186 670 7 CONTINUE
2187 680 DO 8 M=155,156
2188 690 Z(M)=Y(M)**2+SQRT(U(16))**2/(Z*(Y(M)**2+D))
2189 700 1*(Z(M)-Z(M-1))**2/(Z*(Y(M)**2+D)+1)**2
2190 710 Z(K)=Z(K-1)+SQRT(U(16))**2/(Z*(Y(K)**2+D))
2191 720 8 CONTINUE
2192 730 DO 9 M=161,163
2193 740 Z(M)=Y(M)**2+SQRT(U(16))**2/(Z*(Y(M)**2+D))
2194 750 1*(Z(M)-Z(M-1))**2/(Z*(Y(M)**2+D)+1)**2
2195 760 9 CONTINUE
2196 770 Z(K)=Z(K-1)+SQRT(U(16))**2/(Z*(Y(K)**2+D))
2197 780 1*(16)**2/(Z*(Y(16))**2+D)+1)**2
2198 790 DO 10 M=161,163
2199 800 Z(M)=Y(M)**2+SQRT(U(16))**2/(Z*(Y(M)**2+D))
2200 810 1*(Z(M)-Z(M-1))**2/(Z*(Y(M)**2+D)+1)**2
2201 820 10 CONTINUE
2202 830

```

```

00402 *DIAGNOSTIC* THIS STATEMENT HAS TOO MANY LEFT PARENTHESES.
00403 000 75 FORMAT(11M,07M)AT THE 15,1X25MTH ITERATION WE HAVF)
00404 000 WRITE(6,26) COUNT
00405 000 $ FORMAT(11M,07M)AT THE 15,1X25MTH ITERATION WE HAVF)
00406 000 WRITE(6,26) COUNT
00407 000 $ FORMAT(11M,07M)AT THE 15,1X25MTH ITERATION WE HAVF)
00408 000 END

```

END OF COMPILATION 1 DIAGNOSTICS.

```

ACT 0026-11/04-15 BY
APC STATUS OF OUTPUT ELEMENT=UNKNOWN

```

```

ADDRESS LIMITS 00100 011574 4445 16444 40005 DECIMAL
STARTING ADDRESS 010034 2492 08444 40005 DECIMAL

```

SEGMENT	4MINS	00100	011534	040000	044661
N0100/F0000-6	0111	001000	001024		
N0100/F0000-6	0111	001025	001047		
N0100/F0000-6	0111	001050	001131	0121	040000 040011
N0100/F0000-6	0111	001132	001335	0121	040012 040031
N0100/F0000-6	0111	001336	001463	0121	040032 040074
N0100/F0000-6	0111	001464	001746	0121	040075 040110
N0100/F0000-6	0111	001747	001771		
N0100/F0000-6	0111	001772	002213	0121	040111 040205
N0100/F0000-6	0111	002214	002404	0121	040206 040236
N0100/F0000-6	0111	002405	002516		
N0100/F0000-6	0111	002517	002557		
N0100/F0000-6	0111	002560	002613		
N0100/F0000-6	0111	002614	003110	0121	040237 042440
N0100/F0000-6	0111	003111	004265	0121	042441 042444
N0100/F0000-6	0111	004266	004455	0121	042445 042503
N0100/F0000-6	0111	004456	004646	0121	042504 042642
N0100/F0000-6	0111	004647	005655	0121	042643 042646
N0100/F0000-6	0111	005656	006532	0121	042647 042677
N0100/F0000-6	0111	006533	007520	0121	042700 042754
N0100/F0000-6	0111	007521	010121	0140	042755 043130
N0100/F0000-6	0111	010122	010146	0121	043131 043202
N0100/F0000-6	0111	010147	010707	0121	043203 043241
N0100/F0000-6	0111	010708	010832	0121	043242 043432
N0100/F0000-6	0111	010833	010932	0121	043433 043462
N0100/F0000-6	0111	010934	010932	0121	043463 043494
N0100/F0000-6	0111	010933	010932	0121	043495 043575
N0100/F0000-6	0111	010932	010932	0121	043576 043576
N0100/F0000-6	0111	010933	010933	0121	043577 043615

ORIGINAL PAGE IS
OF POOR QUALITY

*(1) 010534 011534 *(10) 043616 044661
*(12) BLANKSCOMMON

*(11) 010534 011534

*(14)

SYSTEMS. LEVEL 109-11
END OF COLLECTION - TIME 1.788 SECONDS

AT THE 1000 TH ITERATION WE HAVE

(11)

1

- 1 .129160000000
- 2 .135573900000
- 3 .159786710000
- 4 .188113400000
- 5 .202910180000
- 6 .221422200000
- 7 .267165780000
- 8 .340900180000
- 9 .482654500000
- 10 .682612730000
- 11 .112249860000
- 12 .181675550000
- 13 .217416450000
- 14 .261768400000
- 15 .313846500000
- 16 .412222750000
- 17 .611300670000
- 18 .822555160000
- 19 .124801000000
- 20 .185575000000
- 21 .282866600000
- 22 .420102750000
- 23 .621156700000
- 24 .924210000000
- 25 .138607050000
- 26 .207272400000
- 27 .306934400000
- 28 .455122800000
- 29 .682636900000
- 30 .102408500000
- 31 .152408500000
- 32 .224817000000
- 33 .337225500000
- 34 .502043500000
- 35 .741262000000
- 36 .109347800000
- 37 .162687800000
- 38 .241405800000
- 39 .356793300000
- 40 .528198300000
- 41 .784491800000
- 42 .115668800000
- 43 .172417300000
- 44 .257235300000
- 45 .381053300000
- 46 .558261300000
- 47 .824479300000
- 48 .121664300000
- 49 .179472800000
- 50 .265680800000
- 51 .395488800000
- 52 .584296800000
- 53 .864104800000
- 54 .127620800000
- 55 .188428800000
- 56 .277236800000
- 57 .409644800000
- 58 .604452800000
- 59 .888260800000
- 60 .131641800000
- 61 .194449800000
- 62 .284257800000
- 63 .421465800000
- 64 .621273800000
- 65 .904481800000
- 66 .132629800000
- 67 .194437800000
- 68 .284245800000
- 69 .421453800000
- 70 .621261800000
- 71 .904469800000
- 72 .132633800000
- 73 .194441800000
- 74 .284249800000
- 75 .421457800000
- 76 .621265800000
- 77 .904473800000
- 78 .132639800000
- 79 .194445800000
- 80 .284253800000
- 81 .421461800000
- 82 .621269800000
- 83 .904479800000
- 84 .132643800000
- 85 .194449800000
- 86 .284257800000
- 87 .421465800000
- 88 .621273800000
- 89 .904481800000
- 90 .132647800000
- 91 .194453800000
- 92 .284261800000
- 93 .421469800000
- 94 .621277800000
- 95 .904485800000
- 96 .132651800000
- 97 .194457800000
- 98 .284265800000
- 99 .421473800000
- 100 .621281800000

ORIGINAL PAGES
OF FOUR QUALITY

49	.8044881-01
50	.8442265-01
51	.11191759-00
52	.13171768-00
53	.14218104-00
54	.15545622-00
55	.18811845-00
56	.24362246-00
57	.27740524-00
58	.75542346-00
59	.12351450-01
60	.17443867-01
61	.22524388-01
62	.27417992-01
63	.21875903-01
64	.75447792-01
65	.77589766-01
66	.81431447-01
67	.05947965-01
68	.11489439-00
69	.12145948-00
70	.13322841-00
71	.16149657-00
72	.21046405-00
73	.33508440-00
74	.71059171-00
75	.12449106-01
76	.17140586-01
77	.22228151-01
78	.27111933-01
79	.31477911-01
80	.62547132-01
81	.64649413-01
82	.67572062-01
83	.70963597-01
84	.04037946-01
85	.10156574-00
86	.31450775-00
87	.13474805-00
88	.17626620-00
89	.28465115-00
90	.65942049-00
91	.11655457-01
92	.16296699-01
93	.21368890-01
94	.26768610-01
95	.71050278-01
96	.80441405-01
97	.51716003-01
98	.46254453-01
99	.63477616-01
100	.75256592-01
101	.81601449-01
102	.90750657-01
103	.10771065-00
104	.14145467-00
105	.24068281-00

106 -59831696+00
 107 -11157328+01
 108 -18372463+01
 109 -21488974+01
 110 -28373804+01
 111 -30673063+01
 112 -37519744+01
 113 -38757750+01
 114 -80734181+01
 115 -87987180+01
 116 -56480280+01
 117 -60958619+01
 118 -66984105+01
 119 -81007468+01
 120 -1C887605+00
 121 -19768257+00
 122 -52486883+00
 123 -10567261+01
 124 -15853485+01
 125 -20548393+01
 126 -25925149+01
 127 -30249705+01
 128 -25013834+01
 129 -23558857+01
 130 -27158404+01
 131 -31033296+01
 132 -37636018+01
 133 -40539528+01
 134 -88655236+01
 135 -59039444+01
 136 -71501608+01
 137 -13277528+00
 138 -82787752+00
 139 -89728225+00
 140 -18438185+01
 141 -20339039+01
 142 -25527033+01
 143 -28780034+01
 144 -22007155+01
 145 -25228976+01
 146 -13576887+01
 147 -11592200+01
 148 -11127115+01
 149 -23307070+01
 150 -22133181+01
 151 -27100004+01
 152 -35100071+01
 153 -87185716+01
 154 -28481448+00
 155 -45882388+00
 156 -17448677+01
 157 -18126880+01
 158 -24241116+01
 159 -28082000+01
 160 -52180086+00
 161 -111000000+01
 162 -118700000+01

11-11-68

165
164
163

FC-44442922
FC-66665522

17

ORIGINAL PAGE IS
OF POOR QUALITY

V. I AND Z COMPUTER PROGRAM/FINITE PLATE/(R₀/L = 1/2)

DATE 120374 PAGE 2

FINITE PLATE

FOR IS MAIN
FOR D114-12/03/74-12 56 39 1.01

MAIN PROGRAM

STORAGE USED CODE(1) 000050: DATA(1) 017271: BLANK COMMON(2) 000000

EXTERNAL REFERENCES (BLOCK, NAME)

0003 FOMS
0004 MINIRS
0005 MRDUS
0006 MIOZS
0007 MIOZS
0010 MSTOPA

STORAGE ASSIGNMENT (BLOCK, TYPE, RELATIVE LOCATION, NAME)

0000 017261 100F 0001 00014 1076 0000 R 017256 ACC
0000 000062 F 0000 017254 IPRINT 0000 I 017253 J
0000 017255 STEP 0000 R 005050 M 0000 R 000000 X

0000 R 000144 AJINV
0000 I 017257 MAXFUN

0000 R 01726C DMAX
0000 I 017252 N

0101 10 DIMENSION X(50),F(50),AJINV(50),M(52501)
0103 20 100 FORMAT (8F10.23)
0104 30 N=4
0105 40 READ(5,100)(X(J),J=1,N)
0115 50 IPRINT=1
0114 60 STEP=001
0115 70 ACC=00001
0116 80 MAXFUN=200
0117 90 DMAX=1.0
0120 100 CALL CONS(M,X,F,AJINV,STEP,DMAX,ACC,MAXFUN,IPRINT,M)
0121 110 END

END OF COMPILATION NO DIAGNOSTICS.

ORIGINAL PAGE IS
OF POOR QUALITY

DATE 120378 PAGE 15

FINITE PLATE

FORM 15 CAL
FORM 5112-12/53/79-12 57 72 1-02

SUBROUTINE CALFUN ENTRY POINT 01455

STORAGE USED CODE(1) CODE(2) DATA(1) CODE(2); PLANK COMMON(2) CODE(0)

EXTERNAL REFERENCES (ALCOM, NAME)

CODE NAME

STORAGE ASSIGNMENT (BLOCK, TYPE, RELATIVE LOCATION, NAME)

001	00233 131	0001	000006 1466	0001	000577 1566	0001	000660 1716	0001	000744 2006
001	00104 210	0001	000456 31	0000	000150 AL	0000	000146 D	0000	000200 IMJPS
000	00151 15	0001	000154 17	0000	000152 M	0000	000155 MR	0000	000144 MS
000	002197 2510	0000	000161 10	0000	000000 U	0000	000145 US	0000	000062 Z

```

0101 SUBROUTINE CALFUN(M,Y,F)
0102 DIMENSION U(57)
0103 DIMENSION Y(57)
0104 DIMENSION F(57)
0105 DIMENSION Z(57)
0106 Z(1)=.25*
0107 Z(9)=.267
0108 Z(17)=.294
0109 Z(25)=.301
0110 Z(33)=.317
0111 Z(41)=.333
0112 PFAL MS
0113 NS=1.
0114 USENS=2
0115 DE=0.12
0116 PSIS=5/2.
0117 AL=PSI6/5.
0118 RD=2.0
0119 ROZL=1/2
0120 C ALL STATEMENT NUMBERS LOCAL TO CAL
0121 C DEFINE F(1) IN TERMS OF Y(1)
0122 50 U(1)=AL*(Z(1)-Y(1)+Z(1))-(Z(1))**2
0123 Y(1)=U(1)-AL*(Z(1)-Y(1))
0124 F(1)=Y(1)*Y(1)-Y(1)*Z(1)+Z(1)**2
0125 Y(1)=0*(Y(1)-Y(1)+Z(1))-Z(1)*Z(1)
0126 Z(1)=Z(1)+Z(1)
0127 DO 1 K=2,7
0128 U(K)=AL*(Z(K)-Y(K)+Z(K))
0129 Y(K)=U(K)-AL*(Z(K)-Y(K))
0130 F(K)=Y(K)*Y(K)-Y(K)*Z(K)+Z(K)**2
0131 Y(K)=0*(Y(K)-Y(K)+Z(K))-Z(K)*Z(K)
0132 Z(K)=Z(K)+Z(K)
0133 IF (F(1).LT.0.) U(1)=0.
0134 F(1)=Y(1)*Y(1)-Y(1)*Z(1)+Z(1)**2
0135 Y(1)=0*(Y(1)-Y(1)+Z(1))-Z(1)*Z(1)

```

ORIGINAL PAGE
OF POOR QUALITY

DATE 120374 PAGE 16

FINITE PLATE

```

320 242.0D*(Y(K+1)-Y(K-1))**2-4.0*AL**2/US)/8.
330 1 CONTINUE
340 U(I)=4.0*AL**2/US-DEL1.-Y(I))**2
350 IF(U(I))LE-0.0(U(I))=0
360 F(I)=Y(I)*0.0-V(I)*0.3*Y(I)*V(I)+V(I)**2-ID-.5*SORT(U(I)))-
370 Y(I)*0.0*11.-Y(I)**2.0
380 242.0D*11.-Y(I)**2-4.0*AL**2/US)/8.
390 DO 2 N=9,33,8
400 F(N)=Y(K)*0.0-Y(K)*0.3*Y(K-8)+Y(K+8))/2.0
410 Y(K)**2-ID-(Y(K-8)-Y(K+8))**2/8.0)-
420 2.5*Y(K)*0.0*12.-Y(K)*Y(K+1)*Y(K+1)*(K-8)-Z(K+8))/SORT(ID))
430 Y(K)**2-17*(K-8)-Z(K+8))**2/8.
440 2 CONTINUE
450 15=10
460 3 Y=15+5
470 DO 4 N=15,17
480 F(N)=Y(K)*0.0-Y(K)*0.3*Y(K-8)+Y(K+8))/2.0
490 Y(K)**2-ID-(Y(K-8)-Y(K+8))**2/8.0)-
500 2*DEL1*(K+1)-Y(K-1))**2/8.
510 4 CONTINUE
520 15=15+8
530 IF(15.LE.26) GO 70 3
540 REAL MR
550 MR=1.
560 DO 5 N=16,32,8
570 F(N)=Y(K)*0.0-Y(K)*0.3*Y(K-8)+Y(K+8))/2.0
580 Y(K)**2-ID-(Y(K-8)-Y(K+8))**2/8.0)-
590 2*Y(K)*0.0*15.-MR*AL/NS)+Y(K-1))**2.0
600 3D*(SORT(12.0*15.-MR*AL/NS)-Y(K-1))**2/8.
610 MR=MR+1.
620 5 CONTINUE
630 DO 6 N=34,35
640 F(N)=Y(K)*0.0-Y(K)*0.3*Y(K-8)+Y(K+8))/2.0
650 Y(K)**2-ID-(Y(K-8)-Y(K+8))**2/8.0)-Y(K)*0.0*Y(K+1)+Y(K-1))**2.0
660 2*DEL1*(K+1)-Y(K-1))**2/8.
670 6 CONTINUE
680 F(36)=Y(I)*0.0-Y(I)*0.3*Y(I+28)+Y(I+28))/2.0
690 Y(I)*0.0*2-ID-(Y(I+28)-Y(I))**2/8.0)-
700 2*Y(I)*0.0*Y(I+35)+Y(I+35))/2.0+0.0*(Y(I+37)-Y(I+35))**2/8.
710 F(37)=Y(I)*0.0-Y(I)*0.3*Y(I+29)+Y(I+29))/2.0
720 Y(I)*0.0*2-ID-(Y(I+29)-Y(I))**2/8.0)-
730 2*Y(I)*0.0*Y(I+36)+Y(I+36))/2.0+0.0*(Y(I+38)-Y(I+36))**2/8.
740 10 7 N=7,30
750 F(N)=Y(K)*0.0-Y(K)*0.3*Y(K-8)+Y(K+8))/2.0+Y(K)*0.0*2-ID-.125*Y(K-8)**2)-
760 Y(K)*0.0*Y(K+1)+Y(K-1))**2/2.0+DEL1*(K+1)-Y(K-1))**2/8.
770 7 CONTINUE
780 F(40)=Y(K)*0.0-Y(K)*0.3*Y(K+32))/2.0+Y(K)*0.0*2-ID-.125*Y(K+32)**2)-
790 2*DEL1*(K+32)+5*DEL1*(K+32).0*AL/NS)+Y(I+30))
800 U(I)=AL**2/US-V(I)*0.3*Y(I)*V(I)**2/8.
810 IF(U(I))LE-0.0(U(I))=0
820 F(41)=Y(K)*0.0-Y(K)*0.3*Y(K+33)+
830 Y(K)**2-ID-(Y(K+33)-Y(K))**2/8.0)-
840 2*Y(K)*0.0*Y(K+40)+Y(K+40))/2.0
850 Y(K)**2-ID-(Y(K+40)-Y(K))**2/8.0)-
860 2*Y(K)*0.0*Y(K+47)+Y(K+47)-Z(K+41))/SORT(ID))
870 Y(K)**2-ID-(Y(K+47)-Z(K+41))**2/8.0)-
880 2*Y(K)*0.0*AL**2/US-0.0*Y(K+3)-Y(K+3))**2
890 IF(U(I))LE-0.0(U(I))=0
900 8 CONTINUE

```


ORIGINAL PAGE IS
OF POOR QUALITY

DATE 120378 PAGE 153

FINDING PLATE

3	.26339368+01	.89025083-03
4	.20496590+01	.26680096-02
5	.10388339+01	.26338730-03
6	.10024565+01	.13316098-03
7	.99488555+00	.13352246-02
8	.99317597+00	.13506668-02
9	.39148330+01	.99317597-02
10	.33799877+01	.74407990-02
11	.26106275+01	.13415673-02
12	.20334483+01	.12815797-02
13	.95377931+00	.35519752-03
14	.89745270+00	.84258498-04
15	.89014006+00	.10337803-02
16	.88891198+00	.10970674-02
17	.5854268+01	.91589284-02
18	.33609975+01	.76580360-02
19	.25889103+01	.81492195-03
20	.20194086+01	.21384814-03
21	.83271550+00	.12440665-03
22	.7723162+00	.19464283-03
23	.76885365+00	.89114238-04
24	.76702218+00	.25911929-05
25	.38756332+01	.91445014-02
26	.3819447+01	.77525818-02
27	.25628153+01	.18746395-02
28	.20090393+01	.12175383-02
29	.72295893+00	.13866366-03
30	.63203345+00	.25482670-03
31	.62298401+00	.30392579-03
32	.62162420+00	.22793029-03
33	.38558731+01	.88254769-02
34	.33228296+01	.75184951-02
35	.25381564+01	.1858411-02
36	.23023854+01	.99075942-04
37	.54323023+00	.46073110-04
38	.43624437+00	.20977520-03
39	.42829492+00	.25629085-03
40	.42754654+00	.23920318-03
41	.38349783+01	.46051143-02
42	.23736727+01	.39352653-02
43	.25124594+01	.77474740-03
44	.24444511+00	.37299299-04

TOTAL SUM OF SQUARES IS .66368485-03
AT THE 163 TH CALL OF CALFUN WE HAVE
F III

1	.19334570+01	.86992741-02
2	.33986154+01	.35526160-02
3	.26339368+01	.97243446-03
4	.22895352+01	.26114430-02
5	.13386733+01	.1656282-03
6	.15224502+01	.13255415-03
7	.99488555+00	.13623016-02
8	.99317597+01	.14614231-02
9	.74407990+01	.92544466-02
10	.13415673+01	.74521824-02
11	.12815797+01	.71167508-02

9F04-JS MAIN
PCR 1119-12/24/74-11 29 57 (50)

MAIN PROGRAM

STORAGE USED CODE(1) 2C1105; DATA(0) 000324; BLANK COMMENT(2) 000000

EXTERNAL REFERENCES (BLOCK, NAME)

0004 NINTRS
0006 MRBUS
0005 NIOIS
0008 NIOZS
0007 MRSUS
0010 SORT
0011 NSTOP5

STORAGE ASSIGNMENT (BLOCK, TYPE, RELATIVE LOCATION, NAME)

000	00046 100F	0001	000037 1226	0001	000051 1306	0001	000134 1516
001	000303 1706	0001	000016 2060	0001	000465 2176	0001	000566 2336
002	000250 24F	0001	000347 3L	0001	000060 50L	0001	001103 99L
000 R	000134 4L	0000 I	000241 COUNT	0000 R	000232 D	0000 I	000242 I
001 I	000245 17	0000 I	000240 J	0000 I	000243 K	0000 I	000244 IS
000 I	000230 4M	0000 I	000235 N	0000 R	000236 NS	0000 R	000237 NO
000 R	000000 U	0000 R	000231 JS	0000 R	000062 Y	0000 R	000238 PD

0101	10	DIMENSION U15C1
0104	20	DIMENSION Y15C1
0108	30	DIMENSION Z15C1
0109	40	REAL N5
0106	50	REAL K0
0107	60	MM250
0110	70	N511
0111	80	US245+2
0112	90	DZ-D118
0113	100	PSIG=NS42
0114	110	ALPSIG175
0115	120	N505
0116	130	ROZ20
0117	140	MF204
0120	150	REAR15,1700 17410,JE1,NEJ
0126	160	REAR15,1700 17410,JE1,N
0130	170	170 FORWARD1810,213
0135	180	WZ113
0136	190	INTEGER COUNT
0137	200	COUNT50
0138	210	50 COUNT=COUNT+1
0139	220	IF(COUNTAGE,MM) GO TO 90
0140	230	THIS STATEMENT HAS TOO MANY LEFT PARENTHESES.
0141	240	70 FORWARD1810,213WAY THE IS,1825WHM ITERATION WE HAVE!
0142	250	WRITE(16,261) COUNT
0148	260	

ORIGINAL PAGE IS
OF POOR QUALITY.

```

0187 256 8 FORMAT(IHK,IXIMI,9XNZI11//I15,E17.8))
0150 257 WRITE(6,8) (I,ZI1),I=1,N)
217 258 ZI1=-25
0160 259 DO 1 N=2,7
0163 260 UMI=-9.9AL*2/US-D*(ZIK-1)-Z(K-1))**2
0164 261 IF(UMI).LT.0.0) UMI=0.0
0166 262 Z(K)=Y(K)**2+SORT(U(K)/Y(K)+Z*(K+8))/I2.*Y(K)**2+D)))
0167 263 I(Z(K)-Z(K-1))/I2.*Y(K)**2/D+1.))
0168 264 Z(K)=Z(K-1)+SORT(U(K)/I4.*Y(K)**2/USORT(I)*SORT(I))
0169 265 1 CONTINUE
0170 266 U(I)=9.9AL*2/US-D*(INO-ZI1))**2
0171 267 IF(U(I).LT.0.0)U(I)=0.0
0172 268 Z(I)=Y(I)**2+SORT(U(I)/Y(I)+Z*(I+8))/I2.*Y(I)**2+D))
0173 269 I(I(Z(I)-Z(I-1))/I2.*Y(I)**2/D+1.))
0174 270 Z(I)=Z(I-1)+SORT(U(I)/I4.*Y(I)**2/USORT(I)*SORT(I))
0175 271 DO 2 N=9,35
0176 272 Z(N)=Y(N)**2+Z*(N-8)+Z*(N+8))/I2.*Y(N)**2+D))
0177 273 I(Z(N)-Z(N-1)-Y(N)+Y(N-8)-Y(N+8))/SORT(I)))/I2.*Y(N)**2/D+1.))
0178 274 Z(N)=Z(N-1)+Y(N-8)+Y(N+8))/I4.*Y(N)**2+D))
0179 275 2 CONTINUE
0180 276 I=33
0181 277 3 I=75+5
0182 278 DO 4 N=15,17
0183 279 Z(N)=Y(N)**2+Z*(N-6)+Z*(N+6))/I2.*Y(N)**2+D))
0184 280 I(Z(N)-Z(N-1))/I2.*Y(N)**2/D+1.))
0185 281 Z(N)=Z(N-1)+SORT(U(N)/I4.*Y(N)**2/USORT(I)*SORT(I))
0186 282 * CONTINUE
0187 283 I=15+9
0188 284 IF(I).LT.26) GO TO 3
0189 285 DO 5 N=16,32
0190 286 Z(N)=Y(N)**2+Z*(N-8)+Z*(N+8))/I2.*Y(N)**2+D))
0191 287 I(I(Z(N)-Z(N-1))/I2.*Y(N)**2/D+1.))
0192 288 Z(N)=Z(N-1)+SORT(U(N)/I4.*Y(N)**2/USORT(I)*SORT(I))
0193 289 5 CONTINUE
0194 290 DO 6 N=33,35
0195 291 Z(N)=Y(N)**2+Z*(N-8)+Z*(N+8))/I2.*Y(N)**2+D))
0196 292 I(Z(N)-Z(N-1))/I2.*Y(N)**2/D+1.))
0197 293 Z(N)=Z(N-1)+SORT(U(N)/I4.*Y(N)**2/USORT(I)*SORT(I))
0198 294 6 CONTINUE
0199 295 DO 7 N=36,38
0200 296 Z(N)=Y(N)**2+Z*(N-9)+Z*(N+9))/I2.*Y(N)**2+D))
0201 297 I(Z(N)-Z(N-1))/I2.*Y(N)**2/D+1.))
0202 298 Z(N)=Z(N-1)+SORT(U(N)/I4.*Y(N)**2/USORT(I)*SORT(I))
0203 299 7 CONTINUE
0204 300 Z(39)=Y(39)**2+Z*(39+2)/I2.*Y(39)**2+D))
0205 301 I(Z(39)-Z(38))/I2.*Y(39)**2/D+1.))
0206 302 Z(39)=Z(38)+SORT(U(39)/I4.*Y(39)**2/USORT(I)*SORT(I))
0207 303 I(Z(39)-Z(38))/I2.*Y(39)**2/D+1.))
0208 304 Z(39)=Z(38)+SORT(U(39)/I4.*Y(39)**2/USORT(I)*SORT(I))
0209 305 I(Z(39)-Z(38))/I2.*Y(39)**2/D+1.))
0210 306 Z(39)=Z(38)+SORT(U(39)/I4.*Y(39)**2/USORT(I)*SORT(I))
0211 307 U(41)=9.9AL*2/US-D*(INO-ZI1))**2
0212 308 U(42)=9.9AL*2/US-D*(INO-ZI1))**2
0213 309 I(U(41).LT.0.0)U(41)=0.0
0214 310 I(U(42).LT.0.0)U(42)=0.0
0215 311 Z(41)=Y(41)**2+SORT(U(41)/Y(41)+Z*(41+8))/I2.*Y(41)**2+D))
0216 312 I(Z(41)-Z(40))/I2.*Y(41)**2/D+1.))
0217 313 Z(41)=Z(40)+SORT(U(41)/I4.*Y(41)**2/USORT(I)*SORT(I))
0218 314 8 CONTINUE
0219 315 DO 9 N=42,44
0220 316 Z(N)=Y(N)**2+Z*(N-8)+Z*(N+8))/I2.*Y(N)**2+D))
0221 317 I(Z(N)-Z(N-1))/I2.*Y(N)**2/D+1.))
0222 318 Z(N)=Z(N-1)+SORT(U(N)/I4.*Y(N)**2/USORT(I)*SORT(I))
0223 319 9 CONTINUE
0224 320 DO 10 N=45,47
0225 321 Z(N)=Y(N)**2+Z*(N-8)+Z*(N+8))/I2.*Y(N)**2+D))
0226 322 I(Z(N)-Z(N-1))/I2.*Y(N)**2/D+1.))
0227 323 Z(N)=Z(N-1)+SORT(U(N)/I4.*Y(N)**2/USORT(I)*SORT(I))
0228 324 10 CONTINUE
0229 325 DO 11 N=48,50
0230 326 Z(N)=Y(N)**2+Z*(N-8)+Z*(N+8))/I2.*Y(N)**2+D))
0231 327 I(Z(N)-Z(N-1))/I2.*Y(N)**2/D+1.))
0232 328 Z(N)=Z(N-1)+SORT(U(N)/I4.*Y(N)**2/USORT(I)*SORT(I))
0233 329 11 CONTINUE
0234 330 DO 12 N=51,53
0235 331 Z(N)=Y(N)**2+Z*(N-8)+Z*(N+8))/I2.*Y(N)**2+D))
0236 332 I(Z(N)-Z(N-1))/I2.*Y(N)**2/D+1.))
0237 333 Z(N)=Z(N-1)+SORT(U(N)/I4.*Y(N)**2/USORT(I)*SORT(I))
0238 334 12 CONTINUE
0239 335 DO 13 N=54,56
0240 336 Z(N)=Y(N)**2+Z*(N-8)+Z*(N+8))/I2.*Y(N)**2+D))
0241 337 I(Z(N)-Z(N-1))/I2.*Y(N)**2/D+1.))
0242 338 Z(N)=Z(N-1)+SORT(U(N)/I4.*Y(N)**2/USORT(I)*SORT(I))
0243 339 13 CONTINUE
0244 340 DO 14 N=57,59
0245 341 Z(N)=Y(N)**2+Z*(N-8)+Z*(N+8))/I2.*Y(N)**2+D))
0246 342 I(Z(N)-Z(N-1))/I2.*Y(N)**2/D+1.))
0247 343 Z(N)=Z(N-1)+SORT(U(N)/I4.*Y(N)**2/USORT(I)*SORT(I))
0248 344 14 CONTINUE
0249 345 DO 15 N=60,62
0250 346 Z(N)=Y(N)**2+Z*(N-8)+Z*(N+8))/I2.*Y(N)**2+D))
0251 347 I(Z(N)-Z(N-1))/I2.*Y(N)**2/D+1.))
0252 348 Z(N)=Z(N-1)+SORT(U(N)/I4.*Y(N)**2/USORT(I)*SORT(I))
0253 349 15 CONTINUE
0254 350 DO 16 N=63,65
0255 351 Z(N)=Y(N)**2+Z*(N-8)+Z*(N+8))/I2.*Y(N)**2+D))
0256 352 I(Z(N)-Z(N-1))/I2.*Y(N)**2/D+1.))
0257 353 Z(N)=Z(N-1)+SORT(U(N)/I4.*Y(N)**2/USORT(I)*SORT(I))
0258 354 16 CONTINUE
0259 355 DO 17 N=66,68
0260 356 Z(N)=Y(N)**2+Z*(N-8)+Z*(N+8))/I2.*Y(N)**2+D))
0261 357 I(Z(N)-Z(N-1))/I2.*Y(N)**2/D+1.))
0262 358 Z(N)=Z(N-1)+SORT(U(N)/I4.*Y(N)**2/USORT(I)*SORT(I))
0263 359 17 CONTINUE
0264 360 DO 18 N=69,71
0265 361 Z(N)=Y(N)**2+Z*(N-8)+Z*(N+8))/I2.*Y(N)**2+D))
0266 362 I(Z(N)-Z(N-1))/I2.*Y(N)**2/D+1.))
0267 363 Z(N)=Z(N-1)+SORT(U(N)/I4.*Y(N)**2/USORT(I)*SORT(I))
0268 364 18 CONTINUE
0269 365 DO 19 N=72,74
0270 366 Z(N)=Y(N)**2+Z*(N-8)+Z*(N+8))/I2.*Y(N)**2+D))
0271 367 I(Z(N)-Z(N-1))/I2.*Y(N)**2/D+1.))
0272 368 Z(N)=Z(N-1)+SORT(U(N)/I4.*Y(N)**2/USORT(I)*SORT(I))
0273 369 19 CONTINUE
0274 370 DO 20 N=75,77
0275 371 Z(N)=Y(N)**2+Z*(N-8)+Z*(N+8))/I2.*Y(N)**2+D))
0276 372 I(Z(N)-Z(N-1))/I2.*Y(N)**2/D+1.))
0277 373 Z(N)=Z(N-1)+SORT(U(N)/I4.*Y(N)**2/USORT(I)*SORT(I))
0278 374 20 CONTINUE
0279 375 DO 21 N=78,80
0280 376 Z(N)=Y(N)**2+Z*(N-8)+Z*(N+8))/I2.*Y(N)**2+D))
0281 377 I(Z(N)-Z(N-1))/I2.*Y(N)**2/D+1.))
0282 378 Z(N)=Z(N-1)+SORT(U(N)/I4.*Y(N)**2/USORT(I)*SORT(I))
0283 379 21 CONTINUE
0284 380 DO 22 N=81,83
0285 381 Z(N)=Y(N)**2+Z*(N-8)+Z*(N+8))/I2.*Y(N)**2+D))
0286 382 I(Z(N)-Z(N-1))/I2.*Y(N)**2/D+1.))
0287 383 Z(N)=Z(N-1)+SORT(U(N)/I4.*Y(N)**2/USORT(I)*SORT(I))
0288 384 22 CONTINUE
0289 385 DO 23 N=84,86
0290 386 Z(N)=Y(N)**2+Z*(N-8)+Z*(N+8))/I2.*Y(N)**2+D))
0291 387 I(Z(N)-Z(N-1))/I2.*Y(N)**2/D+1.))
0292 388 Z(N)=Z(N-1)+SORT(U(N)/I4.*Y(N)**2/USORT(I)*SORT(I))
0293 389 23 CONTINUE
0294 390 DO 24 N=87,89
0295 391 Z(N)=Y(N)**2+Z*(N-8)+Z*(N+8))/I2.*Y(N)**2+D))
0296 392 I(Z(N)-Z(N-1))/I2.*Y(N)**2/D+1.))
0297 393 Z(N)=Z(N-1)+SORT(U(N)/I4.*Y(N)**2/USORT(I)*SORT(I))
0298 394 24 CONTINUE
0299 395 DO 25 N=90,92
0300 396 Z(N)=Y(N)**2+Z*(N-8)+Z*(N+8))/I2.*Y(N)**2+D))
0301 397 I(Z(N)-Z(N-1))/I2.*Y(N)**2/D+1.))
0302 398 Z(N)=Z(N-1)+SORT(U(N)/I4.*Y(N)**2/USORT(I)*SORT(I))
0303 399 25 CONTINUE
0304 400 DO 26 N=93,95
0305 401 Z(N)=Y(N)**2+Z*(N-8)+Z*(N+8))/I2.*Y(N)**2+D))
0306 402 I(Z(N)-Z(N-1))/I2.*Y(N)**2/D+1.))
0307 403 Z(N)=Z(N-1)+SORT(U(N)/I4.*Y(N)**2/USORT(I)*SORT(I))
0308 404 26 CONTINUE
0309 405 DO 27 N=96,98
0310 406 Z(N)=Y(N)**2+Z*(N-8)+Z*(N+8))/I2.*Y(N)**2+D))
0311 407 I(Z(N)-Z(N-1))/I2.*Y(N)**2/D+1.))
0312 408 Z(N)=Z(N-1)+SORT(U(N)/I4.*Y(N)**2/USORT(I)*SORT(I))
0313 409 27 CONTINUE
0314 410 DO 28 N=99,101
0315 411 Z(N)=Y(N)**2+Z*(N-8)+Z*(N+8))/I2.*Y(N)**2+D))
0316 412 I(Z(N)-Z(N-1))/I2.*Y(N)**2/D+1.))
0317 413 Z(N)=Z(N-1)+SORT(U(N)/I4.*Y(N)**2/USORT(I)*SORT(I))
0318 414 28 CONTINUE
0319 415 DO 29 N=102,104
0320 416 Z(N)=Y(N)**2+Z*(N-8)+Z*(N+8))/I2.*Y(N)**2+D))
0321 417 I(Z(N)-Z(N-1))/I2.*Y(N)**2/D+1.))
0322 418 Z(N)=Z(N-1)+SORT(U(N)/I4.*Y(N)**2/USORT(I)*SORT(I))
0323 419 29 CONTINUE
0324 420 DO 30 N=105,107
0325 421 Z(N)=Y(N)**2+Z*(N-8)+Z*(N+8))/I2.*Y(N)**2+D))
0326 422 I(Z(N)-Z(N-1))/I2.*Y(N)**2/D+1.))
0327 423 Z(N)=Z(N-1)+SORT(U(N)/I4.*Y(N)**2/USORT(I)*SORT(I))
0328 424 30 CONTINUE
0329 425 DO 31 N=108,110
0330 426 Z(N)=Y(N)**2+Z*(N-8)+Z*(N+8))/I2.*Y(N)**2+D))
0331 427 I(Z(N)-Z(N-1))/I2.*Y(N)**2/D+1.))
0332 428 Z(N)=Z(N-1)+SORT(U(N)/I4.*Y(N)**2/USORT(I)*SORT(I))
0333 429 31 CONTINUE
0334 430 DO 32 N=111,113
0335 431 Z(N)=Y(N)**2+Z*(N-8)+Z*(N+8))/I2.*Y(N)**2+D))
0336 432 I(Z(N)-Z(N-1))/I2.*Y(N)**2/D+1.))
0337 433 Z(N)=Z(N-1)+SORT(U(N)/I4.*Y(N)**2/USORT(I)*SORT(I))
0338 434 32 CONTINUE
0339 435 DO 33 N=114,116
0340 436 Z(N)=Y(N)**2+Z*(N-8)+Z*(N+8))/I2.*Y(N)**2+D))
0341 437 I(Z(N)-Z(N-1))/I2.*Y(N)**2/D+1.))
0342 438 Z(N)=Z(N-1)+SORT(U(N)/I4.*Y(N)**2/USORT(I)*SORT(I))
0343 439 33 CONTINUE
0344 440 DO 34 N=117,119
0345 441 Z(N)=Y(N)**2+Z*(N-8)+Z*(N+8))/I2.*Y(N)**2+D))
0346 442 I(Z(N)-Z(N-1))/I2.*Y(N)**2/D+1.))
0347 443 Z(N)=Z(N-1)+SORT(U(N)/I4.*Y(N)**2/USORT(I)*SORT(I))
0348 444 34 CONTINUE
0349 445 DO 35 N=120,122
0350 446 Z(N)=Y(N)**2+Z*(N-8)+Z*(N+8))/I2.*Y(N)**2+D))
0351 447 I(Z(N)-Z(N-1))/I2.*Y(N)**2/D+1.))
0352 448 Z(N)=Z(N-1)+SORT(U(N)/I4.*Y(N)**2/USORT(I)*SORT(I))
0353 449 35 CONTINUE
0354 450 DO 36 N=123,125
0355 451 Z(N)=Y(N)**2+Z*(N-8)+Z*(N+8))/I2.*Y(N)**2+D))
0356 452 I(Z(N)-Z(N-1))/I2.*Y(N)**2/D+1.))
0357 453 Z(N)=Z(N-1)+SORT(U(N)/I4.*Y(N)**2/USORT(I)*SORT(I))
0358 454 36 CONTINUE
0359 455 DO 37 N=126,128
0360 456 Z(N)=Y(N)**2+Z*(N-8)+Z*(N+8))/I2.*Y(N)**2+D))
0361 457 I(Z(N)-Z(N-1))/I2.*Y(N)**2/D+1.))
0362 458 Z(N)=Z(N-1)+SORT(U(N)/I4.*Y(N)**2/USORT(I)*SORT(I))
0363 459 37 CONTINUE
0364 460 DO 38 N=129,131
0365 461 Z(N)=Y(N)**2+Z*(N-8)+Z*(N+8))/I2.*Y(N)**2+D))
0366 462 I(Z(N)-Z(N-1))/I2.*Y(N)**2/D+1.))
0367 463 Z(N)=Z(N-1)+SORT(U(N)/I4.*Y(N)**2/USORT(I)*SORT(I))
0368 464 38 CONTINUE
0369 465 DO 39 N=132,134
0370 466 Z(N)=Y(N)**2+Z*(N-8)+Z*(N+8))/I2.*Y(N)**2+D))
0371 467 I(Z(N)-Z(N-1))/I2.*Y(N)**2/D+1.))
0372 468 Z(N)=Z(N-1)+SORT(U(N)/I4.*Y(N)**2/USORT(I)*SORT(I))
0373 469 39 CONTINUE
0374 470 DO 40 N=135,137
0375 471 Z(N)=Y(N)**2+Z*(N-8)+Z*(N+8))/I2.*Y(N)**2+D))
0376 472 I(Z(N)-Z(N-1))/I2.*Y(N)**2/D+1.))
0377 473 Z(N)=Z(N-1)+SORT(U(N)/I4.*Y(N)**2/USORT(I)*SORT(I))
0378 474 40 CONTINUE
0379 475 DO 41 N=138,140
0380 476 Z(N)=Y(N)**2+Z*(N-8)+Z*(N+8))/I2.*Y(N)**2+D))
0381 477 I(Z(N)-Z(N-1))/I2.*Y(N)**2/D+1.))
0382 478 Z(N)=Z(N-1)+SORT(U(N)/I4.*Y(N)**2/USORT(I)*SORT(I))
0383 479 41 CONTINUE
0384 480 DO 42 N=141,143
0385 481 Z(N)=Y(N)**2+Z*(N-8)+Z*(N+8))/I2.*Y(N)**2+D))
0386 482 I(Z(N)-Z(N-1))/I2.*Y(N)**2/D+1.))
0387 483 Z(N)=Z(N-1)+SORT(U(N)/I4.*Y(N)**2/USORT(I)*SORT(I))
0388 484 42 CONTINUE
0389 485 DO 43 N=144,146
0390 486 Z(N)=Y(N)**2+Z*(N-8)+Z*(N+8))/I2.*Y(N)**2+D))
0391 487 I(Z(N)-Z(N-1))/I2.*Y(N)**2/D+1.))
0392 488 Z(N)=Z(N-1)+SORT(U(N)/I4.*Y(N)**2/USORT(I)*SORT(I))
0393 489 43 CONTINUE
0394 490 DO 44 N=147,149
0395 491 Z(N)=Y(N)**2+Z*(N-8)+Z*(N+8))/I2.*Y(N)**2+D))
0396 492 I(Z(N)-Z(N-1))/I2.*Y(N)**2/D+1.))
0397 493 Z(N)=Z(N-1)+SORT(U(N)/I4.*Y(N)**2/USORT(I)*SORT(I))
0398 494 44 CONTINUE
0399 495 DO 45 N=150,152
0400 496 Z(N)=Y(N)**2+Z*(N-8)+Z*(N+8))/I2.*Y(N)**2+D))
0401 497 I(Z(N)-Z(N-1))/I2.*Y(N)**2/D+1.))
0402 498 Z(N)=Z(N-1)+SORT(U(N)/I4.*Y(N)**2/USORT(I)*SORT(I))
0403 499 45 CONTINUE
0404 500 DO 46 N=153,155
0405 501 Z(N)=Y(N)**2+Z*(N-8)+Z*(N+8))/I2.*Y(N)**2+D))
0406 502 I(Z(N)-Z(N-1))/I2.*Y(N)**2/D+1.))
0407 503 Z(N)=Z(N-1)+SORT(U(N)/I4.*Y(N)**2/USORT(I)*SORT(I))
0408 504 46 CONTINUE
0409 505 DO 47 N=156,158
0410 506 Z(N)=Y(N)**2+Z*(N-8)+Z*(N+8))/I2.*Y(N)**2+D))
0411 507 I(Z(N)-Z(N-1))/I2.*Y(N)**2/D+1.))
0412 508 Z(N)=Z(N-1)+SORT(U(N)/I4.*Y(N)**2/USORT(I)*SORT(I))
0413 509 47 CONTINUE
0414 510 DO 48 N=159,161
0415 511 Z(N)=Y(N)**2+Z*(N-8)+Z*(N+8))/I2.*Y(N)**2+D))
0416 512 I(Z(N)-Z(N-1))/I2.*Y(N)**2/D+1.))
0417 513 Z(N)=Z(N-1)+SORT(U(N)/I4.*Y(N)**2/USORT(I)*SORT(I))
0418 514 48 CONTINUE
0419 515 DO 49 N=162,164
0420 516 Z(N)=Y(N)**2+Z*(N-8)+Z*(N+8))/I2.*Y(N)**2+D))
0421 517 I(Z(N)-Z(N-1))/I2.*Y(N)**2/D+1.))
0422 518 Z(N)=Z(N-1)+SORT(U(N)/I4.*Y(N)**2/USORT(I)*SORT(I))
0423 519 49 CONTINUE
0424 520 DO 50 N=165,167
0425 521 Z(N)=Y(N)**2+Z*(N-8)+Z*(N+8))/I2.*Y(N)**2+D))
0426 522 I(Z(N)-Z(N-1))/I2.*Y(N)**2/D+1.))
0427 523 Z(N)=Z(N-1)+SORT(U(N)/I4.*Y(N)**2/USORT(I)*SORT(I))
0428 524 50 CONTINUE
0429 525 DO 51 N=168,170
0430 526 Z(N)=Y(N)**2+Z*(N-8)+Z*(N+8))/I2.*Y(N)**2+D))
0431 527 I(Z(N)-Z(N-1))/I2.*Y(N)**2/D+1.))
0432 528 Z(N)=Z(N-1)+SORT(U(N)/I4.*Y(N)**2/USORT(I)*SORT(I))
0433 529 51 CONTINUE
0434 530 DO 52 N=171,173
0435 531 Z(N)=Y(N)**2+Z*(N-8)+Z*(N+8))/I2.*Y(N)**2+D))
0436 532 I(Z(N)-Z(N-1))/I2.*Y(N)**2/D+1.))
0437 533 Z(N)=Z(N-1)+SORT(U(N)/I4.*Y(N)**2/USORT(I)*SORT(I))
0438 534 52 CONTINUE
0439 535 DO 53 N=174,176
0440 536 Z(N)=Y(N)**2+Z*(N-8)+Z*(N+8))/I2.*Y(N)**2+D))
0441 537 I(Z(N)-Z(N-1))/I2.*Y(N)**2/D+1.))
0442 538 Z(N)=Z(N-1)+SORT(U(N)/I4.*Y(N)**2/USORT(I)*SORT(I))
0443 539 53 CONTINUE
0444 540 DO 54 N=177,179
0445 541 Z(N)=Y(N)**2+Z*(N-8)+Z*(N+8))/I2.*Y(N)**2+D))
0446 542 I(Z(N)-Z(N-1))/I2.*Y(N)**2/D+1.))
0447 543 Z(N)=Z(N-1)+SORT(U(N)/I4.*Y(N)**2/USORT(I)*SORT(I))
0448 544 54 CONTINUE
0449 545 DO 55 N=180,182
0450 546 Z(N)=Y(N)**2+Z*(N-8)+Z*(N+8))/I2.*Y(N)**2+D))
0451 547 I(Z(N)-Z(N-1))/I2.*Y(N)**2/D+1.))
0452 548 Z(N)=Z(N-1)+SORT(U(N)/I4.*Y(N)**2/USORT(I)*SORT(I))
0453 549 55 CONTINUE
0454 550 DO 56 N=183,185
0455 551 Z(N)=Y(N)**2+Z*(N-8)+Z*(N+8))/I2.*Y(N)**2+D))
0456 552 I(Z(N)-Z(N-1))/I2.*Y(N)**2/D+1.))
0457 553 Z(N)=Z(N-1)+SORT(U(N)/I4.*Y(N)**2/USORT(I)*SORT(I))
0458 554 56 CONTINUE
0459 555 DO 57 N=186,188
0460 556 Z(N)=Y(N)**2+Z*(N-8)+Z*(N+8))/I2.*Y(N)**2+D))
0461 557 I(Z(N)-Z(N-1))/I2.*Y(N)**2/D+1.))
0462 558 Z(N)=Z(N-1)+SORT(U(N)/I4.*Y(N)**2/USORT(I)*SORT(I))
0463 559 57 CONTINUE
0464 560 DO 58 N=189,191
0465 561 Z(N)=Y(N)**2+Z*(N-8)+Z*(N+8))/I2.*Y(N)**2+D))
0466 562 I(Z(N)-Z(N-1))/I2.*Y(N)**2/D+1.))
0467 563 Z(N)=Z(N-1)+SORT(U(N)/I4.*Y(N)**2/USORT(I)*SORT(I))
0468 564 58 CONTINUE
0469 565 DO 59 N=192,194
0470 566 Z(N)=Y(N)**2+Z*(N-8)+Z*(N+8))/I2.*Y(N)**2+D))
0471 567 I(Z(N)-Z(N-1))/I2.*Y(N)**2/D+1.))
0472 568 Z(N)=Z(N-1)+SORT(U(N)/I4.*Y(N)**2/USORT(I)*SORT(I))
0473 569 59 CONTINUE
0474 570 DO 60 N=195,197
0475 571 Z(N)=Y(N)**2+Z*(N-8)+Z*(N+8))/I2.*Y(N)**2+D))
0476 572 I(Z(N)-Z(N-1))/I2.*Y(N)**2/D+1.))
0477 573 Z(N)=Z(N-1)+SORT(U(N)/I4.*Y(N)**2/USORT(I)*SORT(I))
0478 574 60 CONTINUE
0479 575 DO 61 N=198,200
0480 576 Z(N)=Y(N)**2+Z*(N-8)+Z*(N+8))/I2.*Y(N)**2+D))
0481 577 I(Z(N)-Z(N-1))/I2.*Y(N)**2/D+1.))
0482 578 Z(N)=Z(N-1)+SORT(U(N)/I4.*Y(N)**2/USORT(I)*SORT(I))
0483 579 61 CONTINUE
0484 580 DO 62 N=201,203
0485 581 Z(N)=Y(N)**2+Z*(N-8)+Z*(N+8))/I2.*Y(N)**2+D))
0486 582 I(Z(N)-Z(N-1))/I2.*Y(N)**2/D+1.))
0487 583 Z(N)=Z(N-1)+SORT(U(N)/I4.*Y(N)**2/USORT(I)*SORT(I))
0488 584 62 CONTINUE
0489 585 DO 63 N=204,206
0490 586 Z(N)=Y(N)**2+Z*(N-8)+Z*(N+8))/I2.*Y(N)**2+D))
0491 587 I(Z(N)-Z(N-1))/I2.*Y(N)**2/D+1.))
0492 588 Z(N)=Z(N-1)+SORT(U(N)/I4.*Y(N)**2/USORT(I)*SORT(I))
0493 589 63 CONTINUE
0494 590 DO 64 N=207,209
0495 591 Z(N)=Y(N)**2+Z*(N-8)+Z*(N+8))/I2.*Y(N)**2+D))
0496 592 I(Z(N)-Z(N-1))/I2.*Y(N)**2/D+1.))
0497 593 Z(N)=Z(N-1)+SORT(U(N)/I4.*Y(N)**2/USORT(I)*SORT(I))
0498 594 64 CONTINUE
0499 595 DO 65 N=210,212
0500 596 Z(N)=Y(N)**2+Z*(N-8)+Z*(N+8))/I2.*Y(N)**2+D))
0501 597 I(Z(N)-Z(N-1))/I2.*Y(N)**2/D+1.))
0502 598 Z(N)=Z(N-1)+SORT(U(N)/I4.*Y(N)**2/USORT(I)*SORT(I))
0503 599 65 CONTINUE
0504 600 DO 66 N=213,215
0505 601 Z(N)=Y(N)**2+Z*(N-8)+Z*(N+8))/I2.*Y(N)**2+D))
0506 602 I(Z(N)-Z(N-1))/I2.*Y(N)**2/D+1.))
0507 603 Z(N)=Z(N-1)+SORT(U(N)/I4.*Y(N)**2/USORT(I)*SORT(I))
0508 604 66 CONTINUE
0509 605 DO 67 N=216,218
0510 606 Z(N)=Y(N)**2+Z*(N-8)+Z*(N+8))/I2.*Y(N)**2+D))
0511 607 I(Z(N)-Z(N-1))/I2.*Y(N)**2/D+1.))
0512 608 Z(N)=Z(N-1)+SORT(U(N)/I4.*Y(N)**2/USORT(I)*SORT(I))
0513 609 67 CONTINUE
0514 610 DO 68 N=219,221
0515 611 Z(N)=Y(N)**2+Z*(N-8)+Z*(N+8))/I2.*Y(N)**2+D))
0516 612 I(Z(N)-Z(N-1))/I2.*Y(N)**2/D+1.))
0517 613 Z(N)=Z(N-1)+SORT(U(N)/I4.*Y(N)**2/USORT(I)*SORT(I))
0518 614 68 CONTINUE
0519 615 DO 69 N=222,224
0520 616 Z(N)=Y(N)**2+Z*(N-8)+Z*(N+8))/I2.*Y(N)**2+D))
0521 617 I(Z(N)-Z(N-1))/I2.*Y(N)**2/D+1.))
0522 618 Z(N)=Z(N-1)+SORT(U(N)/I4.*Y(N)**2/USORT(I)*SORT(I))
0523 619 69 CONTINUE
0524 620 DO 70 N=225,227
0525 621 Z(N)=Y(N)**2+Z*(N-8)+Z*(N+8))/I2.*Y(N)**2+D))
0526 622 I(Z(N)-Z(N-1))/I2.*Y(N)**2/D+1.))
0527 623 Z(N)=Z(N-1)+SORT(U(N)/I4.*Y(N)**2/USORT(I)*SORT(I))
0528 624 70 CONTINUE
0529 625 DO 71 N=228,230
0530 626 Z(N)=Y(N)**2+Z*(N-8)+Z*(N+8))/I2.*Y(N)**2+D))
0531 627 I(Z(N)-Z(N-1))/I2.*Y(N)**2/D+1.))
0532 628 Z(N)=Z(N-1)+SORT(U(N)/I4.*Y(N)**2/USORT(I)*SORT(I))
0533 629 71 CONTINUE
0534 630 DO 72 N=231,233
0535 631 Z(N)=Y(N)**2+Z*(N-8)+Z*(N+8))/I2.*Y(N)**2+D))
0536 632 I(Z(N)-Z(N-1))/I2.*Y(N)**2/D+1.))
0537 633 Z(N)=Z(N-1)+SORT(U(N)/I4.*Y(N)**2/USORT(I)*SORT(I))
0538 634 72 CONTINUE
0539 635 DO 73 N=234,236
0540 636 Z(N)=Y(N)**2+Z*(N-8)+Z*(N+8))/I2.*Y(N)**2+D))
0541 637 I(Z(N)-Z(N-1))/I2.*Y(N)**2/D+1.))
0542 638 Z(N)=Z(N-1)+SORT(U(N)/I4.*Y(N)**2/USORT(I)*SORT(I))
0543 639 73 CONTINUE
0544 640 DO 74 N=237,239
0545 641 Z(N)=Y(N)**2+Z*(N-8)+Z*(N+8))/I2.*Y(N)**2+D))
0546 642 I(Z(N)-Z(N-1))/I2.*Y(N)**2/D+1.))
0547 643 Z(N)=Z(N-1)+SORT(U(N)/I4.*Y(N)**2/USORT(I)*SORT(I))
0548 644 74 CONTINUE
0549 645 DO 75 N=240,242
0550 646 Z(N)=Y(N)**2+Z*(N-8)+Z*(N+8))/I2.*Y(N)**2+D))
0551 647 I(Z(N)-Z(N-1))/I2.*Y(N)**2/D+1.))
0552 648 Z(N)=Z(N-1)+SORT(U(N)/I4.*Y(N)**2/USORT(I)*SORT(I))
0553 649 75 CONTINUE
0554 650 DO 76 N=243,245
0555 651 Z(N)=Y(N)**2+Z*(N-8)+Z*(N+8))/I2.*Y(N)**2+D))
0556 652 I(Z(N)-Z(N-1))/I2.*Y(N)**2/D+1.))
0557 653 Z(N)=Z(N-1)+SORT(U(N)/I4.*Y(N)**2/USORT(I)*SORT(I))
0558 654 76 CONTINUE
0559 655 DO 77 N=246,248
0560 656 Z(N)=Y(N)**2+Z*(N-8)+Z*(N+8))/I2.*Y(N)**2+D))
0561 657 I(Z(N)-Z(N-1))/I2.*Y(N)**2/D+1.))
0562 658 Z(N)=Z(N-1)+SORT(U(N)/I4.*Y(N)**2/USORT(I)*SORT(I))
0563 659 77 CONTINUE
0564 660 DO 78 N=249,251
0565 661 Z(N)=Y(N)**2+Z*(N-8)+Z*(N+8))/I2.*Y(N)**2+D))
0566 662 I(Z(N)-Z(N-1))/I2.*Y(N)**2/D+1.))
0567 663 Z(N)=Z(N-1)+SORT(U(N)/I4.*Y(N)**2/USORT(I)*SORT(I))
0568 664 78 CONTINUE
0569 665 DO 79 N=252,254
0570 666 Z(N)=Y(N)**2+Z*(N-8)+Z*(N+8))/I2.*Y(N)**2+D))
0571 667 I(Z(N)-Z(N-1))/I2.*Y(N)**2/D+1.))
0572 668 Z(N)=Z(N-1)+SORT(U(N)/I4.*Y(N)**2/USORT(I)*SORT(I))
0573 669 79 CONTINUE
0574 670 DO 80 N=255,257
0575 671 Z(N)=Y(N)**2+Z*(N-8)+Z*(N+8))/I2.*Y(N)**2+D))
0576 672 I(Z(N)-Z(N-1))/I2.*Y(N)**2/D+1.))
0577 673 Z(N)=Z(N-1)+SORT(U(N)/I4.*Y(N)**2/USORT(I)*SORT(I))
0578 674 80 CONTINUE
0579 675 DO 81 N=258,260
0580 676 Z(N)=Y(N)**2+Z*(N-8)+Z*(N+8))/I2.*Y(N)**2+D))
0581 677 I(Z(N)-Z(N-1))/I2.*Y(N)**2/D+1.))
0582 678 Z(N)=Z(N-1)+SORT(U(N)/I4.*Y(N)**2/USORT(I)*SORT(I))
0583 679 81 CONTINUE
0584 680 DO 82 N=261,263
0585 681 Z(N)=Y(N)**2+Z*(N-8)+Z*(N+8))/I2.*Y(N)**2+D))
0586 682 I(Z(N)-Z(N-1))/I2.*Y(N)**2/D+1.))
0587 683 Z(N)=Z(N-1)+SORT(U(N)/I4.*Y(N)**2/USORT(I)*SORT(I))
0588 684 82 CONTINUE
0589 685 DO 83 N=264,266
0590 686 Z(N)=Y(N)**2+Z*(N-8)+Z*(N+8))/I2.*Y(N)**2+D))
0591 687 I(Z(N)-Z(N-1))/I2.*Y(N)**2/D+1.))
0592 688 Z(N)=Z(N-1)+SORT(U(N)/I4.*Y(N)**2/USORT(I)*SORT(I))
0593 689 83 CONTINUE
0594 690 DO
```


VI. FINITE PLATE/(R₀/L) = 1/2

$\gamma_1 = 1.93$	$\gamma_2 = 1.085$	$\gamma_3 = 1.051$	$\gamma_4 = 1.040$	$\gamma_5 = 1.037$	$\gamma_6 = 1.113$	$\gamma_7 = 1.111$	$\gamma_8 = 1.111$
$\gamma_9 = 1.94$	$\gamma_{10} = 1.115$	$\gamma_{11} = 1.093$	$\gamma_{12} = 1.199$	$\gamma_{13} = 1.059$	$\gamma_{14} = 1.095$	$\gamma_{15} = 1.111$	$\gamma_{16} = 1.111$
$\gamma_{17} = 1.91$	$\gamma_{18} = 1.137$	$\gamma_{19} = 1.101$	$\gamma_{20} = 1.193$	$\gamma_{21} = 1.058$	$\gamma_{22} = 1.092$	$\gamma_{23} = 1.111$	$\gamma_{24} = 1.111$
$\gamma_{25} = 1.89$	$\gamma_{26} = 1.155$	$\gamma_{27} = 1.095$	$\gamma_{28} = 1.191$	$\gamma_{29} = 1.059$	$\gamma_{30} = 1.098$	$\gamma_{31} = 1.111$	$\gamma_{32} = 1.111$
$\gamma_{33} = 1.89$	$\gamma_{34} = 1.173$	$\gamma_{35} = 1.094$	$\gamma_{36} = 1.191$	$\gamma_{37} = 1.057$	$\gamma_{38} = 1.097$	$\gamma_{39} = 1.111$	$\gamma_{40} = 1.111$
$\gamma_{41} = 1.88$	$\gamma_{42} = 1.191$	$\gamma_{43} = 1.093$	$\gamma_{44} = 1.191$	$\gamma_{45} = 1.057$	$\gamma_{46} = 1.097$	$\gamma_{47} = 1.111$	$\gamma_{48} = 1.111$
$\gamma_{49} = 1.85$	$\gamma_{50} = 1.210$	$\gamma_{51} = 1.093$	$\gamma_{52} = 1.191$	$\gamma_{53} = 1.056$	$\gamma_{54} = 1.097$	$\gamma_{55} = 1.111$	$\gamma_{56} = 1.111$
$\gamma_{57} = 1.85$	$\gamma_{58} = 1.228$	$\gamma_{59} = 1.093$	$\gamma_{60} = 1.191$	$\gamma_{61} = 1.056$	$\gamma_{62} = 1.097$	$\gamma_{63} = 1.111$	$\gamma_{64} = 1.111$

KATHY...
 SI 85...

FINITE PLATE

CC136	32a	212*0000*(Y11-Y10-11)**2-4*0AL**2/US1/8.
CC137	33a	1 CONTINUE
CC141	34a	U193=0*0AL**2/US-0*11-(Y17)**2
CC142	35a	Y10U17*LT*0.C*U18)E*0
CC144	36a	F101=V101**4-V101**3*V101**2*(Y19)**2*(C-5*SORT(U18))-
CC186	37a	1 V101**4*(Y17)**2**2
CC188	38a	2(2*00011-(Y17)**2-4*0AL**2/US1/8.
CC189	39a	CC 2 P25*73*E
CC190	40a	F101=V101**4*(Y10)**3*(V101-8)*(Y10+8))/2**
CC191	41a	2 V101**2*(C-2*(Y10-8)-Y10+8)**2/8.1-
CC192	42a	2.5*(Y10-2*(Y10-8)-Y10+8)*(210-8)-2*(Y10+8))/SORT(U10))*
CC193	43a	3 Y10**2*(Y10-8)*2*(Y10+8)**2/8.
CC194	44a	2 CONTINUE
CC195	45a	3 IT25*5
CC196	46a	CC 4 P25*73*E
CC197	47a	IS*IC
CC198	48a	3 IT25*5
CC199	49a	F101=V101**4*(Y10)**3*(V101-8)*(Y10+8))/2**
CC200	50a	2*(Y10+8)-Y10-8)*Y10**2/8.1-
CC201	51a	6 CONTINUE
CC202	52a	IS*IS*P
CC203	53a	3 F101*F.261 50 TO 3
CC204	54a	3*AL PR
CC205	55a	3*AL PR
CC206	56a	CC 5 P25*73*E
CC207	57a	F101=V101**4*(Y10)**3*(V101-8)*(Y10+8))/2**
CC208	58a	1 V101**2*(C-2*(Y10-8)-Y10+8)**2/8.1-
CC209	59a	2*(Y10+8)-Y10-8)*Y10**2/8.1-
CC210	60a	3*0AL**2/US-0*11-(Y17)**2
CC211	61a	3*0AL**2/US-0*11-(Y17)**2
CC212	62a	3*0AL**2/US-0*11-(Y17)**2
CC213	63a	3*0AL**2/US-0*11-(Y17)**2
CC214	64a	3*0AL**2/US-0*11-(Y17)**2
CC215	65a	3*0AL**2/US-0*11-(Y17)**2
CC216	66a	3*0AL**2/US-0*11-(Y17)**2
CC217	67a	3*0AL**2/US-0*11-(Y17)**2
CC218	68a	3*0AL**2/US-0*11-(Y17)**2
CC219	69a	3*0AL**2/US-0*11-(Y17)**2
CC220	70a	3*0AL**2/US-0*11-(Y17)**2
CC221	71a	3*0AL**2/US-0*11-(Y17)**2
CC222	72a	3*0AL**2/US-0*11-(Y17)**2
CC223	73a	3*0AL**2/US-0*11-(Y17)**2
CC224	74a	3*0AL**2/US-0*11-(Y17)**2
CC225	75a	3*0AL**2/US-0*11-(Y17)**2
CC226	76a	3*0AL**2/US-0*11-(Y17)**2
CC227	77a	3*0AL**2/US-0*11-(Y17)**2
CC228	78a	3*0AL**2/US-0*11-(Y17)**2
CC229	79a	3*0AL**2/US-0*11-(Y17)**2
CC230	80a	3*0AL**2/US-0*11-(Y17)**2
CC231	81a	3*0AL**2/US-0*11-(Y17)**2
CC232	82a	3*0AL**2/US-0*11-(Y17)**2
CC233	83a	3*0AL**2/US-0*11-(Y17)**2
CC234	84a	3*0AL**2/US-0*11-(Y17)**2
CC235	85a	3*0AL**2/US-0*11-(Y17)**2
CC236	86a	3*0AL**2/US-0*11-(Y17)**2
CC237	87a	3*0AL**2/US-0*11-(Y17)**2
CC238	88a	3*0AL**2/US-0*11-(Y17)**2
CC239	89a	3*0AL**2/US-0*11-(Y17)**2
CC240	90a	3*0AL**2/US-0*11-(Y17)**2
CC241	91a	3*0AL**2/US-0*11-(Y17)**2
CC242	92a	3*0AL**2/US-0*11-(Y17)**2
CC243	93a	3*0AL**2/US-0*11-(Y17)**2
CC244	94a	3*0AL**2/US-0*11-(Y17)**2
CC245	95a	3*0AL**2/US-0*11-(Y17)**2
CC246	96a	3*0AL**2/US-0*11-(Y17)**2
CC247	97a	3*0AL**2/US-0*11-(Y17)**2
CC248	98a	3*0AL**2/US-0*11-(Y17)**2
CC249	99a	3*0AL**2/US-0*11-(Y17)**2
CC250	100a	3*0AL**2/US-0*11-(Y17)**2

ORIGINAL PAGE IS
OF POOR QUALITY

DATE 10/5/76 PAGE 100

FINITE PLATE

16 7134945901
 17 7134945902
 18 7134945903
 19 7134945904
 20 7134945905
 21 7134945906
 22 7134945907
 23 7134945908
 24 7134945909
 25 7134945910
 26 7134945911
 27 7134945912
 28 7134945913
 29 7134945914
 30 7134945915
 31 7134945916
 32 7134945917
 33 7134945918
 34 7134945919
 35 7134945920
 36 7134945921
 37 7134945922
 38 7134945923
 39 7134945924
 40 7134945925
 41 7134945926
 42 7134945927
 43 7134945928
 44 7134945929
 45 7134945930

THE SET OF SEQUENCES IS 5209278-32
 PLATE SOLUTION BECAUSE THERE HAVE BEEN 150 CALLS OF CALFUN
 FOR FINITE SOLUTION PROBERT 150 CALLS OF CALFUN AND IS

46 7134945931
 47 7134945932
 48 7134945933
 49 7134945934
 50 7134945935
 51 7134945936
 52 7134945937
 53 7134945938
 54 7134945939
 55 7134945940
 56 7134945941
 57 7134945942
 58 7134945943
 59 7134945944
 60 7134945945
 61 7134945946
 62 7134945947
 63 7134945948
 64 7134945949
 65 7134945950
 66 7134945951
 67 7134945952
 68 7134945953
 69 7134945954
 70 7134945955
 71 7134945956
 72 7134945957
 73 7134945958
 74 7134945959
 75 7134945960

000015 MAIN
FOR 011A-12/76/79-11 39 JA (,7)

MAIN PROGRAM

STORAGE USED (CORE) 00115: DATA(1) 00125: PLAN(COMMONIZ) 00000

EXTERNAL REFERENCES (BLOCK, NAME)

0001 NINTPS
0002 NRDUS
0003 NIOIS
0004 NI02S
0007 N00US
0010 SQNT
0011 NSTOPS

STORAGE ASSIGNMENT (BLOCK, TYPE, RELATIVE LOCATION, NAME)

0001	00096	100F	0001	00027	1220	0001	00051	1206	0001	00121	1426	0001	000134	1816	
0002	00033	176K	0001	00046	2266	0001	00065	2176	0001	00027	2256	0001	000566	2335	
0003	00050	267	0001	00037	21	0001	00060	50L	0001	00021	8F	0001	001103	99L	
0004	00039	8L	0001	00028	COUAT	0001	00027	U	0001	00028	1	0001	000284	15	
0007	000245	1F	0001	00024	J	0001	00024	M	0001	00027	ME	0000	R	000227	K0
0010	000230	M	0001	00023	N	0001	00023	N	0001	00023	PS16	0000	R	000236	RU
0011	00000	U	0000	P	000231	US	0000	P	000062	V	0000	R	000104	Z	

0101	19	DIMENSION (USER)
0102	20	DIMENSION (USER)
0104	20	DIMENSION (USER)
0105	00	REAL (S)
0106	00	REAL (U)
0107	00	MM(25)
0110	74	AS(1)
0111	00	US(55002)
0112	00	01(40027)
0113	100	PSIGEN(72)
0119	110	AL(01070)
0120	120	1205
0128	170	00(10733)
0129	180	MEMM
0131	100	HEAD(5) (1) (E)(U)(J)(DELIM)
0132	100	HEAD(5) (1) (E)(U)(J)(DELIM)
0133	170	170 (FORMAT(1)(1)(2))
0135	100	MM(25)
0136	100	INTEGR COUNT
0137	100	COUNT
0139	210	01 (CONTIGUOUS)
0141	200	IF (CONTIGUOUS) 00 TO 00
0142	200	THIS STATEMENT HAS TOO MANY LEFT PARENTHESES.
0143	200	TO EXCEED THE LIMIT OF THE 15-ARGUMENT INFORMATION. (E HAVE)
0144	200	01 (FORMAT(1) (1) (2))

```

2167 6 FORMAT(1P,4XHE,9X02(T1//C25,C17,0))
2168 WRITE(6,3) (1,2,19,1E1,N)
2169 Z(1)=1.04
2170 DO 1 K=2,7
2171   U(K)=0.04*ZUS-D*(Z(K)+1)-Z(K-1)*0.2
2172   IF(U(K).LE.0) U(K)=0
2173   Z(K)=U(K)*0.2+(SORT(U(K)/Y(K)+2.7*(K+8)))/(2.0*Y(K)*0.2+0.3)+
2174   1.2*(K+1)-Z(K-1)/12.0*(Y(K)+0.2*Z(K+1))
2175   Z(1)=1.04
2176   1 CONTINUE
2177   U(1)=0.04*ZUS-D*(0.0-Z(1)*0.2
2178   IF(U(1).LE.0) U(1)=0
2179   2 GO TO 1
2180   3 SORT(U(1)/Y(1)+2.7*(1+8)))/(2.0*Y(1)*0.2+0.3)+
2181   2*(1+2.7*(1+8)*U(1)/Y(1)+0.2*(1+8))
2182   4 GO TO 2
2183   5 CONTINUE
2184   6 CONTINUE
2185   7 CONTINUE
2186   8 CONTINUE
2187   9 CONTINUE
2188   10 CONTINUE
2189   11 CONTINUE
2190   12 CONTINUE
2191   13 CONTINUE
2192   14 CONTINUE
2193   15 CONTINUE
2194   16 CONTINUE
2195   17 CONTINUE
2196   18 CONTINUE
2197   19 CONTINUE
2198   20 CONTINUE
2199   21 CONTINUE
2200   22 CONTINUE
2201   23 CONTINUE
2202   24 CONTINUE
2203   25 CONTINUE
2204   26 CONTINUE
2205   27 CONTINUE
2206   28 CONTINUE
2207   29 CONTINUE
2208   30 CONTINUE
2209   31 CONTINUE
2210   32 CONTINUE
2211   33 CONTINUE
2212   34 CONTINUE
2213   35 CONTINUE
2214   36 CONTINUE
2215   37 CONTINUE
2216   38 CONTINUE
2217   39 CONTINUE
2218   40 CONTINUE
2219   41 CONTINUE
2220   42 CONTINUE
2221   43 CONTINUE
2222   44 CONTINUE
2223   45 CONTINUE
2224   46 CONTINUE
2225   47 CONTINUE
2226   48 CONTINUE
2227   49 CONTINUE
2228   50 CONTINUE
2229   51 CONTINUE
2230   52 CONTINUE
2231   53 CONTINUE
2232   54 CONTINUE
2233   55 CONTINUE
2234   56 CONTINUE
2235   57 CONTINUE
2236   58 CONTINUE
2237   59 CONTINUE
2238   60 CONTINUE
2239   61 CONTINUE
2240   62 CONTINUE
2241   63 CONTINUE
2242   64 CONTINUE
2243   65 CONTINUE
2244   66 CONTINUE
2245   67 CONTINUE
2246   68 CONTINUE
2247   69 CONTINUE
2248   70 CONTINUE
2249   71 CONTINUE
2250   72 CONTINUE
2251   73 CONTINUE
2252   74 CONTINUE
2253   75 CONTINUE
2254   76 CONTINUE
2255   77 CONTINUE
2256   78 CONTINUE
2257   79 CONTINUE
2258   80 CONTINUE
2259   81 CONTINUE
2260   82 CONTINUE
2261   83 CONTINUE
2262   84 CONTINUE
2263   85 CONTINUE
2264   86 CONTINUE
2265   87 CONTINUE
2266   88 CONTINUE
2267   89 CONTINUE
2268   90 CONTINUE
2269   91 CONTINUE
2270   92 CONTINUE
2271   93 CONTINUE
2272   94 CONTINUE
2273   95 CONTINUE
2274   96 CONTINUE
2275   97 CONTINUE
2276   98 CONTINUE
2277   99 CONTINUE
2278   100 CONTINUE

```


ORIGINAL PAGE IS
OF POOR QUALITY

43 --4910963*E1
44 --1170000*E1
45 --2210000*E1
 AT THE 249 TH ITERATION WE HAVE
 1
 2 --18700000*E1
 3 --4616036*E1
 4 --3300033*E0
 5 --302452 *E0
 6 --5705644*E0
 7 --8933582*E0
 8 --17222387*E1
 9 --28459164*E1
 10 --19177222*E1
 11 --9065479*E0
 12 --36431603*E0
 13 --28277105*E0
 14 --47660711*E0
 15 --80372937*E0
 16 --16317861*E1
 17 --27757206*E1
 18 --18352173*E1
 19 --9315911*E0
 20 --39831503*E0
 21 --1624438*E0
 22 --37593754*E0
 23 --59901792*E1
 24 --19286174*E1
 25 --27026399*E1
 26 --16525366*E1
 27 --95584374*E1
 28 --42880629*E0
 29 --12166324*E0
 30 --26627696*E0
 31 --6899156*E0
 32 --15544137*E1
 33 --26144431*E1
 34 --14696506*E1
 35 --98240872*E0
 36 --45975687*E0
 37 --60706190*E1
 38 --14376329*E0
 39 --37923098*E0
 40 --19354850*E1
 41 --24927655*E1
 42 --14965498*E1
 43 --13082602*E1
 44 --4911324*E0
 45 --11000000*E1
 46 --22100000*E1

VIII. FINITE PLATE/(R₀/L) = 3/4

$z_1 = 1.40$	$z_2 = 1.887$	$z_3 = 2.341$	$z_4 = 2.796$	$z_5 = 3.2597$	$z_6 = 3.703$	$z_7 = 4.188$	$z_8 = 4.693$	A E: 3.3 r=1
$y_1 = 1.05$	$y_2 = 1.49$	$y_3 = 1.67$	$y_4 = 1.55$	$y_5 = 1.05$	$y_6 = 1.00$	$y_7 = 1.995$	$y_8 = 1.995$	K: 3.3 r=1.895
$z_9 = 1.417$	$z_{10} = 1.473$	$z_{11} = 1.533$	$z_{12} = 1.598$	$z_{13} = 1.665$	$z_{14} = 1.748$	$z_{15} = 1.833$	$z_{16} = 1.886$	
$y_9 = 1.03$	$y_{10} = 1.47$	$y_{11} = 1.66$	$y_{12} = 1.50$	$y_{13} = 1.956$	$y_{14} = 1.897$	$y_{15} = 1.889$	$y_{16} = 1.888$	K: 3.3 r=1.775
$z_{17} = 1.434$	$z_{18} = 1.948$	$z_{19} = 2.505$	$z_{20} = 3.179$	$z_{21} = 3.904$	$z_{22} = 4.682$	$z_{23} = 5.577$	$z_{24} = 6.577$	
$y_{17} = 1.01$	$y_{18} = 1.45$	$y_{19} = 1.64$	$y_{20} = 1.46$	$y_{21} = 1.845$	$y_{22} = 1.776$	$y_{23} = 1.768$	$y_{24} = 1.767$	K: 3.3 r=1.63
$z_{25} = 1.457$	$z_{26} = 1.965$	$z_{27} = 2.537$	$z_{28} = 3.119$	$z_{29} = 3.790$	$z_{30} = 4.502$	$z_{31} = 5.268$	$z_{32} = 6.087$	
$y_{25} = 1.00$	$y_{26} = 1.43$	$y_{27} = 1.62$	$y_{28} = 1.42$	$y_{29} = 1.710$	$y_{30} = 1.641$	$y_{31} = 1.633$	$y_{32} = 1.632$	K: 3.3 r=1.57
$z_{33} = 1.468$	$z_{34} = 1.997$	$z_{35} = 2.670$	$z_{36} = 3.359$	$z_{37} = 4.159$	$z_{38} = 5.091$	$z_{39} = 6.155$	$z_{40} = 7.355$	
$y_{33} = 1.02$	$y_{34} = 1.41$	$y_{35} = 1.61$	$y_{36} = 1.41$	$y_{37} = 1.533$	$y_{38} = 1.436$	$y_{39} = 1.429$	$y_{40} = 1.428$	K: 3.3 r=1.57
$z_{41} = 1.483$	$z_{42} = 2.037$	$z_{43} = 2.733$				$z_{44} = 3.570$	$z_{45} = 4.550$	
$y_{41} = 1.06$	$y_{42} = 1.37$	$y_{43} = 1.57$				$y_{44} = 1.37$	$y_{45} = 1.37$	

Handwritten notes or scribbles at the bottom left of the page.

IX. COMPUTER LISTING/SURFACE TENSION MODEL

FINITE PLATE

TOP, IS MAIN
FOR D11A-09/10/75-17 35 SR (60)

MAIN PROGRAM

STORAGE USED CODE(1) 00050; DATA(1) 00010; COMMON(1) 00000

COMMON BLOCKS

0001 A 057420
0002 B 057420
0003 C 165180
0004 D 057420

EXTERNAL REFERENCES (BLOCK, NAME)

0007 FONS
0010 N10705
0011 N10705
0012 N1015
0013 N1025
0014 N1025

STORAGE ASSIGNMENT (BLOCK, TYPE, RELATIVE LOCATION, NAME)

000 000077 1000 000017 1050 0000 P 000074 ACC 0004 000000 0J1NY
000 000076 1000 000030 F 0000 I 000077 1P1NT 0000 I 000075 J 0000 I 000075 MARFUM
000 000075 1000 000071 STEP 0000 I 000000 5 0000 A 000000 X

0011 14 COMPLETION(1)
0012 14 DIMENSION N1(56),F(156)
0013 14 COMMON/COMMON/156
0014 14 COMMON/COMMON/156
0015 14 COMMON/COMMON/156
0016 14 COMMON/COMMON/156
0017 14 COMMON/COMMON/156
0018 14 COMMON/COMMON/156
0019 14 COMMON/COMMON/156
0020 14 COMMON/COMMON/156
0021 14 COMMON/COMMON/156
0022 14 COMMON/COMMON/156
0023 14 COMMON/COMMON/156
0024 14 COMMON/COMMON/156
0025 14 COMMON/COMMON/156
0026 14 COMMON/COMMON/156
0027 14 COMMON/COMMON/156
0028 14 COMMON/COMMON/156
0029 14 COMMON/COMMON/156
0030 14 COMMON/COMMON/156
0031 14 COMMON/COMMON/156
0032 14 COMMON/COMMON/156
0033 14 COMMON/COMMON/156
0034 14 COMMON/COMMON/156
0035 14 COMMON/COMMON/156
0036 14 COMMON/COMMON/156
0037 14 COMMON/COMMON/156
0038 14 COMMON/COMMON/156
0039 14 COMMON/COMMON/156
0040 14 COMMON/COMMON/156
0041 14 COMMON/COMMON/156
0042 14 COMMON/COMMON/156
0043 14 COMMON/COMMON/156
0044 14 COMMON/COMMON/156
0045 14 COMMON/COMMON/156
0046 14 COMMON/COMMON/156
0047 14 COMMON/COMMON/156
0048 14 COMMON/COMMON/156
0049 14 COMMON/COMMON/156
0050 14 COMMON/COMMON/156
0051 14 COMMON/COMMON/156
0052 14 COMMON/COMMON/156
0053 14 COMMON/COMMON/156
0054 14 COMMON/COMMON/156
0055 14 COMMON/COMMON/156
0056 14 COMMON/COMMON/156
0057 14 COMMON/COMMON/156
0058 14 COMMON/COMMON/156
0059 14 COMMON/COMMON/156
0060 14 COMMON/COMMON/156
0061 14 COMMON/COMMON/156
0062 14 COMMON/COMMON/156
0063 14 COMMON/COMMON/156
0064 14 COMMON/COMMON/156
0065 14 COMMON/COMMON/156
0066 14 COMMON/COMMON/156
0067 14 COMMON/COMMON/156
0068 14 COMMON/COMMON/156
0069 14 COMMON/COMMON/156
0070 14 COMMON/COMMON/156
0071 14 COMMON/COMMON/156
0072 14 COMMON/COMMON/156
0073 14 COMMON/COMMON/156
0074 14 COMMON/COMMON/156
0075 14 COMMON/COMMON/156
0076 14 COMMON/COMMON/156
0077 14 COMMON/COMMON/156
0078 14 COMMON/COMMON/156
0079 14 COMMON/COMMON/156
0080 14 COMMON/COMMON/156
0081 14 COMMON/COMMON/156
0082 14 COMMON/COMMON/156
0083 14 COMMON/COMMON/156
0084 14 COMMON/COMMON/156
0085 14 COMMON/COMMON/156
0086 14 COMMON/COMMON/156
0087 14 COMMON/COMMON/156
0088 14 COMMON/COMMON/156
0089 14 COMMON/COMMON/156
0090 14 COMMON/COMMON/156
0091 14 COMMON/COMMON/156
0092 14 COMMON/COMMON/156
0093 14 COMMON/COMMON/156
0094 14 COMMON/COMMON/156
0095 14 COMMON/COMMON/156
0096 14 COMMON/COMMON/156
0097 14 COMMON/COMMON/156
0098 14 COMMON/COMMON/156
0099 14 COMMON/COMMON/156
0100 14 COMMON/COMMON/156

END OF COMPILATION NO DIAGNOSTICS.

ORIGINAL PAGE IS
OF POOR QUALITY

DATE 0010:5 PAGE 15

FD-415 CAL
PLP 011A-CR/11/75-17 16 07 167

SUPERSTIC CULTUM ENVPY POINT J02223

STORAGE USED C000111 002200: DATA09 000675: FLVW C0000123 C00000

COMPON LEGENS

0007 557020
0008 557020
0009 165100
0010 557020

LETTERAL REFERENCES (BLOCK, NAME)

0007 5570
0010 557020

STORAGE ASSIGNMENT (BLOCK, TYPE, RELATIVE LOCATION, NAME)

0001	000129 12W	001	000357 313C	0004	000517 1065	0001	000707 1035	0001	000657 2L
0001	00100A 230P	0001	001161 211P	0001	001265 276C	0001	001350 235C	0001	001415 2075
0001	00110 251C	0001	001537 257C	0001	001602 265C	0001	001805 273C	0001	001714 301C
001	001129 377C	0001	002010 315P	0001	007052 323C	0001	002113 331C	0001	002151 337C
001	001129 5L	0001	001234 6A	0000	000877 A	0004	000000 0010V	0000	000078 0L
0007	000507 5L	0000	000000 0010V	0007	000571 C	0000	000000 0010V	0000	000078 0L
0000	000507 10W	0001	000507 10W	0001	000503 1S	0000	000504 1L	0000	000078 0L
0000	000507 0P	0000	000507 0P	0000	000000 0010V	0000	000000 0010V	0000	000078 0L
0000	000507 0P	0000	000507 0P	0000	000000 0010V	0000	000000 0010V	0000	000078 0L
0000	000507 0P	0000	000507 0P	0000	000000 0010V	0000	000000 0010V	0000	000078 0L
0000	000507 0P	0000	000507 0P	0000	000000 0010V	0000	000000 0010V	0000	000078 0L

00101	10	COMPILE(PIRME1)
00103	70	SUBROUTINE CALC(UNENY,F)
00105	30	DIMENSION 301563
00106	00	DIMENSION 411563
00107	50	DIMENSION 411563
00110	60	DIMENSION 411563
00111	70	COMMON/4/1156,1163
00112	00	COMMON/4/1156,1163
00113	00	COMMON/4/1156,1163
00114	100	COMMON/4/1156,1163
00115	170	COMMON/4/1156,1163
00116	120	COMMON/4/1156,1163
00117	130	COMMON/4/1156,1163
00120	100	COMMON/4/1156,1163
00121	100	COMMON/4/1156,1163
00122	100	COMMON/4/1156,1163
00123	100	COMMON/4/1156,1163
00124	100	COMMON/4/1156,1163
00125	100	COMMON/4/1156,1163

ROUTE PLATE

0012
 0012
 0013
 0014
 0015
 0016
 0017
 0018
 0019
 0020
 0021
 0022
 0023
 0024
 0025
 0026
 0027
 0028
 0029
 0030
 0031
 0032
 0033
 0034
 0035
 0036
 0037
 0038
 0039
 0040
 0041
 0042
 0043
 0044
 0045
 0046
 0047
 0048
 0049
 0050
 0051
 0052
 0053
 0054
 0055
 0056
 0057
 0058
 0059
 0060
 0061
 0062
 0063
 0064
 0065
 0066
 0067
 0068
 0069
 0070
 0071
 0072
 0073
 0074
 0075
 0076
 0077
 0078
 0079
 0080
 0081
 0082
 0083
 0084
 0085
 0086
 0087
 0088
 0089
 0090
 0091
 0092
 0093
 0094
 0095
 0096
 0097
 0098
 0099
 0100

SOURCE
 0001 WE1010135
 0002 1012-0111-CQU-T0AL-RC001
 0003 0001-0001-01
 0004 CONTINUF
 0005 0001-01-01
 0006 ADV1000/2A
 0007 0001-01-01-0002/2A
 0008 0001-01-01-0002/2A
 0009 0001-01-01-0002/2A
 0010 0001-01-01-0002/2A
 0011 0001-01-01-0002/2A
 0012 0001-01-01-0002/2A
 0013 0001-01-01-0002/2A
 0014 0001-01-01-0002/2A
 0015 0001-01-01-0002/2A
 0016 0001-01-01-0002/2A
 0017 0001-01-01-0002/2A
 0018 0001-01-01-0002/2A
 0019 0001-01-01-0002/2A
 0020 0001-01-01-0002/2A
 0021 0001-01-01-0002/2A
 0022 0001-01-01-0002/2A
 0023 0001-01-01-0002/2A
 0024 0001-01-01-0002/2A
 0025 0001-01-01-0002/2A
 0026 0001-01-01-0002/2A
 0027 0001-01-01-0002/2A
 0028 0001-01-01-0002/2A
 0029 0001-01-01-0002/2A
 0030 0001-01-01-0002/2A
 0031 0001-01-01-0002/2A
 0032 0001-01-01-0002/2A
 0033 0001-01-01-0002/2A
 0034 0001-01-01-0002/2A
 0035 0001-01-01-0002/2A
 0036 0001-01-01-0002/2A
 0037 0001-01-01-0002/2A
 0038 0001-01-01-0002/2A
 0039 0001-01-01-0002/2A
 0040 0001-01-01-0002/2A
 0041 0001-01-01-0002/2A
 0042 0001-01-01-0002/2A
 0043 0001-01-01-0002/2A
 0044 0001-01-01-0002/2A
 0045 0001-01-01-0002/2A
 0046 0001-01-01-0002/2A
 0047 0001-01-01-0002/2A
 0048 0001-01-01-0002/2A
 0049 0001-01-01-0002/2A
 0050 0001-01-01-0002/2A
 0051 0001-01-01-0002/2A
 0052 0001-01-01-0002/2A
 0053 0001-01-01-0002/2A
 0054 0001-01-01-0002/2A
 0055 0001-01-01-0002/2A
 0056 0001-01-01-0002/2A
 0057 0001-01-01-0002/2A
 0058 0001-01-01-0002/2A
 0059 0001-01-01-0002/2A
 0060 0001-01-01-0002/2A
 0061 0001-01-01-0002/2A
 0062 0001-01-01-0002/2A
 0063 0001-01-01-0002/2A
 0064 0001-01-01-0002/2A
 0065 0001-01-01-0002/2A
 0066 0001-01-01-0002/2A
 0067 0001-01-01-0002/2A
 0068 0001-01-01-0002/2A
 0069 0001-01-01-0002/2A
 0070 0001-01-01-0002/2A
 0071 0001-01-01-0002/2A
 0072 0001-01-01-0002/2A
 0073 0001-01-01-0002/2A
 0074 0001-01-01-0002/2A
 0075 0001-01-01-0002/2A
 0076 0001-01-01-0002/2A
 0077 0001-01-01-0002/2A
 0078 0001-01-01-0002/2A
 0079 0001-01-01-0002/2A
 0080 0001-01-01-0002/2A
 0081 0001-01-01-0002/2A
 0082 0001-01-01-0002/2A
 0083 0001-01-01-0002/2A
 0084 0001-01-01-0002/2A
 0085 0001-01-01-0002/2A
 0086 0001-01-01-0002/2A
 0087 0001-01-01-0002/2A
 0088 0001-01-01-0002/2A
 0089 0001-01-01-0002/2A
 0090 0001-01-01-0002/2A
 0091 0001-01-01-0002/2A
 0092 0001-01-01-0002/2A
 0093 0001-01-01-0002/2A
 0094 0001-01-01-0002/2A
 0095 0001-01-01-0002/2A
 0096 0001-01-01-0002/2A
 0097 0001-01-01-0002/2A
 0098 0001-01-01-0002/2A
 0099 0001-01-01-0002/2A
 0100 0001-01-01-0002/2A

ORIGINAL FROM
CALIFORNIA

LINE	AMOUNT	DATE	DESCRIPTION
112	-1374988901	1003509-02	
113	-2073448101	00000000	
114	-13770278901	38955729-02	
115	-8969666700	-32924126-02	
116	-580817900	4875812-03	
117	-5117933000	-32818407-03	
118	-5895867900	-5895402-04	
119	-5998469300	-83145680-05	
120	-5981075900	-77982000-05	
121	-9978877300	-13638503-03	
122	-9977657900	-19531507-03	
123	-9992828700	-15184014-03	
124	-9512025900	-196885968-03	
125	-8941285100	-64953074-03	
126	-5613103900	-36694615-02	
127	-1362414901	30222110-02	
128	-2093990101	00000000	
129	-1368761801	-33995816-02	
130	-5617159800	-36786399-02	
131	-9941266500	-64512353-03	
132	-9512023800	-19645684-03	
133	-998285700	-15185056-03	
134	-998764300	-14531991-03	
135	-9978877000	-13638160-03	
136	-3740262500	-37820806-03	
137	-3150197800	-31294888-03	
138	-3163775900	-30752488-03	
139	-3199643600	-28722718-03	
140	-3949164800	-14894305-03	
141	-9748997100	-95549141-02	
142	-3353160701	-28534887-02	
143	-2028845701	00000000	
144	-3358929101	-33374926-02	
145	-970632300	-6559598-02	
146	-3821899500	-1895713-03	
147	-3199644700	-272459-03	
148	-3163775900	-36752997-03	
149	-3150197800	-3129525-03	
150	-3142262500	-30667949-03	
151	-2972576000	-1500302-02	
152	-946018100	-30220743-02	
153	-1351774601	-13546498-02	
154	-1355633501	-16685955-02	
155	-9463295800	-30111035-02	
156	-2472602900	-15008058-02	
THE SUM OF SQUARES IS 63935093-03			
ERROR RETURN BECAUSE THERE HAVE BEEN 400 CALLS OF CALFUN			
THE FINAL SOLUTION REQUIRED 400 CALLS OF CALFUN AND 75			
1	1000337301	-2655924-74	
2	1000726601	-32745402-04	
3	1001651001	-34883735-04	
4	1005931501	-15685400-03	
5	1019615801	-13530743-03	
6	1029932701	-15972726-02	
7	1038969801	-10145134-01	

0-3

FINDIF CLAMP

10	0573000000	0573000000
11	0573000000	0573000000
12	0573000000	0573000000
13	0573000000	0573000000
14	0573000000	0573000000
15	0573000000	0573000000
16	0573000000	0573000000
17	0573000000	0573000000
18	0573000000	0573000000
19	0573000000	0573000000
20	0573000000	0573000000
21	0573000000	0573000000
22	0573000000	0573000000
23	0573000000	0573000000
24	0573000000	0573000000
25	0573000000	0573000000
26	0573000000	0573000000
27	0573000000	0573000000
28	0573000000	0573000000
29	0573000000	0573000000
30	0573000000	0573000000
31	0573000000	0573000000
32	0573000000	0573000000
33	0573000000	0573000000
34	0573000000	0573000000
35	0573000000	0573000000
36	0573000000	0573000000
37	0573000000	0573000000
38	0573000000	0573000000
39	0573000000	0573000000
40	0573000000	0573000000
41	0573000000	0573000000
42	0573000000	0573000000
43	0573000000	0573000000
44	0573000000	0573000000
45	0573000000	0573000000
46	0573000000	0573000000
47	0573000000	0573000000
48	0573000000	0573000000
49	0573000000	0573000000
50	0573000000	0573000000
51	0573000000	0573000000
52	0573000000	0573000000
53	0573000000	0573000000
54	0573000000	0573000000
55	0573000000	0573000000
56	0573000000	0573000000
57	0573000000	0573000000
58	0573000000	0573000000
59	0573000000	0573000000
60	0573000000	0573000000
61	0573000000	0573000000
62	0573000000	0573000000
63	0573000000	0573000000
64	0573000000	0573000000
65	0573000000	0573000000
66	0573000000	0573000000

ORIGINAL PAGE IS
OF POOR QUALITY

DATE 091075 PAGE 31

	VALUE	PERTE
122	-0087760+00	-1652983-03
123	-0992868+00	-15187012-03
124	-05120281+00	-116831273-03
125	-09912981+00	-60916998-03
126	-0513108+00	-36890759-02
127	-134-0151+01	-30195750-02
128	-2093901+01	-00000000
129	-13667589+01	-35961998-02
130	-5671661+00	-36782055-02
131	-09912796+00	-60976176-03
132	-05120216+00	-14651188-03
133	-0992808+00	-15183060-03
134	-00877636+00	-16530819-03
135	-09788766+00	-13637028-03
136	-31902831+00	-39661240-03
137	-31501983+00	-33295281-03
138	-31557765+00	-36753011-03
139	-31996447+00	-28723609-03
140	-38819173+00	-19889267-03
141	-07189087+00	-65508266-02
142	-13551628+01	-28577865-02
143	-20288457+01	-00000000
144	-13589257+01	-33208710-02
145	-07906639+00	-65598721-02
146	-38819008+00	-19886535-03
147	-31996458+00	-28725278-03
148	-31657785+00	-36753523-03
149	-31501983+00	-33295928-03
150	-31902831+00	-30661377-03
151	-20725767+00	-15008318-02
152	-09501818+00	-10227850-02
153	-13517915+01	-13566950-02
154	-13589299+01	-16909209-02
155	-00632929+00	-30113108-02
156	-20726076+00	-15008970-02
	THE SUM OF SQUARES IS	-63937107-03

4FIN

Handwritten notes in the left margin, possibly including a date or reference number.

00115	115	
00116	116	READ5
00122	116	READ5,100121(10,23)
00130	130	100 FORWAT(10,23)
00131	130	WZ85
00132	160	INTEGR (COUNT
00133	170	COUNTSC
00134	170	50 COUNTSCOUNTS
00135	190	IF(COUNT,CE,MM) GO TO 50
00137	200	CN(14,0AL,02)/ID(172)K0(0002)
00140	210	C111-2,7NE
00141	220	C227/100V(11)
00142	210	A1-C3/C1
00143	240	RECZ/C1
00144	250	AF(8,02/0,0002)Z7Z
00145	260	IF(ARG,LT,0,2) GO TO 30
00147	270	PAT-0/2--SOFT(AR5)
00150	290	POP1-DAY
00151	290	
00153	300	IF(SOP,ALL,VAR) GO TO 77
00154	310	TIP-00000333
00154	310	GO TO 74
00155	320	77 TIP=0,0
00156	330	78 CAPA=-TIP
00157	340	SAYZ-0/2--SORT(AR5)
00160	350	
00161	360	IF(SOP,ALL,VAR) GO TO 73
00161	370	TOP-SOP000333
00164	380	GO TO 84
00165	390	93 TOP=0,0
00166	400	04 CAPA=-TOP
00167	410	T-CAPA-CAPB
00170	420	IF(1,GT,0,1) T=-1.
00171	430	50 TO 51
00173	440	30 E-3,09/12,081
00174	450	IF(1,LT,-1) E=-1.
00176	460	PHI=ACOS(E)
00177	470	1E-2,SSQ(1-E/2)*COS(PI/3)
00200	480	TZ2=SSORT(1-A/3)*COS(PI/3)
00201	490	TZ2=SSORT(1-A/3)*COS(PI/3)
00202	500	WZ85-475)
00203	510	IF(1,LT,-1) T1=100.
00205	520	IF(1,LT,-1) T2=100.
00207	530	IF(ANY,ALL,ANY)E=103.
00211	540	IF(1,GT,0) GO TO 1
00212	550	IF(1,GT,0) GO TO 2
00215	560	SMALL=1
00214	570	GO TO 3
00217	580	1 SMALL=2
00220	590	IF(1,GT,0) SMALL=NY
00222	600	GO TO 3
00223	610	2 SMALL=NY
00224	620	IF(ANY,GT,72) SMALL=2
00224	630	GO TO 3
00227	640	3 CONTINUE
00230	650	T=SMALL
00231	660	T=21.
00232	670	31. RT=(212)*NO)*SORT(10)*SORT(10)*2-1,3/111

ORIGINAL PAGE IS
OF POOR QUALITY

00296	IF11A400111 121	1296
00297	IF11A400111 121	1297
00298	IF11A400111 121	1298
00299	IF11A400111 121	1299
00300	IF11A400111 121	1300
00301	IF11A400111 121	1301
00302	IF11A400111 121	1302
00303	IF11A400111 121	1303
00304	IF11A400111 121	1304
00305	IF11A400111 121	1305
00306	IF11A400111 121	1306
00307	IF11A400111 121	1307
00308	IF11A400111 121	1308
00309	IF11A400111 121	1309
00310	IF11A400111 121	1310
00311	IF11A400111 121	1311
00312	IF11A400111 121	1312
00313	IF11A400111 121	1313
00314	IF11A400111 121	1314
00315	IF11A400111 121	1315
00316	IF11A400111 121	1316
00317	IF11A400111 121	1317
00318	IF11A400111 121	1318
00319	IF11A400111 121	1319
00320	IF11A400111 121	1320
00321	IF11A400111 121	1321
00322	IF11A400111 121	1322
00323	IF11A400111 121	1323
00324	IF11A400111 121	1324
00325	IF11A400111 121	1325
00326	IF11A400111 121	1326
00327	IF11A400111 121	1327
00328	IF11A400111 121	1328
00329	IF11A400111 121	1329
00330	IF11A400111 121	1330
00331	IF11A400111 121	1331
00332	IF11A400111 121	1332
00333	IF11A400111 121	1333
00334	IF11A400111 121	1334
00335	IF11A400111 121	1335
00336	IF11A400111 121	1336
00337	IF11A400111 121	1337
00338	IF11A400111 121	1338
00339	IF11A400111 121	1339
00340	IF11A400111 121	1340
00341	IF11A400111 121	1341
00342	IF11A400111 121	1342
00343	IF11A400111 121	1343
00344	IF11A400111 121	1344
00345	IF11A400111 121	1345
00346	IF11A400111 121	1346
00347	IF11A400111 121	1347
00348	IF11A400111 121	1348
00349	IF11A400111 121	1349
00350	IF11A400111 121	1350
00351	IF11A400111 121	1351
00352	IF11A400111 121	1352
00353	IF11A400111 121	1353
00354	IF11A400111 121	1354
00355	IF11A400111 121	1355
00356	IF11A400111 121	1356
00357	IF11A400111 121	1357
00358	IF11A400111 121	1358
00359	IF11A400111 121	1359
00360	IF11A400111 121	1360
00361	IF11A400111 121	1361
00362	IF11A400111 121	1362
00363	IF11A400111 121	1363
00364	IF11A400111 121	1364
00365	IF11A400111 121	1365
00366	IF11A400111 121	1366
00367	IF11A400111 121	1367
00368	IF11A400111 121	1368
00369	IF11A400111 121	1369
00370	IF11A400111 121	1370
00371	IF11A400111 121	1371
00372	IF11A400111 121	1372
00373	IF11A400111 121	1373
00374	IF11A400111 121	1374
00375	IF11A400111 121	1375
00376	IF11A400111 121	1376
00377	IF11A400111 121	1377
00378	IF11A400111 121	1378
00379	IF11A400111 121	1379
00380	IF11A400111 121	1380
00381	IF11A400111 121	1381
00382	IF11A400111 121	1382
00383	IF11A400111 121	1383
00384	IF11A400111 121	1384
00385	IF11A400111 121	1385
00386	IF11A400111 121	1386
00387	IF11A400111 121	1387
00388	IF11A400111 121	1388
00389	IF11A400111 121	1389
00390	IF11A400111 121	1390
00391	IF11A400111 121	1391
00392	IF11A400111 121	1392
00393	IF11A400111 121	1393
00394	IF11A400111 121	1394
00395	IF11A400111 121	1395
00396	IF11A400111 121	1396
00397	IF11A400111 121	1397
00398	IF11A400111 121	1398
00399	IF11A400111 121	1399
00400	IF11A400111 121	1400

ORIGINAL COPY
 5/11/68

```

2567 2870 7181=VIR1002ZEM-03/VIR10020D30
2568 2870 1878=1327M-113/12.01VIR10027D01.33
2569 2870 63 CONTINUE
2570 2870 00 00 M=156.156
2571 2870 7181=VIR1002ZEM-03/VIR10020D30
2572 2870 1878=1327M-113/12.01VIR10027D01.33
2573 2870 63 CONTINUE
2574 2870 60 13.50
2575 2870 99 CONTINUE
2576 2870 76 FORMATTING AT THE 15, LARGEST ITERATION HE HAVED
2577 2870 82115663 COUNT
2578 2870 A FORMATTING, XMINI, XMMZ, X115, F17, 000
2579 2870 20716.01 11.711, 11.1, 1.1
2580 2870 END
  
```

END OF COMPILATION 1 DIAGNOSTICS.

207
 MAP 0225-0917-14 07
 AFCH STATUS OF OUTPUT ELEMENTS:0000

ADDRESS 11102 101000 011500 5477 1FRANK 10005 DECIMAL
 STARTING ADDRESS 011001 7423 0FRANK 10005 DECIMAL

ADDRESS	STARTING ADDRESS	101000 011500	5477 1FRANK 10005 DECIMAL	7423 0FRANK 10005 DECIMAL
011001	011001	011001	011001	011001
011002	011002	011002	011002	011002
011003	011003	011003	011003	011003
011004	011004	011004	011004	011004
011005	011005	011005	011005	011005
011006	011006	011006	011006	011006
011007	011007	011007	011007	011007
011008	011008	011008	011008	011008
011009	011009	011009	011009	011009
011010	011010	011010	011010	011010
011011	011011	011011	011011	011011
011012	011012	011012	011012	011012
011013	011013	011013	011013	011013
011014	011014	011014	011014	011014
011015	011015	011015	011015	011015
011016	011016	011016	011016	011016
011017	011017	011017	011017	011017
011018	011018	011018	011018	011018
011019	011019	011019	011019	011019
011020	011020	011020	011020	011020
011021	011021	011021	011021	011021
011022	011022	011022	011022	011022
011023	011023	011023	011023	011023
011024	011024	011024	011024	011024
011025	011025	011025	011025	011025
011026	011026	011026	011026	011026
011027	011027	011027	011027	011027
011028	011028	011028	011028	011028
011029	011029	011029	011029	011029
011030	011030	011030	011030	011030
011031	011031	011031	011031	011031
011032	011032	011032	011032	011032
011033	011033	011033	011033	011033
011034	011034	011034	011034	011034
011035	011035	011035	011035	011035
011036	011036	011036	011036	011036
011037	011037	011037	011037	011037
011038	011038	011038	011038	011038
011039	011039	011039	011039	011039
011040	011040	011040	011040	011040
011041	011041	011041	011041	011041
011042	011042	011042	011042	011042
011043	011043	011043	011043	011043
011044	011044	011044	011044	011044
011045	011045	011045	011045	011045
011046	011046	011046	011046	011046
011047	011047	011047	011047	011047
011048	011048	011048	011048	011048
011049	011049	011049	011049	011049
011050	011050	011050	011050	011050
011051	011051	011051	011051	011051
011052	011052	011052	011052	011052
011053	011053	011053	011053	011053
011054	011054	011054	011054	011054
011055	011055	011055	011055	011055
011056	011056	011056	011056	011056
011057	011057	011057	011057	011057
011058	011058	011058	011058	011058
011059	011059	011059	011059	011059
011060	011060	011060	011060	011060
011061	011061	011061	011061	011061
011062	011062	011062	011062	011062
011063	011063	011063	011063	011063
011064	011064	011064	011064	011064
011065	011065	011065	011065	011065
011066	011066	011066	011066	011066
011067	011067	011067	011067	011067
011068	011068	011068	011068	011068
011069	011069	011069	011069	011069
011070	011070	011070	011070	011070
011071	011071	011071	011071	011071
011072	011072	011072	011072	011072
011073	011073	011073	011073	011073
011074	011074	011074	011074	011074
011075	011075	011075	011075	011075
011076	011076	011076	011076	011076
011077	011077	011077	011077	011077
011078	011078	011078	011078	011078
011079	011079	011079	011079	011079
011080	011080	011080	011080	011080
011081	011081	011081	011081	011081
011082	011082	011082	011082	011082
011083	011083	011083	011083	011083
011084	011084	011084	011084	011084
011085	011085	011085	011085	011085
011086	011086	011086	011086	011086
011087	011087	011087	011087	011087
011088	011088	011088	011088	011088
011089	011089	011089	011089	011089
011090	011090	011090	011090	011090
011091	011091	011091	011091	011091
011092	011092	011092	011092	011092
011093	011093	011093	011093	011093
011094	011094	011094	011094	011094
011095	011095	011095	011095	011095
011096	011096	011096	011096	011096
011097	011097	011097	011097	011097
011098	011098	011098	011098	011098
011099	011099	011099	011099	011099
011100	011100	011100	011100	011100

ORIGINAL PAGE IS
OF POOR QUALITY

37 --32503012-00
 38 --11290075-00
 39 --52942087-00
 40 --12717999-00
 41 --10770883-01
 42 --20330395-01
 43 --20129058-01
 44 --27788898-01
 45 --11988740-00
 46 --11500899-01
 47 --27553171-01
 48 --21933555-01
 49 --29089585-01
 50 --10276092-01
 51 --12076801-01
 52 --30396294-01
 53 --12270362-01
 54 --40093208-01
 55 --12082101-01
 56 --10493000-01
 57 --10781311-01
 58 --10486648-01
 59 --10478782-01
 60 --10493000-01
 61 --10493000-01
 62 --10493000-01
 63 --10493000-01
 64 --10493000-01
 65 --10493000-01
 66 --10493000-01
 67 --10493000-01
 68 --10493000-01
 69 --10493000-01
 70 --10493000-01
 71 --10493000-01
 72 --10493000-01
 73 --10493000-01
 74 --10493000-01
 75 --10493000-01
 76 --10493000-01
 77 --10493000-01
 78 --10493000-01
 79 --10493000-01
 80 --10493000-01
 81 --10493000-01
 82 --10493000-01
 83 --10493000-01
 84 --10493000-01
 85 --10493000-01
 86 --10493000-01
 87 --10493000-01
 88 --10493000-01
 89 --10493000-01
 90 --10493000-01
 91 --10493000-01
 92 --10493000-01
 93 --10493000-01
 94 --10493000-01
 95 --10493000-01
 96 --10493000-01
 97 --10493000-01
 98 --10493000-01
 99 --10493000-01
 100 --10493000-01

DR...
05 1957 4...

94	-18987292-01
95	-18318820-01
96	-25875191-02
97	-32338070-00
98	-17001381-04
99	-32362363-00
100	-28728125-00
101	-18318716-03
102	-18481138-01
103	-2271897-01
104	-28921488-01
105	-31300457-01
106	-20727895-01
107	-26521955-01
108	-22287687-01
109	-17053887-01
110	-13287597-01
111	-25388789-00
112	-25835921-02
113	-18627598-04
114	-22925316-02
115	-85061176-00
116	-13260707-01
117	-17929958-01
118	-22228161-01
119	-26523585-01
120	-2793932-01
121	-2589813-01
122	-25945778-01
123	-21398525-01
124	-18352578-01
125	-2179888-01
126	-2838398-00
127	-17487156-00
128	-10281228-01
129	-17899256-00
130	-88811676-00
131	-11701253-01
132	-16830302-01
133	-21388198-01
134	-2595221-01
135	-2909508-01
136	-29739238-01
137	-2001878-01
138	-19945378-01
139	-18788170-01
140	-8220816-00
141	-2331182-00
142	-23328212-01
143	-2298998-05
144	-2137381-01
145	-2338163-00
146	-68190138-02
147	-18489578-01
148	-17111262-01
149	-2908959-01
150	-2922975-01

151 --26250000001
152 --17500000000
153 --8788888888888
154 --8788888888888
155 --17500000001
156 26250000001

214

X. SURFACE TENSION DOMINATED τ FORMULATION

	M															A
	1.0005	1.0007	1.0015	1.0058	1.018	1.032	1.432	2.236	1.432	1.032	1.018	1.0058	1.0015	1.0007	1.0003	
	Y1	Y2	Y3	Y4	Y5	Y6	Y7	Y8	Y9	Y10	Y11	Y12	Y13	Y14	Y15	
1.0	.9489	.9493	.9500	.9540	.9679	.9970	1.431	2.213	1.431	.9970	.9679	.9540	.9500	.9493	.9489	1.0
.949	.8947	.8950	.8959	.8990	.9141	.9561	1.428	2.190	1.428	.9561	.9141	.8990	.8959	.8950	.8947	.949
.895	.8368	.8372	.8381	.8410	.8576	.9090	1.421	2.167	1.421	.9090	.8576	.8410	.8381	.8372	.8368	.895
.837	.7758	.7752	.7761	.7794	.7972	.8552	1.411	2.144	1.411	.8552	.7972	.7794	.7761	.7752	.7748	.837
.775	.7073	.7078	.7087	.7121	.7331	.7941	1.398	2.121	1.398	.7941	.7331	.7121	.7087	.7078	.7073	.775
.707	.6327	.6333	.6342	.6380	.6656	.7250	1.383	2.097	1.383	.7250	.6656	.6380	.6342	.6333	.6327	.707
.632	.5581	.5585	.5595	.5517	.5886	.6469	1.369	2.073	1.369	.6469	.5886	.5517	.5495	.5488	.5481	.632
.548	.4477	.4486	.4497	.4511	.4941	.5610	1.358	2.049	1.358	.5610	.4941	.4511	.4497	.4486	.4477	.548
.447	.3139	.3149	.3164	.3198	.3890	.4789	1.351	2.024	1.351	.4789	.3890	.3198	.3164	.3149	.3139	.447
.316	.249	.2507	.2518	.2539	.2871	.3460	1.348	2.000	1.348	.3460	.2871	.249	.2471	.2460	.2450	.316
							Y151	Y152	Y153	Y154	Y155	Y156				0.0
																0.0
																0.0

C'

D

C

0.0

B

XII. BIBLIOGRAPHY

1. Allen, D. N. G.: Relaxation Methods. McGraw-Hill. 1954.
2. Amsden, A. A., and Harlow, F. H.: The Smac Method: A Numerical Technique for Calculating Incompressible Fluid Flows. Los Alamos Scientific Laboratory Rep. LA-4370, May, 1970.
3. Arbbahhirama, A.: Free Streamline Analysis of Two-Dimensional Jet. Jour. of the Hydraulics Division. July, 1969, pp. 1139-1148.
4. Batchelor, G. K.: An Introduction to Fluid Mechanics. Cambridge University Press. 1967.
5. Brennan, C.: A Numerical Solution of Axisymmetric Cavity Flows. Jour. Fluid Mech., vol. 37, part 4, 1969, pp. 671-688.
6. Brunauer, E. A.: Axially Symmetric Free Streamline Flow About Tandem Discs. M.S. Thesis, Illinois Inst. of Tech., 1951.
7. Chan, S. T. K.: Finite Element Analysis of Irrotational Flows of an Ideal Fluid. Ph.D. Thesis, Univ. of California, Davis. 1971.
8. Chan, S. T. K., and Larock, B. E.: Fluid Flows from Axisymmetric Orifices and Valves. Journ. of the Hydraulics Division, Jan. 1973, pp. 81-97.
9. Chang, H. Y., and Conly, J. F.: Potential Flow of Segmental Jet Deflectors. Jour. Fluid Mech., Vol. 46, Part 3, 1971, pp. 465-475.
10. Davis, A. L., and Jeppson, R. W.: Solving Three-Dimensional Potential Flow Problems by Means of an Inverse Formulation and Finite Differences. Utah State Univ., Mar. 1973.
11. Donnelly, R. J., and Glaberson, W.: Experiments on the Capillary Instability of a Liquid Jet. pp. 547-556. 1965.
12. Feng, G. C., and Robertson, S. J.: Study of Propellant Dynamics During Docking. NASA CR-124055, 1972.
13. Fox, L.: A Short Account of Relaxation Methods. 1947.
14. Gurevich, M. J.: Theory of Jets in Ideal Fluids. Academic Press, 1965.

15. Hirt, C. W., Cook, J. I., and Butler, T. D.: A LaGrangian Method for Calculating the Dynamics of an Incompressible Fluid with Free Surface. *Jour. of Comp. Physics*, vol. 5, 1970, pp. 103-124.
16. Hirt, C. W., and Shannon, J. P.: Free-Surface Stress Conditions for Incompressible-Flow Calculations. *Jour. of Com. Physics*, vol. 2, 1968, pp. 403-411.
17. Huang, Y. C., Hammit, F. G., and Yang, W-J.: Hydrodynamics Phenomena During High-Speed Collision Between Liquid Droplet and Rigid Plane. *Jour. of Fluids Engineering*. June, 1973. pp. 276-294.
18. Huang, Y. C., Hammit, F. G., and Yang, W-J.: Normal Impact of a Finite Cylindrical Liquid Jet on a Flat Rigid Plane. Rep. No. U Mich 03371-9-T, The Univ. of Michigan, Aug. 1971.
19. Jeppson, R. W.: Techniques for Solving Free-Streamline, Cavity, Jet and Seepage Problems by Finite Differences. Tech. Rep. 68. Stanford Univ., Sept. 1966.
20. Jeppson, R. W.: Inverse Formulation and Finite Difference Solution for Flow From a Circular Orifice. *Jour. Fluid Mech.*, vol. 40, part 1, 1970, pp. 215-223.
21. Kochin, N. E., Kibel, I. A., and Roze, N. V.: *Theoretical Hydro-mechanics*. Interscience Publishers, 1964.
22. Koloseus, H. J., and Ahmad, D.: Circular Hydraulic Jump. *Jour. of the Hydraulics Division*. Jan. 1969, pp. 409-422.
23. Krantz, W. B.: Scaling Initial and Boundary Value Problems. *Chem. Engr. Education*. Summer 1970. pp. 145-151.
24. Labus, T. L., and Symons, E. P.: Experimental Investigation of an Axisymmetric Free Jet with an Initially Uniform Velocity Profile. NASA TN D-6783, May, 1972.
25. LeClerc, A.: Deflection of a Liquid Jet by a Perpendicular Boundary. M.S. Thesis, Univ. of Iowa, 1948.
26. Lieberstein, H. M.: Overrelaxation for Non-Linear Elliptic Partial Differential Problems. MRC Technical Summary Report, No. 87, March, 1959.
27. McNown, J. S., Hsu, E., and Yih, C.: Applications of the Relaxation Technique in Fluid Mechanics. *Trans. Amer. Soc. of Civil Engs.* Paper No. 2758, 1953.
28. Michelson, I.: Fluid Jet Impingement-Analytical Solution and Novel Physical Characteristic. *Nature*, Vol. 223, Aug. 9, 1969, pp. 610-611.

29. Michelson, I.: A Solution to the Three-Dimensional Oblique-Incidence Liquid Jet Problem. Rev. Roum. Math. Pures et Appl. Tome, XV, no 2, pp. 279-284. Bucarest, 1970.
30. Milne-Thomson, L. M.: Theoretical Hydrodynamics. The Macmillan Co., 1968.
31. Moayeri, M. S., and Strelkoff, T. S.: Potential Flow at a Two-Dimensional Conduit Outlet. Jour. of the Hydraulics Division. 1973, pp. 653-671.
32. Moss, W. D.: Flow Separation at the Upstream Edge of a Square-Edged Broad-Crested Weir. Jour. Fluid Mech., vol. 52, part 2, 1972, pp. 307-320.
33. Nirapathdongporn, S.: Circular Hydraulic Jump. M.S. Thesis, Asian Inst. of Tech., Bangkok (Thailand), 1968.
34. Powell, M. J. D.: A Fortran Subroutine For Solving Systems of Non-Linear Algebraic Equations. United Kingdom Atomic Energy Authority Research Group Report, 1968.
35. Roache, P. J.: Computational Fluid Dynamics. Hermosa Publishers, 1972, pp. 18-23.
36. Rouse, H., and Abel-Fetouh, A.: Characteristics of Irrotational Flow through Axially Symmetric Orifices. Jour. of Appl. Mech., Dec. 1950, pp. 421-426.
37. Rupe, J. H.: On the Dynamic Characteristics of Free-Liquid Jets and a Partial Correlation with Orifice Geometry. Tech. Rep. 32-207. Jet Propulsion Laboratory. Jan. 1962.
38. Schach, Von W.: Umlenkung eines freien Flussigkeitsstrahles an einer ebenen Platte. (Deflection of a Free Fluid Jet at a Flat Panel). Ingenieur-Archiv, vol. 5, 1934, pp. 245-265.
39. Schach, Von W.: Umlenkung eines Kreisformigen Flussigkeitsstrahles an einer ebenen Platte Senkrecht Zur Stromungstrichtung. (Deflection of a Circular Liquid Jet on a Plane Plate Normal to the Stream.) Ingenieur Archiv, vol. VI, 1935, pp. 51-59.
40. Southwell, R. V., and Vaisey, G.: Relaxation Methods Applied to Engineering Problems. Phil Trans. Roy. Soc. of London A(240), 1946, pp. 117-161.
41. Stephens, D. G.: Experimental Investigation of Liquid Impact in a Model Propellant Tank. NASA TN D-2913, 1965.
42. Thom, A., and Apelt, C. J.: Field Computations in Engineering and Physics. D. Van Nostrand Co., 1961.

43. Watson, E. J.: The Radial Spread of a Liquid Jet Over a Horizontal Plane. *J. Fluid Mech.* (1968), vol. 20, part 3, pp. 481-499.
44. Yih, C.: *Dynamics of Nonhomogeneous Fluids*. The Macmillan Co., 1965.
45. Young, D. M., Gates, L. D., Arms, R. J., and Eliczer, D. F.: The Computation of an Axially Symmetric Free Boundary Problem on NORC. NPG Rep. 1413, Dec. 1955.
46. Zhukovskii, N. Ye.: Opred' Leniye Dvizheniya Zhidkosti Pri Kakom'-Nibud' Uslovii, Dannom' Na Linii Toka. (Determining the Movement of a Liquid for a Condition Specified on a Streamline.) *Zhurnal Obshchei Khimii*, Number 2, vol. XXIII, pp. 89-100, 1891.

TABLE 1. - LIQUID PROPERTIES AT 20° C

Liquid	Surface tension, N/cm	Density, g/cm ³	Absolute viscosity, g/cm-sec
Anhydrous ethanol	22.3×10^{-5}	0.789	1.200×10^{-2}
Trichlorotrifluoroethane	18.6	1.579	0.700
Distilled water	72.5	1.00	1.0037

TABLE 2. - SUMMARY OF PARAMETERS - ZERO GRAVITY

Test liquid	Nozzle radius, R ₀ , cm	Disk radius, L, cm	Ratio, R ₀ /L	Velocity of jet, cm/sec	Reynolds number, $\rho V R_0 / \nu$	Weber number, $\rho V^2 R_0 / \sigma$	Flow category
Freon TF	0.25	1.0	0.23	34.3	1934	24.8	S
Freon TF				38.0	2133	30.5	S
Freon TF				43.7	2464	40.4	T
Ethanol				77.0	1278	52.2	T
Freon TF				50.5	2848	54.0	T
Ethanol				58.8	3316	73.4	T
Freon TF				101.0	1662	90.1	T
Ethanol				79.0	4460	113.2	I
Freon TF				131.3	2160	151.9	I
Ethanol				88.6	5000	161.5	I
Freon TF	.50	1.5	.33	149.8	2465	197.8	I
Ethanol				237.7	3911	498	I
Freon TF				282.2	4642	703	I
Ethanol				365.6	6014	1180	I
Ethanol				26.4	868	12.2	S
Ethanol				19.5	1815	16.1	S
Ethanol				37.7	1240	25.1	S
Freon TF				27.4	3090	31.8	T
Ethanol				46.0	1513	37.2	T
Freon TF				53.9	1773	51.2	T
Ethanol	37.6	4240	60.0	T			
Ethanol	59.6	1900	62.0	T			
Freon TF	↓	↓	↓	42.75	4830	77.6	I
Ethanol							
Freon TF							

TABLE 2. - Concluded.

Test liquid	Nozzle radius, R_o , cm	Disk radius, L, cm	Ratio, R_o/L	Velocity of jet, cm/sec	Reynolds number, $\rho VR_o/\mu$	Weber number, $\rho V^2 R_o/\sigma$	Flow category
Ethanol	0.75	1.5	0.50	15.4	760	6.2	S
Ethanol	.75	1.5	↓	19.1	942	9.6	S
Ethanol	.75	1.5	↓	19.9	986	10.5	S
Ethanol	.50	1.0	↓	26.4	868	12.2	S
Freon TF	.50	1.0	↓	17.7	1996	13.2	S
Ethanol	.75	1.5	↓	28.2	1891	21.0	S
Ethanol	.50	1.0	↓	34.9	1148	21.3	T
Freon TF	.50	1.0	↓	23.3	2628	23.0	T
Ethanol	.75	1.5	↓	34.4	1697	31.2	T
Ethanol	.50	1.0	↓	46.1	1516	37.4	T
Freon TF	.50	1.0	↓	31.9	3490	43.2	T
Ethanol	.75	1.5	↓	41.2	2036	44.7	I
Ethanol	.50	1.0	↓	52.3	1720	48.2	T
Freon TF	.50	1.0	↓	37.5	4230	59.5	I
Ethanol	.75	1.5	↓	47.5	2347	59.6	I
Ethanol	.50	1.0	↓	85.7	2820	129.0	I
Ethanol	.75	1.0	.75	12.7	630	4.2	S
Ethanol	↓	↓	↓	22.5	1110	13.3	S
Ethanol	↓	↓	↓	24.8	1227	16.2	S
Ethanol	↓	↓	↓	27.3	1350	19.7	T
Ethanol	↓	↓	↓	29.4	1454	22.9	T
Ethanol	↓	↓	↓	32.0	1580	27.0	T
Ethanol	↓	↓	↓	35.0	1730	32.3	T
Ethanol	↓	↓	↓	39.1	1930	40.2	I

ORIGINAL PAGE IS
OF POOR QUALITY.

TABLE 3. - Concluded.

Test liquid	Nozzle radius, R_o , cm	Disk radius, l , cm	Ratio, R_o/l	Ratio, H/R_o	Weber number, $\sqrt{V^2 R_o / \sigma}$	Reynolds number, VR_o/ν	Bond number, $\rho g R_o^2 / \sigma$	Ratio, R_p/R_o						
Distilled water	0.25	0.50	0.50	4	235	6573	0.857	35.14						
		.50	.50	20	6922	6922		38.80						
		.75	.33	4	6573	6573		38.50						
		.75	.33	20	6922	6922		43.86						
		1.0	.25	4	6573	6573		37.96						
		1.0	.25	20	6922	6922		41.56						
		1.5	.167	4	6573	6573		35.64						
		1.5	.167	20	6922	6922		38.27						
		2.0	.125	4	6573	6573		33.55						
		Ethanol	0.25	.50	.50	4		62.5	1558	2.16	12.08			
				.50	.50	20			2128		15.36			
				.75	.33	20			2128		16.98			
↓	↓			↓	↓	↓	↓		↓		↓			
												4	1558	11.66
												4	2307	24.30
												20	2725	31.80
												20	2725	30.76
												4	2307	23.28
↓	↓			↓	↓	↓	↓		↓		↓			
												2	200	26.02
												4	2571	24.12
								10				2720	27.12	
								20				2953	29.82	
								2				224	32.80	
↓	↓			↓	↓	↓	↓	↓	↓					
											4	1866	35.02	
											10	1892	32.28	
											20	1936	32.60	
											?	177	35.92	
											4	1667	30.87	
↓	↓			↓	↓	↓	↓	↓	↓					
											10	1696	30.65	
											20	1744	28.32	
		4	213							26.35				
		20	3119							31.22				
		20	3119							36.38				
↓	↓	↓	↓	↓	↓	↓	↓							
								4	2761	32.02				
								4	2761	32.02				
								20	3119	32.05				

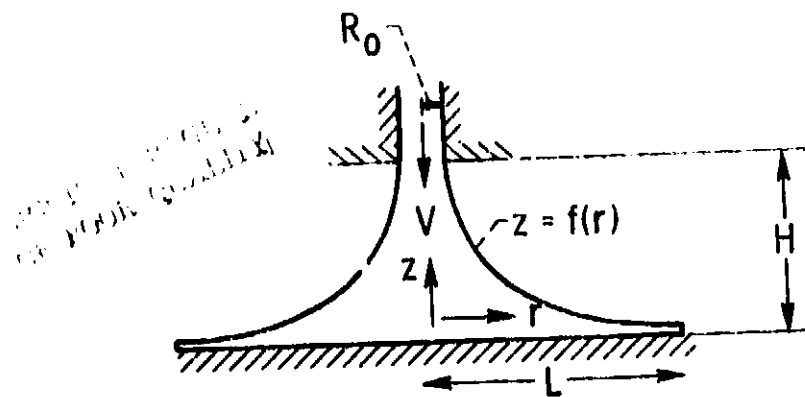


Figure 1. - Schematic of liquid jet impinging on a flat plate.

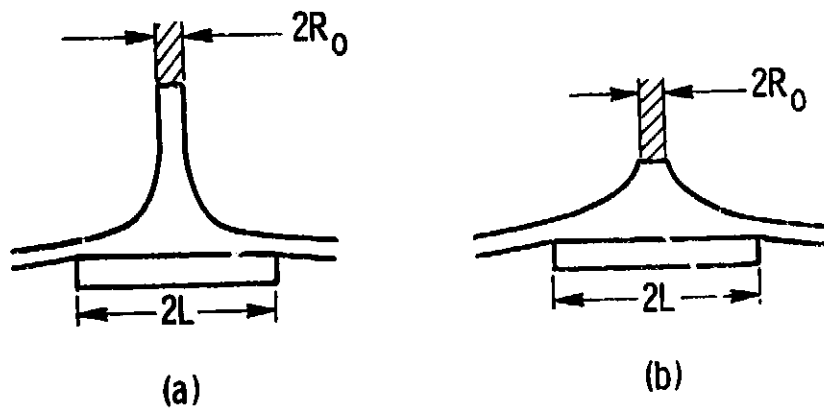


Figure 2. - Flow pattern as a function of nozzle height.

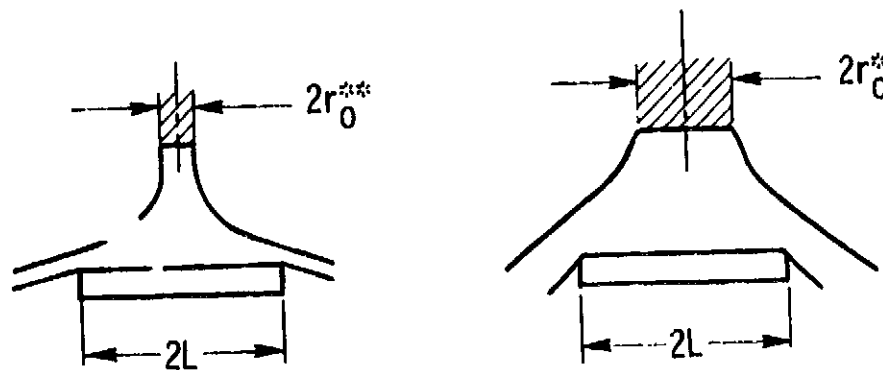


Figure 3. - Flow pattern as a function of jet radius.

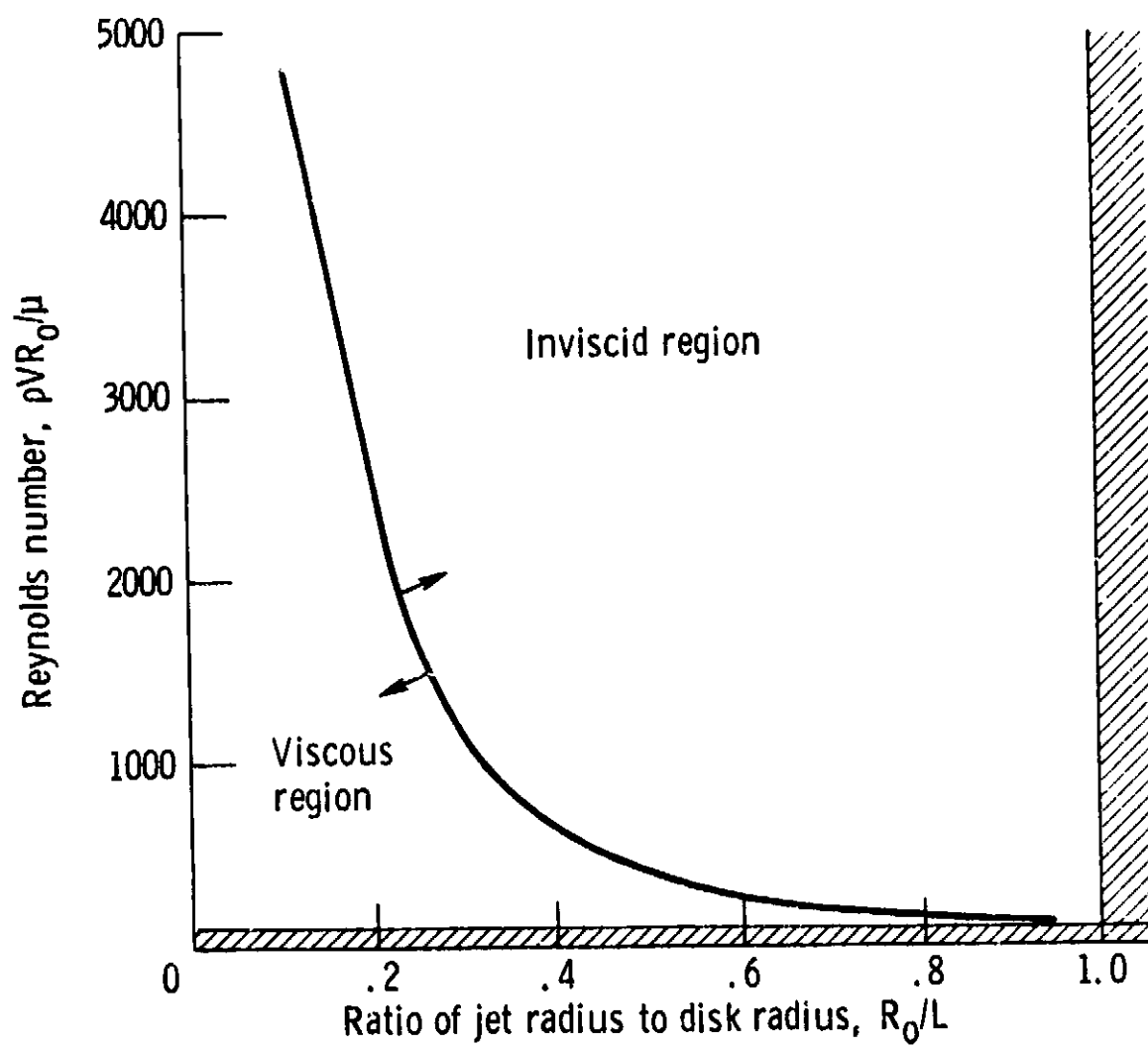


Figure 4. - Results of order of magnitude analysis.

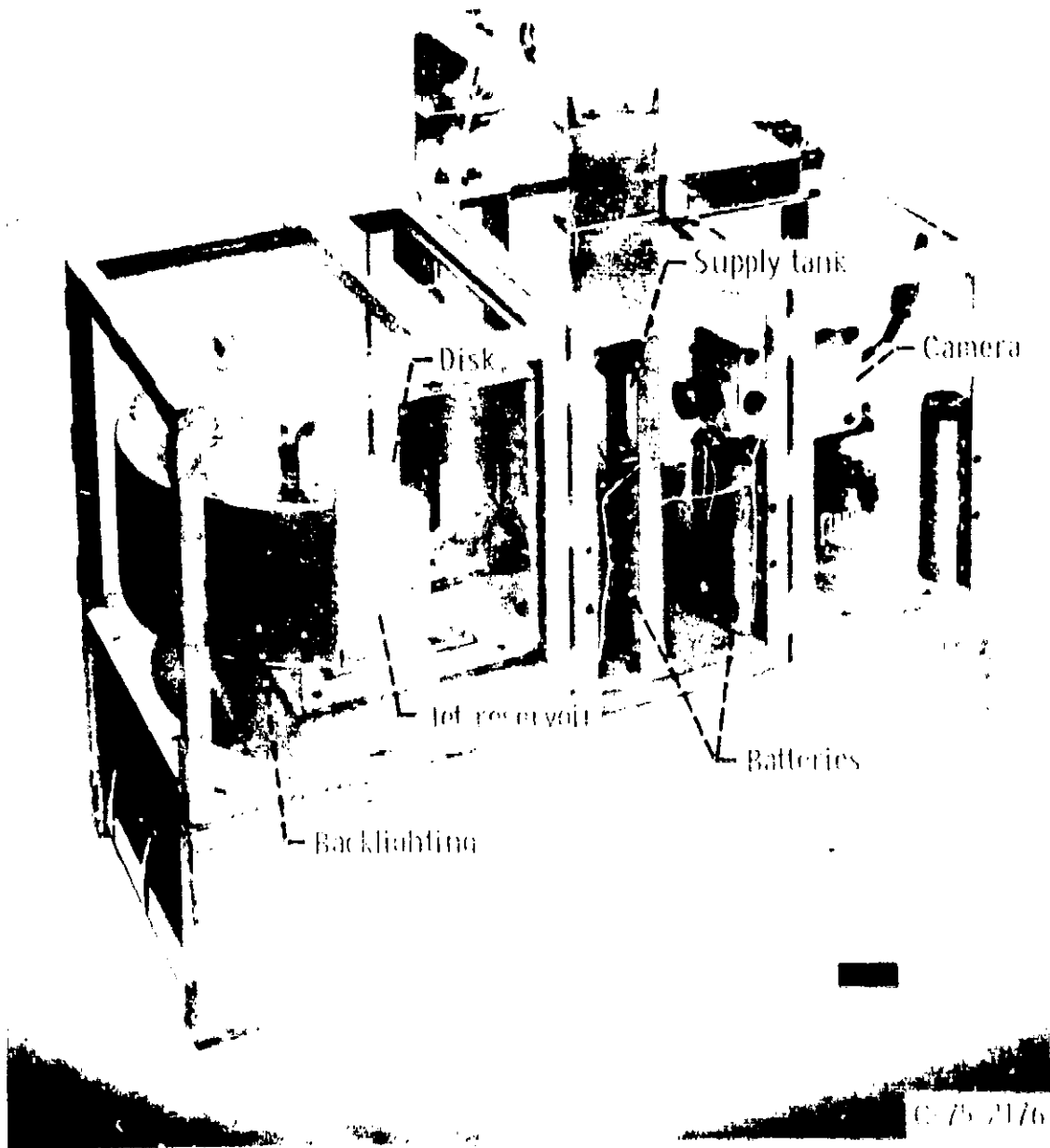


Figure 5. - Experiment package.

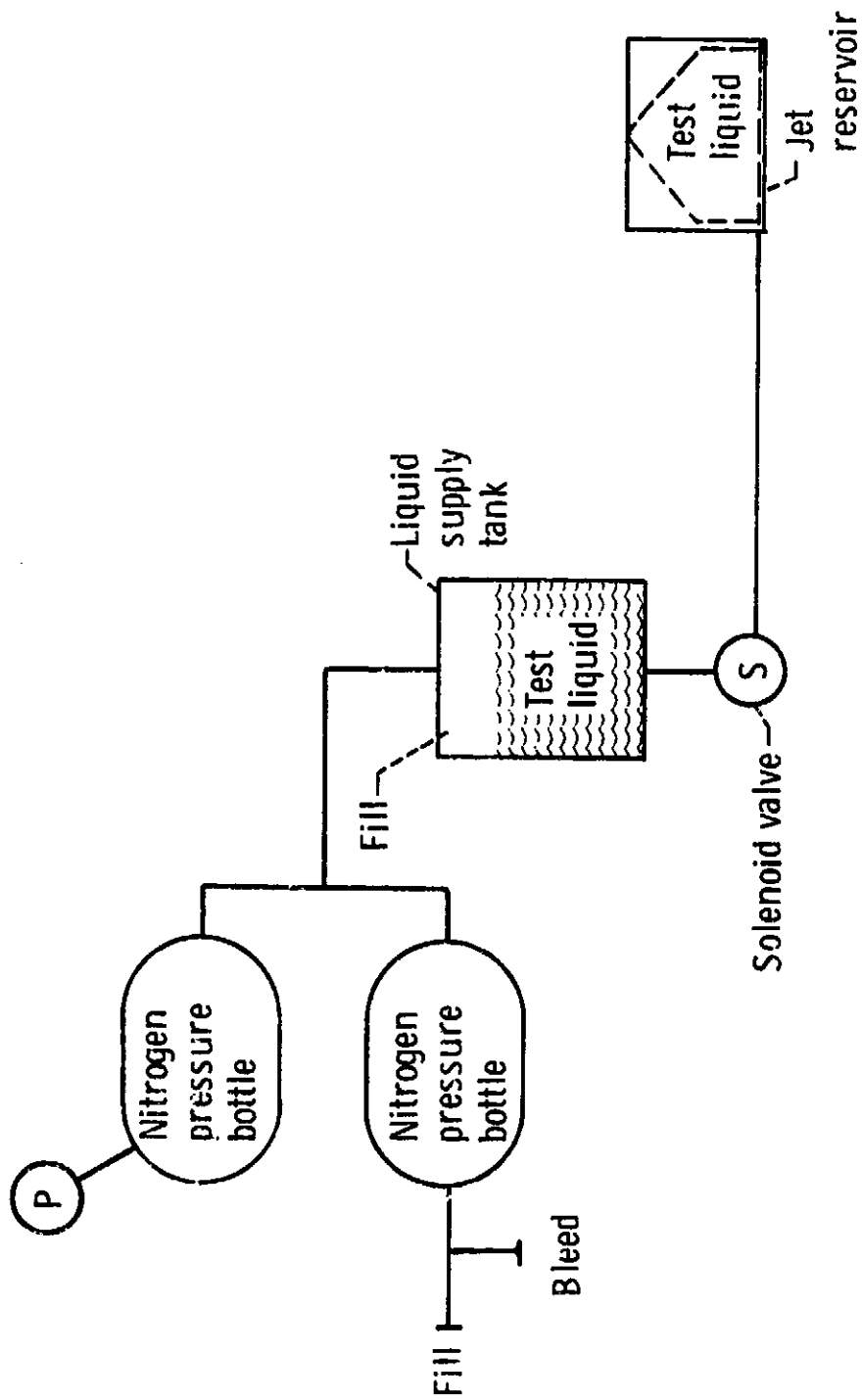


Figure 6. - Flow system schematic.

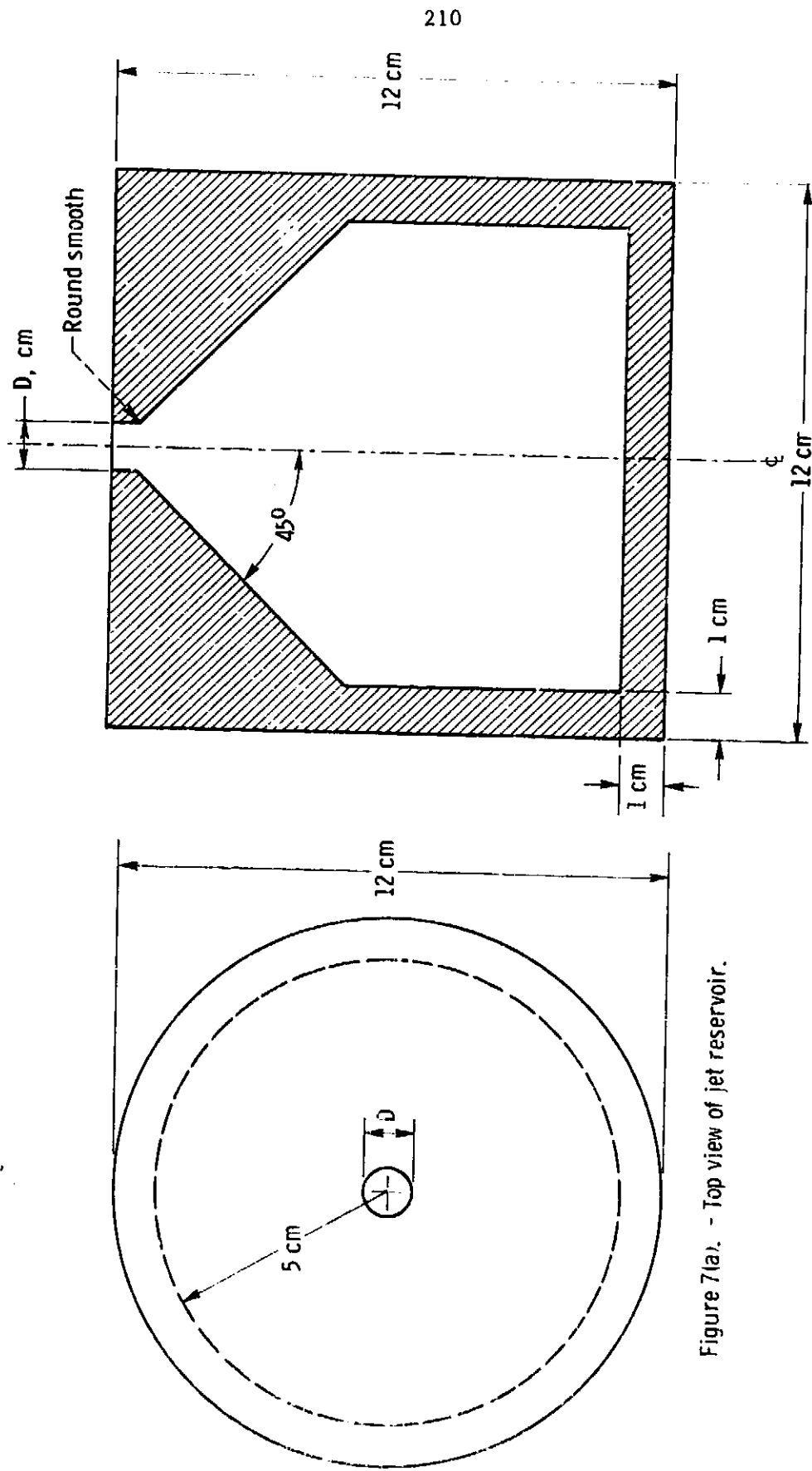


Figure 7(a). - Top view of jet reservoir.

Figure 7(b). - Side view of jet reservoir.

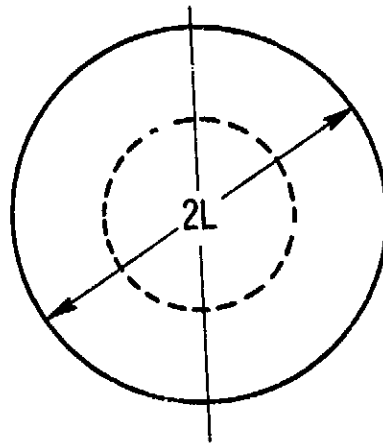
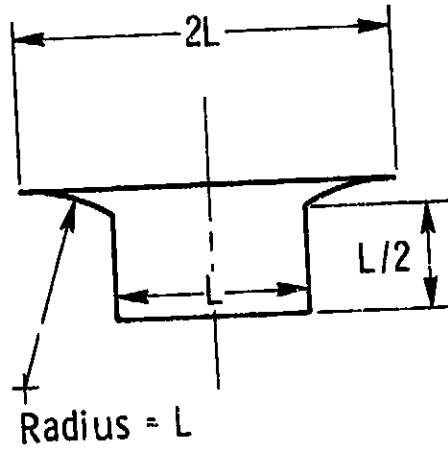
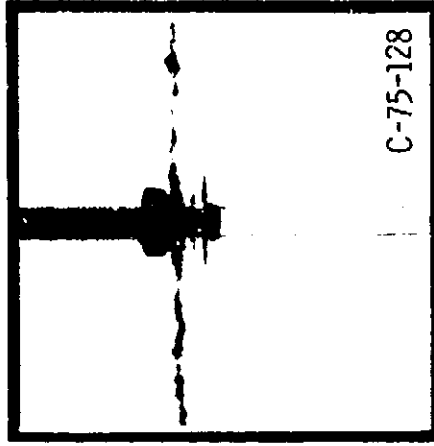
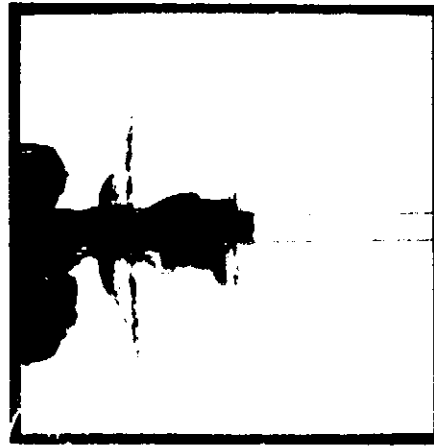


Figure 8. - Schematic diagram of sharp-edged disk.

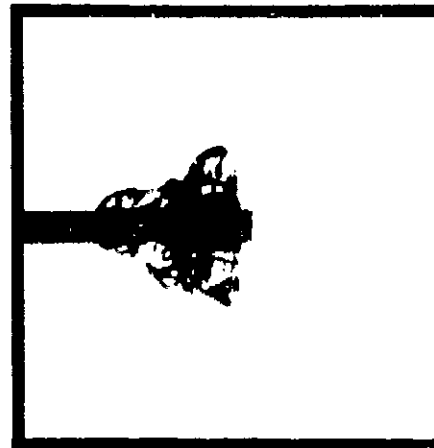
ORIGINAL PAGE IS
OF POOR QUALITY



(c) Inertia flow.



(b) Transition flow.



(a) Surface tension flow.

Figure 9. - Liquid jet impinging on flat solid plate.

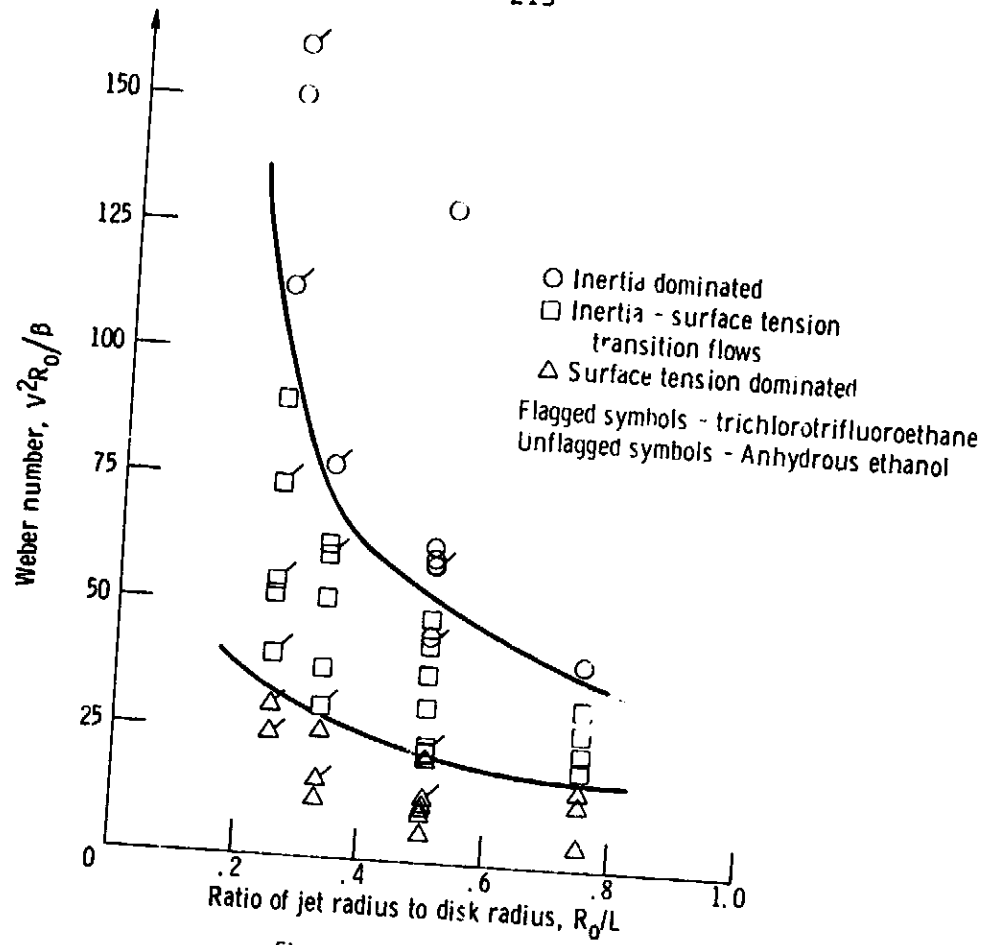


Figure 10. - Zero gravity experimental results.

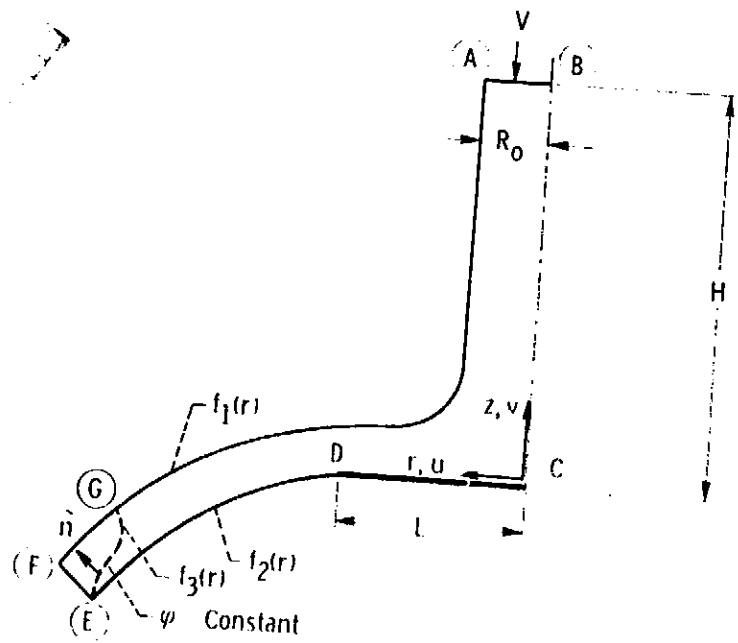


Figure 11. - Physical plane model of liquid jet impingement.

$$\psi_{z^2 z^2} + \psi_{r^2 r^2} - \frac{1}{r^2} \psi_{r^2} = 0$$

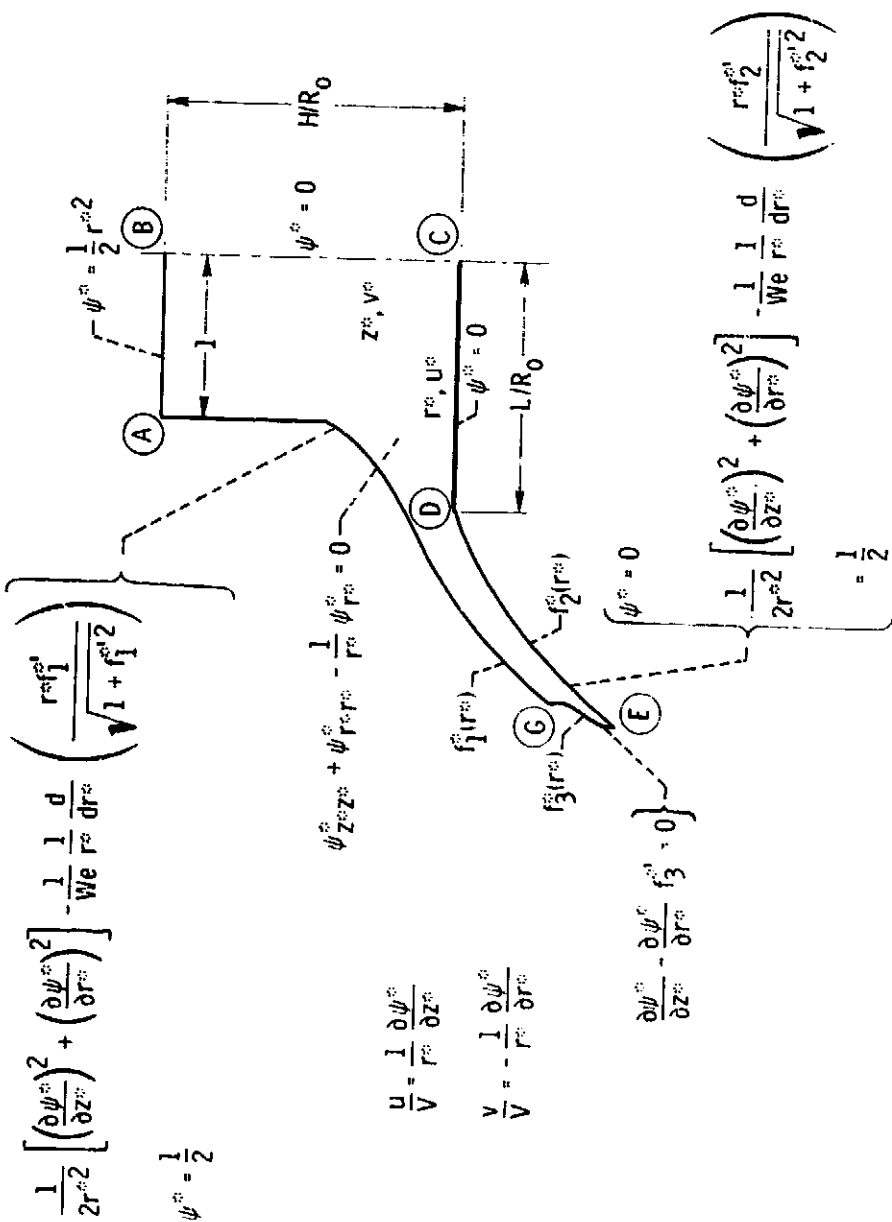


Figure 12. - Dimensionless governing equation and boundary conditions in physical plane employing Stokes' stream function.

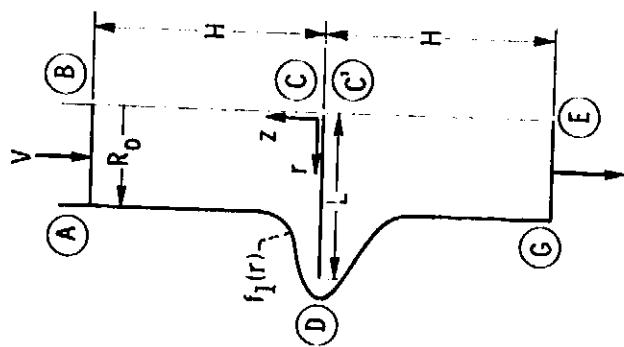


Figure 13. - Surface tension model in physical plane.

$$\psi_{z^*z^*}^* + \psi_{r^*r^*}^* - \frac{1}{r^*} \psi_{r^*}^* = 0$$

where $We = \frac{\rho V^2 R_0}{\sigma}$

$$u^* = \frac{1}{r^*} \frac{\partial \psi^*}{\partial z^*}$$

$$v^* = -\frac{1}{r^*} \frac{\partial \psi^*}{\partial r^*}$$

$$\frac{\partial^2 \psi^*}{\partial z^{*2}} + \frac{\partial^2 \psi^*}{\partial r^{*2}} - \frac{1}{r^*} \frac{\partial \psi^*}{\partial r^*} = 0$$

$$\psi^* = \frac{1}{2}$$

$$\frac{1}{2r^{*2}} \left[\left(\frac{\partial \psi^*}{\partial z^*} \right)^2 + \left(\frac{\partial \psi^*}{\partial r^*} \right)^2 \right]$$

$$-\frac{1}{We} \frac{1}{r^*} \frac{d}{dr^*} \left[\frac{r^*}{\sqrt{\left(\frac{\partial \psi^*}{\partial z^*} \right)^2 + 1}} \right]$$

$$= \frac{1}{2} - \frac{1}{We}$$

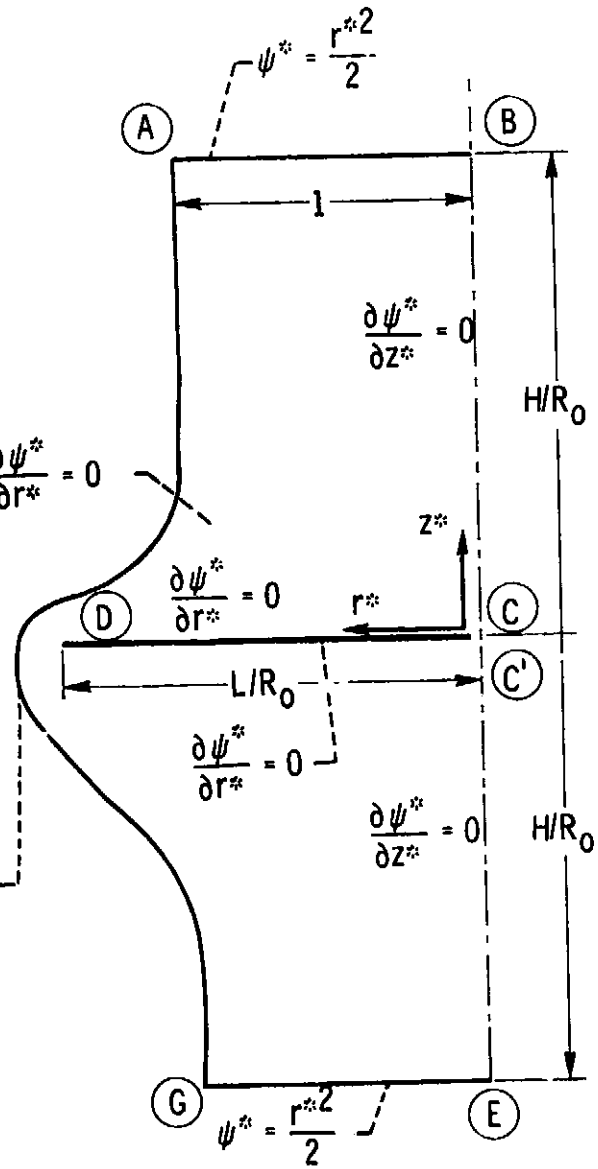


Figure 14. - Dimensionless governing equations and boundary conditions.

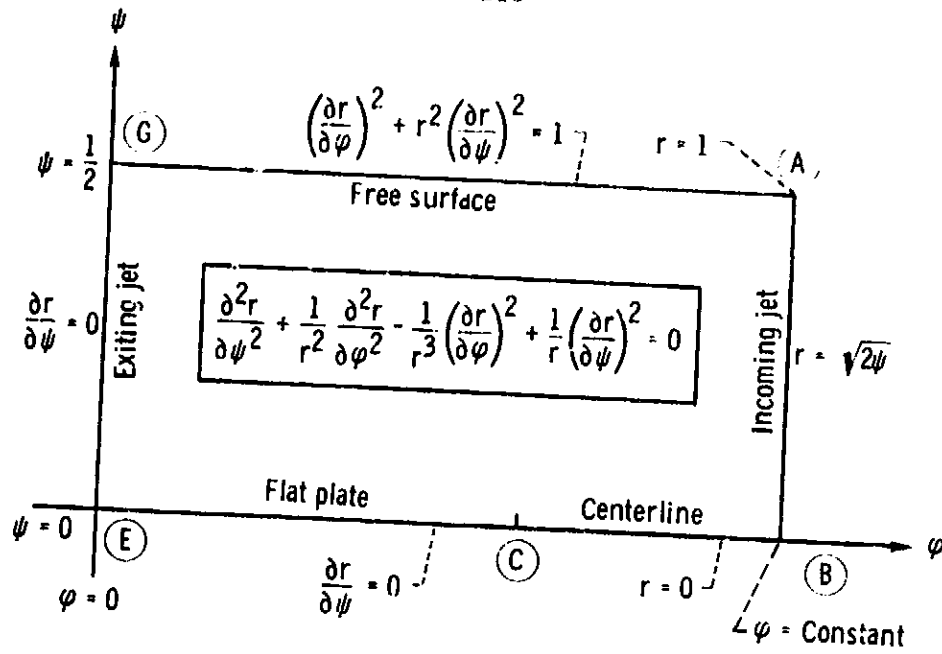


Figure 15(a). - Inverse formulation excluding surface tension (r solution) for infinite plate.

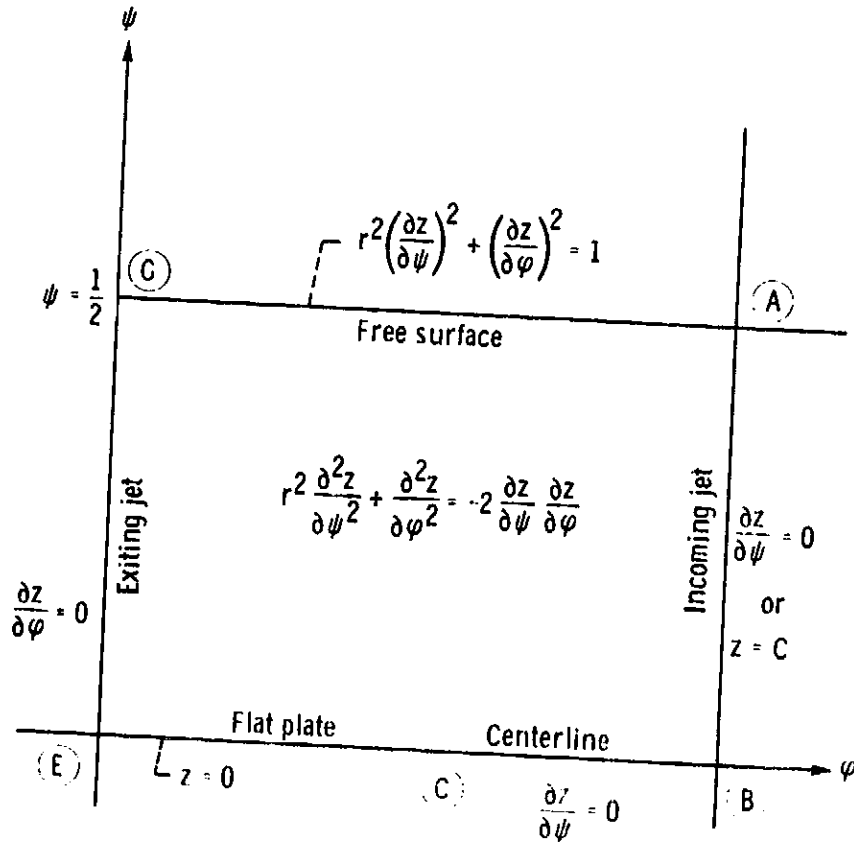


Figure 15(b). - Inverse formulation excluding surface tension (z solution) for infinite plate.

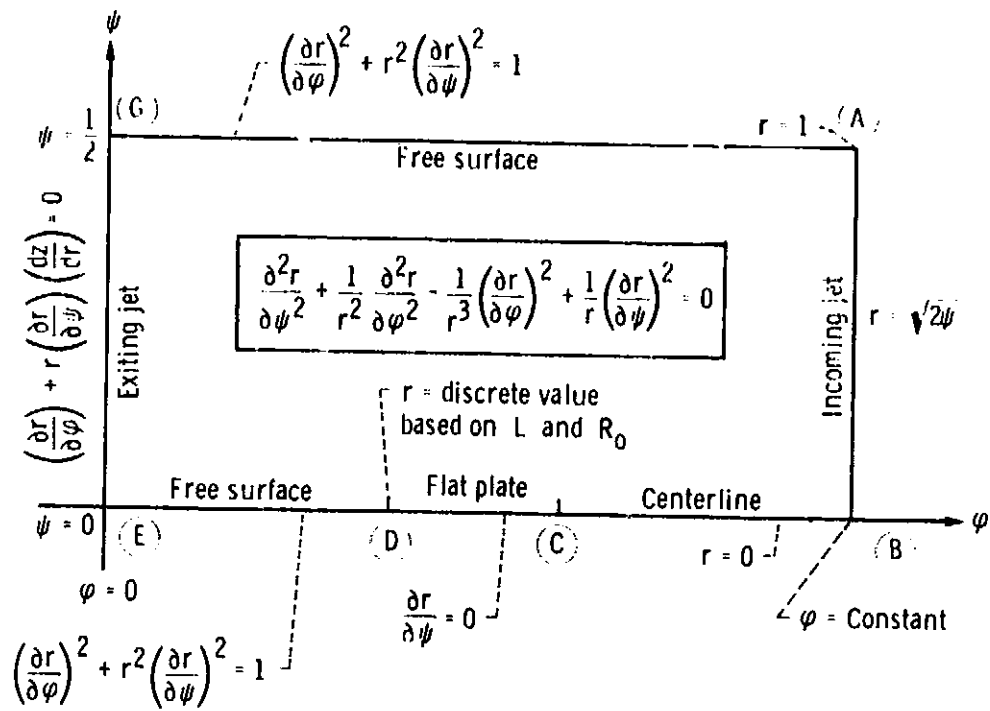


Figure 16(a). - Inverse formulation excluding surface tension (r solution) for finite plate.

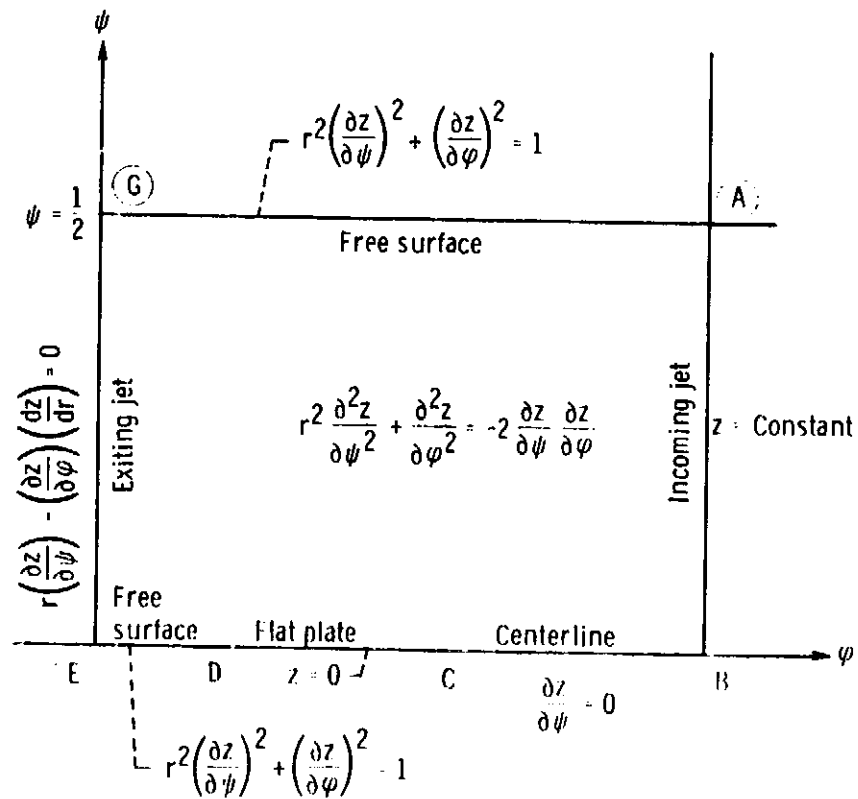


Figure 16(b) - Inverse formulation excluding surface tension (z solution) for finite plate.

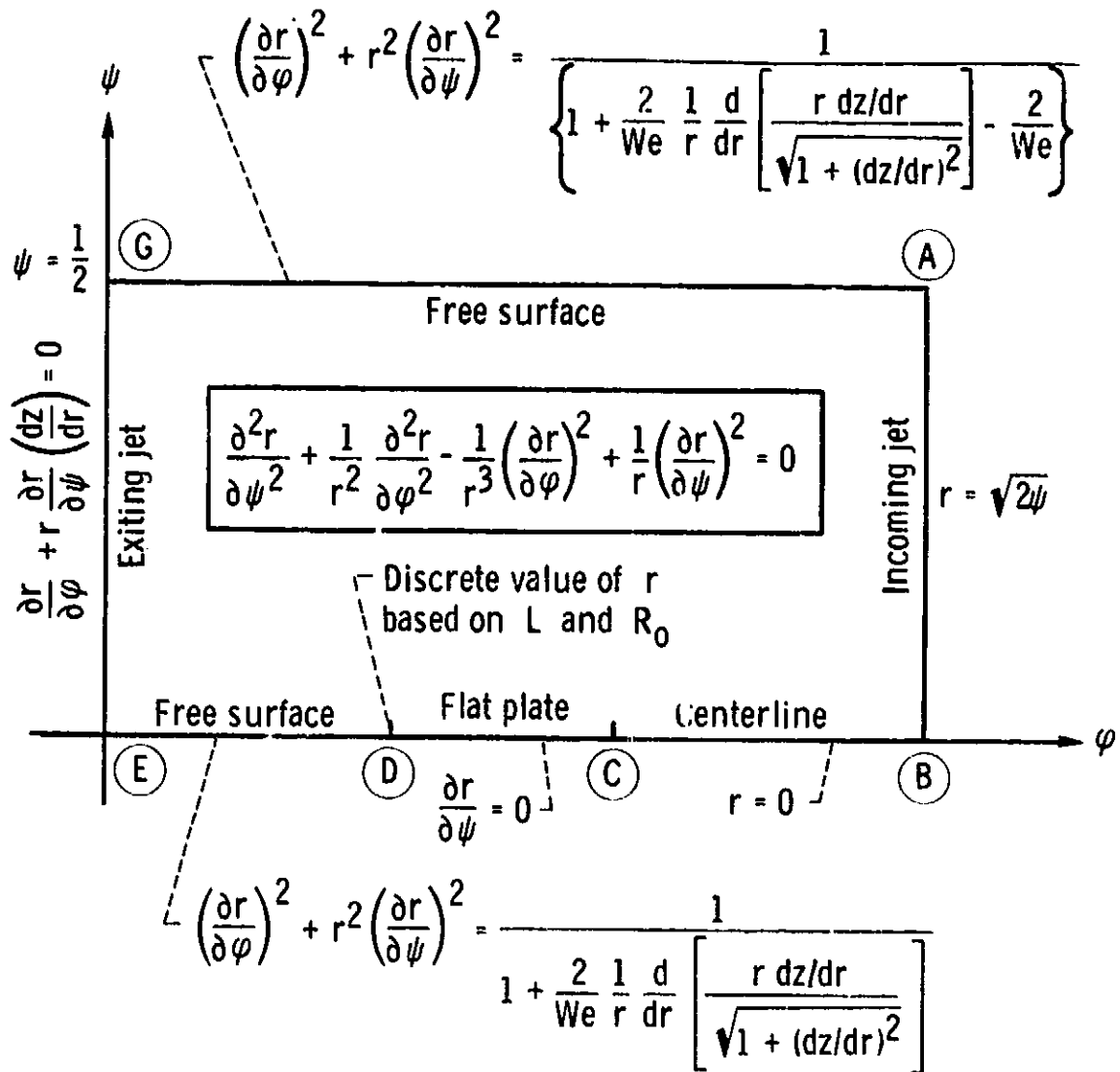


Figure 17. - Inverse formulation including surface tension (r solution) for finite plate.

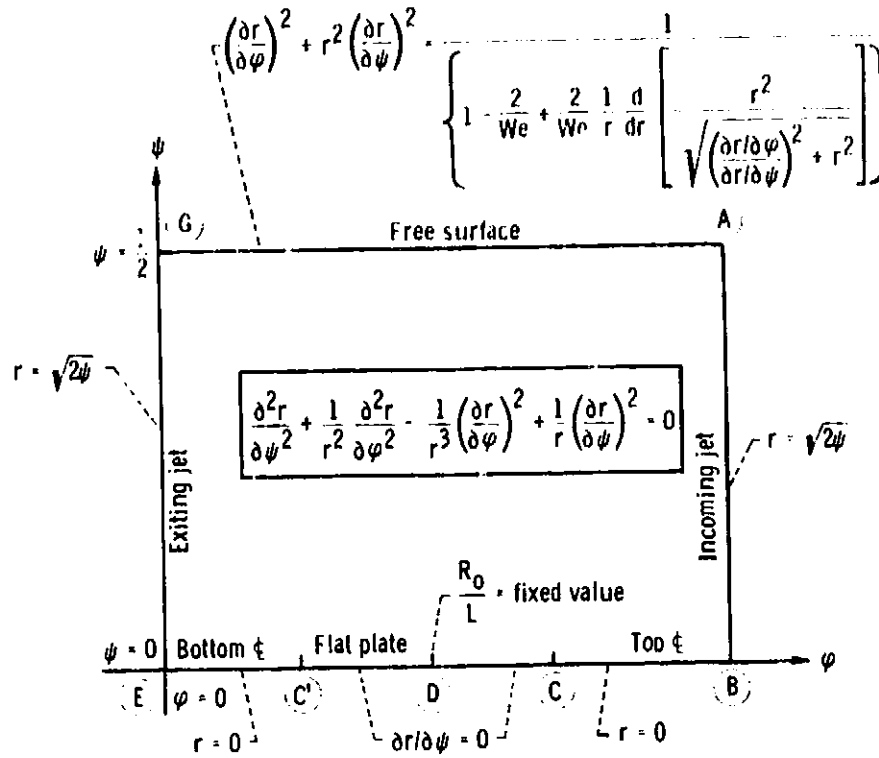


Figure 18(a). - Surface tension model - inverse formulation (r solution).

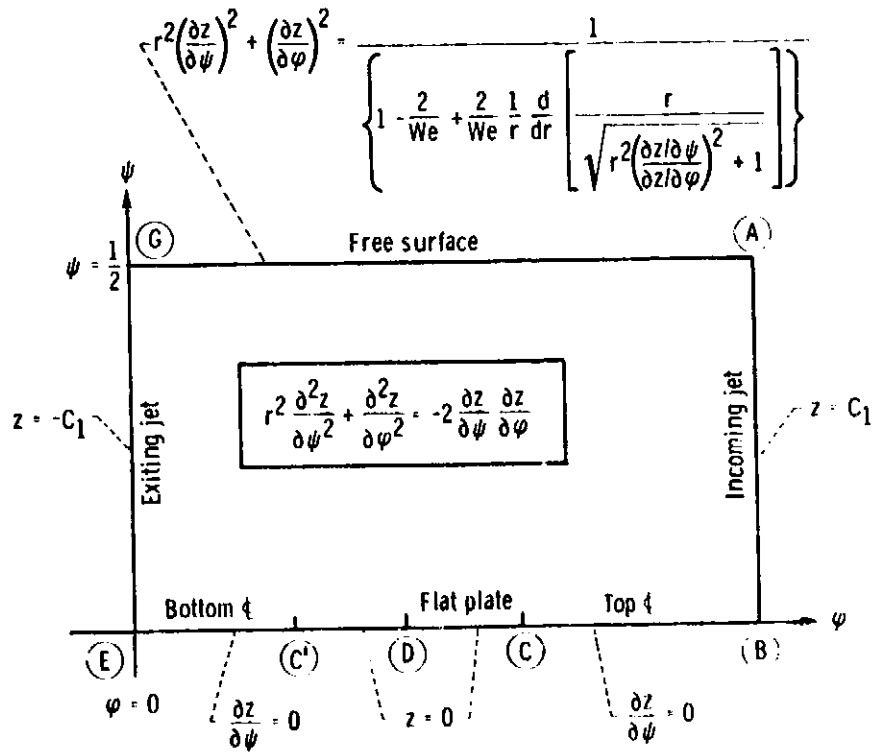


Figure 18(b). - Surface tension model - inverse formulation (z solution).

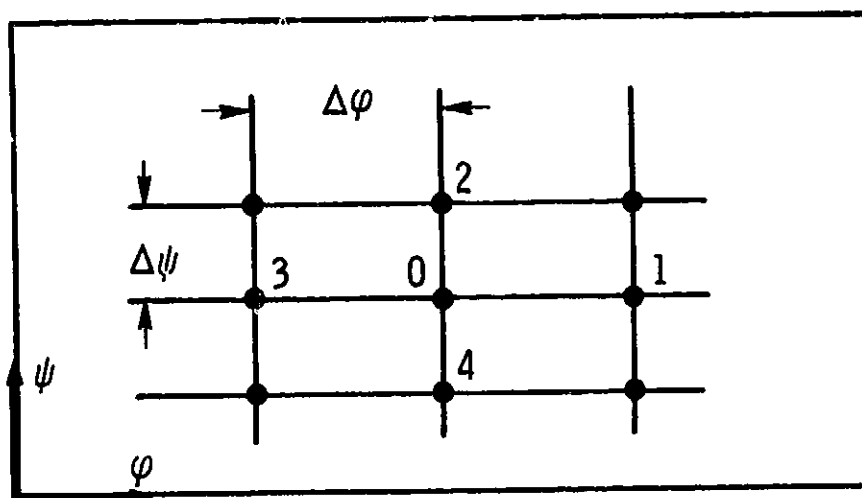


Figure 19. - Nodal point representation for rectangular mesh.

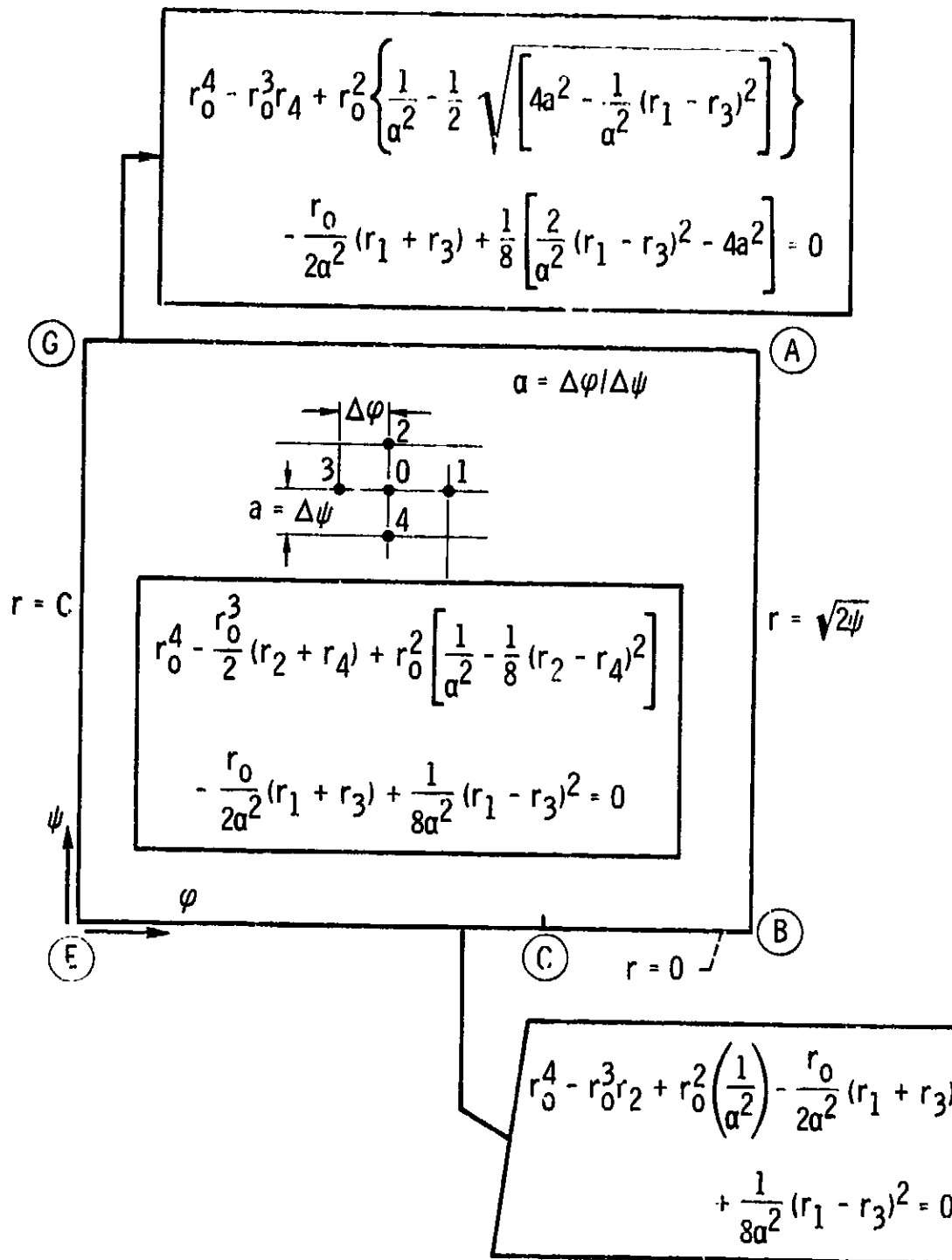


Figure 20(a). - Finite difference representation for infinite plate (r solution).

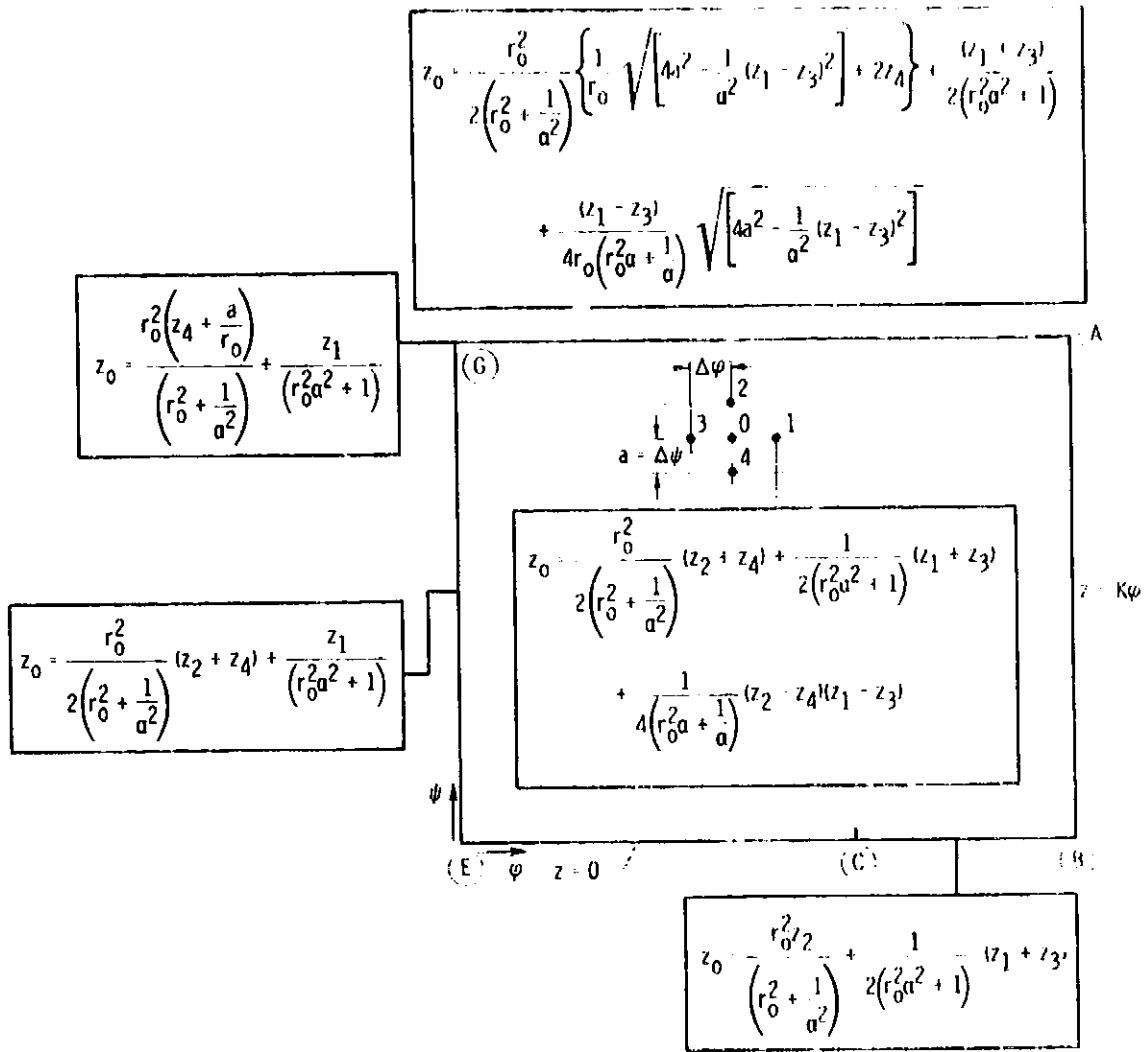


Figure 20(b). - Finite difference representation for infinite plate (z solution).

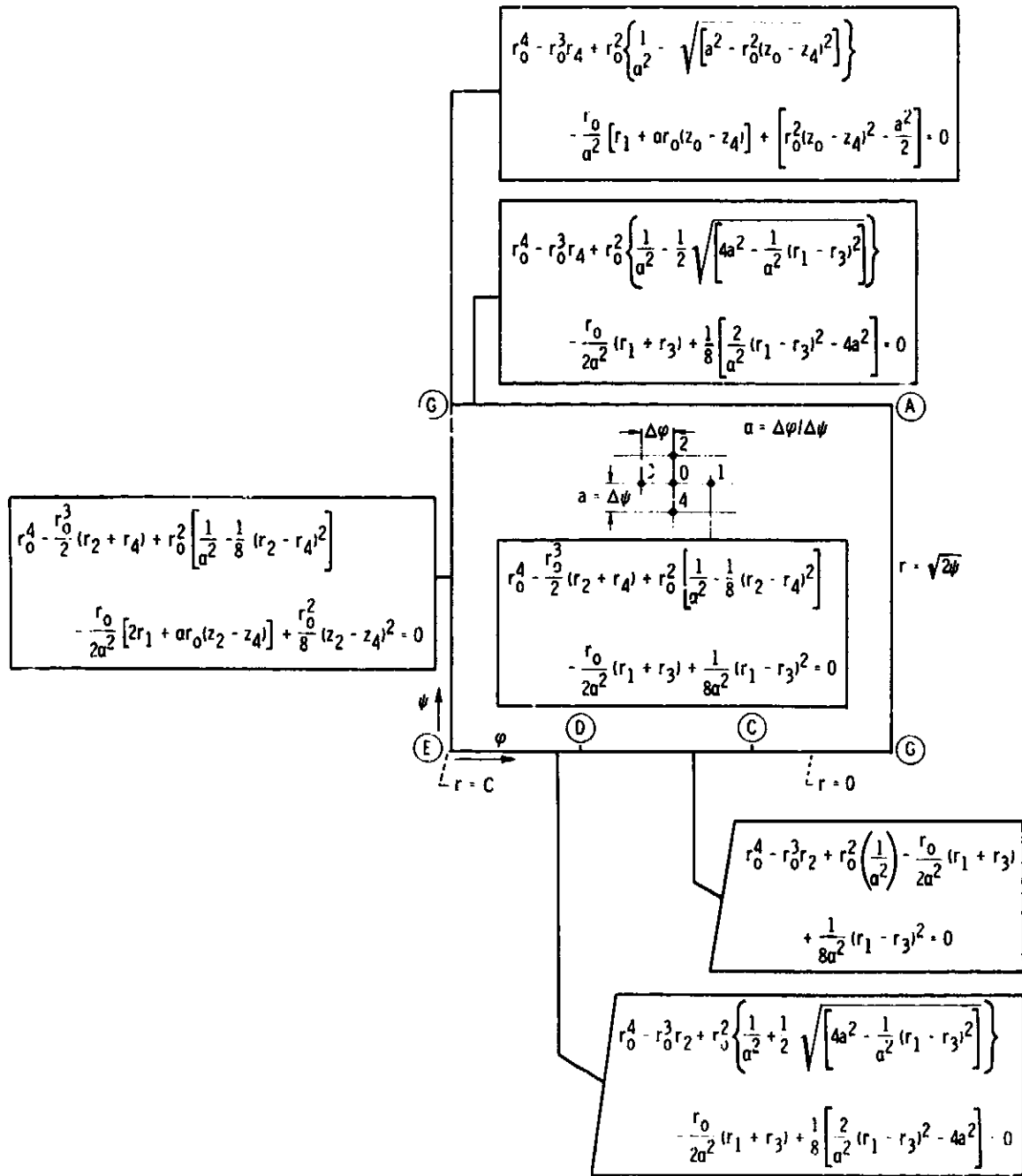
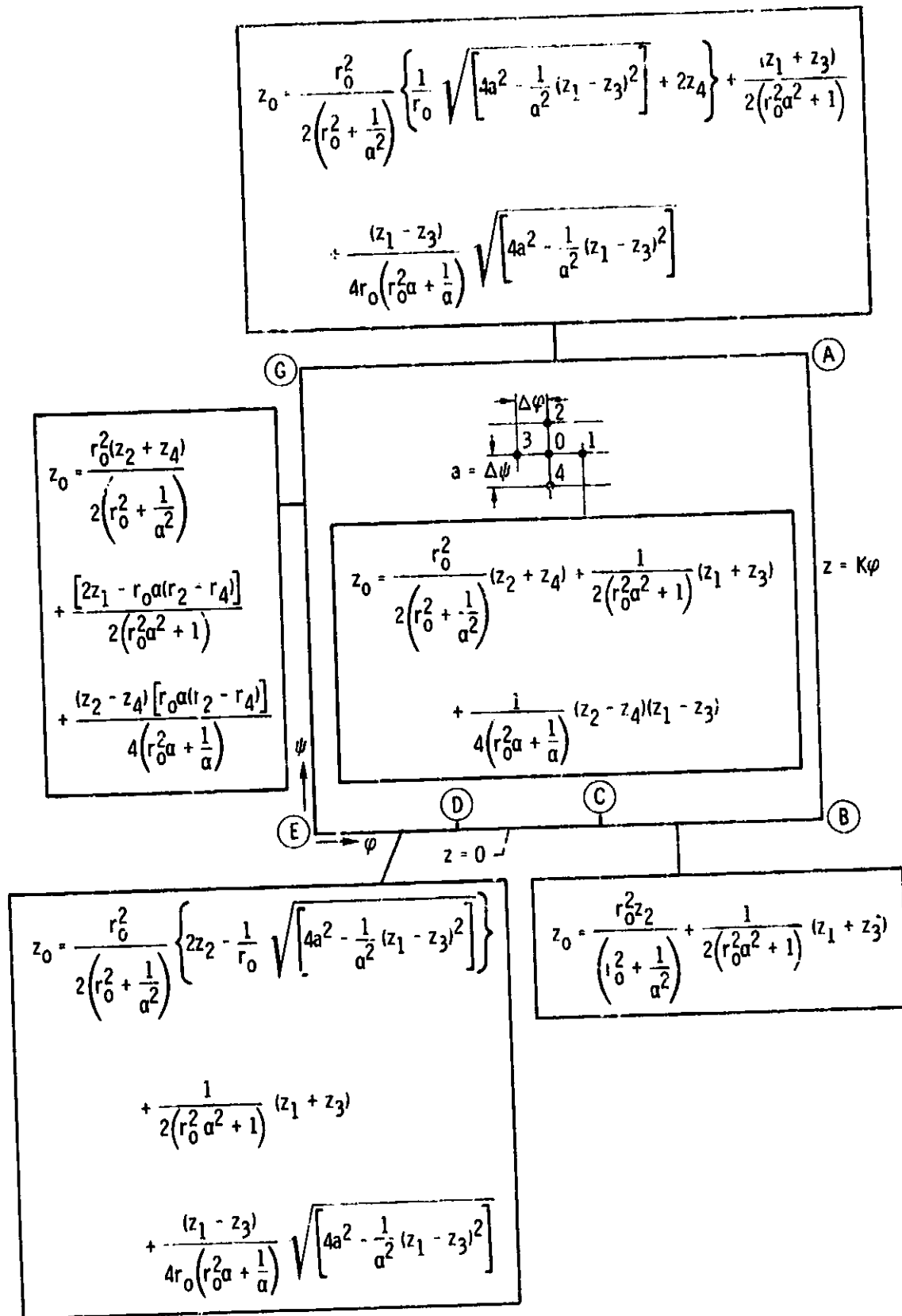


Figure 21(a). - Finite difference representation for finite plate (r solution).

Figure 21(b). - Finite difference representation for finite plate (z solution).

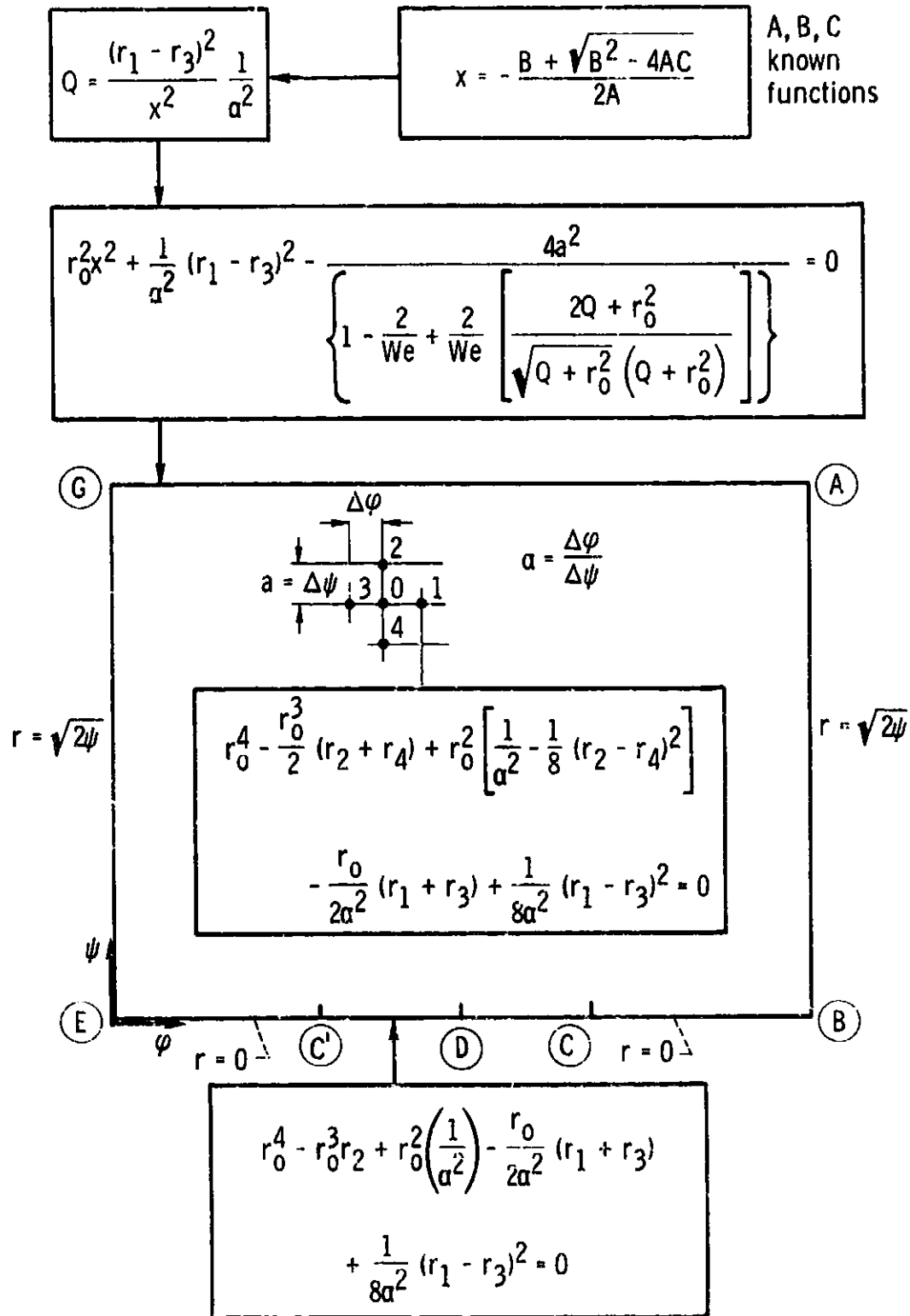


Figure 22(a). - Finite difference representation for surface tension dominated model (r solution).

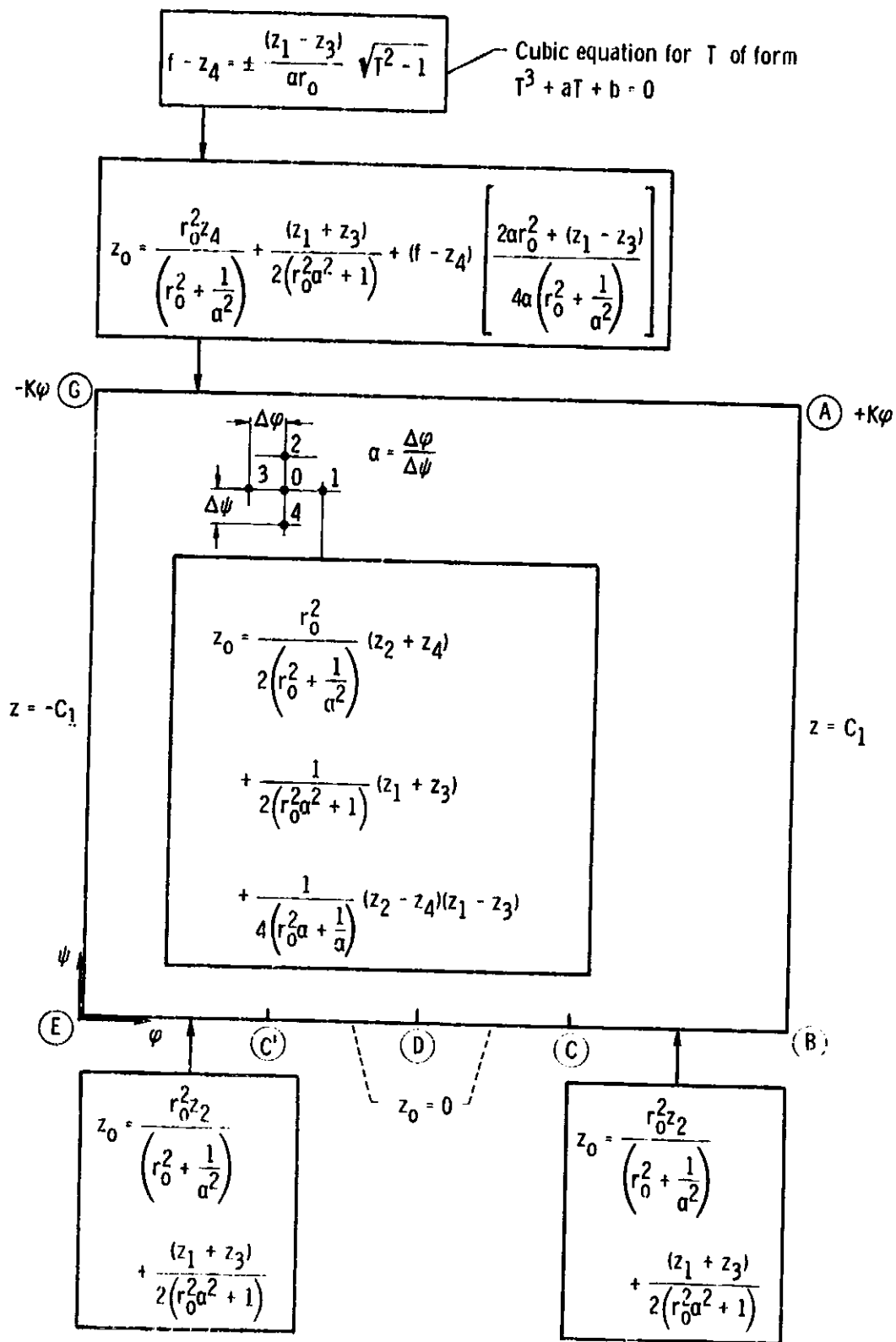


Figure 22(b). - Finite difference representation for surface tension dominated model (z solution).

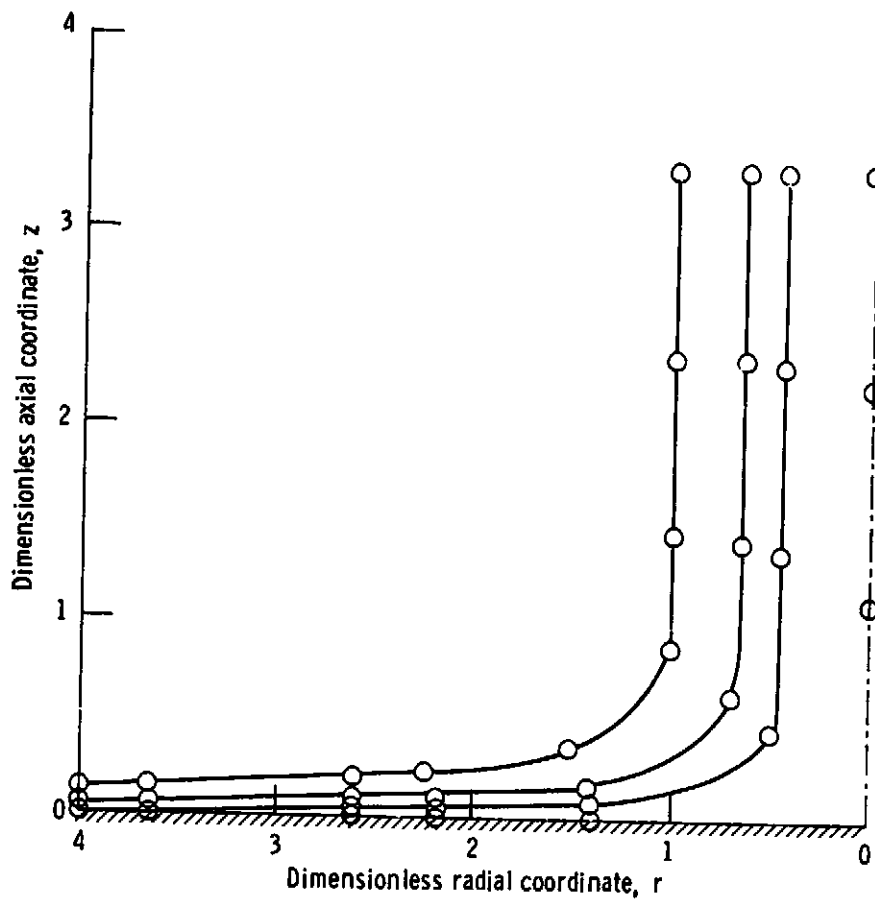


Figure 23. - Numerical solution of liquid jet impinging on infinite flat plate (coarse mesh).

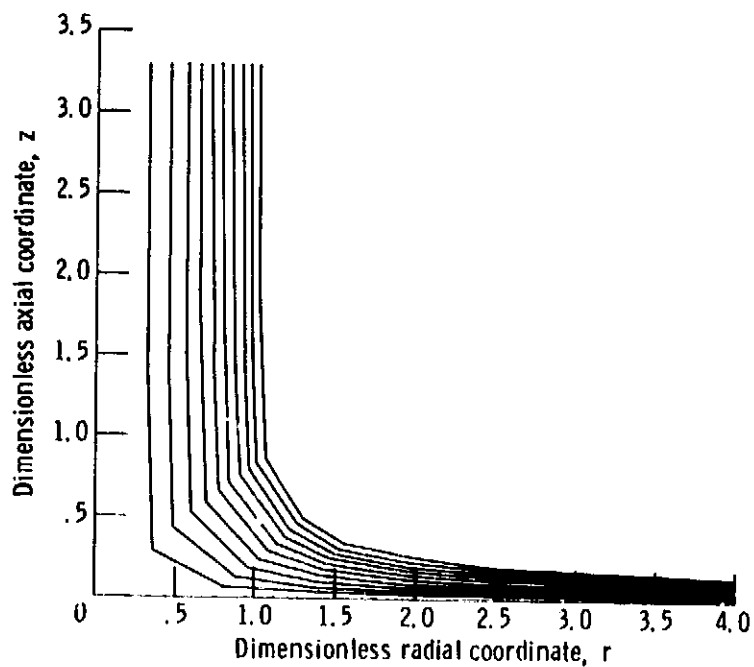


Figure 24. - Print-plot of liquid jet impinging on infinite flat plate (fine mesh).

ORIGINAL PAGE IS
OF POOR QUALITY

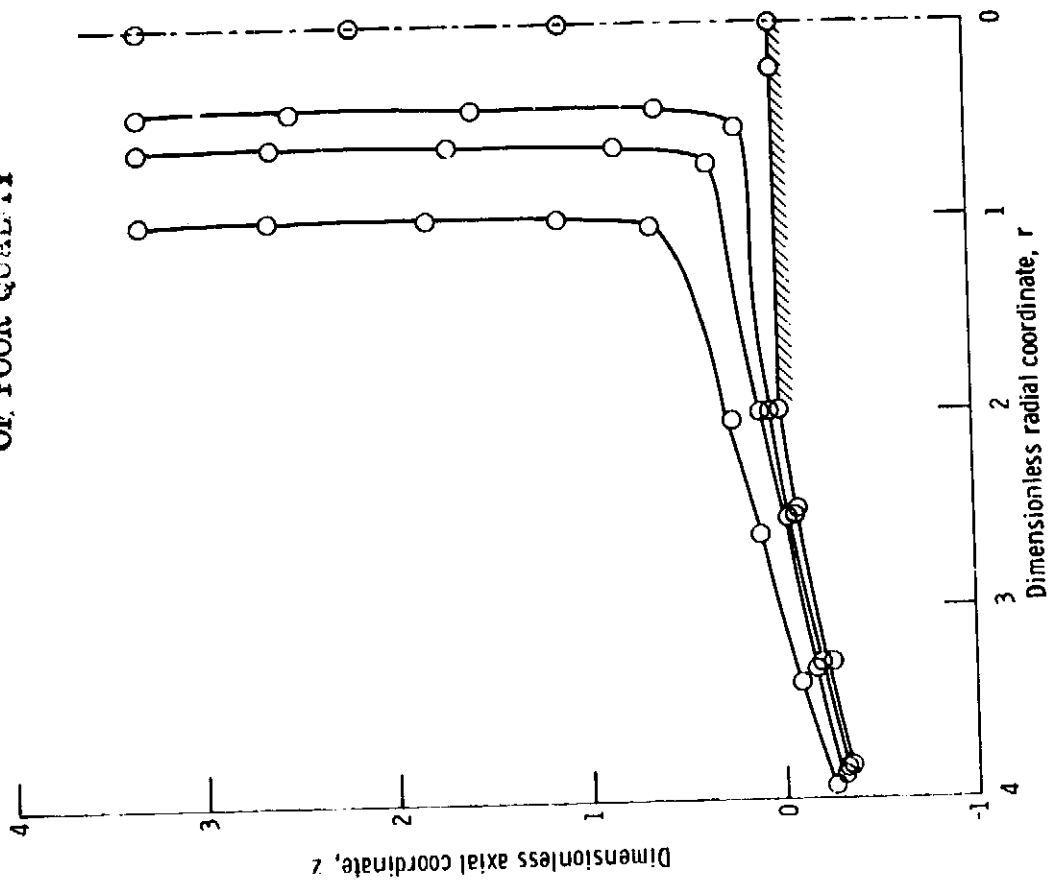


Figure 25. - Numerical solution of liquid jet impinging on finite plate
($R_0/L = 1/2$).

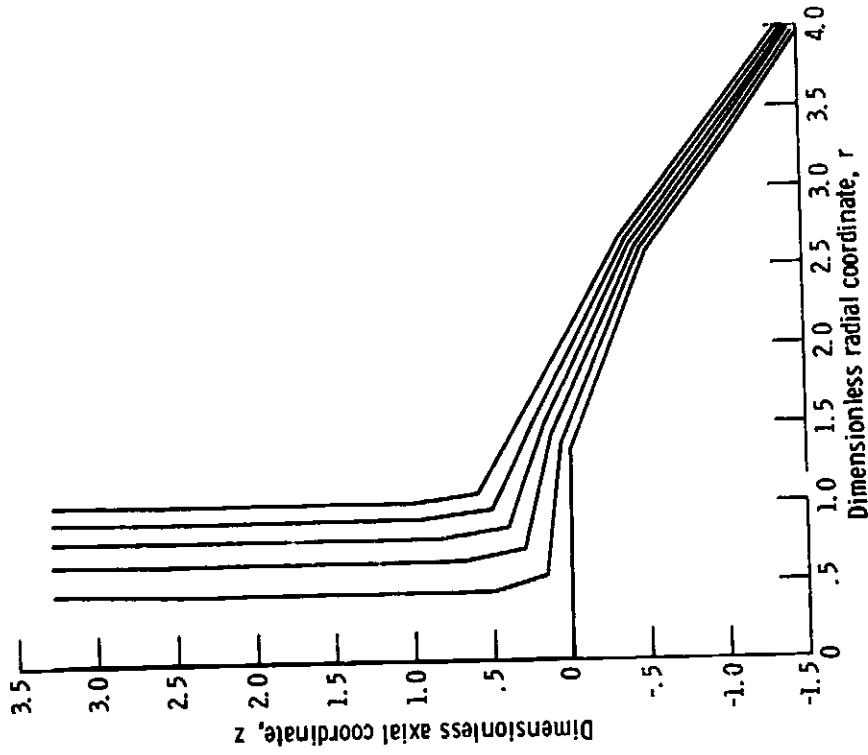


Figure 26. - Print-plot of numerical solution for impingement
on a finite plate ($R_0/L = 3/4$).

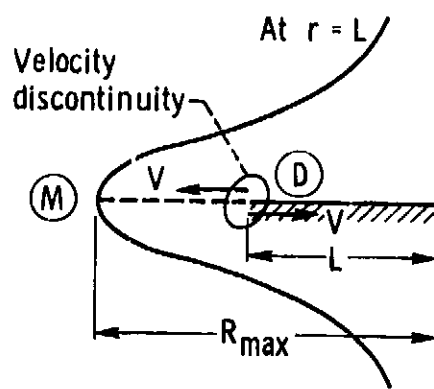


Figure 27. - Schematic diagram of velocity discontinuity occurring in surface tension model.

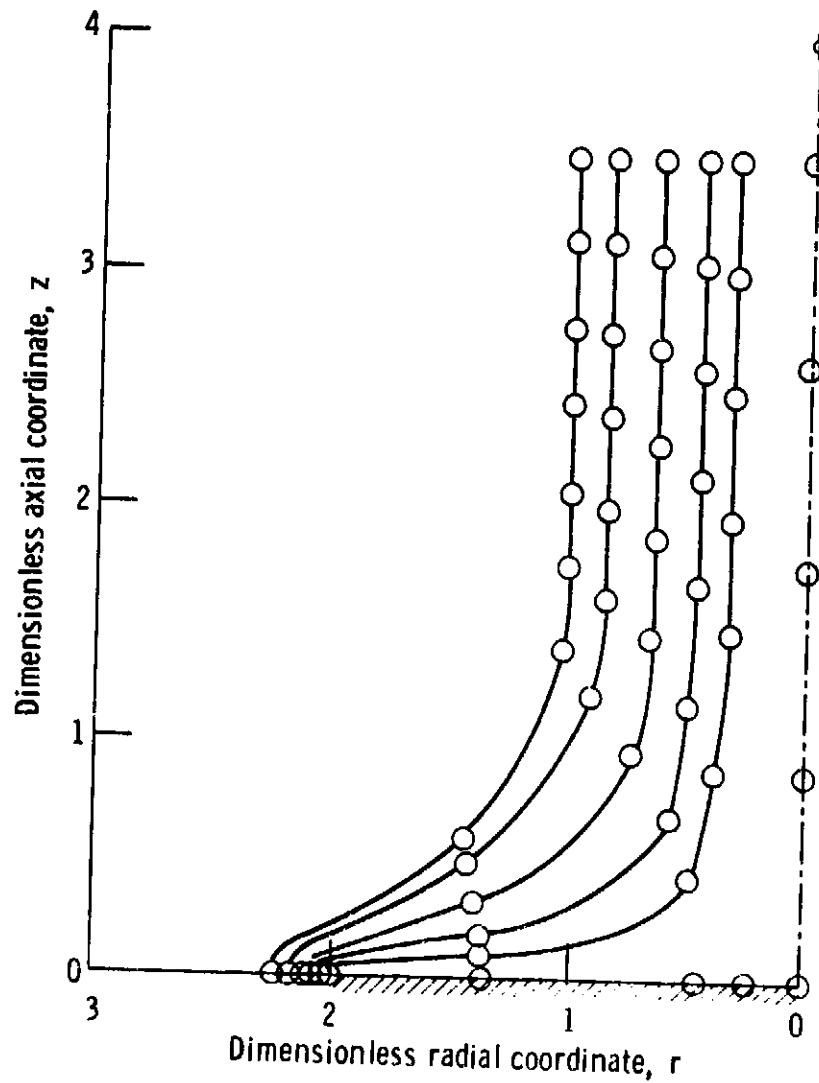


Figure 28. - Numerical solution of surface tension dominated model ($We = 4$, $R_0/L = 1/2$).

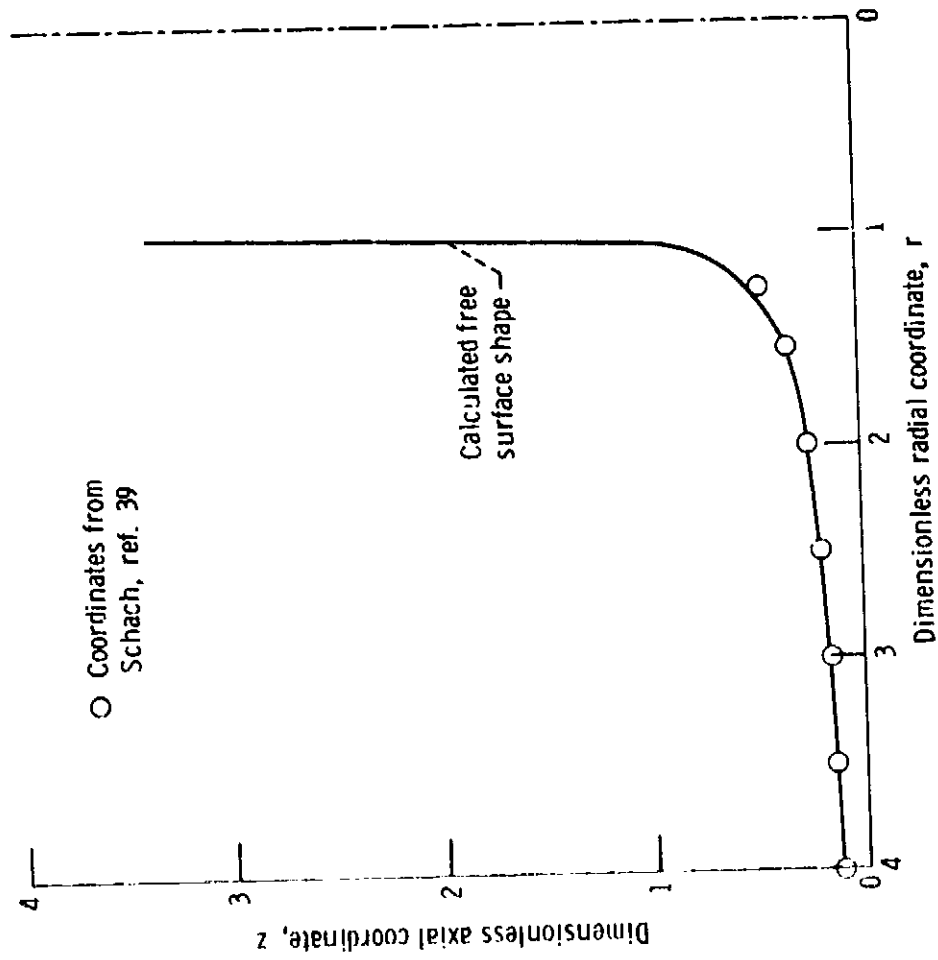


Figure 29. - Comparison of numerical results for infinite plate with reference 39.

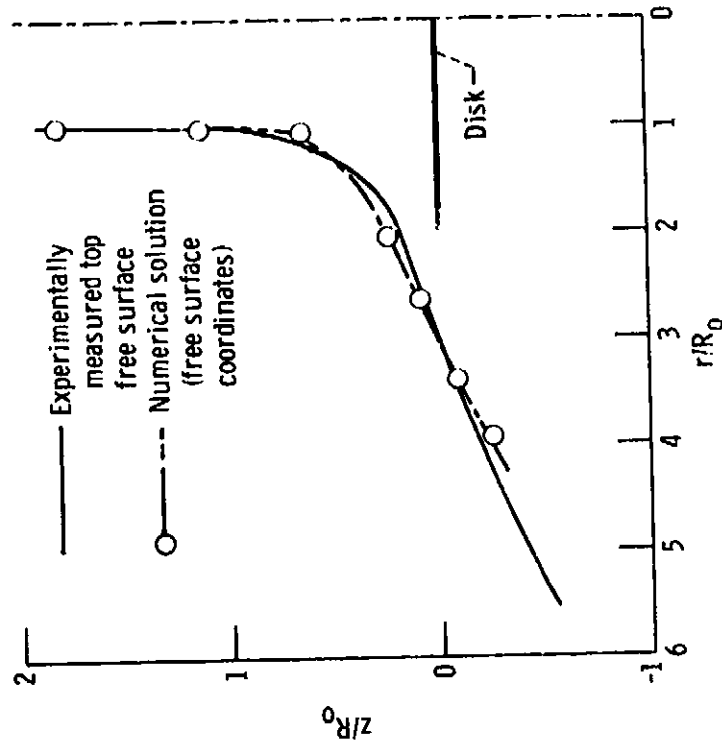


Figure 30. - Comparison of numerical results for finite plate - inertial flow with experiments ($R_0/L = 1/2$).

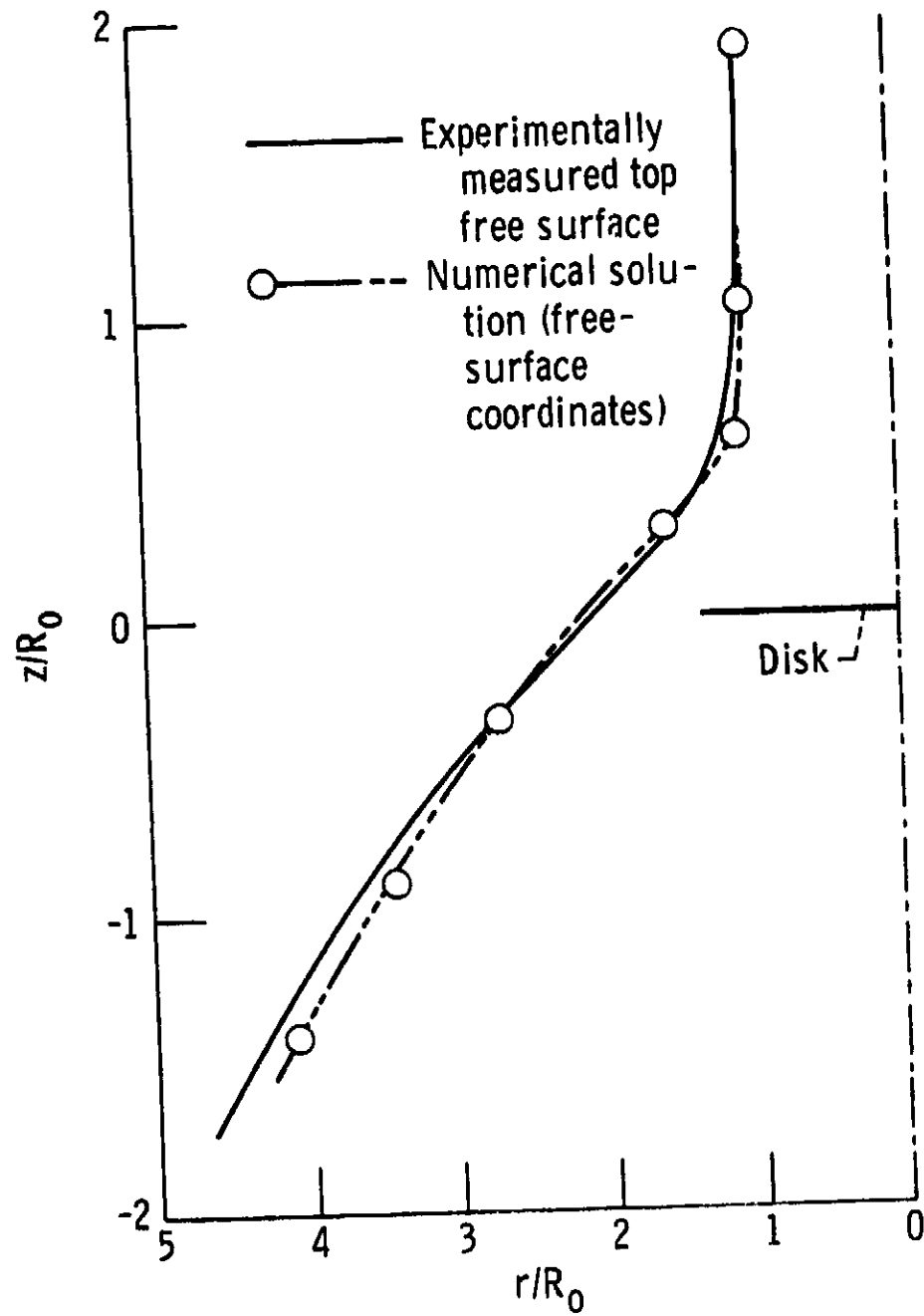


Figure 31. - Comparison of numerical results for finite plate - inertial flow with experiments ($R_0/L = 3/4$).

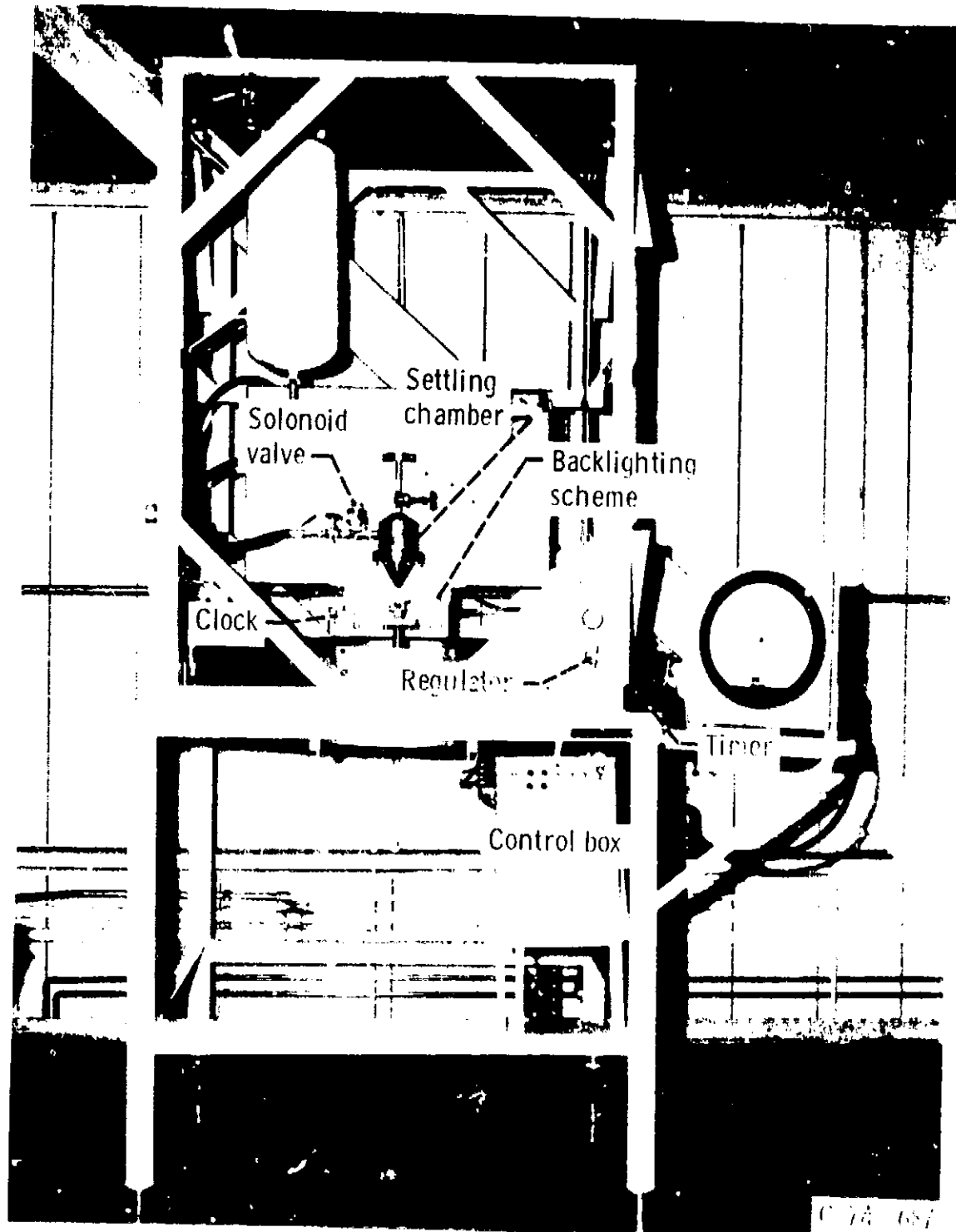


Figure 32(a). - Experimental test rig - front view.

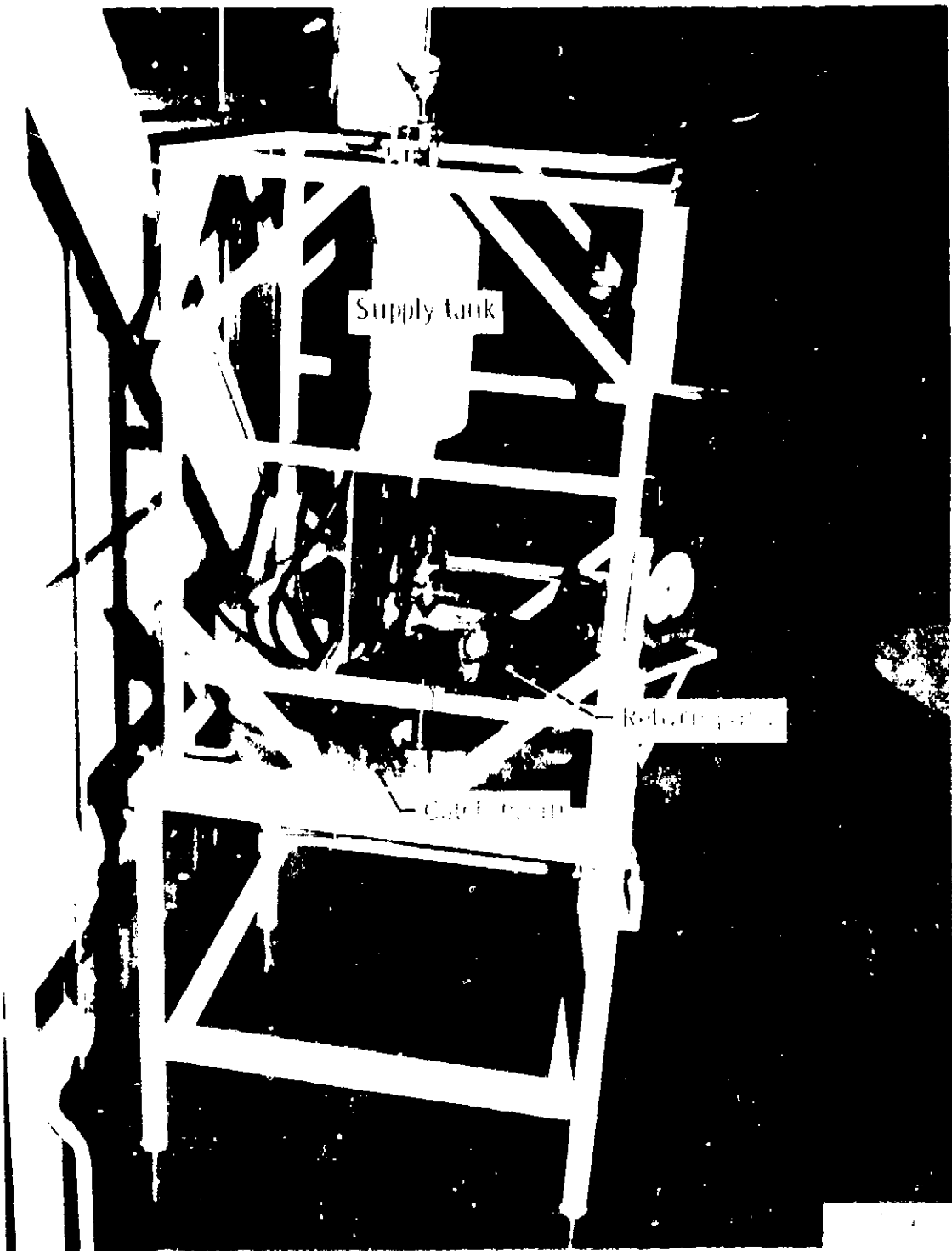


Figure 32(b). - Experimental test rig - side view.

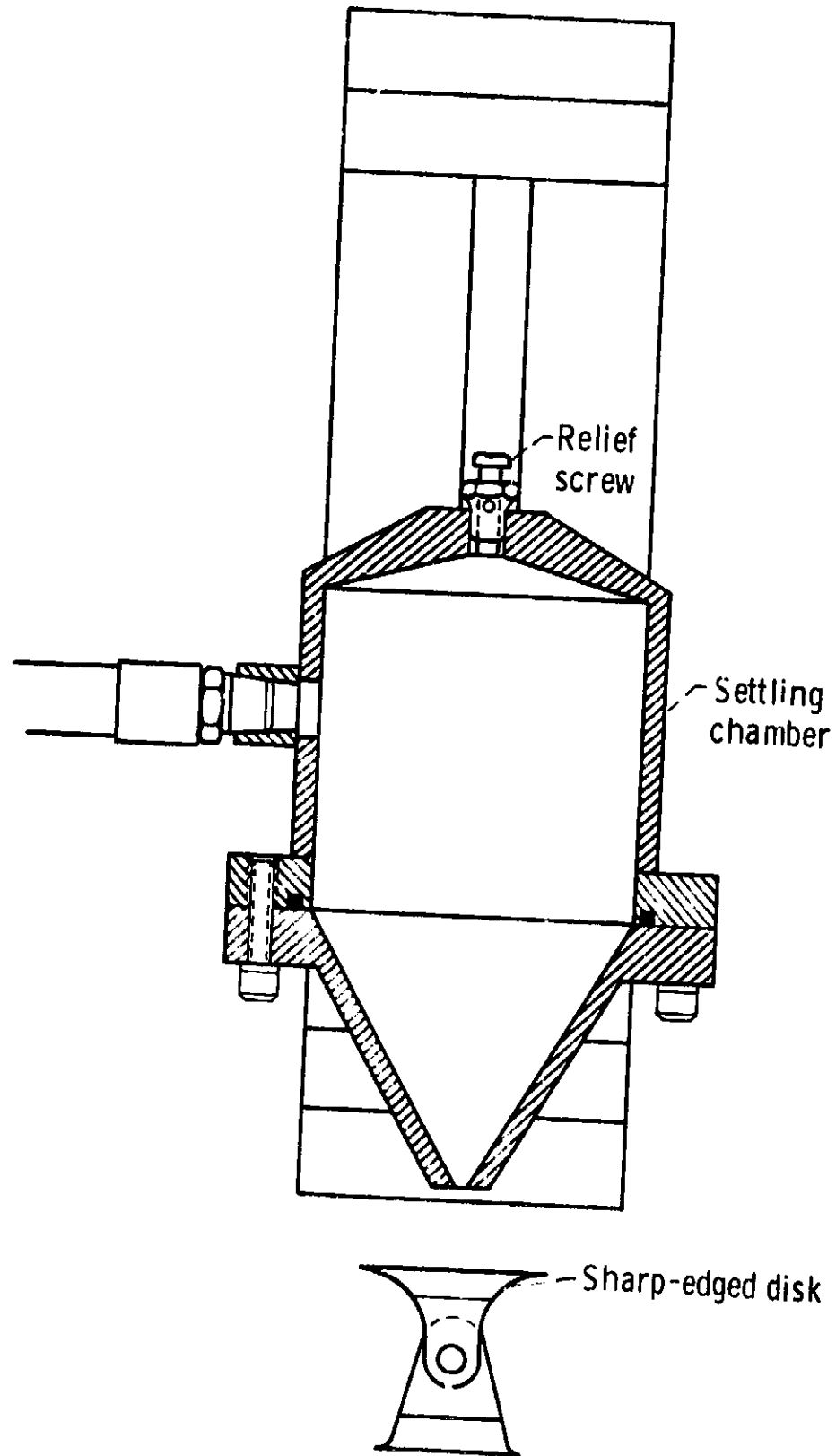


Figure 33. - Cross-section of settling chamber.

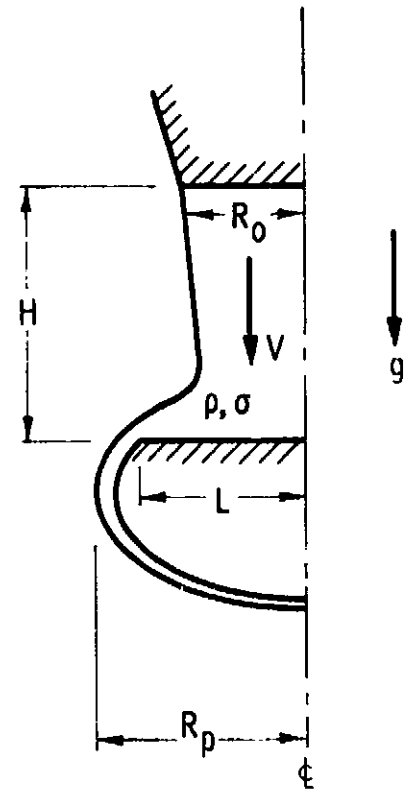
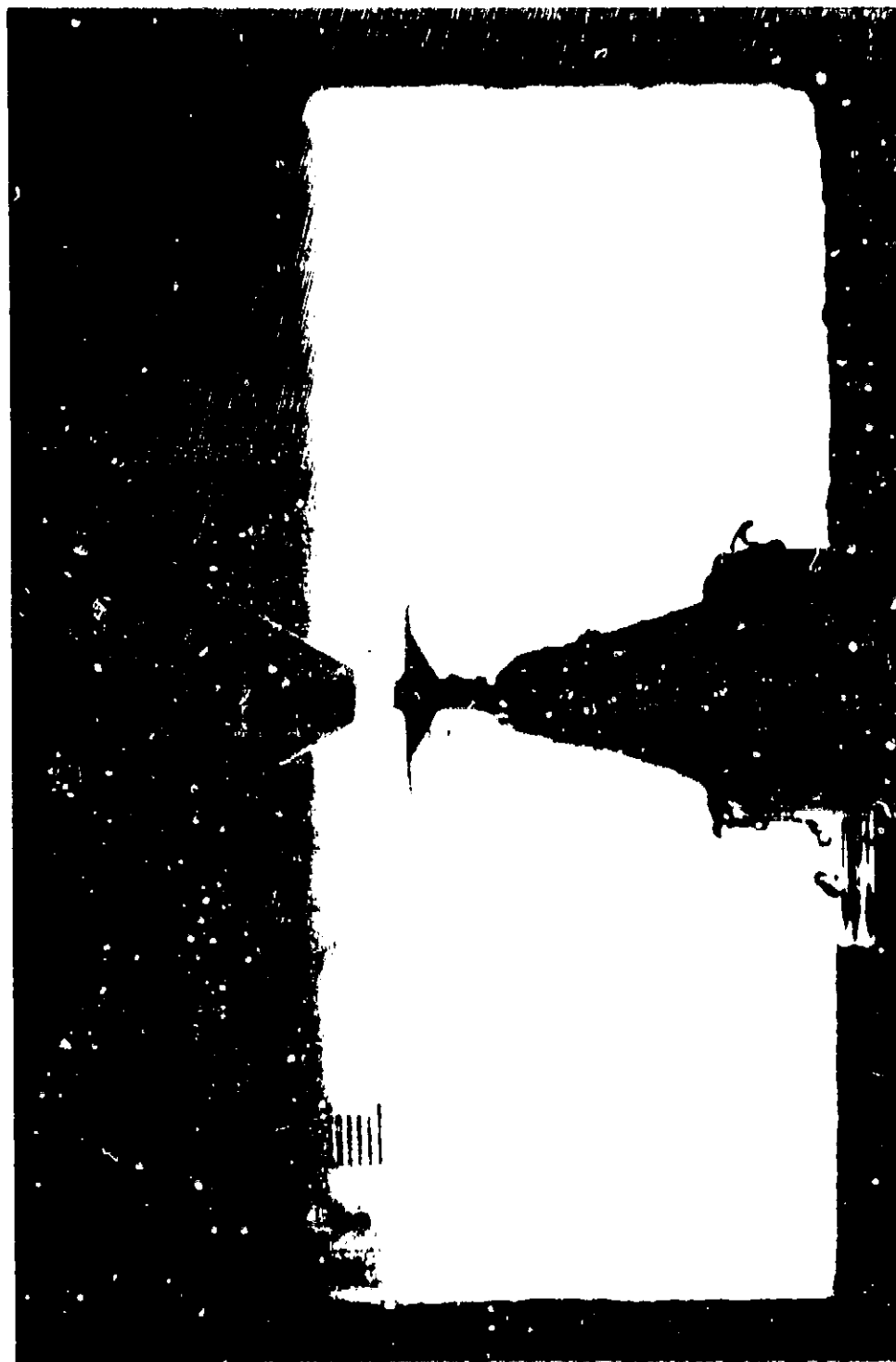


Figure 35. - Schematic of steady state normal gravity impingement.

C-75- 2599

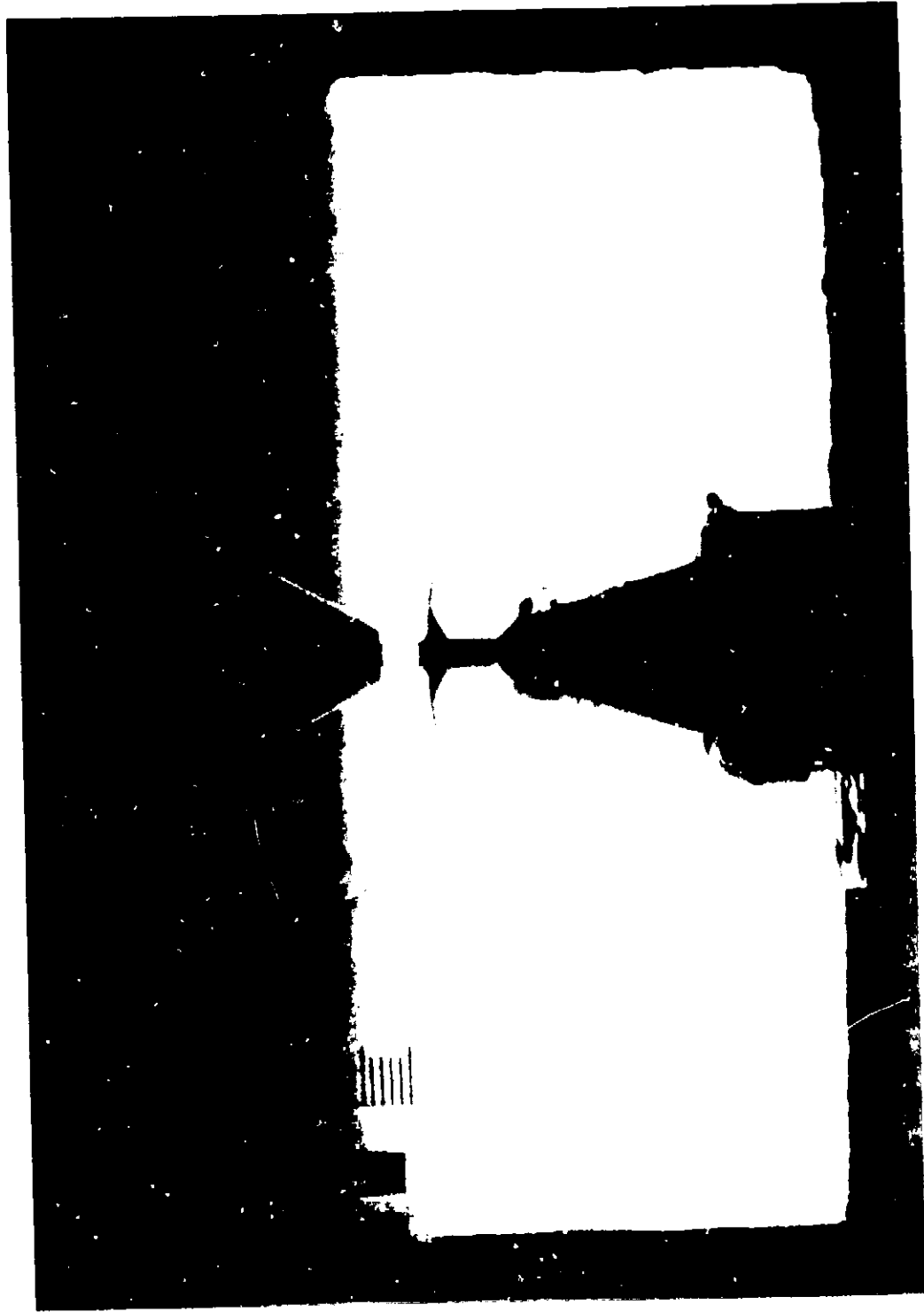
Figure 34. - Photograph of sharp edge disks.

ORIGINAL PAGE IS
OF POOR QUALITY



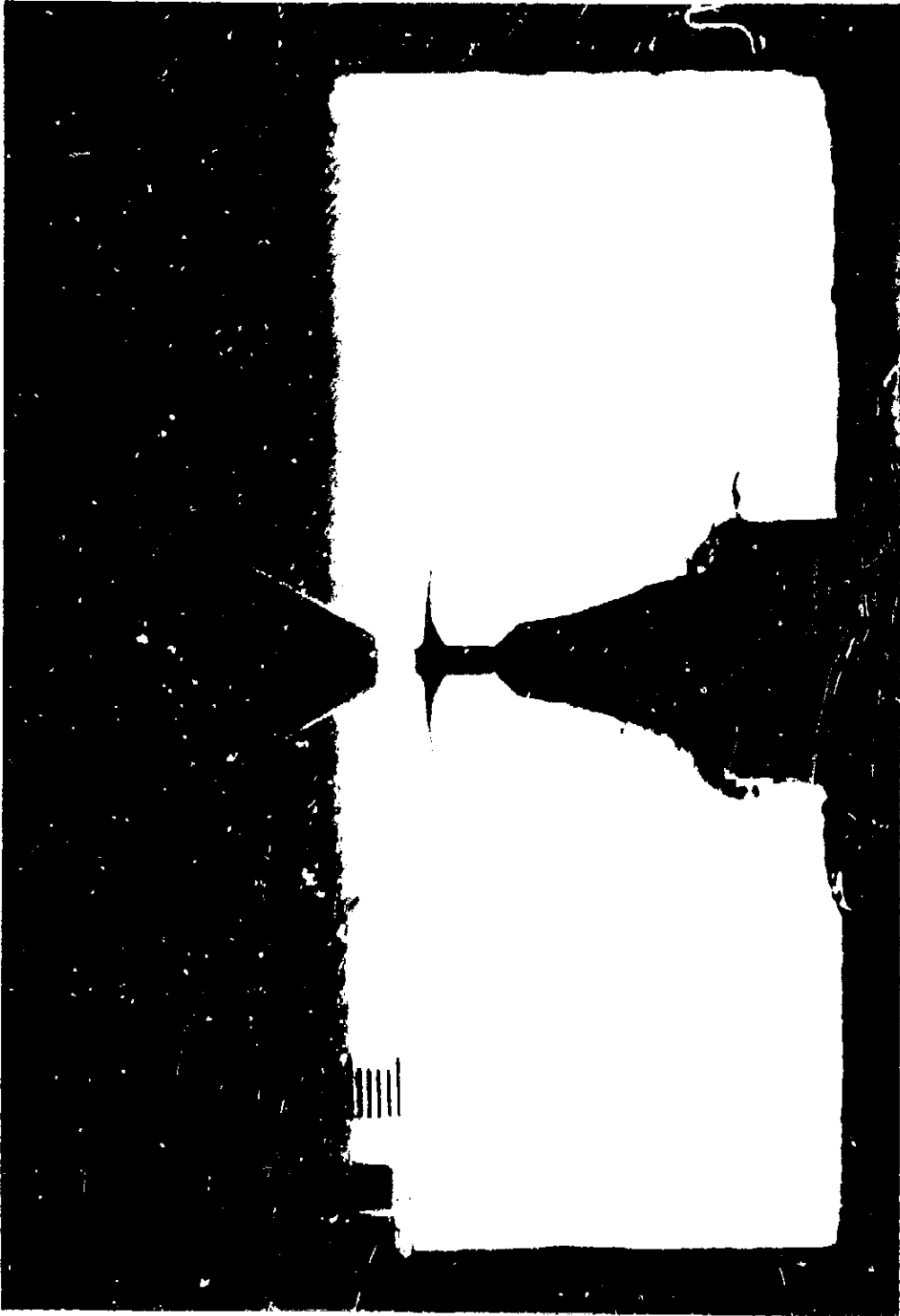
(a) Disc radius, 3.0 cm.

Figure 36. - Test liquid, distilled water; nozzle diameter, 0.5 cm; jet velocity, 286 cm/sec; distance between nozzle and disk, 1 cm.



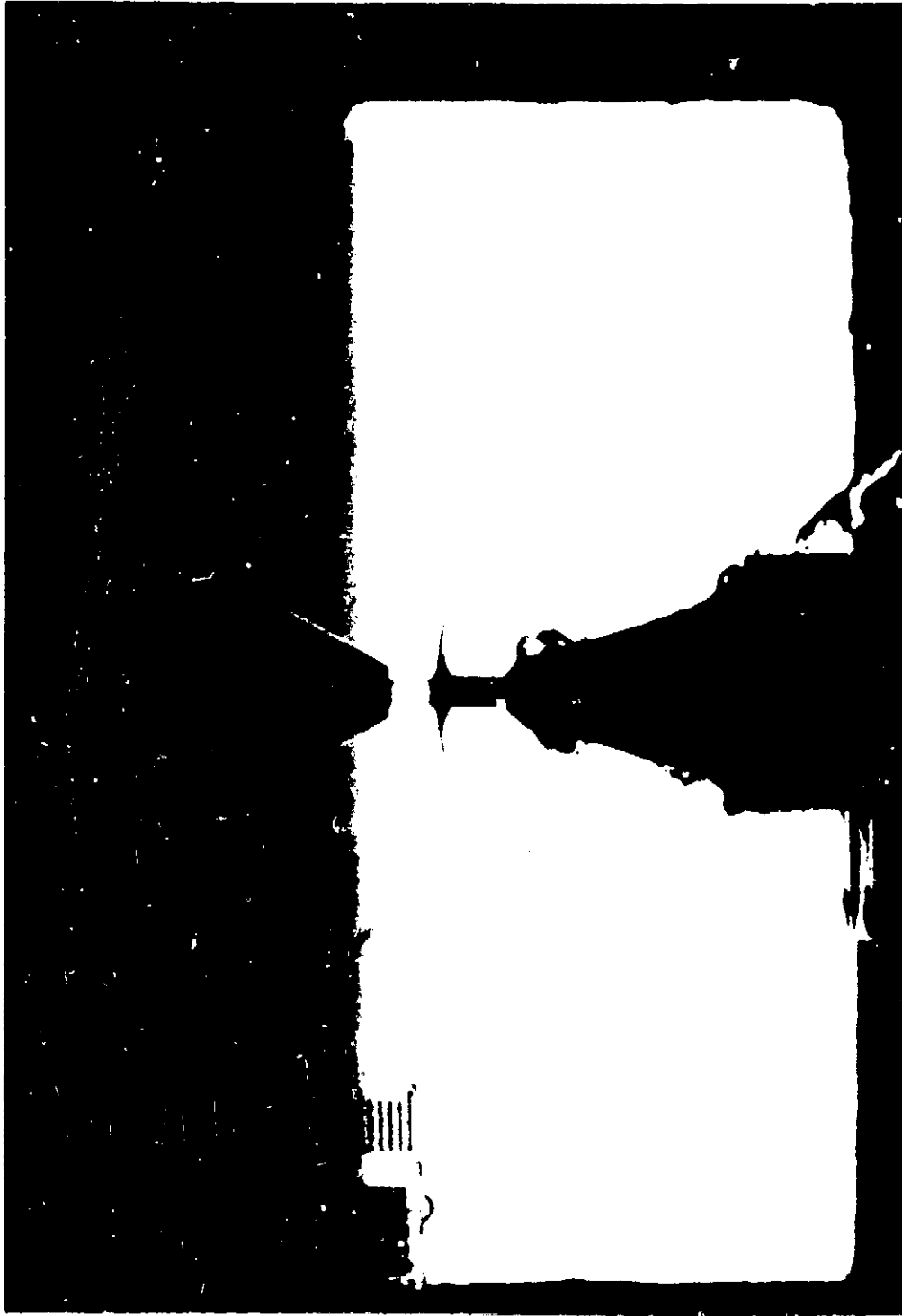
(c) Disk radius, 2.0 cm.

Figure 36. - Continued.



(d) Disk radius, 2.0 cm.

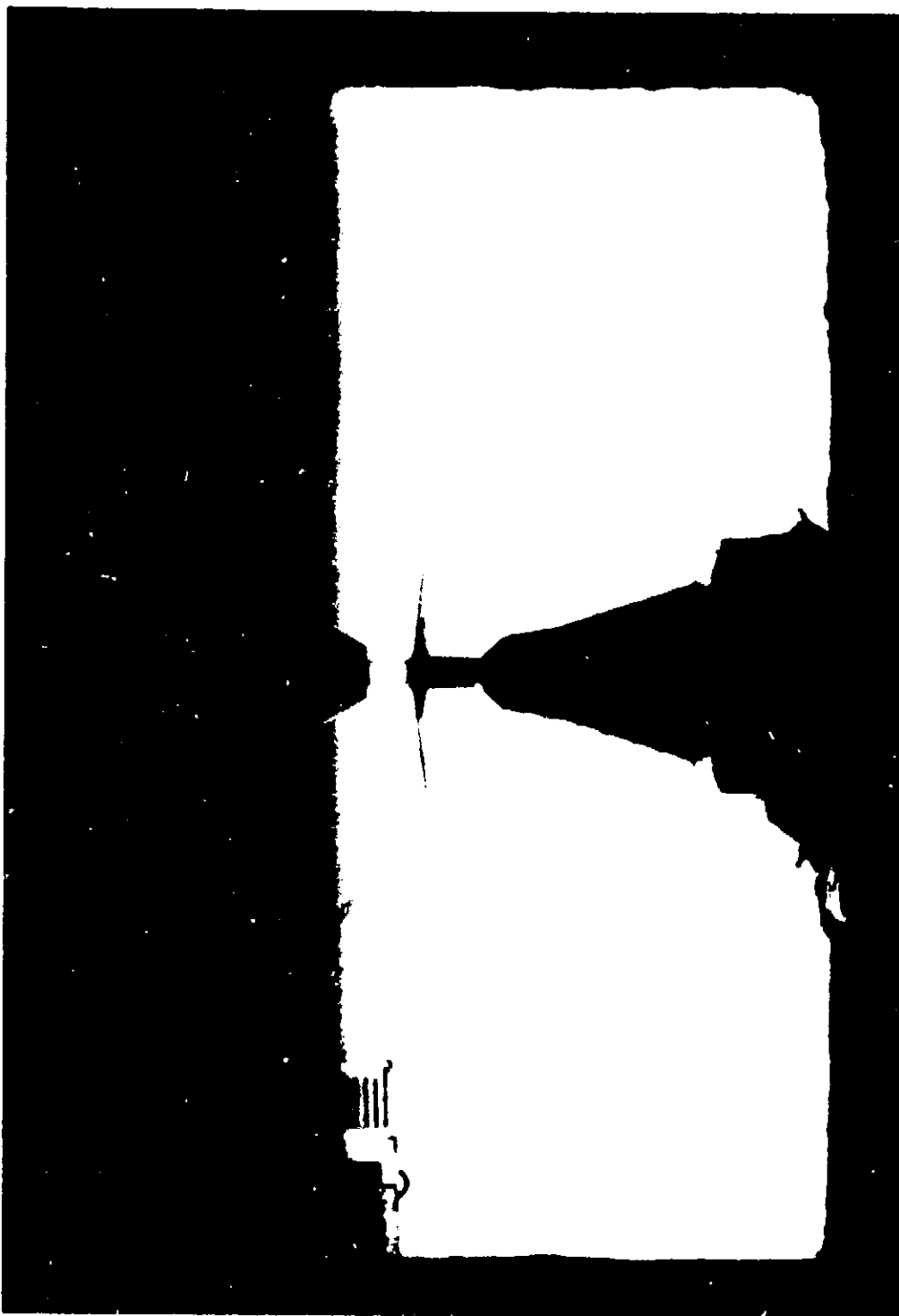
Figure 36. - Continued.



(e) Disk radius, 1.5 cm.

Figure 36. - Continued.

ORIGINAL PAGE IS
OF POOR QUALITY



(f) Disk radius, 1.5 cm.

Figure 36. - Concluded.

ORIGINAL PAGE IS
OF POOR QUALITY

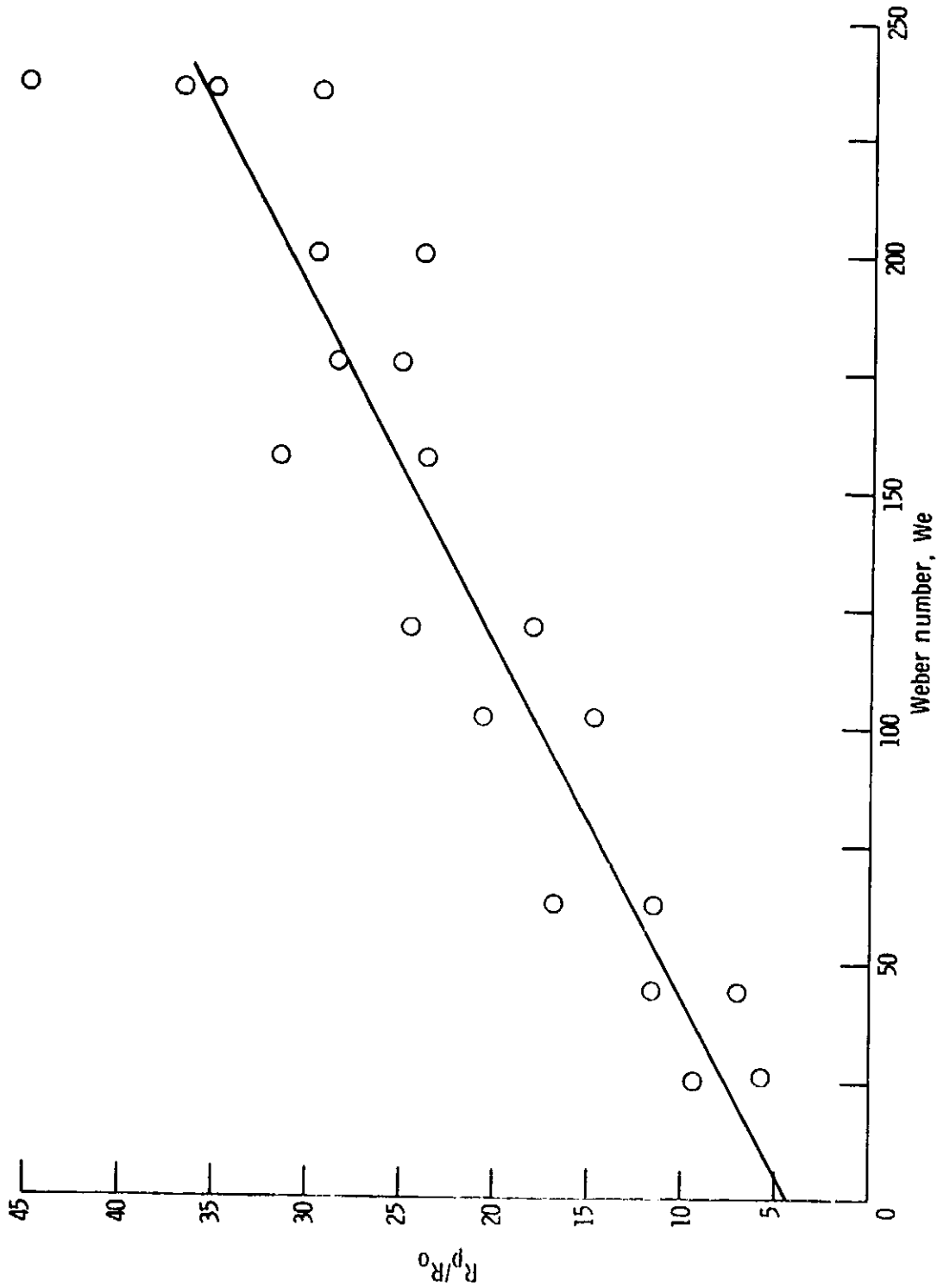
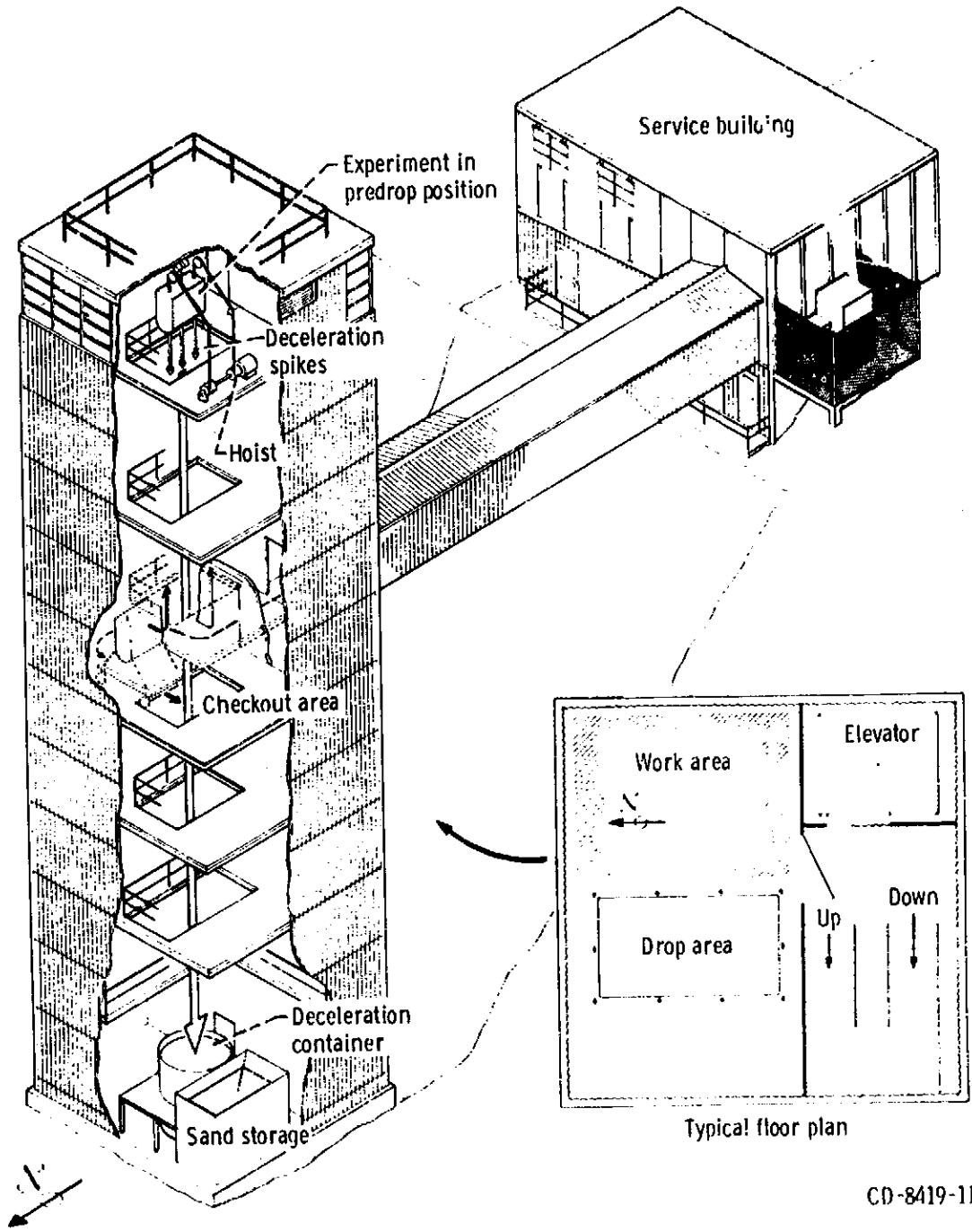
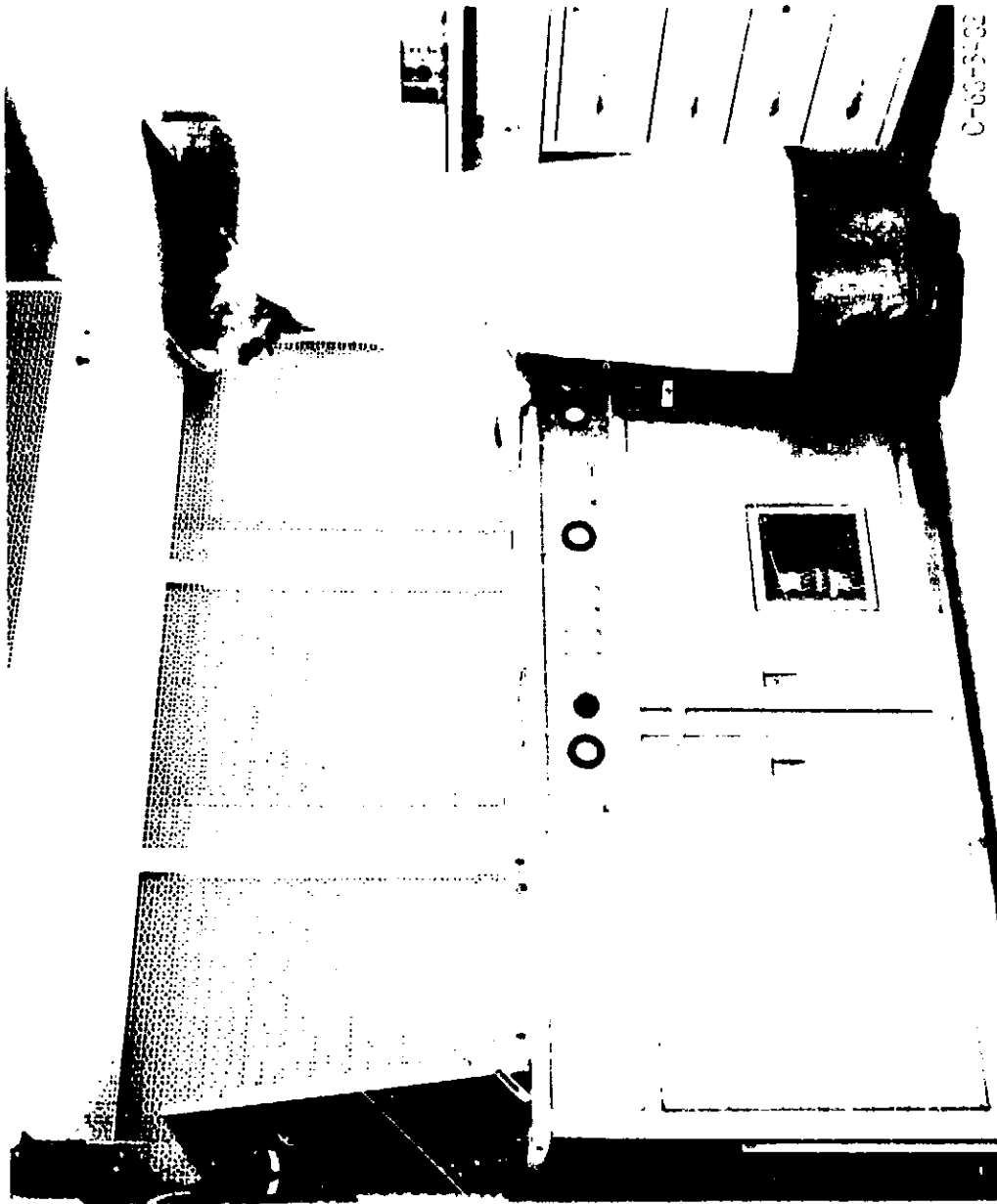


Figure 37. - Variation of plume width with Weber number $R_p/R_0 = 4.3968 + 0.1334 We$.



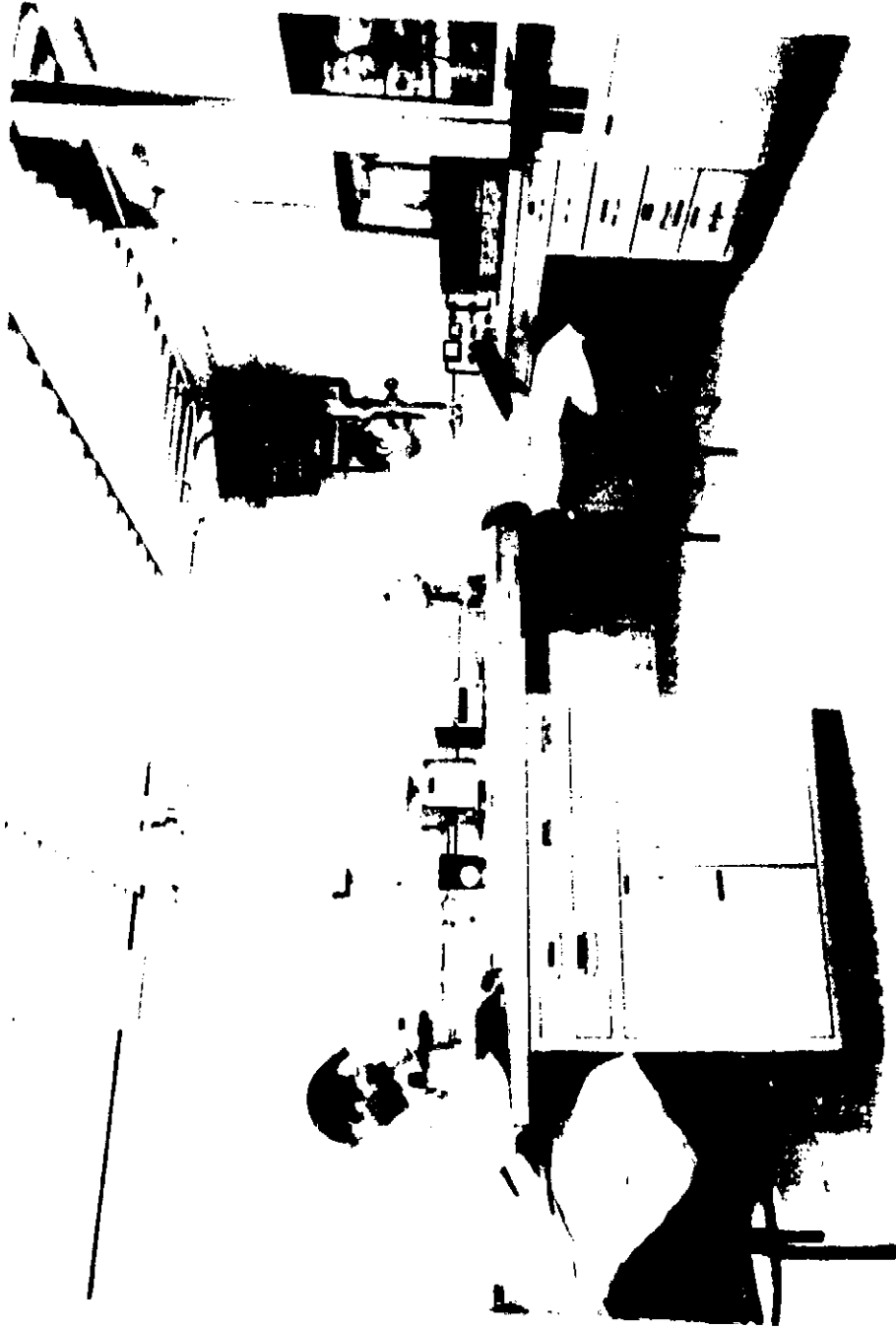
CD-8419-11

Figure B1. - 2.2-Second zero-gravity facility.



(a) Ultrasonic cleaning system.

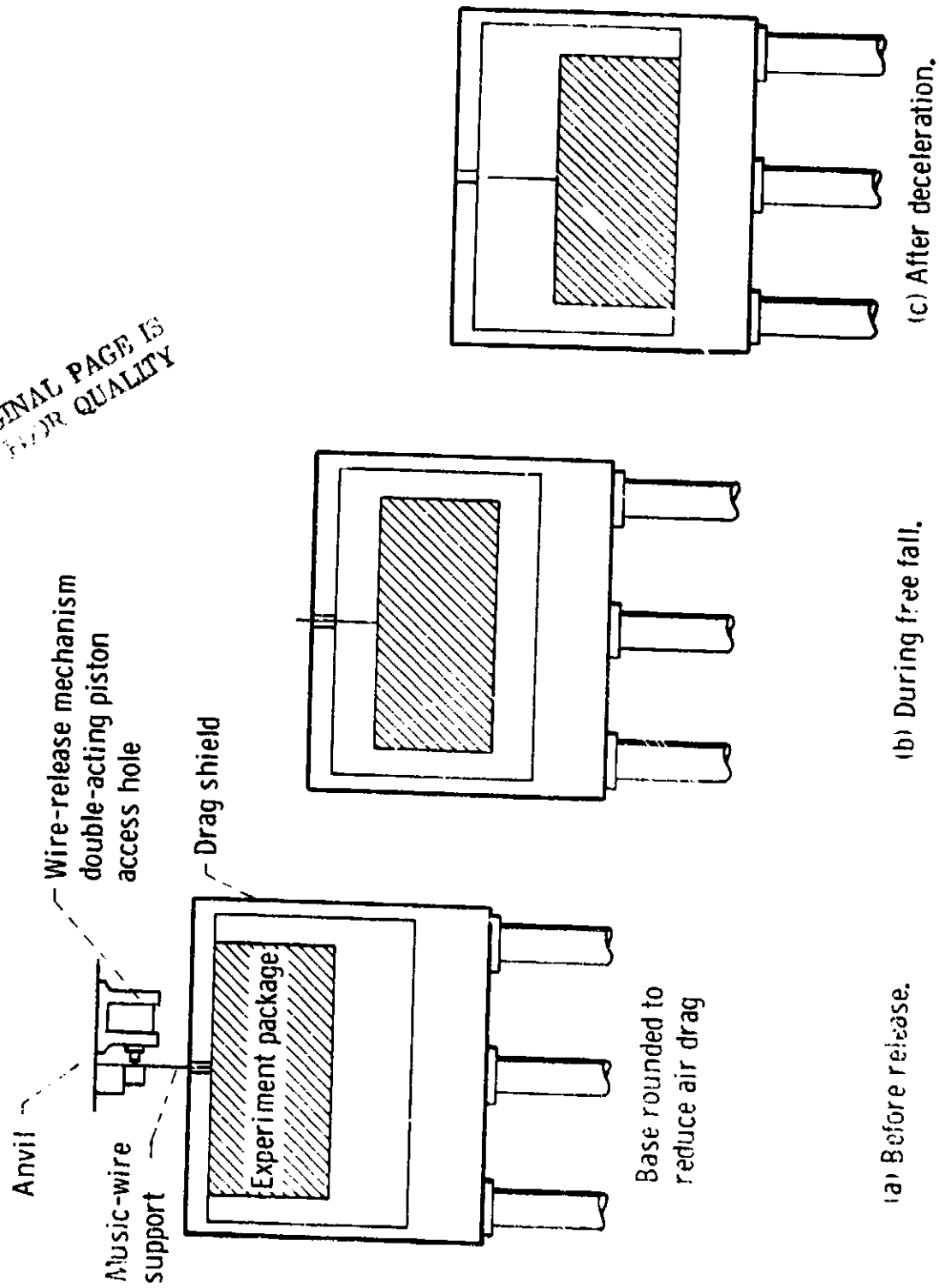
Figure B2. - Controlled environment room.



C-65-3983

(b) Laboratory equipment.
Figure 82. - Concluded.

ORIGINAL PAGE IS
OF POOR QUALITY



(a) Before release. (b) During free fall. (c) After deceleration.

Figure B3. - Position of experiment package and drag shield before, during, and after test drop.